Evolution and Development of the Strepsirrhine Primate Skull

Dissertation
zur
Erlangung der naturwissenschaftlichen Doktorwürde
(Dr. sc. nat.)
vorgelegt der
Mathematisch-naturwissenschaftlichen Fakultät
der
Universität Zürich

Doppeldoktorat

Universität Zürich
-
l'Université Montpellier II

Von
Renaud Lebrun
aus
Frankreich

Promotionskomitee

Dr. Franck Guy
Prof. Dr. Jean-Jacques Jaeger (Leitung der Dissertation)
Dr. Marcia Ponce de León
Prof. Dr. Christoph Zollikofer (Leitung der Dissertation)

Zürich, 2008

T H E S E

pour obtenir le grade de

DOCTEUR DE L'UNIVERSITE MONTPELLIER II
Discipline : Paléontologie
Ecole Doctorale : S.I.B.A.G.H.E
-
Thèse de doctorat double entre
l'UNIVERSITE MONTPELLIER II
et
l'UNIVERSITE de ZÜRICH

présentée et soutenue publiquement
par
Renaud Lebrun
Le 04 avril 2008

Titre :

EVOLUTION AND DEVELOPMENT OF THE STREPSIRRHINE PRIMATE SKULL

Rapporteurs

Prof. Dr. William Hylander, ...Rapporteur
Dr. Christopher Beard, ...Rapporteur

Jury

Prof. Dr. Monique Vianey-Liaud, ...Présidente du Jury
Dr. Franck Guy, ...Examinateur
Prof. Dr. Jean-Jacques Jaeger, ... Directeur de Thèse
Prof. Dr. William Hylander, ... Membre invité
Dr. Marcia Ponce de León,. . . . . .Examinateur
Prof. Dr. Marcelo Sánchez, ...Examinateur
Prof. Dr. Christoph Zollikofer, ... Directeur de Thèse

Abstract

Since Haeckel (1866), the evolutionary modification of ontogeny has been recognized as an important source of morphological innovation. Due to recent advances in developmental genetics and phenotypic analysis, evolutionary developmental (evo-devo) studies have regained considerable interest and led to fundamental changes in our understanding of how ontogeny and phylogeny are related.

This thesis investigates the relationship between ontogeny and phylogeny in strepsirrhine primates. The suborder Strepsirrhini, which comprises galagos, lorises and Malagasy lemurs, is thought to have retained most of the ancestral primate condition (as opposed to the suborder Haplorrhini, which comprises tarsiers and anthropoids). Nevertheless, strepsirrhines are highly diverse in their morphology. Here, the focus is on cranial diversity, which is analyzed from a developmental perspective with a new set of geometric morphometric tools.

First, patterns of cranio-mandibular variability in extant adult primates are analyzed. Taking into account the phylogenetic constraints applying to the skull morphology permits a quantification of how dietary specialization and activity patterns influence cranio-mandibular morphology in both primates suborders. Also, the skull morphology in strepsirrhines and haplorrhines is clearly distinct, and it is shown here that differences between and within infraorders can be traced back to differences in developmental modes.

According to a hypothesis proposed by Beard (1988), "strepsirrhinism" represents the primitive condition of the primate skull. This thesis shows that the cranial morphology of the Omomyidae – a basal haplorrhine taxon comprising the genera *Rooneyia*, *Necrolemur* and *Microchoerus* – is closer to that of extant strepsirrhines than to that of haplorrhines, while the cranial morphology of *Tarsius* is closer to that of other extant haplorrhines, *i.e.*, the anthropoids. Thus, it is probable that the shift towards a modern haplorrhine morphology occurred in one omomyid lineage, to the exclusion of the three genera mentioned above.

New arguments are proposed to support the hypothesis that the cranio-mandibular morphologies of the cheirogaleids and galagids are the least derived from the ancestral condition of toothcombed strepsirrhines.

This thesis presents a comparative geometric morphometric analysis of cranio-mandibular development in ten strepsirrhine and two haplorrhine species. Haplorrhines and strepsirrhines differ widely in ontogenetic trajectory direction, length and position. Within the strepsirrhines, divergence between taxon-specific ontogenetic trajectories and allometric grade shifts are more pronounced in lemurs than in lorises. This pattern of evolutionary modification of ontogenetic trajectories is interpreted in the context of the rapid adaptive radiation of lemurs.

The last section uses insights obtained from the evolutionary developmental analysis of extant taxa for a comparative analysis of fossil strepsirrhine taxa. The morphologies of extant and extinct strepsirrhines are compared. In particular, the morphology of the skull is well known from two adapiform subfamilies, Adapinae and Notharctinae. Among the adapines, a size increase has oc-

curred in the *Leptadapis* lineage via a shift in allometric grade, which suggests phyletic gigantism in this genus. Adapiforms exhibit longer ontogenetic trajectories than extant strepsirrhines. A trend toward a shortening of ontogenetic trajectories has occurred in the evolutionary history of strepsirrhines. This can be related to a context of general increase in encephalization within this lineage.

Table of contents

Since Darwin (1859) and Haeckel (1866), it has been recognized that developmental and evolutionary processes model morphology on different time scales: in the long term, morphology reflects evolution by means of natural selection and adaptation to the environment. On a shorter time scale, morphology is the result of ontogeny and is governed by genetic programs and developmental constraints. The basic thrust behind evolutionary developmental biology, or "evo-devo", is the proposition that the modification of ontogeny is a major source of morphological innovation during evolution. Within a group of species, morphological diversity can be understood in terms of diversity of species-specific developmental trajectories, which results from modification of the ancestral ontogenetic programs. Today, evo-devo is a growing research area, the general aim of which is to establish new ties between development (ontogeny) and evolution (phylogeny) (see Carroll, 2005).

Haeckel's theory of recapitulation inspired research in evolutionary developmental biology for almost a century: its principal postulates are that extant species recapitulate the adult stages of their ancestors during ontogeny, and that evolution of new morphologies proceeds by terminal addition of new features. Haeckels notorious proposition that "ontogeny recapitulates phylogeny" inspired a profusion of theoretical and empirical investigations into the connections between ontogeny and phylogeny.

Notably, Haeckel (1866), in an attempt to account for the exceptions to recapitulation, introduced the concept of heterochrony as the temporal agent of evolutionary change during ontogeny. Heterochrony was redefined by de Beer (1930) as "shifts in timing of an organ relative to the same organ of an ancestor". De Beer's redefinition of heterochrony still prevails and currently forms one of the dominant concepts of evolutionary developmental biology. While Haeckel's original hypothesis of recapitulation was progressively falsified during the 20th century, and while 20th-century evolutionary biology had a strong focus on adaptive changes related to natural selection, Gould's seminal book "Ontogeny and Phylogeny" (1977) has stimulated regained interest in developmental studies, setting the framework of heterochrony at a central place in the evo-devo field. Heterochrony *sensu* Gould applies to comparative analysis of shape-age trajectories (e.g., Gould, 1977, 2000). The terminology has subsequently been expanded to encompass the comparative description of size-age trajectories (Godfrey and Sutherland, 1995; Klingenberg, 1998; Rice, 1997). Originally restricted to the description of morphological patterns, recent advances in molecular developmental genetics have widened the scope of heterochronic analysis to the genetic processes responsible for observed differences in developmental patterns (e.g., see Ambros, 1997; Fondon and Garner, 2004; Moss, 2007; Slack and Ruvkun, 1997).

In parallel with progress in molecular genetics, the advent of geometric morphometric methods marked a milestone in quantitative phenotypic analysis (e.g., see Bookstein, 1991; Dryden and Mardia, 1998; Marcus et al., 1996). Geometric morphometric methods permit to quantify phenotypic changes that occur during ontogeny and phylogeny in a statistically sound and visually comprehensive manner, permitting the analysis of complex patterns of shape vari-

ability at an unprecedented level of detail. These techniques have triggered new interest in the description and analysis of patterns of growth and development from an evo-devo perspective, especially in the field of physical anthropology (e.g. see O'Higgins et al., 2001; O'Higgins and Jones, 1998; Ponce de León and Zollikofer, 2001).

A central topic in the field of evo-devo is the hypothesis of human neoteny, which was initially proposed by Bolk (1926) and contemporaries (see Schultz, 1927). Adult humans present characters, especially in the skull, that correspond to the juvenile condition in great apes. Subsequent to the major review by Gould (1977) in favor of this hypothesis, the question of human neoteny received considerable attention and yielded controversial debates that lack consensus even today (e.g., see Godfrey and Sutherland, 1996; Penin et al., 2002; Raff, 1996; Rice, 1997; Shea, 1989). In primates, another prime example is the case of *Pan paniscus*, the pygmy chimpanzee, which has been regarded as a paedomorphic relative of *Pan troglodytes* since its discovery (see. Coolidge, 1933; Schwarz, 1929). Since then, many studies have attempted to test this hypothesis for cranial ontogeny using either a traditional morphometric approach based on linear measurements (e.g., see Shea, 1983a, 1983b, 1989) or geometric morphometric methods (Lieberman et al., 2007; Mitteroecker et al., 2005; Ponce de León and Zollikofer, 2006). Apart from hominoid primates, geometric morphometrics has also been used to analyze the ontogeny of the skull in long-faced old-world monkey species (mandrills, geladas and baboons) in order to assess whether the similarities in morphological patterns observed in adults are produced via homologous morphogenetic processes (e.g., see Collard and O'Higgins, 2001; Leigh, 2006, 2007).

Evo-devo studies addressing questions of anthropoid primate diversity assume a special place because they concern our own evolutionary history. Nevertheless, it is surprising that the enormous diversity of strepsirrhine primates has little been studied from an evo-devo perspective. This is where the present thesis is situated; it represents an attempt to establish links between ontogenetic and phylogenetic diversity within strepsirrhine primates. Given that diversity concerns almost every aspect of strepsirrhine biology, the prospects for such an approach are promising: the suborder Strepsirrhini consists of two monophyletic infraorders, the Lemuriformes (the Malagasy lemurs) and the Loriformes, which contains lorises and galagos (as opposed to the suborder Haplorrhini, which contains anthropoids and tarsiers, see Figure 1). Lemuriforms have evolved in isolation on Madagascar during most of the Cenozoic era and occupy a wide range of ecological niches (Mittermeier et al., 1994). Malagasy primates exhibit a wide variety of dietary habits (frugivory, insectivory, folivory, gummivory) and activity patterns (diurnality, cathemerality, nocturnality). They also exhibit a wide range of locomotor and postural adaptations (arboreal and terrestrial quadrupedalism, vertical clinging and leaping, and suspension), and body mass ranges between 55 g in *Microcebus* to about 200 kg in *Archaeoindri*. Thus, the model of adaptive radiation (Simpson, 1953) applies well to the evolutionary history of lemuriform primates: their biological diversification is associated with a broad eco-

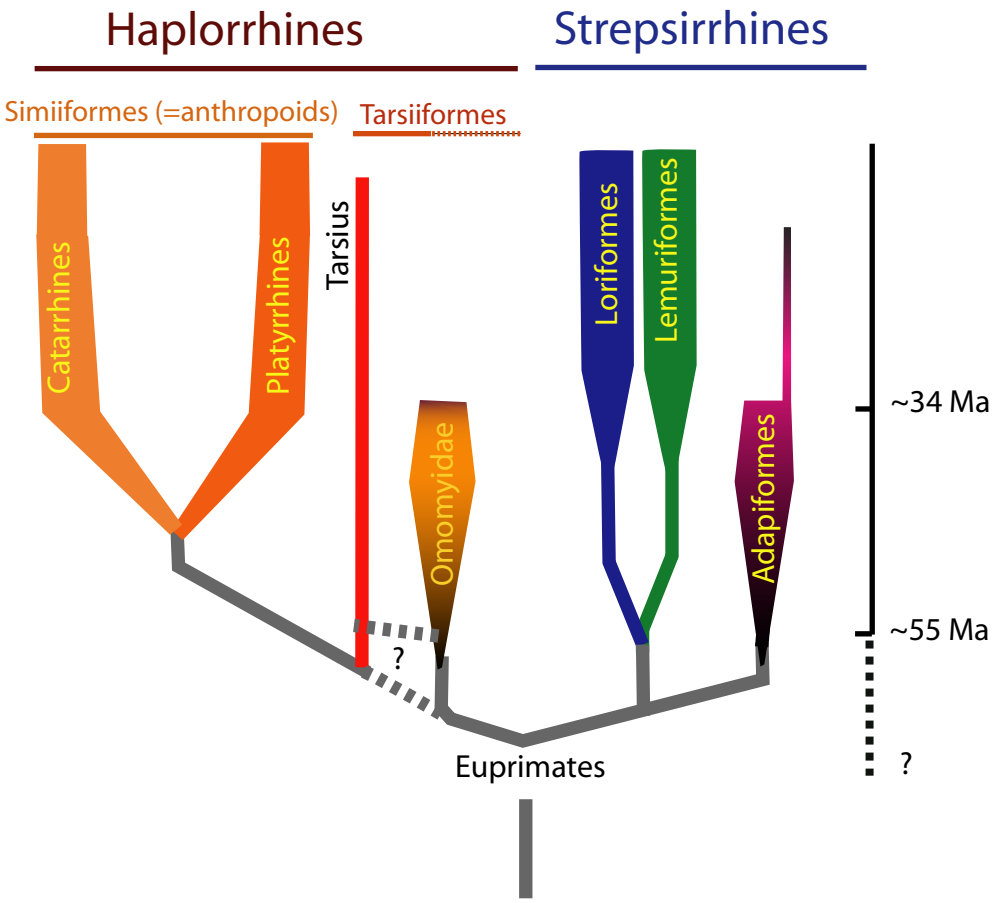

Figure 1: phylogeny of the primate order (modified after Ross et al., 1998).

logical and phenotypic diversity (Martin, 1972). Conversely, loriform species occupy more restricted ecological niches; competition with haplorrhines probably restricted their diversification (Mittermeier et al., 1994). Also, there are still open questions regarding the evolutionary history of strepsirrhines, the major one being that there is currently no clear fossil evidence for the ancestors of extant strepsirrhines. A group of early strepsirrhines is well-represented in the fossil record: the Eocene adapiforms. Their evolution is well-documented in the Eocene deposits of Europe, America and Asia. The best-known morphological diversification episode in their evolutionary history is the radiation of the Adapinae subfamily, which occurred from the middle to the late Eocene in Europe (Franzen, 2003; Godinot, 1998; Lanèque, 1992a, 1992b, 1993). Adapiforms did not evolve a toothcomb (composed of elongated, slender and procumbent incisors and canines on the jaws), which characterizes extant strepsirrhines. Despite the lack of that character in adapiform primates, even in an incipient state, many researchers have attempted to identify a possible ancestor of toothcombed strepsirrhines among the adapiforms (e.g., see Beard et al., 1988; Beard and Godinot, 1988; Godinot, 1998; 2006 ; Rasmussen and Nekaris, 1998; Seiffert, 2005; Seiffert et al., 2003), but the result of these studies still lack consensus. Fortunately, the fossil record comprises complete skulls of several adapiform taxa, the morphology of which can be compared to that of modern forms.

Studies focusing on the development of the skull in strepsirrhine primates are typically based on linear measurements (e.g. see Ravosa, 1992, 2007), and their principal aim is to establish links between patterns of growth and development on the one hand, and life-history parameters and strategies on the other (see Godfrey et al., 2004; Godfrey et al., 2005; Smith, 2000). However, these studies do not provide detailed information on changes in shape and size during the ontogeny of the cranium and mandible. Furthermore, they do not compare data belonging to extant and extinct species. As a result, these studies do not indicate how the evolutionary modification of ontogenetic trajectories is related to morphological diversification and adaptation. Overall, therefore, little is known about possible links between ontogeny patterns of the skull and phylogenetic diversification in strepsirrhine primates. One major reason for the relatively small number of ontogenetic analyses of cranial morphology (e.g., see Godfrey et al., 2004; Godfrey et al., 2005; King et al., 2001; Ravosa, 1992, 2007; Ravosa and Simons, 1994) is that most collections of juvenile strepsirrhine specimens consist of unprepared cadavers, the osseous structures of which are difficult to access. Thanks to recent developments in 3D microtomography (e.g., see Rossi et al., 2003; Silcox, 2003; Spoor, 1998; Tafforeau et al., 2006), it is now possible to perform scans with sufficient spatial resolution to access the skeletal morphology even in juvenile specimens of the smallest strepsirrhine species, such as *Microcebus murinus*. Furthermore, the use of computer-assisted techniques on CT data offers the opportunity to analyze the morphology of fossils from a whole new perspective: reconstructions of incomplete and distorted specimens can be achieved, which permits to conduct comparative analyses of fossil and extinct forms (Zollikofer and Ponce de León, 1995; Zollikofer et al., 1995).

The main aim of this thesis is to investigate how evolutionary modification of developmental programs have contributed to the morphological diversity observed in fossil and extant strepsirrhines. In this thesis, the focus is on skull morphology because:

- the skull conveys a strong phylogenetic signal, which is traditionally used for systematic analyses (for instance, see Cartmill, 1994; Fleagle, 1999; Kay et al., 1997; MacPhee and Cartmill, 1986; Shoshani et al., 1996);
- the skull houses the masticatory apparatus, the brain and the major sense organs; skull morphology is expected to reflect various functional adaptations that are of interest for evolutionary studies;
- the skull is a 3D biological structure with many quantifiable features of interest, and homologous locations; thus, it is possible to conduct comparative analyses using 3D geometric morphometric methods.

The following specific issues are addressed:

1) *Methods*: How can complex and diverse patterns of craniomandibular morphological variation (in phyletic and ontogenetic time) be analyzed comprehensively? What would be the benefits of using an integrated geometric morphometric application framework in order to conduct such analyses?

2) *Functional versus developmental constraints*: What is the relative contribution of functional adaptation and developmental constraints on primate skull size and shape? This issue concerns the debate between adaptationists and structuralists (Gould and Lewontin, 1979).
3) *Ontogenetic sources of phyletic diversity*: What are the relationships between developmental diversity and species diversity?
4) *Evo-devo perspective on fossil taxa*: What is the link between the increase in encephalization in strepsirrhine primates and the evolution of the development of the skull?

These issues are investigated in this manuscript throughout six chapters. Chapter 1 is dedicated to the methods and analytic tools used throughout the thesis. An integrated geometric morphometric software is presented that permits interactive and comprehensive analysis and visualization of patterns of shape variability in 3D biological structures, such as the skull.

In Chapter 2, a sample of adult strepsirrhine and haplorrhine skulls is studied: we examined whether the two suborders share similar patterns of shape variation. Then, taking into account the phylogenetic signal conveyed by the morphology in both infraorders, the extent to which dietary specialization and activity patterns impinge on the morphology of the skull in haplorrhines and strepsirrhines is assessed.

According to a hypothesis proposed by Beard (1988), "anatomical strepsirrhinism" represents the primitive condition in primates. In order to test whether this hypothesis also applies to the global morphology of the cranium, Chapter 3 presents a geometric morphometric analysis of a sample composed of crania of basal haplorrhine fossils belonging to the Omomyidae family and extant haplorrhine and strepsirrhine crania.

Chapter 4 provides an analysis of the morphological variability of the skull of extant adult strepsirrhines. Among strepsirrhines, a popular hypothesis proposes that cheirogaleids and galagids have retained the most of the ancestral toothcombed strepsirrhine condition. This hypothesis is examined for the morphology of the skull using both geometric morphometric and phylogenetically based comparative approaches.

In Chapter 5, a comparative analysis of the developmental patterns of a sample composed of ten strepsirrhine and two haplorrhine species is conducted. The following issues are investigated. What are the differences and commonalities between strepsirrhine and haplorrhine patterns of ontogeny? Is it possible to link the diversity of developmental patterns in lemuriforms with their adaptive radiation? Does this diversity stand in marked contrast with the developmental patterns observed in less diversified groups such as the Loriformes?

In Chapter 6, the morphologies of extant and extinct strepsirrhines are compared. Craniomandibular morphology is well-known in two subfamilies of Adapiformes, the Adapinae and the Notharctinae. Patterns of morphological diversity of the adapiform skull are compared with those of extant strepsirrhines using insights obtained from the developmental analysis of extant

Chapter 1

Materials and Methods

Contents

1. Materials

1.1 Taxonomic framework

In this manuscript, the systematic taxonomy proposed by Groves (2001) was followed, with the following exceptions. Strong molecular evidence suggests that the Malagasy lemurs are monophyletic and that the genus *Daubentonia* is basal in this group (e.g., see Roos et al., 2004; Yoder and Yang, 2004). Therefore, the infraroder "Lemuriformes" was used to designate all Malagasy primates (no use was made of the infraorder "Chiromyiformes", within which Groves (2001) places *Daubentonia*). Thus, it was considered that the suborder Strepsirrhini comprises only two extant infraorders: Loriformes and Lemuriformes. Following Gunnell and Rose (2002), the term Tarsiiformes here designates *Tarsius* and the Omomyidae family.

1.2 Sample

Morphological data were collected from 311 distinct specimens that consisted of 285 complete skulls, 22 isolated crania or crania associated with badly preserved mandibles and 4 isolated mandibles. This sample comprises adults of extant species, juveniles of extant species and adults of extinct species.

1.2.1 Adults belonging to extant and recently extinct species

Morphological data were collected from 205 extant adult primate individuals, 115 of which are strepsirrhines and 90 are haplorrhines, and all of which have crania with associated mandibles. The sample also comprises 4 isolated crania and 3 isolated mandibles belonging to 7 individuals of the genus *Archaeolemur*, a recently extinct lemur of Madagascar. These specimens are listed in Appendix 1.

1.2.2 Extant juveniles

Postnatal ontogenetic data were collected for 10 strepsirrhine species (*Lemur catta*, *Lepilemur ruficaudatus*, *Microcebus murinus*, *Propithecus diadema* and *Propithecus verreauxi*, *Arctocebus calabarensis*, *Nycticebus coucang*, *Perodicticus potto*, *Galago senegalensis*, *Otolemur garnetti*) and 2 haplorrhine species (*Tarsius bancanus* and *Aotus trivirgatus*). The sample comprises 83 skulls (crania + mandibles) and one isolated cranium belonging to juvenile individuals. Two mandibles belonging to individuals of the genus *Propithecus* were badly preserved and, therefore, could not be included in the analyses. As a whole, 81 crania with associated mandibles were analyzed. A comprehensive list of the juvenile specimens is presented in Appendix 1. Additionally, information on the state of dental eruption for each specimen is provided in the Appendices 3.1-12.

1.2.3 Extinct specimens

The fossil sample consists of 11 Eocene adapiform specimens. The sub-family Adapinae is represented by three isolated crania of *Adapis sp*., four isolated crania and one complete skull of *Leptadapis*, and the cranium of the type specimen of *Palaeolemur betillei*, the subfamily Notharctinae by one complete skull of *Notharctus tenebrosus* and one cranium of *Smilodectes gracilis*. Additionally, four crania belonging to the Eocene Omomyidae family are included in the sample. The sub-family Microchoerinae is represented by *Necrolemur* (*N=2)* and *Microchoerus* (*N=1),* and the tribe Rooneyinii is represented by the cranium of the type specimen of *Rooneyia viejaensis*. The cast of the cranium of *Rooneyia* was scanned using a 3D laser scanner by Sai Man Wong, the assistant of Pr. A. Rosenberger, for the purposes of a recently published work (Rosenberger, 2006). The complete Eocene fossil list is presented in Appendix 2.

1.3 CT data acquisition

205 specimens were scanned using tomography (N=8), conventional microtomography (N=166) and microtomography using synchrotron light (N=31). Microtomography yields high-resolution cross-sectional image series of cranial and mandibular structures (see specimen lists presented in Appendix 1 and Appendix 2). Four fossils were scanned at the European Synchrotron Radiation Facility (E.S.R.F) on beamlines ID19 and ID17. The use of synchrotron light for mineralized fossils is recommended because it produces far better results than those achieved with conventional industrial scanners (Tafforeau et al., 2006). For a few fossils, only casts were available. Therefore, these samples were CT scanned to produce a 3D representation of the external fossil surface. Each voxel of the CT images stack consists of a measurement of the density of the object of interest at a given location (x,y,z) in space. For all scanned specimens, 3D surface representations were generated from the µCT volume data using the “isosurface” algorithm of the Amira software package (TGS, San Diego, CA). The position of the interface between air and bone is set using the half-maximum height technique (Baxter and Sorenson, 1981; Spoor et al., 1993). The resulting virtual representations of the mandibles and crania were positioned in dental occlusion.

1.4 Reconstruction

1.4.1 Reconstruction of one neonate Propithecus diadema

The cranium of a specimen belonging to the species *Propithecus diadema* presented several bones that were displaced (see Appendix 4-A). A virtual reconstruction of this specimen was performed in order to recover its original morphology. Groups of bones and individual bones that were displaced were segmented and repositioned in their original anatomical locations. Additionally, bones missing from the left orbital region were reconstructed using mirror images of

the corresponding bones (see Appendix 4 for details).

1.4.2 Fossils

Several fossils and extant specimens were incomplete, were deformed or presented displaced parts. Theses specimens were reconstructed following the recommendations of Zollikofer and Ponce de León (2005). Whenever possible, missing parts were retrieved using symmetry. Pieces that had been displaced but not deformed were moved to their original position. To guarantee accurate virtual reconstructions, only relatively undistorted and almost complete fossils were incorporated in the sample. In seven fossils, several missing parts, mostly situated in the orbital region, were reconstructed by producing a mirror image of the corresponding part (see Appendices 5, 6, 7, 8, 9, 10 and 11).

Recommendations given by Zollikofer and Ponce de León (2005) were followed to correct for plastic deformation of the skull of *Notharctus tenebrosus* that was incorporated in this study. In this case, plastic deformation was principally due to compression. The directions of maximal compression were estimated in the coronal and axial planes, and decompression was subsequently applied to retrieve the bilateral symmetry of the skull (see Appendix 12). The resulting virtual representation of the fossil was almost undistorted, but larger than the original one. Thus, this representation was scaled by a factor of 0.95 in order to recover the original size.

2. Methods used throughout this manuscript

Compared to traditional morphometric methods, which are based on linear and angular measurements, geometric morphometric (GM) methods have two major advantages:

- the biological form is reduced to its size and shape components. In a traditional approach based on linear measurements, this is not possible because the measurements *are* measurements of size, and size is thus expected to be the main source of morphological variation. In a GM context, variation in size does not mask variation in shape, even when the size range of the sample is wide;

- the information conveyed by the geometric structure of the biological object is preserved throughout analysis: it is possible to have a visual representation of the results, which can be interpreted biologically. For a given biological structure, spatial morphological variability patterns can be readily identified and visualized comprehensively.

The use of landmarks is common in studies that analyze primate skull morphology (see for instance Mitteroecker et al., 2004a; O'Higgins and Jones, 1998; Ponce de León and Zollikofer, 2001). When analyzing bones, such as the skull, landmarks can be defined at different loci, such as the intersection of bone sutures, the center of foramina and the tips and maxima of curvature. The basic thrust of GM analyses involving landmarks is the hypothesis of biological homology of the landmark locations across all specimens of a sample. Bookstein (1991)

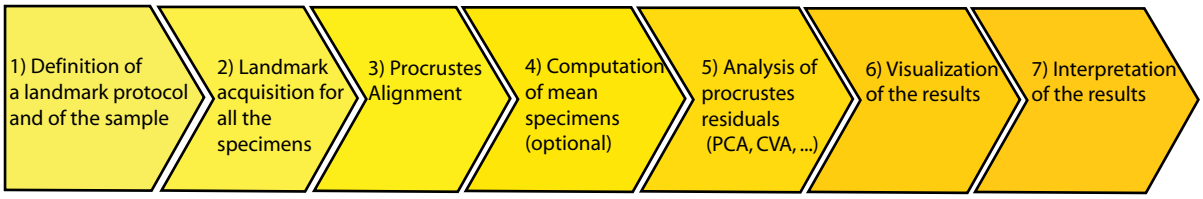

Figure 1.1: Steps of a geometric morphometrics analysis involving landmarks.

proposed a nomenclature that accounts for the quality of the landmarks in terms of homology. Accordingly, type I landmarks are expected to convey more homology information than type II or III landmarks.

All GM analyses performed in this thesis are based on 3D cranial and mandibular landmarks. This methodology provides an efficient means to capture the geometry of the skull in a comprehensive way.

An overview of the different steps of a GM analysis is given in Figure 1.1

Table 1.1: Mandibular landmarks used throughout the manuscript. * No analysis of the mandible is conducted in the 3rd Chapter. ** Not used for the specific sub-analysis using a comparative sample composed of ontogenetic series.

#	Name	Definition	Used in Chapters				
			2	3*	4	5	6
1	Infradentale	midpoint between I1L/I1R on alveolar rim	X		X	X	X
2,3	Foramen mandibulare		X		X	X	X
4,5	M3	medial point on buccal crown surface of permanent M3	X			X	X**
6,7	Ramus	point on the anterior rim of the ramus, where it starts sloping upward from the alveolar plane, in lateral view	X		X	X	X
8,9	Kondylion	highest medial point of the condyle	X		X	X	X
10,11	Incisura	lowest point of mandibular notch	X		X	X	X
12,13	Coronoid process	highest point	X		X	X	X
14	Akanthion	between spinae mentales	X		X	X	X
15	Gnathion	inferiormost point on symphysis	X		X	X	X
16,17	Gonion	location of largest curvature on the gonial edge	X		X	X	X
18	Chin	medial point between 1 and 15	X		X	X	X

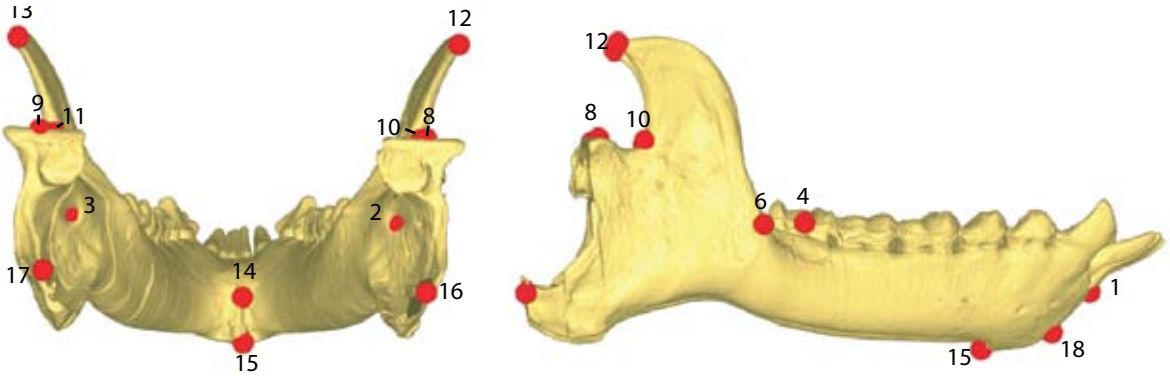

Table 1.2: Cranial landmarks used throughout the manuscript. * Not used for the specific sub-analysis using a comparative sample composed of ontogenetic series.

#	Name	Definition	Used in Chapters				
			2	3	4	5	6
1	Nasion		X		X	X	
2	Mid nasion-bregma	Midpoint of nasion-bregma arch	X	X	X	X	X
3	Bregma		X	X	X	X	X
4	Mid bregma-lambda		X		X	X	
5	Lambda						
6,7	Mid coronale	Midpoint of coronal suture between pterion (fronto-sphenoid suture) and bregma	X	X	X	X	X
8,9	Mid lambda	Midpoint of lambda suture between asterion and lambda	X	X	X	X	X
10,11	Pterion	Meeting poit of coronal with sphenoid suture	X	X	X	X	X
12	Nasospinale		X		X	X	
13	Rhinion		X		X	X	
14,15	Apertura nasalis	Lateralmost points on the nasal aperture	X		X	X	
16,17	Maxillofrontale	Anterior edge of maxillofrontal suture	X	X	X	X	X
18,19	Highest orbital point		X	X	X	X	X
20,21	Orbitale (or)	Zygomatico-maxillary suture	X	X	X	X	X
22,23	Frontomalare-Orbitale (fmo)	Fronto-zygomatic suture at the orbital rim	X		X	X	X
24,25	Mid fmo-or	Midpoint between fmo and or at the orbital rim	X		X	X	X
26,27	Zygomaxillare	Zygomatico-maxillary suture at the tuberosity	X	X	X	X	X
28,29	Jugale	Location of largest curvature of the zygomatic rim in the jugal region	X	X	X	X	X
30, 31	Foramen maxillare	Midpoint at the level of the surface	X	X	X	X	X
32,33	Caninus buccal	Buccal midpoint of crown of canine	X	X	X	X	X
34,35	Third molar (M3)	Buccal midpoint of the crown of the last permanent molar	X	X	X		X*
36,37	Asterion		X	X	X	X	X
38	Mid lambda-opisthion	Midpoint on lambda-opisthion arch	X		X	X	
39	Opisthion	Posteriormost midpoint of foramen magnum	X	X	X	X	X
40	Basion	Anteriormost midpoint of foramen magnum	X	X	X	X	X
41	Sphenobasion	Midpoint of sphenobasilar suture	X	X	X	X	X
42	Staphilion	Posteriormost midpoint of palate	X	X	X	X	X
43	Palatum maxillare	Sagital point at the suture between the palate and maxillar.	X	X	X	X	X
44	Prosthion		X		X	X	
45,46	Porion		X	X	X	X	X
47,48	Stylomastoid foramen		X	X	X	X	X
49,50	Foramen ovale		X	X	X	X	X
51,52	Sutura pterigo-mx		X	X	X	X	X
53,54	Hypogloss canal		X	X	X	X	X

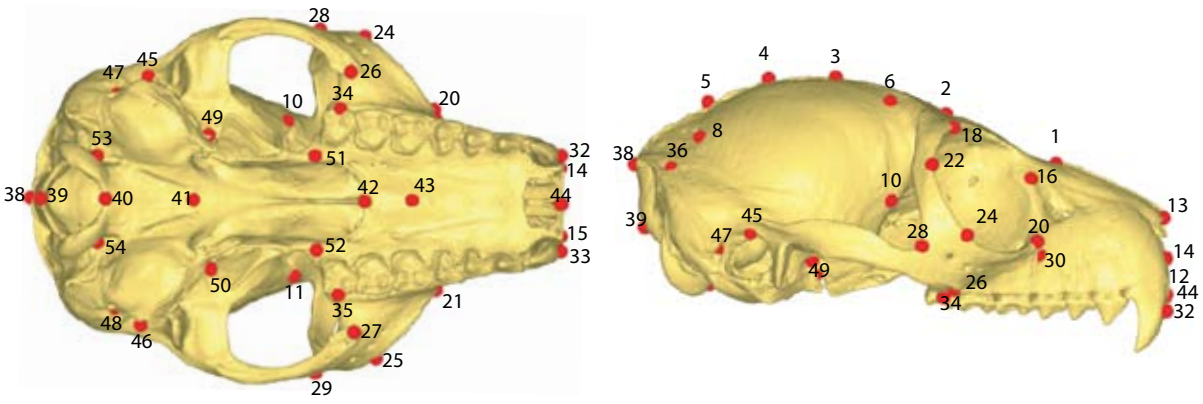

2.1 Landmark protocols and landmark acquisition

2.1.1 Protocols

56 cranial and 18 mandibular landmarks were defined (see Table 1.1 and Table 1.2). The combination of these 2 sets of landmarks results in 3 configurations: the mandible configuration, the cranium configuration and the cranium plus the mandible in occlusion. Throughout this manuscript, the latter configuration is referred to under the term "skull configuration". The term "cranium configuration" thus refers to the cranium *without* the mandible.

Landmarks were defined at the intersection of bone sutures, in the center of foramina and on the tips and maxima of curvature. They consist principally of type I and II landmarks, following the nomenclature defined by Bookstein (1991).

Several landmarks were not used in all of the analyses. In the analyses involving ontogenetic series (in Chapter 5 but also in an analysis presented in Chapter 6), the protocols used for the cranium and the mandibular configurations differed only slightly: the landmarks corresponding to the permanent last molar have been omitted.

Concerning the analyses involving the crania of the Omomyidae family (Chapter 3), the corresponding protocol takes into account the fact that most of these fossils are incomplete in the orbital region. Furthermore, in many omomyids and adapiforms, it is also difficult to satisfactorily estimate the position of the "lambda" landmark because the corresponding region is often badly preserved. Several fossils are also incomplete in the nasal region. Thus, the corresponding points do not form part of the protocols used for analyses of samples comprising fossils.

2.1.2 Landmark acquisition

Concerning the 205 specimens that were CT scanned and the specimen scanned using a laser scanner (see lists presented in Appendix 1, Appendix 2 and Appendices 3.1-12), 3D landmarks were digitized on 3D virtual representations derived from the scans. Landmark data from the remaining 105 specimens were digitized on the original specimens using a Microscribe 3D device (see again the lists presented in Appendix 1, Appendix 2 and Appendices 3.1-12). In these cases, the cranium and mandible were digitized separately. Subsequently, these two sets of landmarks were positioned to retrieve occlusion by applying rotations to one of two configurations: they were manually aligned together using the points taken at the condyles and on the tooth rows as indicators of occlusion.

In neonate specimens exhibiting patent fontanels, the corresponding landmarks were positioned at the location where growing bones are expected to join. All fossils presented canine alveoli, but some of them had lost the corresponding teeth. The corresponding landmark positions were estimated in the following way: they were digitized at the position of the anteriormost point on the canine alveoli at a height corresponding to that of the average height of the

tooth row. Even if this estimation introduced measurement error, these landmarks were kept since they provide a reliable estimate of the total length of the maxilla, an important piece of information that would otherwise be lost.

Concerning the fossils that were measured using the Microscribe 3D device, when one landmark belonging to a couple of symmetric landmarks was missing, a mirror image of the preserved landmark was produced.

2.2 Procrustes superimposition

The landmark configurations measured for the specimens of a given sample are not directly comparable to one another because the system of coordinates in which the specimens are measured and their orientations are not the same. Moreover, the specimens differ in size. Thus, it is necessary to provide a frame of reference within which spatial relationships between landmark configurations can be quantified. One solution was proposed by Lele and Richstmeier (Lele, 1993; Lele and Richtsmeier, 1991; Richtsmeier and Lele, 1993): Euclidean Distance Matrix Analysis (EDMA). This approach consists of including all possible distances within a set of landmarks into a multivariate analysis. However, the results of EDMA are difficult to visualize because it is not possible to re-express variation in distance matrices as morphological variation in physical space.

The alternative approach used here consists of superimposing the landmark configurations using a Generalized Least Squares (GLS) procedure (Rohlf and Slice, 1990) and establishing a multidimensional shape space within which each specimen is represented as a point (Bookstein, 1991; Dryden and Mardia, 1998). This method involves the following steps:

- Size and shape information are separated. Size is estimated by centroid size (CS) (Bookstein, 1991), which is defined as follows:

$$CS = \sqrt{\sum_{i=1}^{i=Dk}(p_i - c)^2} \quad ; \quad c = \frac{1}{Dk}\sum_{i=1}^{i=Dk} p_i$$

  where c is the center of mass of the landmark configuration, p_i is the i-th landmark, D is the dimensionality (2 or 3) and k is the number of landmarks .
- Each landmark configuration is normalized to CS=1.
- All landmark configurations are superimposed using a GLS criterion to minimize deviations between configurations. This is achieved by translating and rotating the size-normalized specimens until the sum of all interspecimen distances (landmark coordinate by landmark coordinate) is minimized.

A consensus configuration is computed as the mean of all aligned specimens. The deviation of each specimen (landmark coordinate by landmark coordinate) from the consensus configuration defines its shape in linearized Procrustes shape space. These so-called Procrustes residuals

have the same dimensionality as the original landmark configurations (Dk). However, 7 degrees of freedom (DF) are lost during the superimposition process. One DF corresponds to the normalization of the configurations to CS=1. Three DF are lost during translation. Finally, 3 DF are lost during rotation. Accordingly, the linearized Procrustes shape space has Dk-7 independent dimensions.

2.3 Principal Component Analysis (PCA)

PCA (Jolliffe, 1986) is a tool that is used to capture statistically significant patterns of variation in a multivariate sample. PCA produces new sets of variables, the principal components (PCs), which are linear combinations of the original variables. The main feature of PCs is that they are statistically independent of each other and capture the largest, second largest, etc., proportions of the total sample variance. Typically, a significant proportion of the total variance is contained in the first few PCs such that it is possible to express the essential patterns of variability in the sample in a low-dimensional subspace of the original multivariate space.

2.4 Canonical Variate Analysis (CVA) and classification procedures.

CVA is a tool that is used to capture the most statistically significant patterns of variation among groups defined *a priori* in a multivariate sample. In CVA, two variance-covariance matrices are examined (see for instance Zelditch et al., 2004). The within-groups variance-covariance matrix, S_W, represents the deviation of individuals from their respective group means. The between-groups variance covariance matrix, S_B, represents the deviation of the group means from the grand mean. CVA provides axes in shape space (the so-called Canonical Variate axes, or CVs) that maximize the ratio S_B/S_W. Maximization of this ratio is achieved by computing the eigenvalues and corresponding eigenvectors of $S_W^{-1}S_B$ (see Zelditch et al., 2004 for further details).

Computation of the inverse of the within-group variance-covariance requires that this matrix be of full rank. Thus, Procrustes residuals cannot be used to compute this matrix because 7 DF are lost during the superimposition process (see above). Rather, a PCA is first performed on the data in linearized Procrustes shape space. The PC scores of the specimens are then used to compute S_B and S_W.

Scores of the specimens on the canonical axes (canonical scores) are used to classify the specimens. The procedure explained by Zelditch et al. (2004) is employed as follows: for each group, the mean projection in CVA space is computed. Then, the Mahalanobis distance between each specimen and all group means is computed. For a given specimen X and a given group M, this distance is obtained by:

$$D=\sqrt{(X-M)^T S^{-1}(X-M)}$$

where S^{-1} is the inverse of the variance-covariance matrix of the CV scores of the specimens. The specimens used as the CVA input are then reallocated *a posteriori* to the group for which D is minimal. The percentage of correct *a posteriori* reallocations is useful to assess whether distinct shapes are associated with the pre-defined categories. A low percentage of correct reallocations indicates that it is not possible to distinguish the classes by shape. Fossils or specimens for which the classification is uncertain can be projected onto the canonical axes and allocated to a category according to their scores.

2.5 Allometry

2.5.1 Common allometric patterns

Allometry refers to the effects of size upon shape (Gould, 1966). Here, allometric patterns are investigated in data sets that involve multiple primate species and different developmental stages. Ontogenetic allometry stands for a change in shape that occurs during growth, i.e., an increase in size. Intraspecific allometry (also called static allometry) is the effect of size upon shape in a set of adult individuals belonging to the same species. Interspecific allometry (also called evolutionary allometry) is the effect of size upon shape in a set of adult individuals belonging to related species. Ontogenetic and interspecific allometries can be detected by multivariate regressions of shape against size (Klingenberg, 1996). In the case of geometric morphometric studies involving 3D landmarks, a multivariate regression of Procrustes residu-

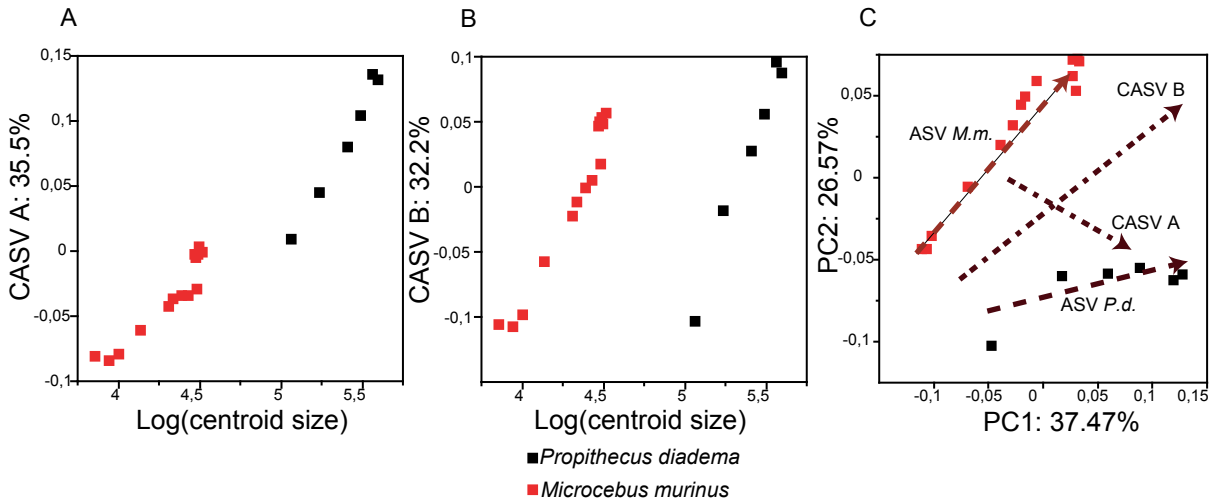

Figure 1.2: Quantification of the common effect of allometry in groups that differ in centroid size. A: Common allometric shape vector (CASV) computed directly on a sample composed of ontogenetic series of specimens belonging to the species *Microcebus murinus* and *Propithecus diadema*. CASV behaves like a discriminant axis, and separates the two species. B: CASV computed as the mean of the allometric shape vectors (ASVs) computed separately for the two species. This CASV better represents the common patterns of allometry shared by the two species. C: PC1-PC2 plot. The projection on PC1-PC2 scatter of the species-specific ASVs are reported, as well as CASV A and CASV B. ASV *M.m.*: ASV computed for *Microcebus murinus*. CASV *P.d.*: ASV computed for *Propithecus diadema*.

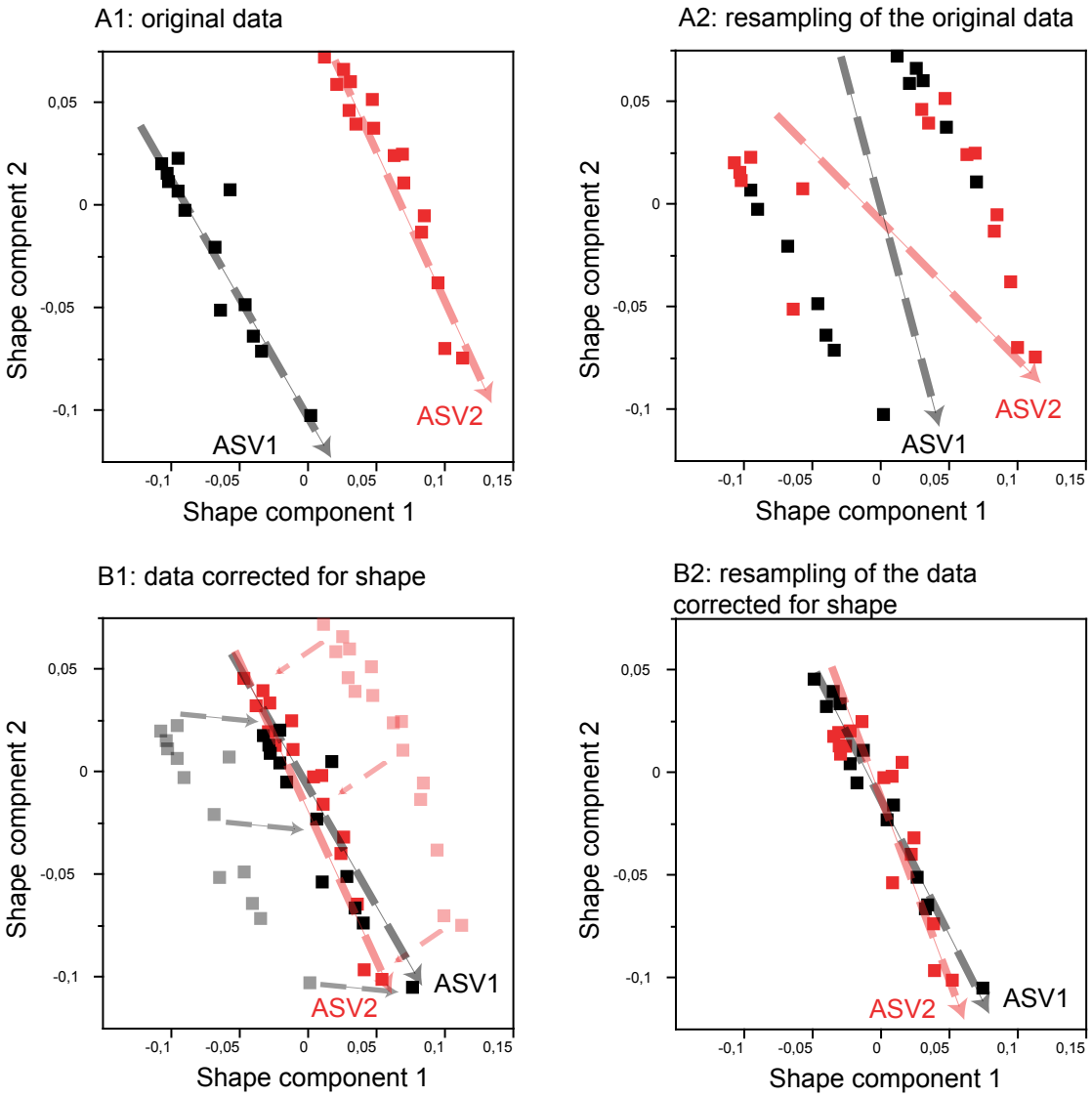

Figure 1.3: Assessment of the statistical significance of the angle of divergence of the allometric vectors in groups that differ in shape. A1: two groups exhibit a significant difference in shape. It is asked whether the angle between ASV1 and ASV2 is significant. A2: individuals are reassigned randomly to one of the two groups. The angle between ASV1 and ASV2 reflects not only divergence in allometric direction, but also difference in shape across the groups. B1: the data are first corrected to achieve a mean shape difference = 0 between the two groups. Here, the angle between ASV1 and ASV2 is the same as in "A1". B2: the same group resampling is applied as in A2, but on data corrected for shape. The angle between ASV1 and ASV2 only reflects divergence in allometric vector direction.

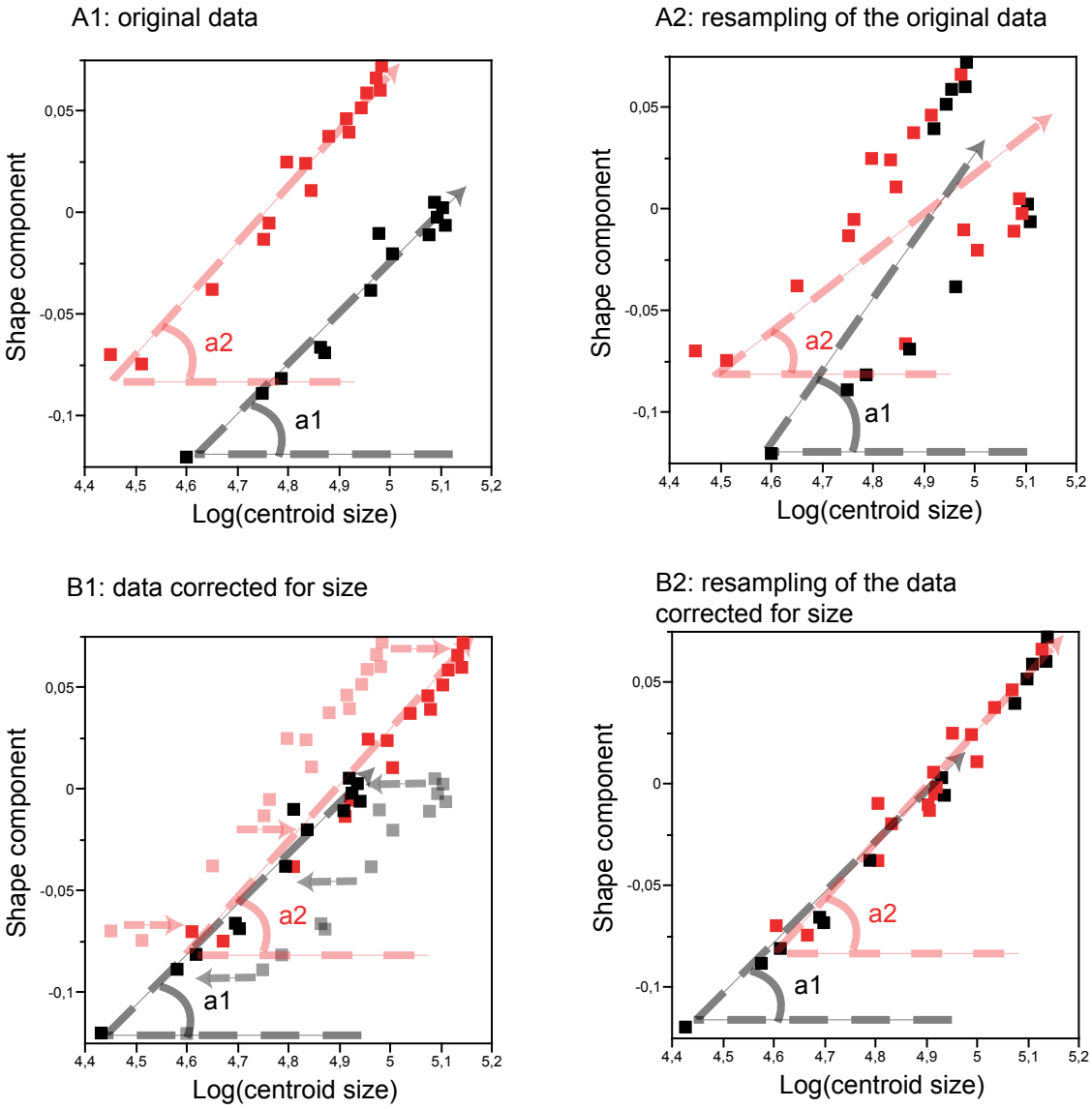

Figure 1.4: Assessment of the statistical significance of the angle of divergence of the allometric vectors in groups that differ in centroid size. A1: two groups exhibit a significant difference in size. It is asked whether their respective allometric shape vectors (ASV1 and ASV2) differ in direction. Each shape component is regressed against the logarithm of centroid size. ASV1 and ASV2 are composed of all regression coefficients (a1 and a2 in this case) of shape coordinates against size. A2: individuals are reassigned randomly to one of the two groups. The regression coefficients a1 and a2 convey a signal that reflects the difference in size across the groups. Therefore, the angle between ASV1 and ASV2 will not reflect divergence in only the allometric direction. B1: the data are corrected to achieve a mean size difference = 0 between the two groups. Here, a1 and a2 are the same as in "A1". B2: the same group resampling is applied as in A2 but on data corrected for size.

als against centroid size or against the logarithm of centroid size may be performed (see for instance Claude et al., 2003; Claude et al., 2004; Ponce de León and Zollikofer, 2006; Zollikofer and Ponce de León, 2004). In practice, choosing centroid size or its logarithm as a proxy for size yields broadly similar results.

Sometimes, samples contain groups that differ widely in size. In such cases, the vector restulting from a direct regression of shape against size often behaves like a discriminant axis; this vector tends to separate groups according to their size. An example is given in Figure 1.2-A: a regression of shape against size is computed in a sample composed of ontogenetic series of specimens belonging to the species *Microcebus murinus*, one of the smallest extant lemurs, and *Propithecus diadema*, one of the largest ones. The resulting common allometric shape vector (CASV) discriminates the two species almost perfectly: *Microcebus murinus* exhibits low scores on the CASV whereas individuals belonging to the species *Propithecus diadema* exhibit high scores (figure 1.2-A).

In order to produce a CASV that does not behave like a discriminant axis, the approach proposed by Ponce de León and Zollikofer (2006) was used. A CASV is computed as the mean of the group-specific allometric shape vectors (ASVs) (see Figure 1.2-B). The resulting axis describes patterns of allometry that are common to the two species.

2.5.2 Divergence in direction between allometric shape vectors

Resampling statistics are used throughout this manuscript to assess inter-group divergence between allometric vectors. When groups differ widely in shape, a considerable heterogeneity in shape is included in each of the resampled groups (see Figure 1.3), resulting in a biased distribution of angles of divergence. Similarly, a considerable heterogeneity in size (Figure 1.4) is introduced in each of the two resampled groups when the groups under study differ significantly in size. In order to avoid these pitfalls, the test sequence proposed by Ponce de León and Zollikofer (2006) was adopted with a slight modification to test for inter-group difference in size.
1) Test for differences between mean group values of shape and size.
2) If differences are significant, correct data to achieve mean shape and size difference = 0 between each group (see Figure 1.3-A2 and Figure 1.4-A2).
3) Test for divergence between group specific allometric vectors (using resampling statistics).

2.6 Visualization of the results.

As mentioned earlier, one important aspect of geometric morphometric methods is that they allow for visualization of the results. It is possible to visualize morphological variations along the axes of PCAs, CVAs and also the vectors resulting from the regressions of shape against scalars. Throughout this manuscript, the visualization methods proposed by Zollikofer and Ponce de León (2002) were used; they help to explore the patterns of shape variability on

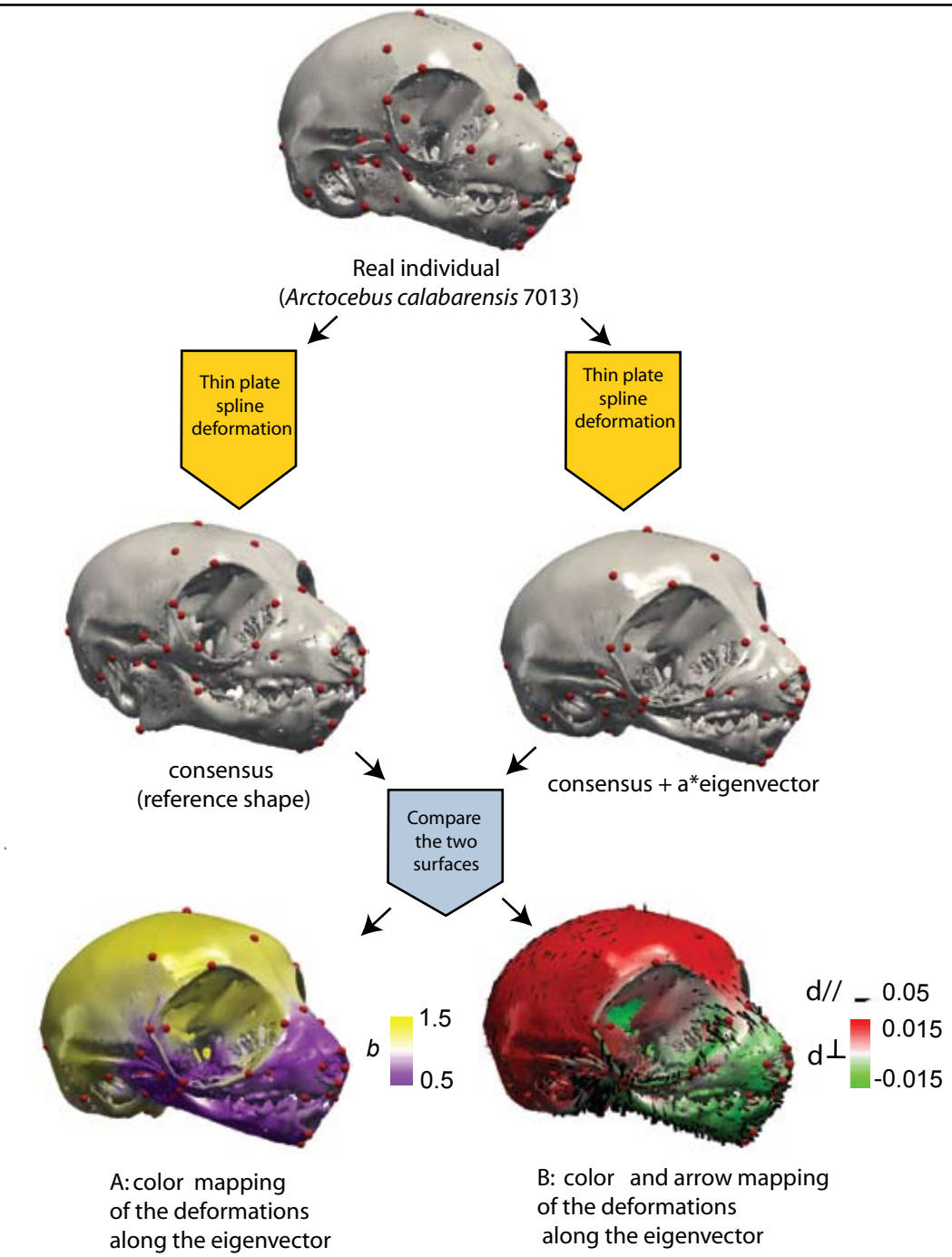

Figure 1.5: Patterns of cranio-mandibular shape transformation along an eigenvector. A: colors indicate the relative amount of change in local area that was necessary to attain that shape, with the reference being in that specific example the consensus shape, e.g., the mean shape of a given sample (yellow and violet code for an increase and decrease in surface area, respectively, and white indicates isometry. Scale unit: local area/ same local area of the reference shape). B: colors and arrows indicate the magnitude and direction of the shape change, with the reference shape being the consensus (d//: shape change parallel to the surface. $d^{\perp}$: shape change perpendicular to the surface. Red and green indicate outward and inward directions, respectively. Scales are in units of centroid size).

3D surfaces (such as virtual reconstructions extracted from CT images).

In all GM analyses presented in this manuscript, changes in shape that occur along vectors of special interest (PCA eigenvectors, CVA canonical vectors or regression vectors) were quantified and mapped onto a given surface using color scales and arrows. In practice, a shape of reference and a shape of interest are needed in order to allow for shape comparison (see Figure 1.5**)**. In all the analyses presented in this thesis, the consensus configuration (e.g., the mean shape of a given sample) was chosen as the reference. In practice, a given individual of the sample is chosen as a template. The corresponding surface is deformed twice using a thin plate spline (TPS) function (Bookstein, 1991) into both the consensus configuration and the configuration of interest (e.g., the corresponding configuration of landmarks along an eigenvector). The different landmark configurations constitute the nodes of the TPS function. Two different ways to quantify differences in shape are used in this manuscript. The first quantifies the relative difference in local surface area (Figure 1.5-A) and is adequate to describe patterns of shape change during ontogeny (see Chapter 5). The other quantifies directional shape change (Figure 1.5-B): shape change parallel to the surface is represented by arrows, and shape change perpendicular to the surface is represented by a color scale.

3. MorphoTools: a geometric morphometric application framework

Typically, a morphometric study aims to measure patterns of morphological variability and test how morphological variability correlates with extrinsic and intrinsic variables. There can be two different kinds of variables: categorical (e.g., a group to which an individual belongs) and continuous (scalars).

The complexity of morphometric analyses increases with the complexity of the sample. What is referred to here under the term “sample complexity” is not sample size but sample structure; when multiple variables are defined, assessing the influence of each individual variable and possible combinations of these variables on morphology is a time-consuming process. Furthermore, the results of the whole analysis also depend on the measurement protocol. It is thus mandatory to test whether the results are robust, i.e., to assess if and how modifications of the measurement protocol influence the results. Another source of potential bias in an analysis is the inclusion of “outliers” (e.g., specimens that deviate considerably from the sample mean). Ordination methods, such as PCA, tend to yield axes that discriminate atypical specimens because they often account for a large part of the total sample variance. Therefore, it is also important to assess how the inclusion of outlier specimens affects the results.

These tests cannot be performed interactively with standard GM software packages. For instance, if one wants to add/remove one specimen or add/remove a landmark, all subsequent steps and associated software manipulations must be redone.

The MorphoTools application framework was specifically designed to address these

issues (Specht, 2007; Specht et al., 2007; Swiss NFS projects N° 205321-102024/1 and 205320-109303/1). MorphoTools facilitates the interactive analysis and visualization of geometric morphometrics datasets. Here, I give a brief overview of the basic architecture of MorphoTools and report on those parts that were implemented within the framework of this thesis.

3.1 General architecture of MorphoTools.

3.1.1 The Visualization Toolkit

The Visualization Toolkit (VTK) (Schroeder et al., 2006) is used at the core of the MorphoTools. VTK is an extensive open source collection of visualization and data processing algorithms, each of which is represented in the form of a *processing object*. A processing object requires an input and returns a specific output (processing objects are also referred to under the term "filter"). Processing objects can be connected to one another to build data processing and visualization *pipelines*. Using pipelines is advantageous for two reasons:

- First, any modification of the input and/or object-specific parameters related to one of the processing objects will have an impact on the objects that depend upon its output, i.e., along the

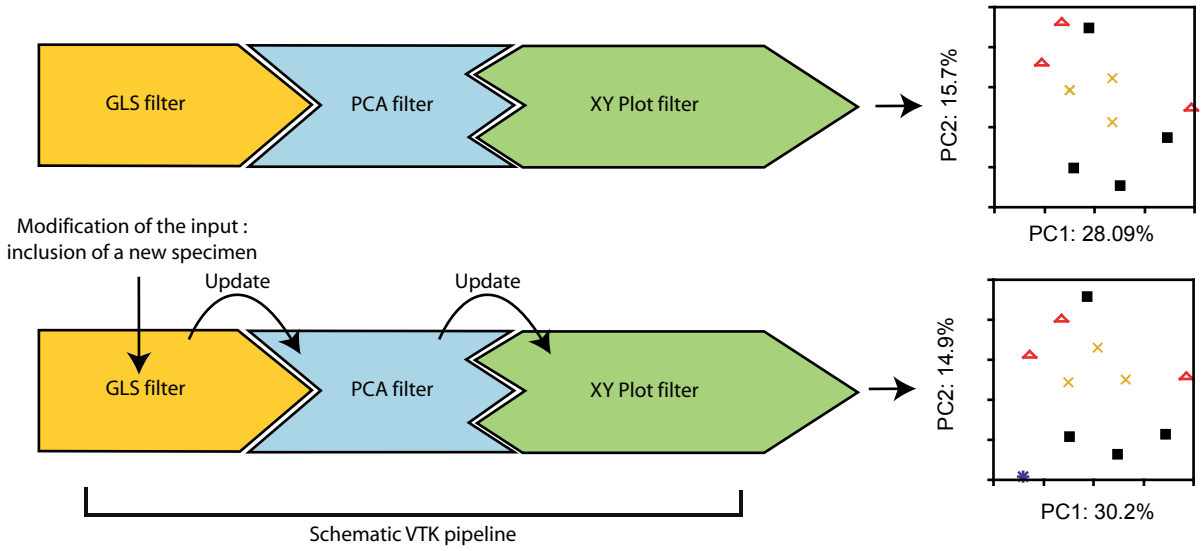

Figure 1.6: Connecting objects into a pipeline. This figure illustrates the fact that the modification of the input of one processing object (or filter) leads to an update of all subsequent pipeline filters. In this specific example, one specimen is included in the sample. The immediate consequence is that all the GM analysis steps are recomputed.

entire pipeline; typically, an "update" procedure is used to account for this change. Step by step calls to "update" procedures will propagate throughout all objects of the pipeline. An example is given in Figure 1.6: the inclusion of an additional specimen in the sample is immediately taken into account and the whole analysis is recomputed, permitting immediate identification of the influence exerted by that specific individual on the results.

- The other major benefit of processing pipelines lies in the evolvability of the application;

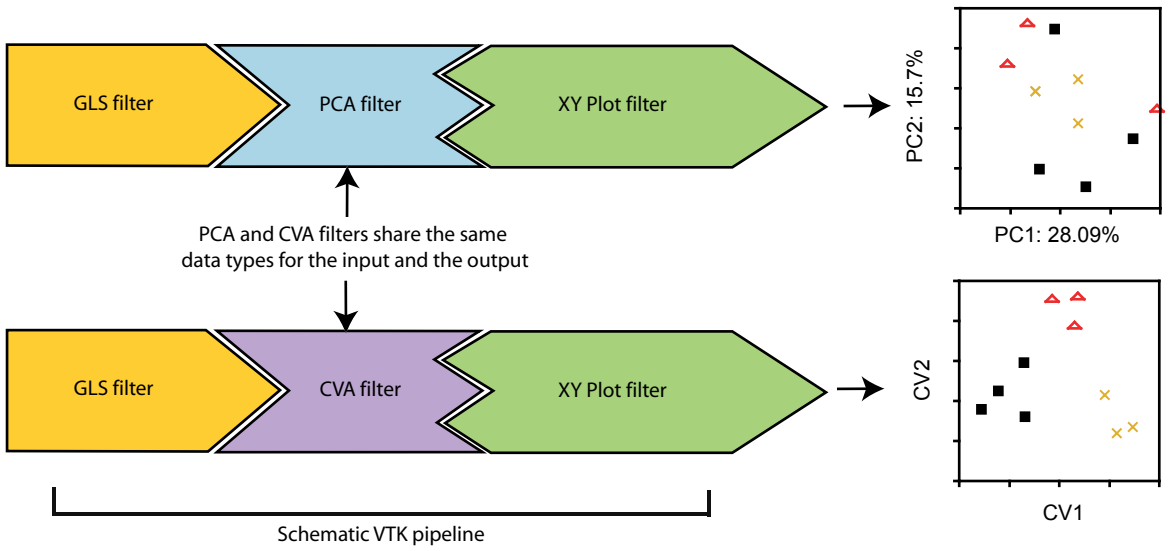

Figure 1.7: Interchangeability of processing objects in a pipeline. Processing objects that share the same data types for the input and output are interchangeable. Here, a Principal Component Analysis (PCA) filter is exchanged with a canonical variate analysis (CVA) Filter. The other elements of the pipeline remain unchanged.

processing objects whose input and output are of the same data type are interchangeable. For instance, in Figure 1.7, a processing object that computes a Principal Component Analysis (PCA) can be easily replaced with a processing object that calculates a Canonical Variate Analysis (CVA). All other objects in the pipeline remain unchanged and can be reused as often as needed. The interchangeability of processing objects is important for the evolvability of the whole application: the process of implementing new functionalities is facilitated.

3.1.2 Interface hierarchy

MorphoTools is mainly written in Java. Java was chosen because it is convenient to design complex user interfaces. As Java is relatively slow for computational purposes, the most cpu-intensive steps are delegated to the VTK classes, which are written in C++. Additional VTK processing objects are created in order to extend the possibilities offered by VTK.

3.2 The sample scheme

3.2.1 Groups and attributes

The information related to each specimen (e.g., age, sex, weight, diet, landmark data…) is specified in a sample file. The format of this file is specific to MorphoTools; an example is presented in Figure 1.8. The sample file begins with a list of *attributes* (continuous variables) and *groups* (categorical variables). This is followed by a list of specimens and their specific groups/attributes. Once groups are defined in the sample file, they cannot be modified in the application. Such groups are referred to as “static groups”. Static groups can be directly used in the analyses, but a buffering system is designed to allow for the creation of dynamic groups

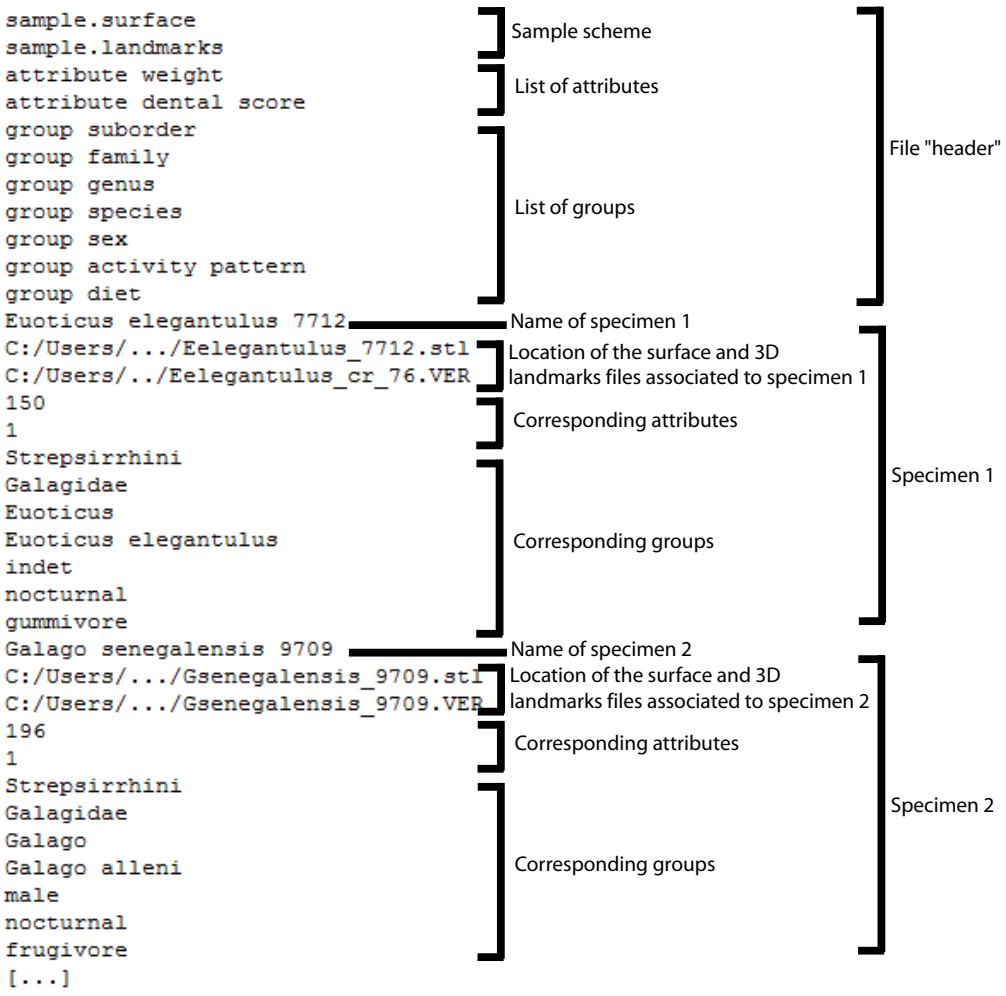

Figure 1.8: Structure of sample files used in MorphoTools.

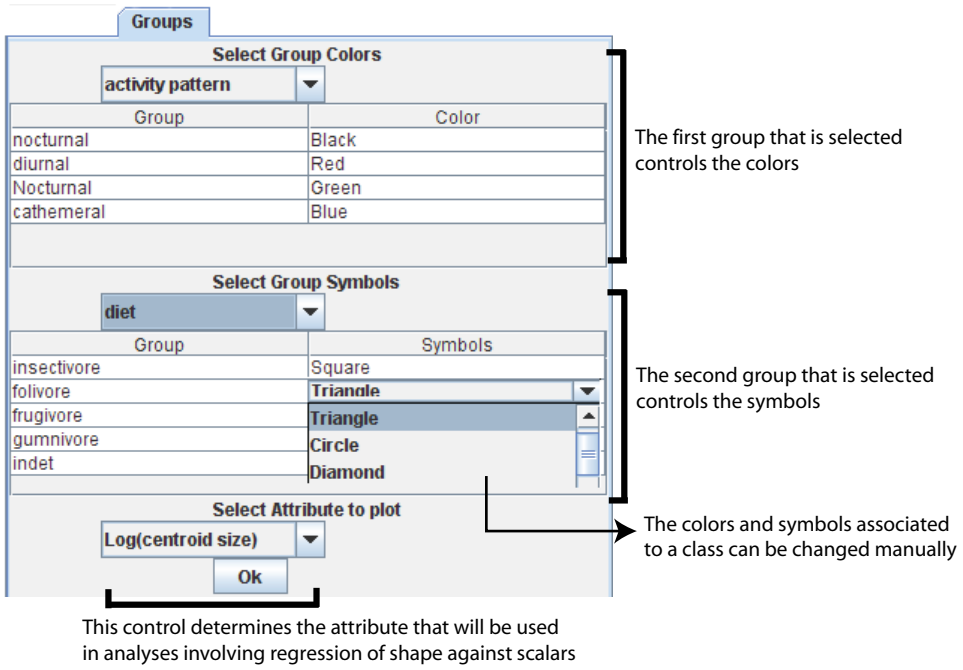

Figure 1.9: Interface dedicated to the definition of the dynamic group and attribute selection.

in order to allow more flexibility. The principle of this buffering system is explained with an example (Figure 1.9). First, two groups must be selected. In the example shown in Figure 1.9, the two selected groups are “diet” and “activity pattern”. Each class of the first group is associated with one color (e.g., all the nocturnal specimens are drawn in black), and the classes of the second group are associated with symbols (e.g., all the insectivores are represented by squares). The association of a color and a symbol defines one dynamic group in the application: groups defined using this association are ultimately used in the analyses requiring group definitions. In the stated example, all nocturnal insectivores will form a group that is represented by black squares. Furthermore, groups can be merged: it is possible to manually change the color or the symbols associated with one class. For instance, it would also be possible to associate the folivore specimens to the color black. In this case, all nocturnal insectivores and nocturnal folivores would be represented by black squares and would form a group (see again Figure 1.9). The names of the individuals also form a static group. Thus, they can be used to define any possible dynamic group, provided that the names defined in the sample file are unique identifiers of the specimens. In the group scheme, there is a close connection between colors, symbols and groups. Dynamic groups form part of the input of all the analysis processing objects that require the definition of groups (e.g., the CVA filter and the filters involving resampling statistics).

Attributes must be chosen from a list (see Figure 1.9). The selected attributes are used in all analyses involving regression of shape against scalars.

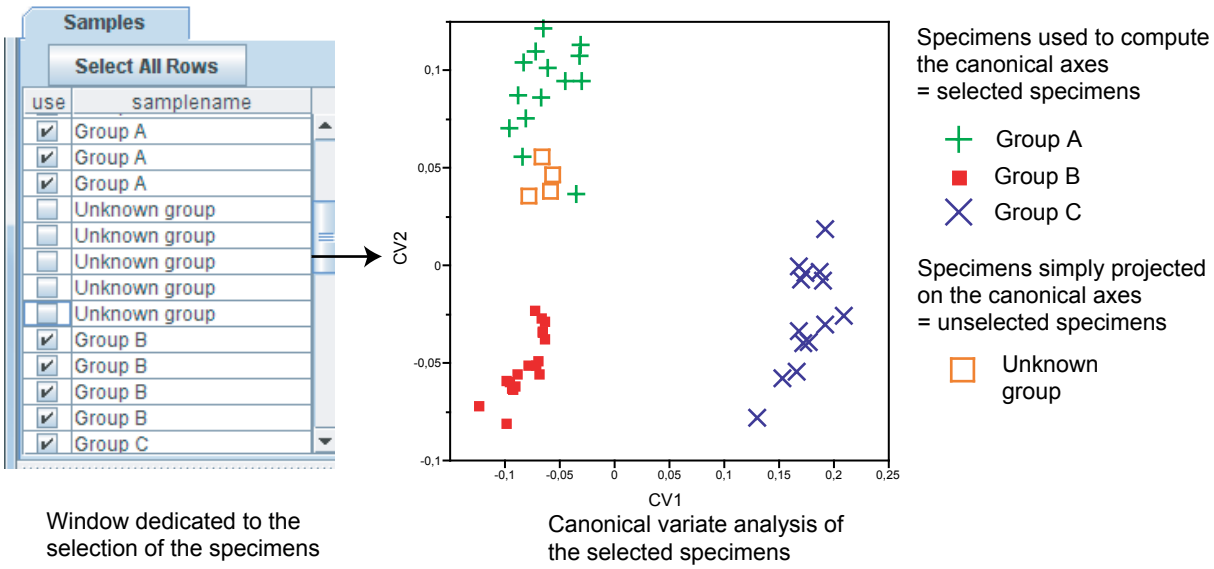

Figure 1.10: Sample structure used in MorphoTools. Selected specimens form the input of the canonical variate analysis, whereas unselected specimens are simply projected on the resulting canonical axes. Their projecting scores on the axes will serve to classify them in either group A, B or C. In this example, the specimens belonging to the “unknown” group are close in shape to the specimens belonging to group A.

3.2.2 Sample structure

In MorphoTools, each sample is divided into three sub-samples: the selected specimens, the unselected specimens and the mean group specimens.

The first sub-sample contains individuals that were selected from the specimen list. They will be used in all analyses (for instance, they can be used to compute the axes of a PCA). This sub-sample is used most of the time.

The second sub-sample contains all specimens that were not selected from the sample list. As stated above, it might be interesting to discard some specimens because they may distort the results of an analysis. However, it may still be interesting to assess where they would be positioned within the scatter data of a given sample. In MorphoTools, non-selected specimens do not play an active part in an analysis: for instance, they are not used during the computation of the axes of a PCA. The important point is that, optionally, they can be projected *a posteriori* on these axes. This option is used in association with classification procedures, which assess the morphological affinities that a specimen of special interest (e.g., a fossil) shares with an *a priori* sample of specimens. The entire procedure works as follows: individuals for which a classification is well-established are first selected as the input of a CVA. The specimens for which the morphological affinities have to be established remain unselected, are projected on the canonical axes (see Figure 1.10) and are classified a posteriori according to their CVA scores

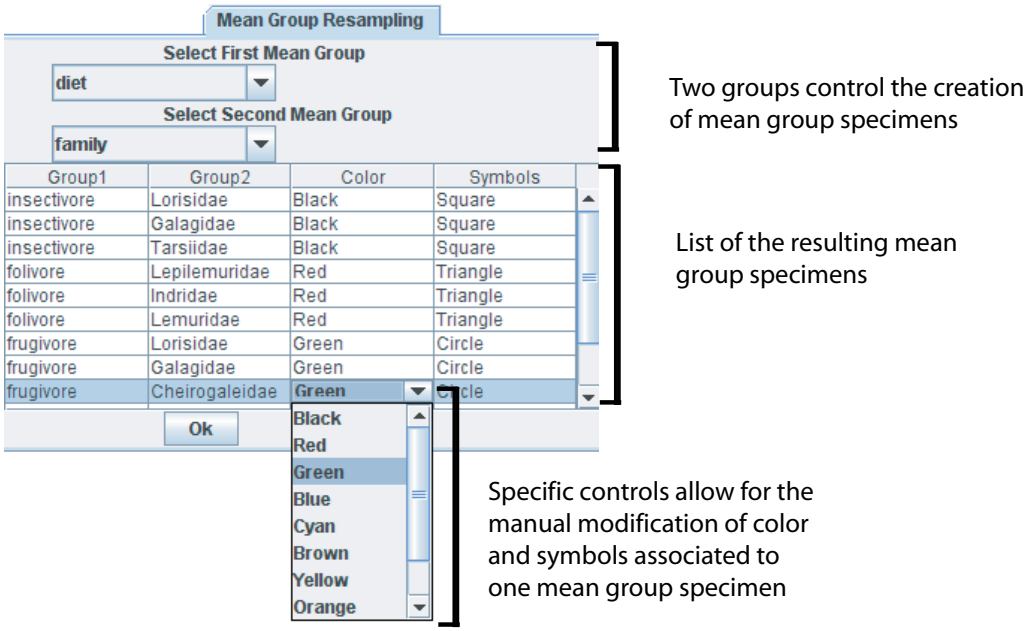

Figure 1.11: Interface dedicated to the creation of the mean group sample. First, two groups are selected in the combo-boxes. The different classes associated with each group are combined to define the mean group specimens. In this example, for instance, one of the mean individuals will be the mean of all insectivore lorisids.

(Zelditch et al., 2004).

In a geometric morphometric analysis, it is often useful to know where the mean of a specific group is situated in shape space. The third sub-sample in MorphoTools contains such group-specific mean specimens. An example is given in Figure 1.11. First, two "groups" are selected (if one wants to work on one static group, the given static group must be selected twice). In this concrete example, the two selected groups are "diet" and "family". The classes associated with each group are then combined to create a list of "mean group" specimens. "Mean group" specimens can then be projected on the axes of an analysis computed using subsample 1 (the original selected specimens). Alternatively, mean specimens can be used as the main input of any further analysis. For instance, it is possible to interactively compute species-specific mean specimens and to use them as the input of a subsequent PCA in an analysis involving a large number of species.

3.3 Visualization and outputs

3.3.1 Surface comparison

VTK processing objects are written in order to allow for interactive visualization of morphological shape change along the axes of PCA and CVA, and to visualize vectors resulting from the regression of shape against attributes. The pattern visualization methods proposed by Zollikofer and Ponce de León (2002) are implemented in MorphoTools. The steps involving the deformation of the surface of reference and its quantification are implemented in VTK processing objects, which are connected together to form a pipeline (see again Figure 1.5**:** the steps "thin plate spline deformation" and "compare the two surfaces" are achieved in MorphoTools using dedicated VTK processing objects). An interface is also provided to visualize the deformations occurring between any two points in shape space. In this case, the shape of reference can be either one of the two endpoints or the mean of these two points.

3.3.2 Outputs

Scores

Routine procedures are defined for each kind of analysis to allow for exportation of the projections scores of the specimens (selected specimens, non-selected specimens and mean group specimens). The eigenvectors, eigenvalues, canonical vectors and regression vectors can also be exported. The file format of the output is ASCII text using the "tab" character as a separator. Thus, the output files can be immediately read in standard applications such as R (Ihaka and Gentelman, 1996), JMP™ or Microsoft Excel™. This allows for further specific statistical treatments that are not part of MorphoTools.

Images

A routine procedure exports image sequences. A starting point and an ending point are cho-

sen in shape space (the complete set of possible shapes). An output image is created for each intermediate step between these two points. These sequence images can be easily transformed into a video file, which can be used for presentation purposes.

In this manuscript, all GM analyses were performed with MorphoTools. Analyses of variance (ANOVAs) and multivariate analyses of variance (MANOVAs) were carried out with "R"2.4 (Ihaka and Gentelman, 1996).

SUMMARY OF CHAPTER 1

The sample consists of 311 individuals, among which 205 were scanned using tomography (N=8), conventional microtomography (N=166), and microtomography using synchrotron light (N=31). One specimen was digitized using a laser scanner. The remaining ones were digitized using a Microscribe 3D device. Several fossils and extant specimens were incomplete, deformed, or presented displaced parts. Theses specimens were reconstructed following the recommendations given by Zollikofer and Ponce de León (Zollikofer and Ponce de León, 2005).

A geometric morphometric (GM) approach is employed throughout this manuscript to analyze the patterns of morphological variability of the strepsirrhine skull. A protocol consisting of 56 cranial and 18 mandibular landmarks was defined. Concerning the specimens for which virtual 3D representations were available, landmarks were directly measured on 3D virtual surfaces. Landmark data from the remaining specimens were digitized using a Microscribe 3D device.

A number of similar methods were employed several times throughout the following chapters of this manuscript in order to analyze different samples. As such, details are given on the following topics:

- Alignment of the specimen through Generalized Procrustes Analysis (GPA).
- Principal Component Analysis (PCA).
- Canonical Variate Analysis (CVA).
- Treatment of allometry.
- Visualization of shape variability patterns.

In order to allow for efficient exploration of GM dataset, the application framework MorphoTools was developed. It consists of an integrated application that is designed to permit interactive analyses. A presentation of the overall architecture of this application is given.

Chapter 2

What determines the morphological variation of the primate skull?

Contents

1. Introduction

In primates, as in other groups, the skull yields information that is widely used for phylogenetic analysis. The morphology of the skull supports the division of primates into two monophyletic suborders, the Strepsirrhini and the Haplorrhini (Fleagle, 1999; Kay et al., 1997; MacPhee and Cartmill, 1986; Shoshani et al., 1996). For instance, the extant representatives of the Haplorrhini suborder, *Tarsius* and the anthropoids, share unique cranial features among primates in the orbital region (Cartmill, 1994; Kay et al., 1997; Le Gros Clark, 1959; see also Figure 2.1); all primates possess a post-orbital bar, but only *Tarsius* and the anthropoids have evolved a postorbital septum. Also, the internal carotid artery is situated within a septum that separates the tympanic cavity from the anterior accessory chamber in all extant haplorrhines (Kay et al., 1997), whereas this is never the case in strepsirrhines. Because only a few dental synapomorphies link the tarsiers and the anthropoids (Kay and Williams, 1994,), skull morphology is important for assessing phylogenetic relationships at the subordinal level in primates. Figure 2.1 presents several cranial traits that are used to identify the different primate groups. These characters are frequently used in phylogenetic analyses.

However, morphology does not only convey phylogenetic information. Morphology responds to natural selection. In particular, the skull houses the masticatory apparatus, the brain and the sense organs of sight, smell and hearing. Hence, the morphology of the skull should reflect functional adaptations (Fleagle, 1999).

- The relationship between orbital size and activity patterns represents a well-studied association between morphological change and functionality**.** Nocturnal species tend to have larger eyes, yielding relatively larger eye sockets. This issue has received much recent attention (e.g., see Heesy and Ross, 2001; Kay and Kirk, 2000; Kirk, 2006; Ross, 1995). Nocturnal and diurnal forms exist in Haplorrhini and Strepsirrhini.
- Diet is another source of adaptive morphological variation. Numerous experimental studies have been conducted to understand the morphology of the cranium and the mandible in terms of adaptation to specific diet types (e.g., see Hylander, 1979; Hylander and Johnson, 1994). Specialization to a specific diet is expected to yield similar morphological patterns in each primate suborder.

Similar adaptations may bring forth similar morphological responses in distantly related taxa. In other terms, adaptation is a source of homoplasy and is expected to disturb the phyletic signal contained in the morphological data.

Allometry is another source of homoplasy. In its broadest sense, allometry refers to the effects of size upon shape (Gould, 1966). When a sample is composed of specimens that encompass a wide range of sizes, a strong allometric signal can be expected. In primates, as in other mammals, there is a general trend toward a relative reduction of the braincase compared

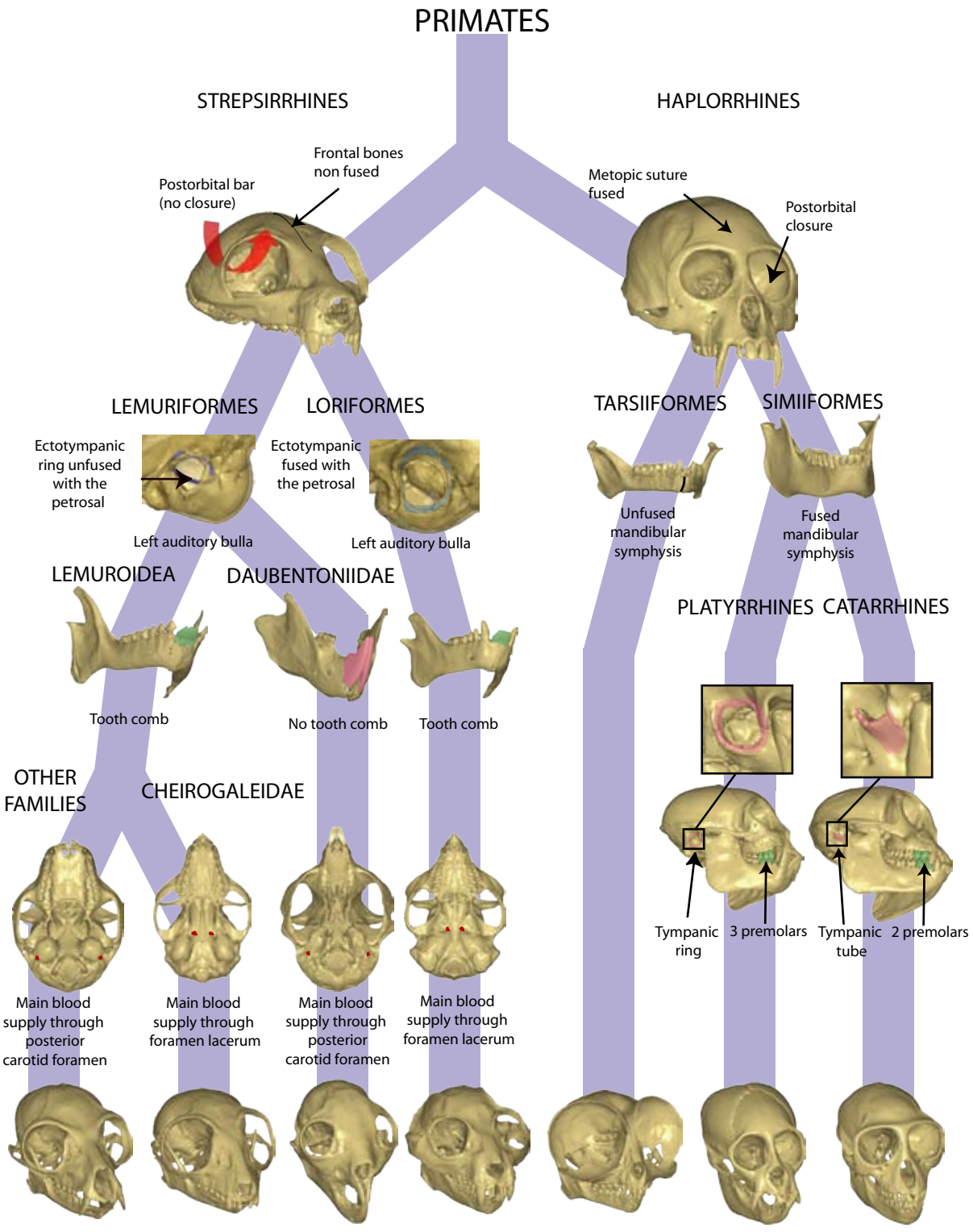

Figure 2.1: Important cranio-mandibular characters used to distinguish the major primate groups.

to the face when size increases (Martin, 1990; Ravosa et al., 2000). In adult primates, allometry is an important source of morphological variation of the skull (e.g see Gould, 1975; Shea, 1983a, 1983b, 1985). Allometry exists at the level of the individual (ontogenetic allometry), of the species (intraspecific or static allometry) and between species (interspecific or evolutionary allometry).

- There is a tight connection between developmental processes and allometry. Shea (1983b; 1985) observed that most of the cranial dimensions of gorillas could be predicted by simple extension of the ontogenetic allometric trajectory of the chimpanzees. This phenomenon is referred to as "ontogenetic scaling". The results of Shea (1983b; 1985) indicate that *Pan* and *Gorilla* share common developmental pathways that they inherited from their common ancestor.
- When examined at a high taxonomic level, allometry can be expected to reflect adaptation. For instance, one can expect that, in a sample of primates encompassing a wide range of body sizes, interspecific allometric patterns reflect adaptation to diet: size distribution among primates is significantly related to diet (Kay, 1984). Thus, there may be nested effects between adaptation and allometry.

In summary, allometry is a complex component of skull morphology, and its quantification and characterization are important for understanding skull morphology from an evolutionary perspective.

The main question asked in this chapter is as follows: what determines the morphology of the skull in haplorrhines and strepsirrhines: phylogenetic or adaptive constraints? The following hypotheses are investigated.

H0: The morphology of the skull mainly reflects adaptive constraints.

H1: The morphology of the skull mainly reflects phylogenetic constraints: the constraints that have previously evolved and now characterize a lineage, and result in biases and limitations the production of phenotypic variability (e.g., Gould and Lewontin, 1979).

The study of adaptation is approached by analyzing the effects of dietary specialization and activity patterns on skull morphology.

- Under H0, we expect that similar dietary specialization and activity patterns yield similar effects on morphology in both primate suborders. In primates, body size distribution is structured by diet and activity patterns (e.g., see Kay, 1984), which neatly supports H0. However, does H0 also stand for shape, the other component of morphology? Here, the shape variability of the skull is analyzed in order to determine whether further support can be given to H0. The investigation of shape using a GM approach is very convenient because morphology is reduced to its size and shape components. However, shape data are expected to convey a strong allometric signal that potentially reflects adaptation (see above). As such, a sub-hypothesis is formulated and tested:

H00: Allometry in primates reflects adaptation to diet and activity patterns

The alternative hypothesis concerning allometric patterns is the following one:

H01: allometric patterns reflect the effect of compensatory mechanisms, the role of which is to maintain functionality when size changes (Emerson and Bramble, 1993).

- H1, the alternative hypothesis, is also investigated. The focus is put on the differences in morphology between Strepsirrhini and Haplorrhini. Under H1, we expect that comparable adaptations would not necessarily result in similar morphologies in the primate skull. Moreover, if phylogenetic constraints determine most of the differences in morphology between haplorrhines and strepsirrhines, we expect that allometry differs in the two suborders. Finally, under H1, it may be expected that the morphospace (e.g., the complete set of possible morphologies) is only sparsely populated and presents no overlap between haplorrhines and strepsirrhines.

2. Materials and methods

2.1 Sample composition

The sample consists of 202 extant primate skulls. 112 extant strepsirrhines and 90 extant haplorrhines were included. The complete list of specimens is presented in Appendix 1.

Additionally, 4 crania and 3 mandibles belonging to 7 distinct individuals of the genus *Archaeolemur* were incorporated into the sample; this sub-fossil strepsirrhine genus shows a skull morphology that is convergent with that of anthropoids, and archaeolemurs were first thought to be extinct anthropoid primates (Major and Forsyth, 1896). However, Lorenz von Liburnau (1902) posited a phylogenetic relationship with extant indriids, a view which has been defended by Grandidier (1905) and the vast majority of morphological studies conducted since then (e.g., see Godfrey et al., 2002; Lamberton, 1939; Schwartz and Tattersall, 1974). Archaeolemurs were incorporated into the sample in order to assess the maximum degree of morphological convergence that occurred between the two primate suborders.

2.2 Dietary and activity patterns categories used for the study of adaptation

2.2.1 Activity patterns

Each species was assigned to an activity pattern category following Heesy and Ross (2001), Kay and Kirk (2000) and Kirk (2006). Three categories were used: nocturnal, diurnal or cathemeral. Cathemeral species have sporadic and random intervals of activity during the day or night (Tattersall, 1987). The assignment of each species to an activity pattern category is presented in Appendix 1.

2.2.2 Diet

The vast majority of primates rely on more than one feeding source. For instance, while some species are strictly insectivores, most of the frugivore species supplement their diets with insects or leaves (Kay, 1984). Nevertheless, each species can be associated with one major dietary source. This study uses four major dietary categories: frugivory, folivory, insectivory and gummivory (exudate feeding). Each species was assigned to one of these groups, illustrating the predominant component of their diet, which is expected to have the most significant impact on skull morphology. The category "gummivore" contains specialized exudate feeders that stimulate the exudate flow by injuring the tree bark with their anterior teeth. The assignment of each species to a diet category was achieved following different sources from the literature (Mittermeier et al., 1994; Nowak, 1999; Rowe, 1996; Vinyard and Hanna, 2005, and references therein). The assignment of each species to a diet category is presented in Appendix 1.

2.3 Methods

The landmark protocols used in this chapter are presented in Chapter 1, section 2.1.

2.3.1 Adaptive constraints and the morphology of the primate skull (H0)

The degree to which diet and activity patterns impinge on the morphology of the skull, cranium and mandible was assessed. To achieve this, we investigated whether shapes can be discriminated according to activity patterns or diet in a particular morphological subspace using Canonical Variate Analyses (CVAs) and classification procedures (see Chapter 1, section 2.4). Samples consisting of mean species configurations were used in these analyses.

Production of shape data corrected for phylogenetic constraints

As a general rule, the more closely related species are phylogenetically, the more they resemble one another morphologically. Correlations in morphology between phylogenetically closely related species result from phylogenetic constraints, and may mask adaptive signals.

As such, it is worth analyzing whether the shape of the skull, cranium or mandible can be better discriminated using raw shape data or shape data "corrected for phylogeny". In this chapter, "correction for phylogeny" means that the effect of phylogenetic constraints (also referred to as the phylogenetic burden) is taken into account. To produce shape data "corrected for phylogeny", we applied the auto-correlation method proposed by Cheverud and Dow (1985) and Cheverud et al. (1985). This technique takes into account the correlation of characters among species due to their shared evolutionary history. The model used is:

$$y = \rho W y + \varepsilon$$

In this model, "y" is an observed data vector, "W" is a matrix representing the phylogenetic distance between taxa, and "ρ" is the auto-regressive coefficient. The term "ε" is the error, which represents the component of the original data that is independent of phylogeny. In

concrete terms, "ε" represents the part of morphology that conveys the adaptive signal in this model.

"W" is constructed the following way:

1) for a given row and column, the value of the matrix corresponds to the inverse of the phylogenetic distance between the two corresponding species; diagonal elements are assigned a value of zero;
2) the matrix is then scaled so each row will sum to one.

Allometry and adaptation

The hypothesis that allometry reflects adaptation to diet or activity patterns (H00) was tested the following way: shape data corrected for both "phylogeny" and allometry were produced and analyzed using the same protocol as described above for raw shape data and shape data corrected for size. Data corrected for size are produced in the following way: an allometric vector is computed for the sample consisting of species-specific shape data "corrected for phylogeny" (e.g., taking into account phylogenetic constraints). This vector is obtained by performing a regression of the shape data corrected for phylogeny against the logarithm of centroid size. All species-specific configurations are projected on this vector. Residuals consist of shape data for which the effect of size has been corrected.

A better discrimination of raw shape data according to diet and activity patterns would lend strong support to H00. Conversely, a better discrimination of the shape data "corrected for size" according to diet and activity pattern categories would lend support to H01. However, this would not mean that allometric patterns do not reflect adaptation *at all*. Therefore, the allometric patterns of the strepsirrhine skull are described and confronted with expectations (that are formulated below) of the effects of diet and activity patterns on the morphology of the skull. In order to quantify the effect of size upon shape that is common to the two suborders, a common allometric shape vector (CASV) was computed as the mean of the two subordinal-specific allometric shape vectors (ASVs). See Chapter 1, section 2.5 for more information on the quantification of allometry.

Expected effects of activity patterns and diet on the skull morphology

With regard to diet and activity patterns, several expectations can be made concerning morphological trends associated with the different categories. The focus is placed on a set of basic cranio-mandibular traits that have been intensively examined in numerous studies, and for which a consensus has been reached regarding adaptive significance. The goal here is not to provide a new assessment of the effects of diet and activity patterns on morphology. Rather, we want to see if cranio-mandibular allometric patterns match these expectations and if CVAs discriminate dietary groups and nocturnal/diurnal species according to these traits.

Expectation 1: Nocturnal species present relatively larger eye sockets than diurnal ones.

Nocturnal species exhibit relatively larger eyes, resulting in relatively larger eye sockets (e.g., see Heesy and Ross, 2001; Kay and Kirk, 2000; Kirk, 2006; Ross, 1995).

Expectation 2: Nocturnal species present a relatively more developed nasal region than diurnal species.

Low light levels require an increased reliance on olfactory means to communicate or locate food (Charles-Dominique, 1977). Although most primates use vision to locate food (e.g., see Dominy et al., 2001), several nocturnal primate species rely heavily on olfaction for foraging (e.g. see, Wright, 1989 concerning owl monkeys, and Hladik, 1979 concerning lorisids). Nocturnal species are thus expected to exhibit relatively more developed nasal regions.

Expectation 3: Folivore species exhibit relatively vertically deeper mandibular corpora than frugivore and insectivore species.

Comparative analyses among anthropoids (e.g., see Bouvier, 1986a, 1986b; Hylander, 1979) and strepsirrhines (Ravosa, 1991) suggest that diet influences the proportion of the mandibular corpus. In primates, folivory affects the robusticity of the corpus. The relative corpus height tends to increase in folivore species.

Expectation 4: Folivore species exhibit relatively larger mandibular symphyses than frugivore and insectivore species.

Folivory affects the robusticity of the mandibular symphysis in strepsirrhines and in anthropoids (e.g., see Hylander, 1979; Ravosa, 1991). The increase in muscle force in folivore or hard-object feeding species causes increased shear stress along the symphysis. Symphyseal fusion or an increase in symphyseal height and length is a response to that stress.

Expectation 5: Folivore species tend to exhibit expanded gonial regions and high condyles

The mandibles of folivorous primates, especially those of folivorous and hard-object feeders (e.g., see Anapol and Lee, 1994; Viguier and Tort, 2000), tend to exhibit expanded gonial regions where the masseter muscles insert. Also, folivore species tend to exhibit relatively high condyles above the occlusal plane (Vinyard et al., 2003). In mammals, high condyles are advantageous during mastication because they increase the moment arms for the masseter and medial pterygoids (e.g., see Greaves, 1974).

Gummivory and the morphological response associated with this specialization recently received much attention (e.g., see Burrows and Smith, 2005; Dumont, 1997; Viguier, 2004; Vinyard et al., 2003). Most authors agree that specialization to gummivory is reflected in the shape of the skull but disagree when describing the associated morphological adaptations. So

far, two major ideas have been proposed to explain how the mandible is adapted to exudate feeding (Burrows and Smith, 2005). Dumont (1997) supposed that the mandible is adapted to exercise greater bite force during the process of opening a wound in the bark (i.e., gouging). According to this hypothesis, short mandibles with a high condyle above the alveolar plane would increase the efficiency of the jaw abductors by moving the lower incisor closer to the temporomandibular joint, thus increasing the efficiency of the muscle force transferred to the biting point. Cartmill (1977) also noted that an increase in the degree of klinorynchy is characteristic of primates and marsupials that use their anterior teeth for gouging. Furthermore, Dumont (1997) showed that the skulls of exudate feeders are wider in the region of the attachment of the nuchal musculature.

Other authors (Vinyard et al., 2003; Williams et al., 2002) suggest that exudate feeders need a large gape; the motion of the incisors is more vertical during the process of scraping the bark. Lower condyles relative to the occlusal plane and longer mandibles would thus be favored according to this scheme.

Since no consensus exists to date concerning the effects of gummivory on the morphology of the skull, no clear expectation is formulated. Rather, potential cranio-mandibular morphological patterns that permit to characterize gummivore species are compared with the competing hypotheses mentioned above.

Outline of the analysis of the effects of adaptation on Morphology

For each species, species-specific mean shape configurations were produced. For the analysis of the effects of diet on skull morphology, 55 species were used. Concerning activity patterns, though occasional cathemeral behavior has been reported in *Alouatta palliata* (Dahl and Hemingway, 1988) and *Aotus trivirgatus* (Wright, 1989), no anthropoid is considered as cathemeral *stricto sensu*. Therefore, cathemerality is only encountered in the Lemuridae family. As such, lemurid cathemeral species were not included in this analysis: the quantification of the s on morphology is difficult when adaptation occurs in a single group. In such a case, it is virtually impossible to distinguish the effects of adaptation and phylogeny on morphology. Thus, only morphological differences between nocturnal and diurnal species were investigated. The analysis of the effects of activity patterns on morphology was thus conducted on 53 species. The primate phylogeny compiled by Spoor et al. (2007) was used to produce the phylogenetic distance matrix “W” defined above. When analyzing the effects of diet on morphology, this phylogeny was simplified to the 55 corresponding species. When analyzing the effects of activity patterns on morphology, the phylogeny was simplified to the 53 corresponding species.

To summarize, analyses were conducted on three kinds of data to assess the effect of adaptation on skull morphology:

- raw shape data,
- shape data corrected for phylogeny and
- shape data corrected for both phylogeny and size.

Two sets of CVA were performed (on raw shape data, shape data corrected for phylogeny, and finally shape data corrected for both phylogeny and size):

- in the first set, diet was employed as the categorical variable and
- in the second set , activity patterns were used as the categorical variable.

A posteriori classification procedures were subsequently set up to reallocate each specimen to the category to which its morphology was closest (see Chapter 1, section 2.4).

2.3.2 Investigation of the alternative hypothesis: the morphology of the primate is determined by structural constraints (H1).

As emphasized by Gould and Lewontin (1979), the attributes of species (including morphology) shall not be interpreted solely from the adaptive perspective: trait expression is also constrained by historical factors, i.e., phylogenetic constraints that prevent the evolution of every possible morphology. The differences in morphology between the skull of strepsirrhines and haplorrhines may be the result of phylogenetic constraints, and this issue is investigated here.

Patterns of shape variability

As the skulls of Haplorrhini and Strepsirrhini differ by an array of discrete anatomical features, the shapes of their skulls are also expected to be distinguishable (see Figure 2.1). A Principal Component Analysis (PCA) of the data in linearized Procrustes shape space was conducted in order to assess the patterns of shape variation within the sample (see Chapter 1, sections 2.2 and 2.3).

Convergence of Archaeolemur with anthropoids

The degree of convergence of *Archaeolemur* with the anthropoids was assessed in the following way. CVA was performed to find the best axis of discrimination between anthropoids and strepsirrhines in linearized Procrustes shape space. *Archaeolemur* specimens were simply projected on this discriminant axis and classified according to their score (see Chapter 1, section 2.4). According to H1, it is expected that the morphology of *Archaeolemur* is still closer to that of other strepsirrhine species than to that of anthropoids.

Allometry and phylogenetic constraints

According to Gould and Lewontin (1979), developmental constraints is probably the most important sub-category of phylogenetic constraints. Developmental constraints are defined by Maynard Smith et al. (1985) as the “biases on the production of variant phenotypes or limitations on phenotypic variability caused by the structure, character, composition, or dynamics of the developmental system”. Differences in developmental pathways may account for the difference in shape between the skulls of haplorrhines and strepsirrhines. Differences in developmental pathways would be expected to result in differences in the evolutionary allometric patterns specific to each suborder. Thus, a comparative study of allometric patterns in haplorrhines and strepsirrhines may provide evidence to support the hypothesis that phylogenetic constraints between the two primate suborders are responsible for their differences in morphology, and that

these phylogenetic constraints are of developmental origin.

Thus, tests were performed to assess interspecific allometric vector divergence between the two primate suborders. Resampling statistics were used to assess the statistical significance of the angle of divergence between the ASVs computed for Haplorrhini and Strepsirrhini. A prerequisite of the assessment of allometric vector divergence is to test for differences in size and shape between the two samples under investigation (see Ponce de León and Zollikofer, 2006, and Chapter 1, section 2.5). Thus, we first tested the difference in centroid size and shape between haplorrhines and strepsirrhines. Subsequently, the statistical significance of the angle of divergence between the two subordinal-specific allometric vectors was assessed (see Chapter 1, section 2.5).

3. Results

3.1 Patterns of shape variability

The results of the PCA of shape are presented in Figures 2.2-2.4.

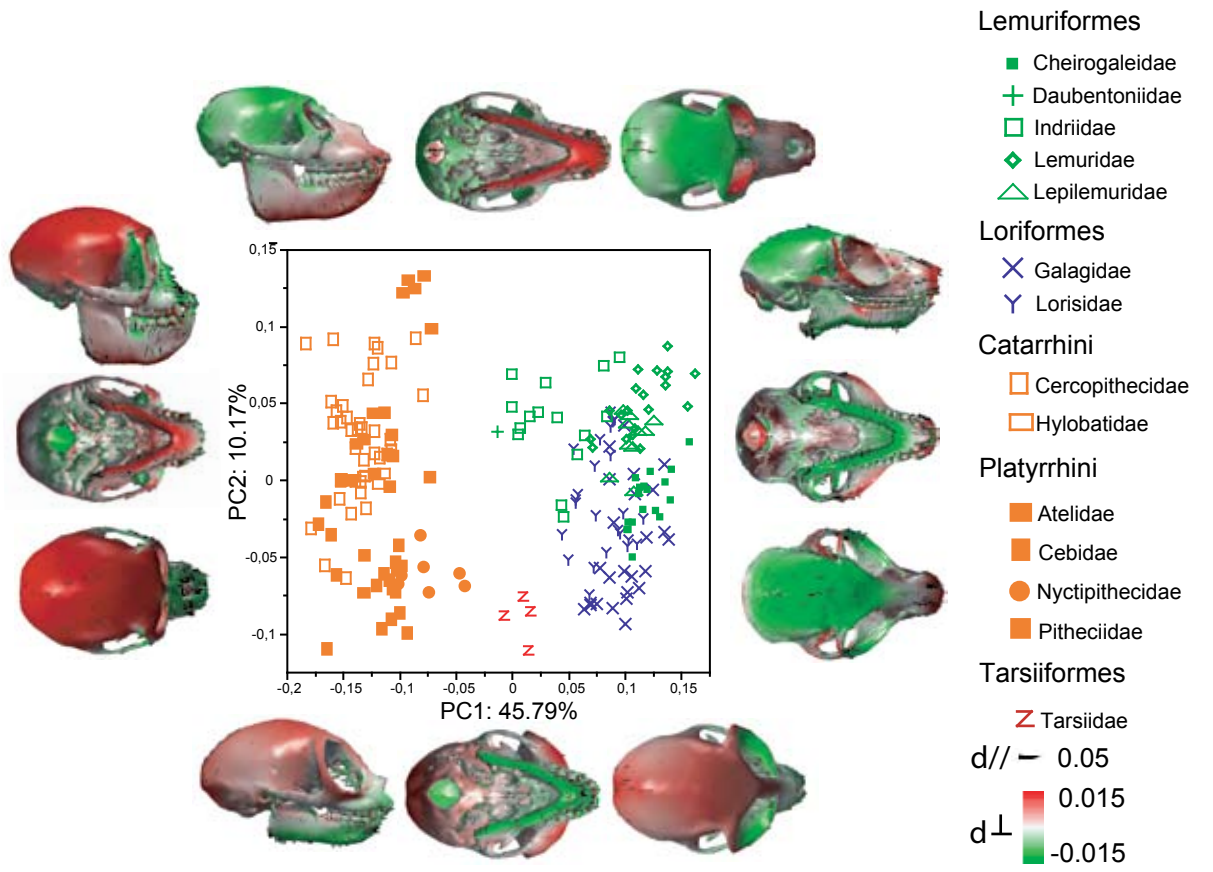

Figure 2.2: PCA of cranio-mandibular shape in primates, and associated patterns of shape variation. The skull of *Cercocebus torquatus* is used to represent the deformations along the two first PC axes with the following exception: concerning PC1, *Lepilemur ruficaudatus* is used for high projection values. d//: displacement parallel to the surface. d⊥: displacement perpendicular to the surface. Scales are in centroid size units.

3.1.1 Skull

The first and second principal components (PC1 and PC2) account respectively for 45.79% and 10.17% of the sample shape variance and summarize many of the shape differences between haplorrhines and strepsirrhines (Figure 2.2). PC1 separates crania having a large braincase, a short face, an anteriorly placed foramen magnum and convergent orbits from crania having a relatively longer snout, comparatively larger and less convergent orbits, a smaller braincase and a posteriorly placed foramen magnum. PC1 separates short mandibles that have short coronoid processes, higher condyles relative to the alveolar plane, vertically deeper corpora and higher and longer mandibular symphyses from narrow and long mandibles that have high coronoid processes pointing backward and mesially, low condyles, low corpora and short mandibular symphyses. The second principal component (PC2) concentrates patterns of shape variation correlated with size. PC2 is significantly correlated with the logarithm of centroid size (r^2=0.46, p<0.0001). In terms of variation in shape, PC2 separates crania with relatively larger orbits, larger braincases and short maxillae from crania having smaller orbits, smaller braincases, and forward projecting maxillae. The mandibles associated with small crania have low and gracile

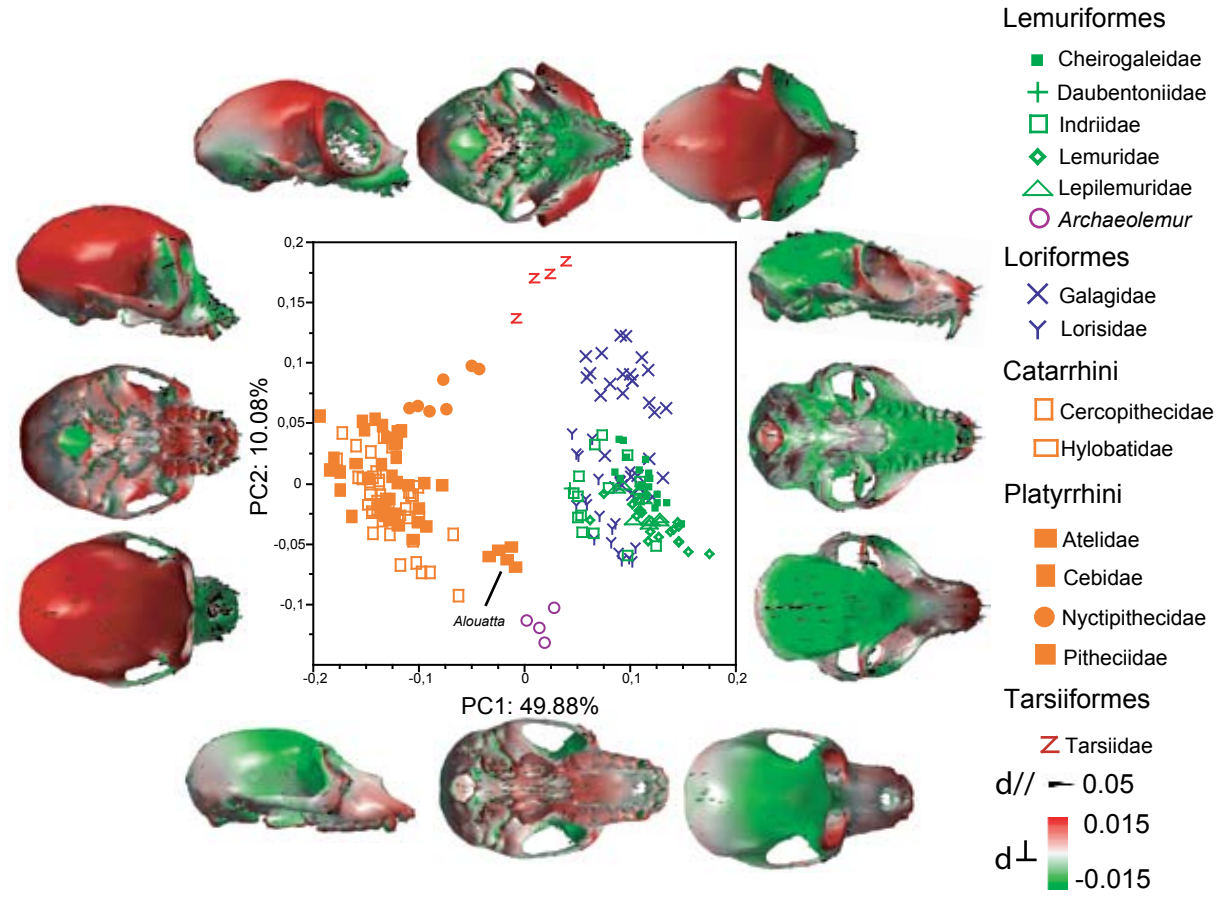

Figure 2.3: PCA of cranial shape in primates and associated patterns of shape variation. The cranium of *Cercocebus torquatus* is used to represent low projection values on PC1 and high projection values on PC2. *Euoticus elegantulus* is used for high projection values on PC1. *Tarsius sirichta* is used for low projection values on PC2. d//: displacement parallel to the surface. d⊥: displacement perpendicular to the surface. Scales are in centroid size units.

corpora and lower condyles relative to the occlusal plane, whereas large crania are associated with mandibles with a large corpus and high condyles. The third PC accounts for 5.39% of the sample shape variance and separates *Tarsius* from the other primates; the tarsiers exhibit relatively larger orbits than any other primate species.

3.1.2 Cranium

The first two PCs, which account respectively for 49.88% and 10.08% of the total shape variance, describe shape variation patterns that are essentially similar to those associated with the first two PCs of the PCA performed on the skull configuration: again, the haplorrhines are clearly separated from the strepsirrhines on the first tow axes. The crania of the genus *Archaeolemur* project in a central position on the first axis. Among haplorrhines, *Alouatta* displays a derived cranial shape for anthropoids and projects closest to the strepsirrhines, near *Archaeolemur* (see Figure 2.3). PC2 scores are significantly correlated with the logarithm of centroid size (r^2=0.4, $p<0.0001$). The tarsier*s* are well discriminated from other primates on this axis. All nocturnal haplorrhines (*Aotus* and *Tarsius*) have high PC2 scores, whereas diurnal haplorrhines exhibit low scores on PC2. The third PC accounts for 6.11% of the sample shape variance and separates shapes with large orbits and long maxillae from crania having small orbits and narrow, short maxillae.

3.1.3 Mandible

PC1 accounts for 42.64% of the total sample shape variance and concentrates most of the mandibular shape differences between strepsirrhines and haplorrhines (Figure 2.4). However, indriids project among the haplorrhines on PC1: indriids display mandibles with a strongly developed angular process and a long mandibular symphysis in the antero-posterior plane.

The second axis accounts for 12.29% of the shape variance and describes variation in the angle formed by the two horizontal branches of the mandibles. PC2 scores are significantly correlated with the logarithm of centroid size (r^2=0.28, $p<0.0001$). Smaller mandibles tend to exhibit a large angle between the two horizontal branches, whereas the separation between the two branches is narrower in large ones. PC3 accounts for 10.8% of the total sample shape variance. For the negative extreme of PC3, the mandibles are gracile and exhibit low condyles relative to the alveolar plane as well as reduced coronoid processes. For positive PC3 scores, the mandibles are more robust and exhibit high condyles and well-developed coronoid processes.

3.2 The effects of adaptation on the skull morphology

3.2.1 Adaptation and size

Common trends are observed in haplorrhines and strepsirrhines for the influence of diet and activity patterns on size (see Table 2.1 and Table 2.2): smaller crania and mandibles are often

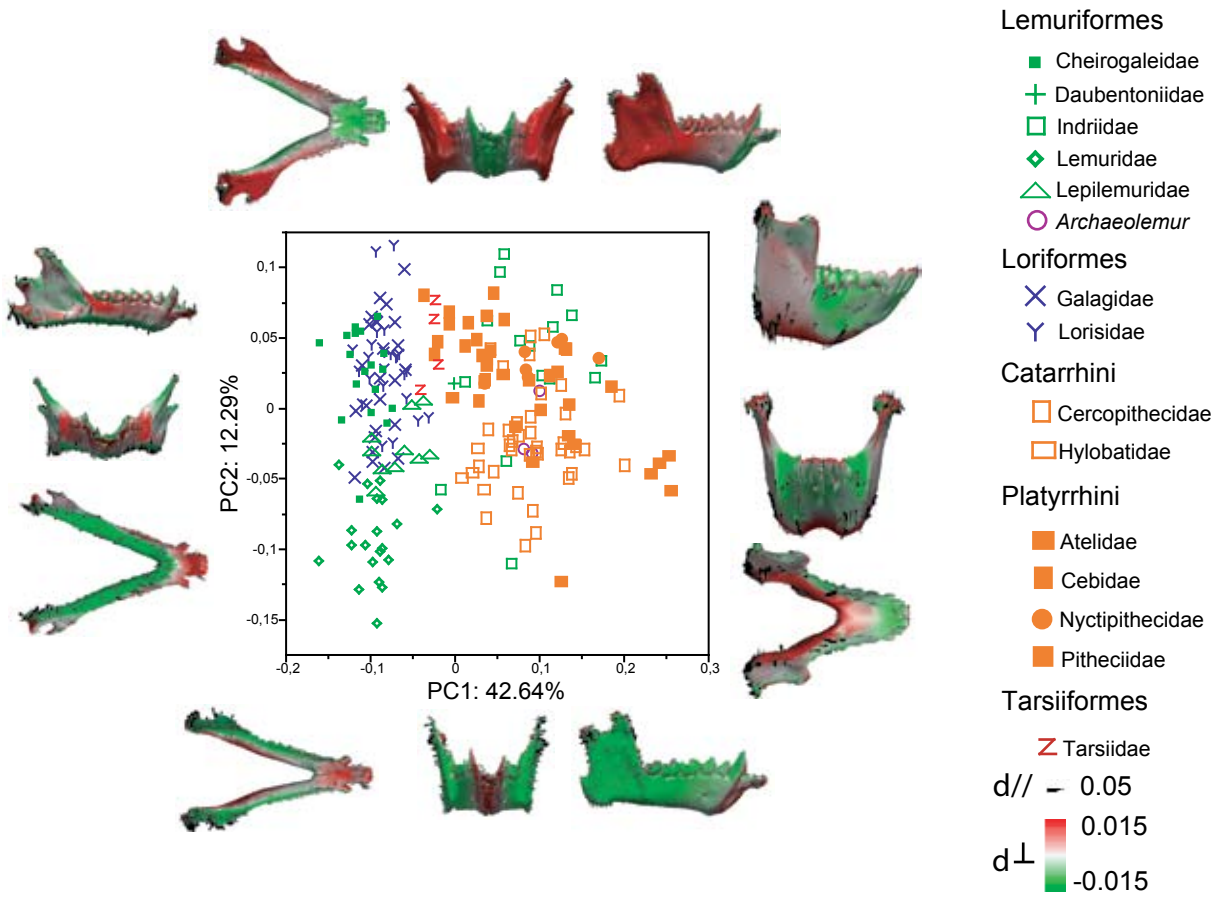

Figure 2.4 : PCA of mandibular shape in primates and associated patterns of shape variation. The mandible of *Euoticus elegantulus* is used to represent the deformations, with the following exception: *Cercocebus torquatus* is used to represent the deformation for high projection values on PC1. d//: displacement parallel to the surface. d⊥: displacement perpendicular to the surface. Scales are in centroid size units.

Table 2.1: Mean and standard deviation of size for the different categories of diet and activity patterns. Haplo: haplorrhines. Strepsi: strepsirrhines. S.d.: standard deviation.

			Skull		Cranium		Md.	
Group	Category	n	Mean	S.d.	Mean	S.d.	Mean	S.d.
Strepsi	Cathemeral	10	237	158	208	110	102	43
	Diurnal	18	245	852	213	628	104	188
	Nocturnal	81	151	1031	134	743	61	211
Haplo	Diurnal	78	265	5037	227	3382	111	1087
	Nocturnal	10	162	1408	142	1082	66	227
Strepsi	Folivore	26	199	2439	174	1768	84	468
	Frugivore	42	193	2024	170	1509	82	419
	Gummivore	15	159	1211	142	869	63	289
	Insectivore	25	131	1267	118	920	51	188
Haplo	Folivore	12	310	484	261	286	135	148
	Frugivore	61	269	3749	232	2502	112	810
	Gummivore	4	128	186	114	132	49	50
	Insectivore	9	137	526	121	405	55	85

Table 2.2: Analysis of variance of species size. Diet and activity pattern factors were considered as the source of variation.

	Effect	D.f.	Mean squares	F	P
Sk	Activity pattern	2	11713	4.85	0.01*
	Residuals	52	2418		
	Diet	3	10373	4.48	0.007*
	Residuals	51	2314		
Cr	Activity pattern	2	8473	4.99	0.01*
	Residuals	52	1697		
	Diet	3	7720	4.4	0.008*
	Residuals	51	1638		
Md	Activity pattern	2	2477	4.97	0.01*
	Residuals	52	498		
	Diet	3	2451	5.32	0.003*
	Residuals	51	460.7		

associated with nocturnal species in both suborders. Larger skulls belong to diurnal species more often. Smaller crania and mandibles mostly belong to insectivore and gummivore species, whereas larger ones usually belong to frugivore and folivore species.

3.2.2 Allometric patterns

Large crania display a relatively smaller neurocranium (see Figure 2.5-A and Figure 2.5-B)**.** The maxillae tend to be longer and wider when size increases. Small crania also exhibit larger and more convergent orbits, and larger temporal fossae. The foramen magnum tends to be placed posteriorly in larger species. Small skulls exhibit mandibles with low and gracile corpora, lower condyles relatively to the alveolar plane and shorter mandibular symphyses, whereas larger skulls exhibit relatively longer mandibles with vertically deeper corpora, higher condyles and longer mandibular symphyses. Similar shape variation patterns can be observed for the mandible (Figure 2.5-C). Small mandibles exhibit a wide angle between the two horizontal branches, whereas large ones display a narrow angle between the branches.

Do these patterns support hypothesis H00? Concerning activity patterns, expectation 1 is fulfilled: relatively smaller species (many of which are nocturnal, see paragraph above) present relatively larger orbits. In contrast, smaller species do not present relatively more developed snouts, which is inconsistent with expectation 2. Allometric patterns also coincide with expectations 3, 4 and 5. Larger species, most of which are folivores, display relatively vertically higher mandibular corpora, higher and longer mandibular symphyses, relatively more expanded gonial regions and higher condyles relative to the alveolar plane. As a whole, H00 is well supported: allometric patterns convey information that is related to dietary specialization

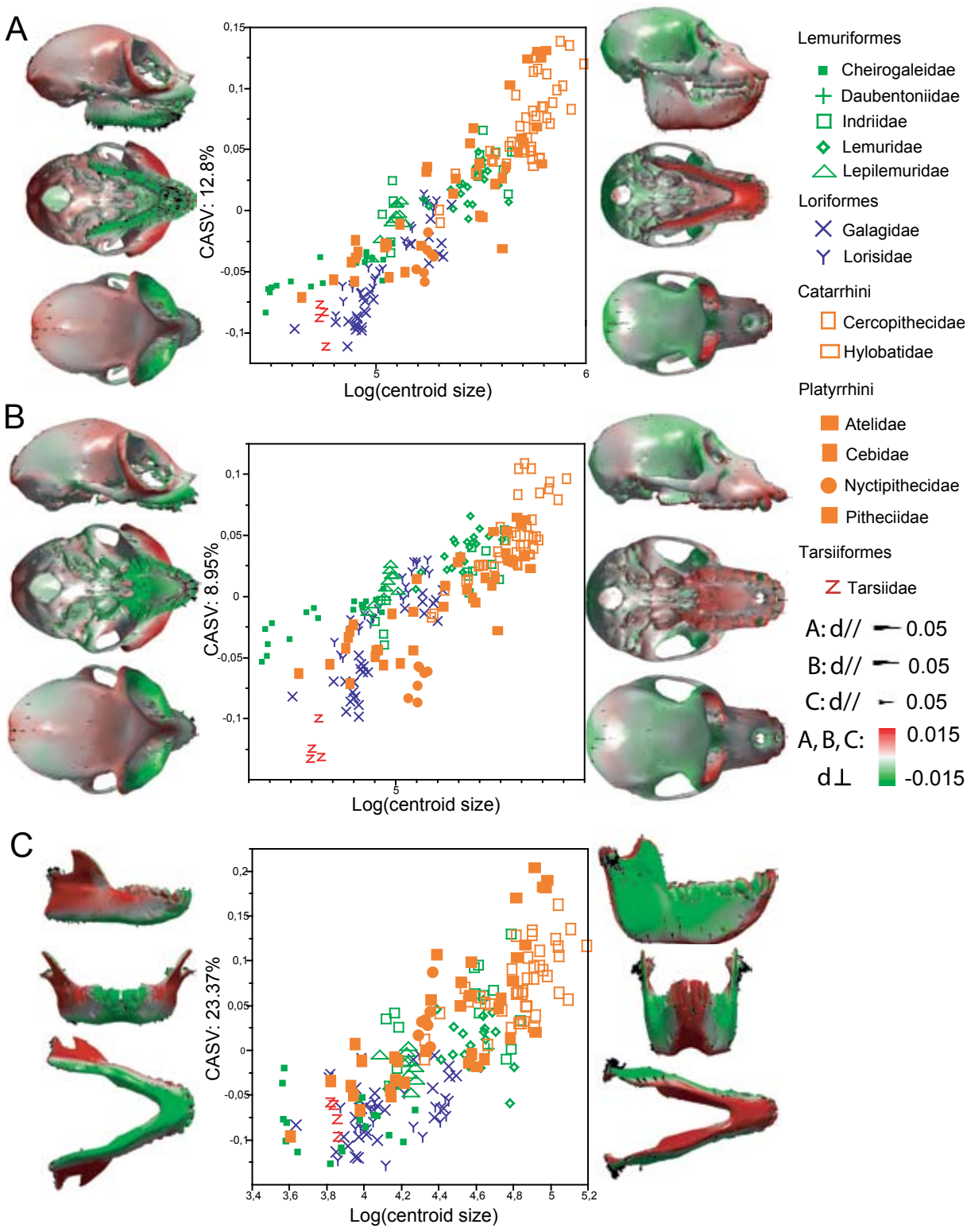

Figure 2.5: Allometric patterns in the primate skull. Plots presenting cranio-mandibular CASV scores versus centroid size in primates are presented along with the associated shape change patterns. A: skull configuration, B: cranium configuration, C: mandible configuration. The mandible and cranium of *Cercocebus torquatus* are used as templates. d//: displacement parallel to the surface. d⊥: displacement perpendicular to the surface. Scales are in centroid size units.

and activity patterns.

3.2.3 Activity patterns, CVA and classification procedures

The percentage of correct classifications is highest when using raw shape data (see Table 2.3). However, the discriminant axis mainly separates haplorrhines from strepsirrhines: all diurnal strepsirrhines are misclassified as "nocturnal", and the nocturnal haplorrhine *Aotus trivirgatus* is misclassified as "diurnal".

When the same analysis is repeated using data "corrected for phylogeny", 50% of the diurnal strepsirrhine specimens are correctly reallocated for cranium configuration, and 86% are correctly reallocated for skull configuration (see Table 2.3). 100% of all nocturnal haplorrhines are correctly reallocated for both the cranium and skull configurations. Finally, when the allometric effect is removed from shape data "corrected for phylogeny", the classification pro-

Table 2.3: Classification procedure for the skull and cranium configurations using "activity patterns" as the categorical variable. See materials and methods for information concerning the differences between raw shape data, shape data "corrected for phylogeny" and shape data corrected for both "phylogeny" and size.

Cranium: raw Procrustes residuals	Diurnal	Nocturnal	%success
Diurnal strepsirrhines (6)		6	0%
Diurnal haplorrhines (25)	25		100%
Nocturnal strepsirrhines (19)		19	100%
Nocturnal haplorrhines (3)	1	2	66%
Total (53)			87%
Cranium: shape corrected for phylogeny	Diurnal	Nocturnal	%success
Diurnal strepsirrhines (6)	3	3	50%
Diurnal haplorrhines (25)	18	7	72%
Nocturnal strepsirrhines (19)	4	15	79%
Nocturnal haplorrhines (3)		3	100%
Total (53)			74%
Cranium: shape corrected for phylogeny and size	Diurnal	Nocturnal	%success
Diurnal strepsirrhines (6)	4	2	67%
Diurnal haplorrhines (25)	20	5	80%
Nocturnal strepsirrhines (19)	3	16	84%
Nocturnal haplorrhines (3)		3	100%
Total (53)			81%

Skull: raw Procrustes residuals	Diurnal	Nocturnal	%success
Diurnal strepsirrhines (6)		6	0%
Diurnal haplorrhines (25)	25		100%
Nocturnal strepsirrhines (19)	1	18	95%
Nocturnal haplorrhines (3)	1	2	66%
Total (53)			85%
Skull: shape corrected for phylogeny	Diurnal	Nocturnal	%success
Diurnal strepsirrhines (6)	5	1	83%
Diurnal haplorrhines (25)	18	7	72%
Nocturnal strepsirrhines (19)	6	13	68%
Nocturnal haplorrhines (3)		3	100%
Total (53)			74%
Skull: shape corrected for phylogeny and size	Diurnal	Nocturnal	%success
Diurnal strepsirrhines (6)	4	2	66%
Diurnal haplorrhines (25)	21	4	84%
Nocturnal strepsirrhines (19)	1	18	95%
Nocturnal haplorrhines (3)		3	100%
Total (53)			87%

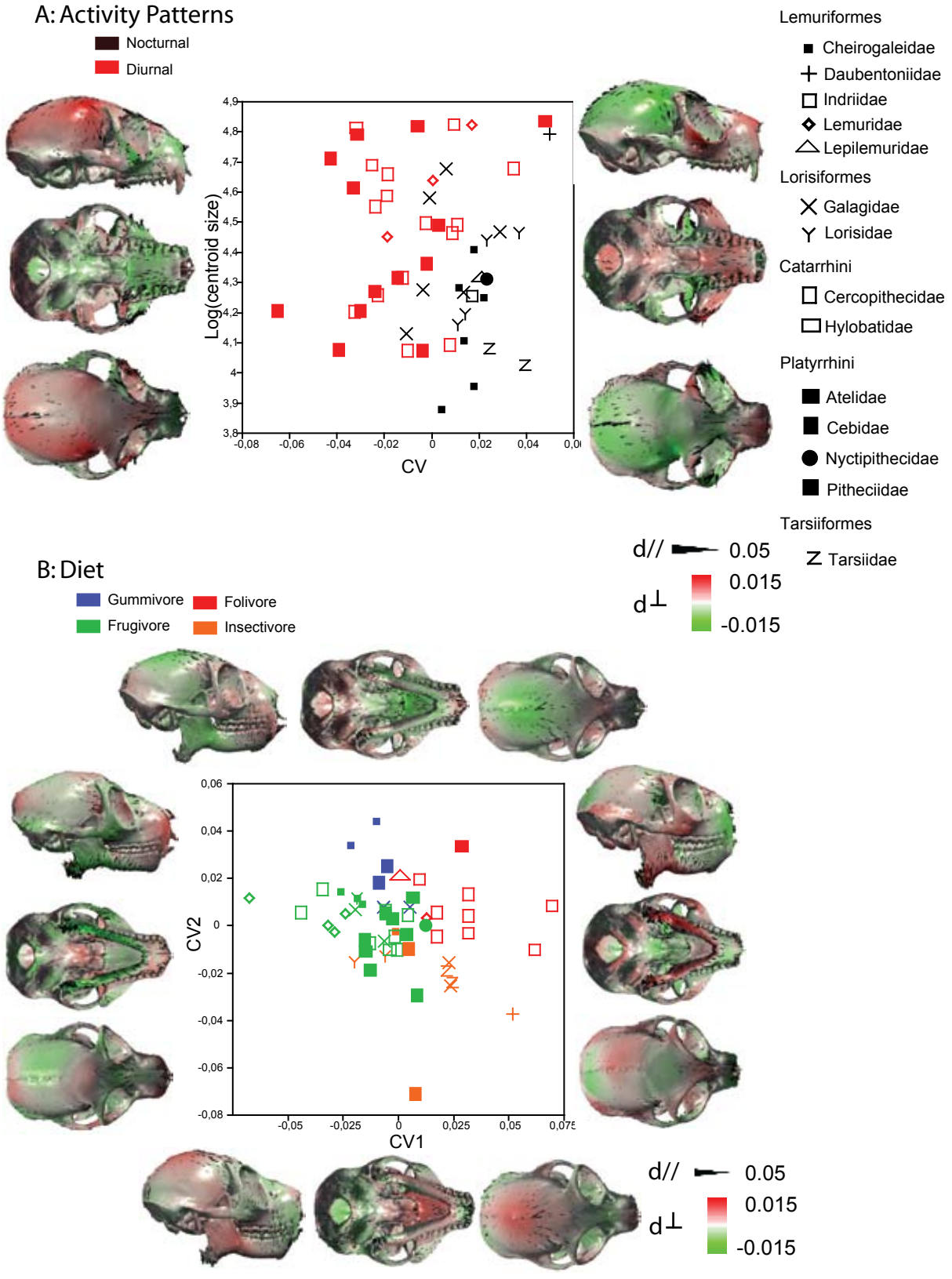

Figure 2.6: CVAs and associated patterns of shape transformation. The input consists of shape data corrected for "phylogeny" and size. A: cranium configuration, activity patterns. B: skull configuration, diet. The mandible and cranium of *Lepilemur ruficaudatus* are used as templates. d//: displacement parallel to the surface. d⊥: displacement perpendicular to the surface. Scales are in centroid size units.

Table 2.4: Classification procedure taking "diet" as the categorical variable. See materials and methods section for information concerning the differences between raw shape data, shape data "corrected for phylogeny" and shape data corrected for both "phylogeny" and size.

Skull: raw Procrustes residuals	Folivore	Frugivore	Gummivore	Insectivore	%success
Folivore(11)	8	3			73%
Frugivore(28)	4	15	7	2	54%
Gummivore (6)		1	4	1	66%
Insectivore (10)	1	1	4	4	40%
Total (55)					56%
Skull: shape corrected for phylogeny	Folivore	Frugivore	Gummivore	Insectivore	%success
Folivore(11)	7	3	1		64%
Frugivore(28)	5	15	3	5	54%
Gummivore (6)		2	3	1	50%
Insectivore (10)	1	2	2	5	50%
Total (55)					55%
Skull: shape corrected for phylogeny and size	Folivore	Frugivore	Gummivore	Insectivore	%success
Folivore(11)	10	1			91%
Frugivore(28)	1	25	1	1	89%
Gummivore (6)		1	5		83%
Insectivore (10)		3		7	70%
Total (55)					86%

Cranium: raw Procrustes residuals	Folivore	Frugivore	Gummivore	Insectivore	%success
Folivore(11)	9	2			82%
Frugivore(28)	8	12	6	2	43%
Gummivore (6)			5	1	83%
Insectivore (10)	1		5	4	40%
Total (55)					55%
Cranium: shape corrected for phylogeny	Folivore	Frugivore	Gummivore	Insectivore	%success
Folivore(11)	9	2			82%
Frugivore(28)	5	13	5	5	46%
Gummivore (6)		2	3	1	50%
Insectivore (10)	1	1	1	7	70%
Total (55)					58%
Cranium: shape corrected for phylogeny and size	Folivore	Frugivore	Gummivore	Insectivore	%success
Folivore(11)	10		1		91%
Frugivore(28)	4	19	3	2	68%
Gummivore (6)		1	5		83%
Insectivore (10)		3		7	70%
Total (55)					75%

Mandible: raw Procrustes residuals	Folivore	Frugivore	Gummivore	Insectivore	%success
Folivore(11)	9	2			82%
Frugivore(28)	1	15	6	6	54%
Gummivore (6)			5	1	83%
Insectivore (10)		1	2	7	70%
Total (55)					65%
Mandible: shape corrected for phylogeny	Folivore	Frugivore	Gummivore	Insectivore	%success
Folivore(11)	7	3		1	64%
Frugivore(28)	3	18	2	5	64%
Gummivore (6)		1	5		83%
Insectivore (10)		2	2	6	60%
Total (55)					65%
Mandible: shape corrected for phylogeny and size	Folivore	Frugivore	Gummivore	Insectivore	%success
Folivore(11)	7	2	1	1	64%
Frugivore(28)	2	20	1	5	71%
Gummivore (6)		1	5		83%
Insectivore (10)	1	1	3	5	50%
Total (55)					67%

cedure performs even better. This result seems to contradict those described in the preceding section: it does not support H00.

The projection of species-specific shape data corrected for size and phylogenetic constraints on the discriminant axis for cranium configuration is represented in Figure 2.6-A, as well as the shape differences associated with nocturnality and diurnality. The discriminant axis separates crania exhibiting relatively smaller orbits from crania that exhibit relatively larger orbits (see Figure 2.6 A). This means that, all things being equal, nocturnal species exhibit relatively larger orbits and more developed nasal regions than diurnal species, which fulfills expectations 1 and 2.

3.2.4 Diet, CVA and classification procedures

For both the cranium and skull configurations, better discrimination was obtained for data corrected for both size and "phylogeny" (see Table 2.4). This result again contradicts those presented in the section dedicated to allometric patterns. For mandible configuration, the percentage of correct *a posteriori* reallocations was never higher than 67%. Discrimination was similar when using either data corrected for size and "phylogeny" or data not corrected for size. This supports the hypothesis that allometric patterns in the mandible reflect dietary specialization. The projection of species-specific shape data corrected for size and "phylogeny" on the discriminant axis for skull configuration are represented in Figure 2.6-B, as well as the associated shape deformations. The first canonical axis (CV1) discriminates skulls that exhibit long and gracile mandibles with low condyles relatively to the occlusal plane, low and gracile corpora and short symphyses from shorter, more robust mandibles that exhibit higher condyles, well developed symphyses, vertically deeper corpora and extremely developed angular processes. CV1 separates crania that exhibit relatively longer maxillae from crania that have shorter snouts. As CV1 separates well folivore species from frugivore species, we can consider that expectations 3, 4 and 5 are well fulfilled. The second discriminant axis (CV2) mainly separates insectivore from gummivore species. The associated morphological changes principally affect the mandibular region. CV2 separates skulls with shorter mandibles from skulls with longer mandibles that exhibit more developed angular processes and lower coronoid processes. Such mandibles are associated to crania that exhibit a relatively higher degree of klinorhynchy.

3.3 Phylogenetic constraints in primate skulls

3.3.1 Divergence in the allometric vector direction.

Size and shape are significantly different between haplorrhines and strepsirrhines for the three configurations ($p<0.001$). Therefore, morphological data were corrected before applying the resampling procedure in order to achieve a mean shape and size difference = 0 between the two suborders (see methods for justifications).

Table 2.5: Percentage of cranio-mandibular shape variance explained by allometry in haplorrhines and strepsirrhines. ASVha : allometric shape vectors computed for haplorrhines. ASVst: allometric shape vectors computed for strepsirrhines. The estimation of statistical significance of the angles of divergence between ASVha and ASVst was performed using resampling statistics (see materials and methods and Chapter 1, section 2.5).

	Percentage of variance explained by ASVha	Percentage of variance explained by ASVst	Cos(angle) between ASVh and ASVst	Angle significance
Skull	24%	17%	0.57	<0.001
Cranium	22%	18%	0.48	<0.001
Mandible	28%	19%	0.53	<0.001

Size explains around 20% of the overall morphological variation in both groups for the three configurations (see Table 2.5). The allometric shape vectors are significantly non-colinear between haplorrhines and strepsirrhines for all configurations (Table 2.5).

The angle of divergence between the two subordinal-specific vector directions is the smallest for mandible configuration.

Morphological convergence of Archaeolemur *with Anthropoids*

For cranium configuration, all specimens were reallocated to the correct suborder. The four crania belonging to the genus *Archaolemur* were allocated to the Strepsirrhini suborder. For mandible configuration, 191 out of 204 specimens were reallocated to their original suborder. Three anthropoid mandibles were wrongly classified *a posteriori*. All strepsirrhine mandibles that were incorrectly reallocated belong to the Indridae family. As a whole, 70% of the mandibles of extant indriids were wrongly reallocated *a posteriori*. The three *Archaeolemur* mandibles were allocated to the Haplorrhini suborder.

4. Discussion

4.1 Morphology and adaptation.

4.1.1 Activity patterns and the orbital region

There is a common trend in haplorrhines and strepsirrhines with regard to the effects of specialization in activity patterns on skull morphology. The results support an observation previously reported by Kirk (2006): nocturnal species tend to display larger orbits. In addition, they display a more developed nasal region, which may be indirect evidence that they rely more on olfaction during foraging than diurnal species.

4.1.2 Diet

There are also common trends in haplorrhines and strepsirrhines with regard to the effects of dietary specialization on mandible morphology. The mandibles of folivorous primates tend to exhibit expanded gonial regions, vertically deep corpora, long and high symphyses and high condyles relative to the alveolar plane, consistent with our expectations.

Concerning gummivory, gummivore species tend to have crania that present a relatively higher degree of klinorhynchy. This latter pattern supports the hypothesis formulated by Dumont (1997) regarding the effects of gummivory on cranial morphology. Concerning the mandible, gummivores are characterized by slightly longer mandibles with developed angular processes and lower coronoid processes. These results neither support the hypotheses of Dumont (1997) nor those of Vinyard et al. (2003). Nonetheless, it should be kept in mind that the data used to discriminate gummivore species from other species are highly modified (in the sense that they do not consist of raw shape data); shape data were corrected for phylogeny and size. As emphasized by Vinyard et al. (2003), functional interpretations are certainly more reliable when comparing a small number of species in a narrower phylogenetic context.

4.1.3 Allometry and adaptation

Allometric patterns certainly reflect dietary specialization and activity patterns to some extent. On the one hand, smaller species, many of which are nocturnal, exhibit relatively larger orbits. On the other hand, the nasal region scales with positive allometry and contradicts our expectations. A positive allometry is found for the corpus breadth and the height of the condyle relative to the alveolar plane, accompanied by an increase in symphyseal length and breadth. Such patterns can be interpreted in biomechanical terms: an augmentation of size is accompanied by an increased robustness in the masseter level arm and the biting force. Coincidentally, the largest species tend to be folivores or process hard food, whereas the smallest are insectivores. Again, allometric patterns also match the expectations concerning the effects of diet on mandible morphology.

Hence, allometric patterns reflect broad morphological trends related to adaptation. This is especially true for the mandible. Then, how can we interpret the seemingly contradictory result that, when the cranium is considered, dietary groups and activity patterns are better discriminated when using data corrected for size? One explanation may be that, if allometric patterns reflect in some ways the adaptive signal, allometry principally acts as a compensatory system on shape for the cranium (H01); functional equivalence is maintained when size changes (see Lockwood and Fleagle, 1999). Changing size while maintaining shape is expected to be maladaptive. If the shape of a skull does not change while size increases, there are important functional consequences: for example, larger skulls would have comparatively less bite force and less tooth surface area (Emerson and Bramble, 1993).

Here, allometry was quantified on a large sample encompassing the two primate suborders. The patterns described are thus very general for primates. However, there may be a departure from this pattern in several taxa. Hence, it cannot be ruled out that cranial allometric patterns may convey a much more important adaptive signal at a lower systematic level (e.g., the family). The different primate families often exhibit specializations in diet, locomotion or activity patterns, which might result in different allometric patterns. This issue is investigated in detail

in Chapter 4, where a sample composed of extant strepsirrhines is analyzed.

4.2 Phylogenetic constraints explain the morphological differences between haplorrhines and strepsirrhines

Considering the present results, several arguments can be proposed to support the hypothesis that strepsirrhines and haplorrhines do not share similar cranio-mandibular phylogenetic constraints. Crania and, to a lesser extent, mandibles of strepsirrhines and haplorrhines differ widely in their shape. *Archaeolemur* and *Hadropithecus* are the strepsirrhine species that exhibit the largest degree of convergence with the anthropoids with regard to the skull. However, in the present analysis, specimens belonging to the genus *Archaeolemur* exhibit a morphology that is closer overall to that of other strepsirrhine individuals than to that of anthropoids. Convergence of *Archaeolemur* with the anthropoids is mostly important for mandible configuration. However, the allocation of the mandible of *Archaeolemur* to the Haplorrhini probably reflects the morphological affinities of *Archaeolemur* with the extant indriids. As mentioned in the results, the majority of the indriid specimens were wrongly reallocated to the Haplorrhini suborder for mandible configuration. Archaeolemurs are thought to be distant relatives of the extant indriids (e.g., see Godfrey et al., 2002; Grandidier, 1905; Lamberton, 1939; Lorenz von Liburnau, 1902; Schwartz and Tattersall, 1974). Thus, the morphological convergence of *Archaeolemur* with the anthropoids is only superficial. No extant haplorrhine fits within the morphological variability of the strepsirrhines: there is no overlap in shape space (e.g., the entire set of possible shapes) between the haplorrhines and the strepsirrhines. Anyhow, the morphological divergence between specimens belonging to different suborders is always far greater than any convergence.

Another line of evidence comes from the comparative study of allometric patterns in haplorrhines and strepsirrhines, at least for the cranium. Their subordinal-specific ASVs diverge significantly, which may reflect differences in developmental constraints between the two suborders. This divergence does not result from differences in activity patterns or dietary specializations across the two groups:

- both groups comprise species belonging to each class of "diet" and "activity pattern"; size is structured similarly by activity patterns and diet in each group;
- cranial allometric patterns reflect the effect of functional equivalence maintenance across size ranges: the discrimination of cranial shape using diet and activity patterns as categorical variables is better achieved using data corrected for size for cranium configuration.

Furthermore, the shape space is only sparsely populated. According to Maynard Smith et al. (1985), this may indicate developmental constraints. No intermediate morphology exists between haplorrhines and strepsirrhines. In both suborders, species belonging to all of the defined dietary and activity pattern groups exist. However, no striking morphological convergence

for the skull exists between species sharing similar dietary specialization and activity patterns across the two primate suborders.

Taken together, these results suggest that the morphology of the primate skull reflects more than the response to natural selection as an agent of optimization. This view converges with the critiques of Gould and Lewontin (1979), which were formulated against what they define as the "adaptationist programme": each trait of an organism must not be considered as the sole product of natural selection. According to their view, organisms must be approached as integrated wholes, with *Baupläne* constraining themselves in the possible pathways of change. This view applies to the morphology of the haplorrhines and strepsirrhines, even though similar adaptations yield similar effects in both suborders. Our results support the hypothesis that the morphology of the skull is strongly constrained by phyletic heritage in each primate suborder. The hypothesis that the phylogenetic constraints are mainly of developmental origin and would explain the differences between haplorrhines and strepsirrhines in the skull morphology is specifically examined in Chapter 5.

The *origin* of these structural differences between haplorrhines and strepsirrhines may be adaptive. Before going further, the structure of the present haplorrhine sample must be considered: it consists mainly of anthropoid species. In that sample, *Tarsius* is the only non-anthropoid haplorrhine genus. Thus, these differences in phylogenetic constraints mostly apply to strepsirrhines *versus* anthropoids. The orbital orientation of primates is among the most convergent among mammals; orbital convergence results in a large binocular field for stereoscopic vision. This pattern is interpreted by many authors as an early adaptation to nocturnal predation (Cartmill, 1972; Fleagle, 1999; Ravosa et al., 2000; but see Soligo and Martin, 2006 and Sussman, 1991), the primitive primates being hypothesized to be nocturnal (Heesy and Ross, 2001; but see Tan et al., 2005). Among non-anthropoid primates, the tarsiers and lorises exhibit the most convergent orbits, which is argued to be an adaptation in response to nocturnal visual predation (Ross, 1995). The anthropoids are highly distinguishable in that they present orbits that are both extremely convergent and highly frontated. As was noted by Ross (1995) and observed in the present study, an increase in skull size is accompanied in both suborders by an increase in the degree of orbital convergence. Ross (1995) proposed that the extreme degree of orbital convergence of anthropoid primates would be the consequence of the following sequence of events. The initial anthropoid orbital configuration would have been acquired in a lineage of omomyid-like nocturnal visual predators. Then, a shift to diurnality and small body size, followed by an increase in body size, would have induced a cumulative allometric increase in convergence. The increased frontation observed in anthropoids would either be an effect of an increase in frontal lobes or would be subsequent to an increased degree of basicranial flexion.

The scenario formulated by Ross (1995) provides an adaptive framework that helps to explain the origin of the morphological differences observed between anthropoids and strepsirrhines. It implies that the morphology of the strepsirrhine skull reflects the primitive primate

condition to a much greater extent.

Then, how do basal haplorrhines, such as *Tarsius* and the omomyids, fit in this scenario? Do all haplorrhines present a derived condition? Szalay (1987) argued that a reorganization of facial development had occurred in haplorrhines. This hypothesis implies that different phylogenetic constraints determine the morphology of the cranium in the two primate suborders. The current evidence does not permit the assessment of whether *Tarsius* presents many more morphological affinities with anthropoids than with strepsirrhines. This issue is treated in detail in the next chapter.

SUMMARY OF CHAPTER 2

The primate order displays great morphological variability of the skull. Additionally, there are also large differences in the morphology of the skull between the two primate suborders, Haplorrhini and Strepsirrhini. Do these differences represent phylogenetic constraints or differences in adaptation? Allometry (the influence of size on shape, *sensu* Gould, 1966) also accounts for a large part of the morphological variability of the skull. Do allometric patterns convey information that can be related to dietary specialization or to activity patterns, or is allometry acting mainly as a compensatory system by which functionality is maintained through size ranges? Do allometric patterns differ between the two primates suborders?

In order to quantify phylogenetic constraints and characterize how morphology reflects adaptation within the two primate suborders, we used the approach proposed by Cheverud et al. (1985). This approach permits the separation of morphological variance into two components. The first component represents phylogenetic constraints, also referred to as the phylogenetic burden. The second component represents evolution independent of phylogenetic constraints.

The influence of adaptation on morphology is important: size is structured by diet and activity patterns (Kay, 1984), and shapes can be discriminated according to diet and activity patterns once the influences of size and phylogenetic constraints on shape are taken into account. Similar dietary specialization and activity patterns yield similar effects on morphology in both suborders. Allometric patterns of the mandible correspond to patterns of dietary specialization. Allometry reflects mostly functional maintenance through size ranges in the cranium.

Nevertheless, phylogenetic constraints explain a lot of the morphological variability in primates. Such constraints account for the differences in skull morphology between strepsirrhines and haplorrhines. Three lines of evidence support this hypothesis. First, there is no overlap in shape-space between haplorrhines and strepsirrhines. Additionally, the skull of the strepsirrhine *Archaeolemur* is convergent with the anthropoids, but it still shares far more morphological similarities with other strepsirrhine species. Finally, allometric patterns differ widely between haplorrhines and strepsirrhines, which suggests a developmental origin of the phylogenetic constraints between the two suborders.

Chapter 3

"Strepsirrhinism": is it a primitive or derived condition in primates?

Contents

1. Introduction

Anatomical strepsirrhinism means continuity of the upper lip with the vomeronasal organ (Asher, 1998), an organ that plays an important role in social and sexual communication (Estes, 1972; Verberne and de Boer, 1976). Rosenberger and Strasser (1985) proposed that a functional tie links the toothcomb and the vomeronasal organ. According to these authors, this link would explain the origin of the mandibular toothcomb, which would have evolved as an accessory appendage to the vomeronasal organ and serve to collect pheromones during grooming. Furthermore, Rosenberger and Strasser (1985) proposed that the Eocene adapiforms, considered by most authors to be either the sister groups of modern strepsirrhines or broadly ancestral to them, displayed a reorganization of their rostrum through both a reduction of the premaxilla and an increase of the gap between their central upper incisors. Such a gap facilitates the connection between the vomeronasal organ and the rhinarium. This gap can also be observed in several non-primate species that exhibit anatomical strepsirrhinism (Asher, 1998). In adapiforms, the reorganization of the rostrum would be related to a reduction of its use during feeding and a concomitant increase in usage of the vomeronasal organ in social behavior. Thus, strepsirrhinism, as observed in extant and fossil strepsirrhines, would be autapomorphic. Asher (1998) gave evidence that some (but not all) extant strepsirrhines display significantly wider interincisal gaps than other anatomically strepsirrhine species. Coincidentally, he observed that all species that display an autapomorphic rostrum also exhibit the most complex social structures and spend a lot of time grooming. This gives credit to the hypothesis that the vomeronasal organ functions in association with the toothcomb. However, Asher (1998) found no support for the hypothesis that extant strepsirrhines and adapiforms share a derived rostrum.

Furthermore, after considering the available fossil evidence, Beard (1988) stated that it could not be excluded that the omomyids, regarded by most researchers as a basal haplorrhine family (e.g., see Gunnell and Rose, 2002; Szalay, 1976), were also, anatomically speaking, strepsirrhines. Therefore, strepsirrhinism would definitely be a plesiomorphic condition in primates. Morphological features that define the strepsirrhine condition would not be apomorphies uniting these animals but an ensemble of plesiomorphic characters. The morphology of the cranium differs significantly between extant strepsirrhines and extant haplorrhines (see Chapter 1). The cranium is well-known for several genera of basal haplorrhines belonging to the Omomyidae family, such as *Rooneyia, Necrolemur,* and *Microchoerus.* The existence of well-preserved omomyid crania makes it possible to assess whether the supposed primitiveness of the "strepsirrhine condition" is a concept that can be extended to the global morphology of the cranium.

The following questions are addressed:

- Does the cranial architecture which characterise the strepsirrhines constitute the primitive condition in primates?

- Are Eocene omomyids primitive for primates, or does their cranial morphology reflect the derived condition observed in extant haplorrhines? In other words, is there evidence for fundamental differences in cranial structure in extant and basal haplorrhines?

2. Materials and Methods

2.1 Materials

The fossil sample consists of 4 omomyid specimens, including 2 crania of *Necrolemur*, 1 cranium of *Microchoerus* and the cranium of the type specimen of *Rooneyia viejaensis* (*Rooneyia* is considered here as an omomyid, following the comprehensive study of Szalay, 1976 and Gunnell and Rose, 2002). *Necrolemur* and *Microchoerus* belong to the Microchoerinae subfamily, whereas *Rooneyia* belongs to the tribe Rooneyini. A complete list of the fossils is given in Appendix 2.

A large comparison sample including extant strepsirrhines and haplorrhines was used for analysis. This sample is almost equivalent to that presented in Chapter 2, with the following exceptions: because the crania that belong to the genus *Alouatta* are atypical for haplorrhines, they are not incorporated in the sample. For the same reason, the crania of *Daubentonia* and of sub-fossil strepsirrhines belonging to the genus *Archaeolemur* and are also excluded.

2.2 Methods

The landmark protocol used in this chapter takes into account the fact that several fossils are incomplete (see Chapter 1, section 2.1).

Shape variability patterns were explored via Principal Component Analysis (PCA) of the shape data in linearized Procrustes shape space (see Chapter 1, sections 2.2 and 2.3).

Is the morphology of the cranium of fossil omomyids more similar to that of extant haplorrhines or to that of extant strepsirrhines? To answer this question, a Canonical Variate Analysis (CVA) was performed. The suborder to which each extant specimen belongs (Haplorrhini or Strepsirrhini) was taken as the categorical variable. Extant specimens were first projected on the common allometric shape vector (CASV), which was computed as the mean of the allometric shape vectors (ASVs) that were computed for both suborders. After projecting the extant specimens on the CASV, shape residuals were used as the CVA inputs. The justification for using shape residuals (e.g., shape data corrected for allometry) rather than raw shape data lies into the fact that the allometric signal is important in the primate cranium (see Chapter 2), and is a source of homoplasy. Each specimen was then reallocated *a posteriori* to one of the two categories “Haplorrhini” or “Strepsirrhini”. It must be noticed that the fossils were not used

to compute the canonical axis (CV). Rather, they were projected *a posteriori* on the CV, and their projection scores were then used to classify them into the suborder to which they were anatomically the closest without making any *a priori* assumption that could have influenced the computation on the axis (see Chapter 1, section 2.5).

Finally, a phenetic analysis was conducted. Procrustes distances were computed among all extant primate mean families available for cranium configuration. Concerning the omomyids, a mean individual was computed for the genus *Necrolemur*, and the other two fossils were included directly in the analysis. Thus, some heterogeneity was introduced into the analysis: the sample consisted of both extant family-specific mean specimens and fossil individuals representative of the generic level. However, the analysis should be only minimally influenced by such heterogeneity because the fossil part was largely a minority. Furthermore, the systematic position of *Rooneyia* is still debated (*Rooneyia* may belong to its own specific family, according to Rosenberger, 2006), it is worth keeping *Rooneyia* separated from the other omomyids. The distance matrix was computed on shape data corrected for size, taking into account the fact that allometry may mask the phylogenetic signal (see Chapters 2 and 4). A tree is computed from this distance matrix using the UPGMA (Unweighted Pair Group Method with Arithmetic mean) procedure. The software PHYLIP (Felsenstein, 1989) was used to compute the UPGMA tree.

3. Results

3.1 PCA and classification procedure

The first principal component (PC1) neatly separates the modern haplorrhines from the modern strepsirrhines. PC1 accounts for 44.67% of the total sample shape variance. PC1 describes patterns of shape variability in the relative size of the neurocranium and the face. PC1 opposes crania displaying a relatively larger braincase, a drastically reduced face, an anteriorly placed foramen magnum and a relatively short inter-orbital space to relatively longer crania that display smaller braincases, a long snout, a posteriorly placed foramen magnum and a wide inter-orbital space. All modern haplorrhines, *Tarsius* included, project on the negative pole of PC1. On the contrary, the four fossils project to positive values, as all the modern strepsirrhines (see Figure 3.1). The second principal component (PC2) accounts for 9.88% of the sample shape variance, and describes patterns of shape variability correlated with size (scores on PC2 are significantly correlated with centroid size: $r^2=0.46$, $p<0.0001$). When size increases, the crania tend to exhibit relatively shorter braincases in the antero-posterior plane, relatively longer and higher maxillae and comparatively smaller orbits. Among the haplorrhines, PC2 separates well all the catarrhines from the platyrrhines and *Tarsius*. This is probably related to the fact that most catarrhines are larger than platyrrhines. Among the strepsirrhines, PC2 tends, though imperfectly, to separate the smallest galagid species from other strepsirrhines. Fossils belonging to

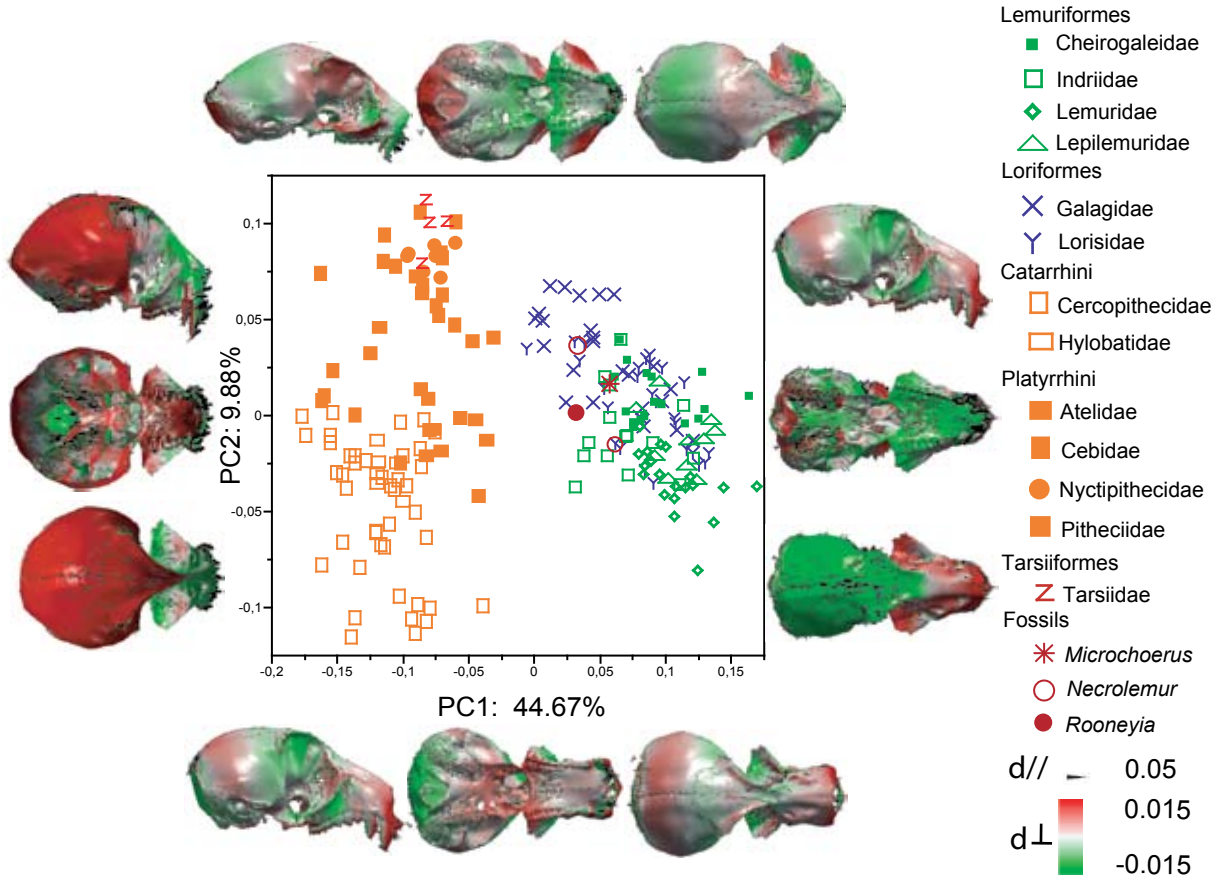

Figure 3.1: PCA of cranial shape in extant primates and fossil haplorrhines and associated patterns of shape variation. The cranium of *Euoticus elegantulus* was used to visualize 3D patterns of shape variability (as the orbital region and zygomatic arch were not preserved in most of the fossil specimens, they were removed from the template using a virtual scalpel). d//: displacement parallel to the surface. d⊥: displacement perpendicular to the surface. Scales in centroid size units.

the Omomyidae family project centrally on this axis. This classification procedure is powerful for the *a posteriori* classification of modern strepsirrhines and modern haplorrhines (Table 3.1): 100% of the specimens were correctly reallocated *a posteriori*. All omomyids were classified among the strepsirrhines.

Table 3.1: Classification procedure derived from the CVA of cranial shape, using “suborder” as the categorical variable. The analysis was performed on shape data that were corrected for size.

	Strepsirrhine	Haplorrhines	%success
Strepsirrhines (113)	113		100%
Haplorrhines (93)		93	100%
Total (206)			100%
Microchoerinae (3)	3		
Rooneyinii(1)	1		

3.2 Phenetic analysis

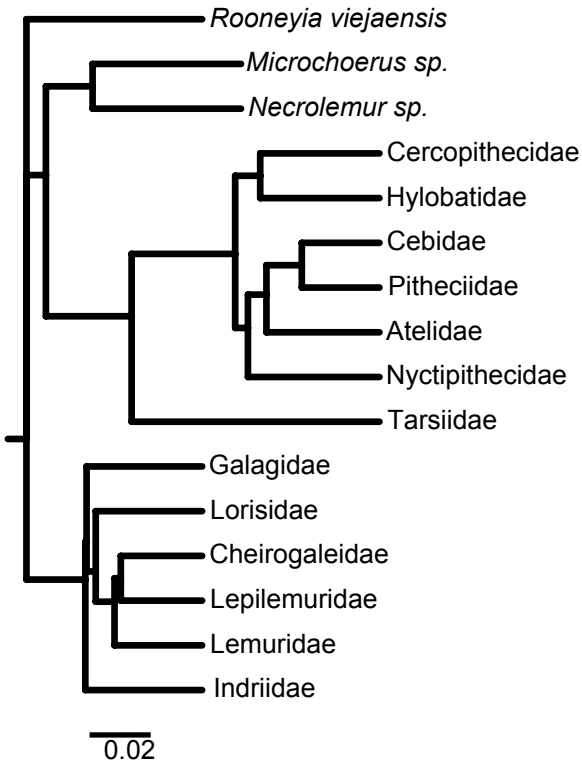

Figure 3.2: UPGMA tree computed on the inter-familial Procrustes distance matrix (shape data were corrected for size).

The UPGMA tree is presented in Figure 3.2. The suborders Strepsirrhini and Haplorrhini are retrieved. Among the haplorrhines, the catarrhines are separated from the platyrrhines. *Tarsius* is situated in basal position among the haplorrhines. A cluster representing the Tarsiiformes infraorder is not retrieved. *Microchoerus* and *Necrolemur* are nested together, and *Rooneyia* displays an intermediate position between the extant strepsirrhines and all the other haplorrhines. Among the strepsirrhines, the Lemuriformes and Loriformes infraorders are not retrieved.

4. Discussion

4.1 Rooneyia and the validity of A Protoanthropoidea taxon

The phylogenetic position of *Rooneyia viejaensis*, which is only known on the basis of a relatively complete cranium from the latest Eocene in Texas, is still enigmatic. *Rooneyia* has been considered to be an omomyid since the comprehensive analysis of this family given by Szalay (1976), who placed it in its own tribe, the Rooneyini. This view is still employed in the

more recent synthesis given by Gunnell and Rose (2002). However, recent parsimony analyses conducted have failed to retrieve an omomyid clade including *Rooneyia* (Beard and MacPhee, 1994; Kay et al., 2004; Ross, 1994). Kay (2004) even classified the genus outside the two suborders, placing it in an *incertae sedis* family. Rosenberger (1985) postulates that *Rooneyia* is more plesiomorphic than *Necrolemur* for several cranial features, a view which is shared by Beard and MacPhee (1994). *Rooneyia* lacks a basioccipital flange and does not exhibit any alisphenoid flange, although it displays broad choanae. Recently, Rosenberger (2006) hypothesized that *Rooneyia* and the anthropoids shared synapomorphies in the orbital regions that justified their placement into their own family, the Rooneyidae, in the Hyporder Protoanthropoidea. The latter would be more closely related to anthropoids than any extant or extinct Tarsiiformes.

The data presented in this study do not support this hypothesis. Indeed, *Rooneyia* is placed closer to the mean shape computed for microchoerines than to that of any extant haplorrhine, *Tarsius* included, in the phenetic analysis. This favors the hypothesis that *Rooneyia* presents a very plesiomorphic morphology for primates. Meanwhile, if the hypothesis presented by Rosenberger (2006) were true, this would imply that the morphological affinities observed between *Tarsiidae* and anthropoids throughout this study would only result from convergence.

4.2 The ancestral condition of the primate skull architecture

4.2.1 Strepsirrhinism

The results presented above strongly uphold the hypothesis proposed by Beard (1988): strepsirrhinism can not be invoked as an innovation underlying the strepsirrhine/haplorrhine dichotomy. Rather, it is a plesiomorphic condition that is probably retained by at least some omomyids, including *Necrolemur*, *Microchoerus* and *Rooneyia*. The tarsiers clearly share more similarities in their cranial geometry with the anthropoids than any of the omomyids present in this sample. There is a vast consensus concerning the hypothesis of monophyly of extant haplorrhines. The first documentation in the fossil record of relatives of the living tarsiers arises from middle Eocene deposits in China (Beard, 1998; Beard et al., 1994; Rossie et al., 2006). Unfortunately, no complete skull for these fossils has been retrieved thus far. Furthermore, there are still competing hypotheses concerning the phylogenetic relationship between *Tarsius*, anthropoids and the extinct omomyids. These hypotheses rely heavily on comparative analyses involving the complete cranial material of several Omomyidae and *Tarsius*. Several researchers favor the theory that tarsiers and anthropoids are more closely related to each other than to any known Omomyidae (Cartmill and Kay, 1978; Cartmill et al., 1981; Conroy, 2005; MacPhee and Cartmill, 1986; Ross, 1994). Other workers support the hypothesis that Tarsiers are more related to some members of the Omomyidae lineage than to anthropoids, especially *Necrolemur* (Gingerich, 1981b; Rosenberger, 1985; Rosenberger and Szalay, 1980; Szalay, 1976). The morphological evidence presented here does not lend much support to a close relationship between

the omomyids and the tarsiers; rather, the results favor the hypothesis of a closer relationship between *Tarsius* and the anthropoids. Still, morphological convergence between *Tarsius* and anthropoids since the Eocene epoch could account for the large morphological difference observed in this study between *Rooneyia, Necrolemur* and *Microchoerus* as compared to *Tarsius.*

Shoshonius, a late early Eocene Omomyidae for which complete skulls have been recently discovered, could be even more closely related to *Tarsius* than any microchoerine (Beard et al., 1991; Beard and MacPhee, 1994). *Shoshonius* is currently known from several skulls, none of which are totally complete or undistorted (Beard and MacPhee, 1994). A reconstruction of *Shoshonius* and its inclusion in the present analysis would give rise to many new arguments in this debate; it could be assessed whether its cranial morphology is closer to that of *Tarsius* or to that of the other omomyids for which the cranium is known.

4.2.2 Is there evidence for a reorganization of the face in the omomyid lineage?

As stated above, Szalay et al. (1987) argued that a reorganization of facial development occurred in basal haplorrhines. The core of their argument is based on the comparison of the orbito-nasal region of short-faced strepsirrhines and haplorrhines. In strepsirrhine species that exhibit a short face and large orbits (e.g., the Asiatic Lorisidae family), the olfactory bulbs pass below the interorbital septum (Cartmill, 1972). In contrast, the olfactory bulbs pass above the region of maximal constriction in the interorbital septum in haplorrhine species (Cave, 1967). Szalay and Delson (1979) observed this condition in the crania of the omomyids *Necrolemur* and *Rooneyia* and insisted that this character could be valuable when assessing phylogenetic affinities in primates. However, the hypothesis that a rearrangement of the face occurred in haplorrhines only holds if the condition observed in lorisids *is not* extremely derived for strepsirrhines. One result reported in Chapter 4 suggests that the lorisids are unique in their orbital region; their orbits point upwards, are extremely convergent and display an unusually thin interorbital septum. A major reorganization of the face, through reorientation of the orbits and a concomitant shortening of the face, certainly occurred in lorisids. Therefore, this tendency in the position of the olfactory processes of the brain observed in several (but not all, see Figure 3.3) lorisid species is probably one consequence of that reorganization. Furthermore, among lorisids, this pattern is mostly expressed within the genus *Loris* (and to a far lesser extent in *Nycticebus*), which exhibits the narrowest interorbital region (see Figure 3.3). Moreover, within the lorisids, *Loris* is the genus that presents the most derived growth patterns (Gomez, 1992). Therefore, using information derived from the morphology of adult *Loris* to infer patterns of developmental constraints for the whole Strepsirrhini suborder is certainly irrelevant. Moreover, the olfactory lobes are positioned upwards in cheirogaleid species such as *Microcebus murinus*, *Cheirogaleus major* and the galagid *Otolemur crassicaudatus*. Thus, it can be concluded that the evidence for shared developmental constraints between the omomyids, *Tarsius* and anthropoids, to the exclusion of strepsirrhines, is weak.

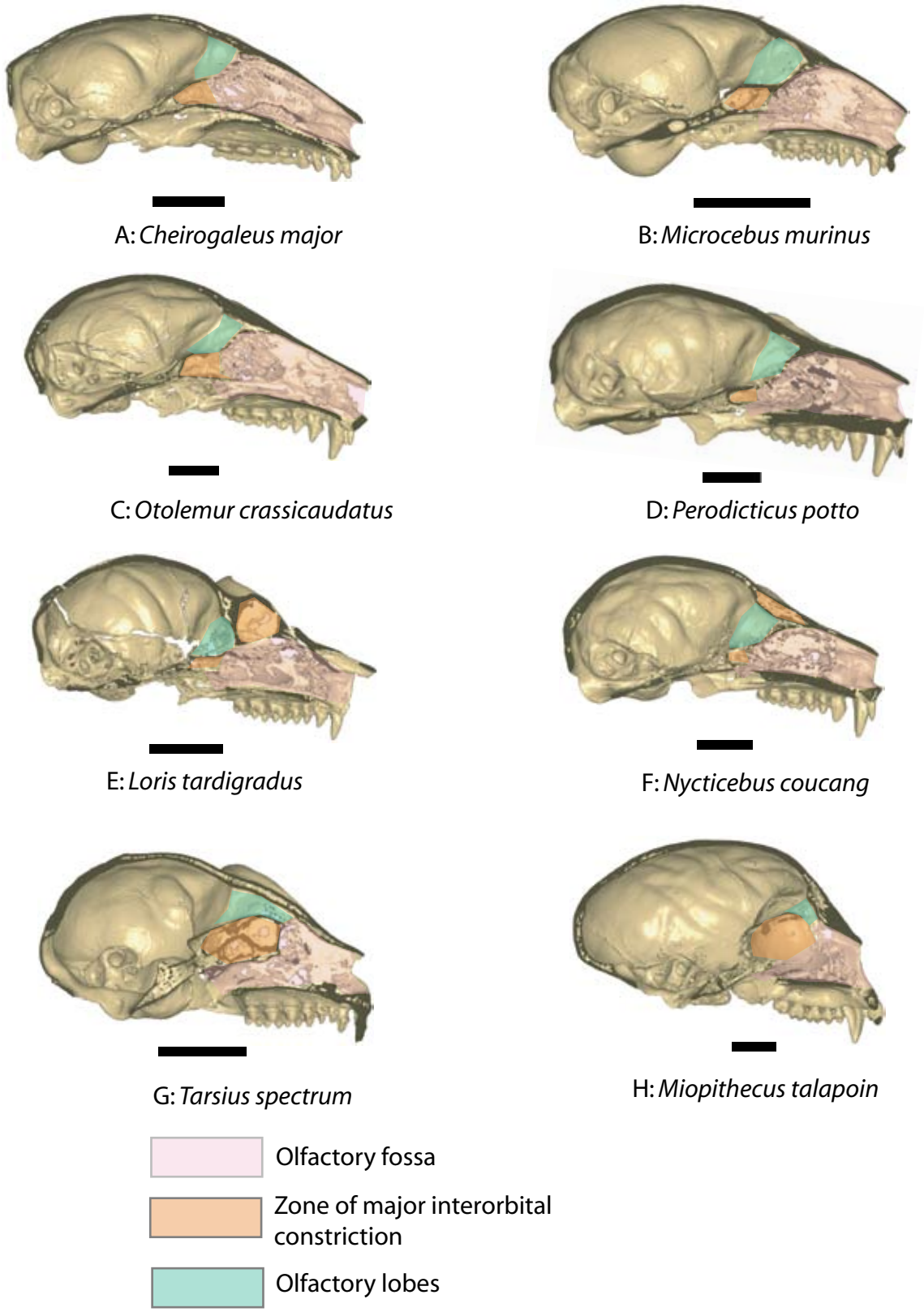

Figure 3.3: Variability in the configuration of the interorbital septum in extant primates. Scale bars: 1cm. This figure illustrates that the zone of major interorbital constriction is situated beneath the olfactory lobes in the region of the orbito-sphenoid bone in most primates (A, B, C, D, G, H). In extant haplorrhines (G, *Tarsius spectrum* and H, *Miopithecus talapoin*), the olfactory lobes are in contact with the nasal fossa through a narrow duct. In Asiatic lorisids (E, F), this zone is principally situated above the olfactory bulbs.

4.2.3 Skeletal strepsirrhinism and haplorrhinism

Contradicting the hypothesis of Szalay et al. (1987), our results strongly suggest that the omomyids belonging to the genera *Necrolemur*, *Microchoerus* and *Rooneyia* demonstrated a cranial shape much more similar to that of extant strepsirrhines than to that of extant haplorrhines, *Tarsius* included. These data give support to the proposition that the notions of "strepsirrhinism" and "haplorrhinism" can be extended to the configuration of the cranium. Thus, it makes sense to employ the terms "skeletal strepsirrhinism" and "skeletal haplorrhinism" to designate the large geometric differences in the cranium that are observed between anatomical strepsirrhines and haplorrhines. It could also be proposed that "skeletal strepsirrhinism" and "skeletal haplorrhinism" can be used as proxies to infer anatomical strepsirrhinism and haplorrhinism. The wide gap that separates the upper incisors of *Necrolemur antiquus* led Beard (1988) to consider that it can not be ruled out that at least some omomyids had conserved anatomical strepsirrhinism. The results presented here support this hypothesis: *Microchoerus erinaceus, Necrolemur antiquus* and *Rooneyia viejaensis* exhibit skeletal strepsirrhinism and thus may have been anatomical strepsirrhines.

As emphasized by Beard (1988), strepsirrhinism cannot defend the monophyly of primate clades, but it still reflects broad biological similarities shared among distantly related species.

SUMMARY OF CHAPTER 3

Beard (1988) stated that the hypothesis that the omomyids were, anatomically speaking, strepsirrhines could not be ruled out. Moreover, there is currently a consensus in favour of the hypothesis that the omoyids are, phylogenetically speaking, haplorrhines. According to these hypotheses, strepsirrhinism would be a primitive condition in primates. Szalay et al. (1987) argued that a reorganization of the development of the face occurred in basal haplorrhines, implying that different developmental constraints determined cranial morphology in the two different primate suborders. These hypotheses were tested.

New arguments are given to support the hypothesis of Beard. In contrast, our results contradict the hypothesis of Szalay et al. The omomyids *Rooneyia*, *Necrolemur* and *Microchoerus* appear to be closer in morphology to the extant strepsirrhines, whereas *Tarsius* exhibits much more morphological resemblance with other extant haplorrhines (i.e., anthropoids). Thus, it is probable that the shift towards a modern haplorrhine morphology occurred in some omomyid lineage to the exclusion of the three genera mentioned above.

Chapter 4

Patterns of morphological variability in the strepsirrhine skull

Contents

1. Introduction

Molecular studies support the division of the extant strepsirrhines into two monophyletic infraorders: the Malagasy primates (the lemuriforms), and the African and Asian loriforms (for a review, see Yoder, 1997). Within the Loriformes infraorder, morphological, molecular and paleontological evidence support the monophyly of Lorisidae and Galagidae (e.g., see Masters et al., 2005; Masters et al., 2007; Masters and Brothers, 2002; Seiffert, 2007; Seiffert et al., 2003). Within the Malagasy primates, the monophyly of each family has also been confirmed. However, there is a lack of consensus regarding the relative positions of the Cheirogaleidae, Lepilemuridae, and a group composed of two sister families, the Indridae and Lemuridae (Roos et al., 2004).

Within the strepsirrhines, the Cheirogaleidae family has created a long-standing phylogenetic controversy. On the basis of morphological, ecological, and behavioral similarities shared by *Microcebus murinus* and *Galagoides demidoff*, Charles-Dominique and Martin (1970) proposed that cheirogaleids and galagids retain most of the ancestral conditions of toothcombed strepsirrhines. However, they admitted that another explanation could account for these shared characteristics: cheirogaleids could be more related to loriforms than to the other Malagasy primates. After the publication by Charles-Dominique and Martin (1970), numerous studies aimed to assess whether the similarities shared by cheirogaleids and galagids represent synapomorphies (Cartmill, 1975; Groves, 1974; Schwartz and Tattersall, 1974; Szalay and Katz, 1973). Systematic taxonomies placing the cheirogaleids among the loriforms were consequently published (Andrews, 1988; Schwartz et al., 1978; Szalay and Delson, 1979). However, the assignment of the Cheirogaleidae family to the Loriformes infraorder can no longer be defended, since the vast majority of molecular studies have placed the Cheirogaleidae family within the Lemuriformes infraorder (for a review, see Yoder, 1997), as well as dental evidence (Marivaux et al., 2001). Therefore, the initial hypothesis of Charles-Dominique and Martin (1970) is reinforced, and cheirogaleids and galagids may be plesiomorphic for extant strepsirrhines. However, does the hypothesis of Charles-Dominique and Martin (1970) also hold true for skull morphology? In other words, does the skull morphology of Cheirogaleidae and Galagidae provide a good model for the ancestral condition of toothcombed strepsirrhines? This chapter re-examines this issue.

The other question addressed within this chapter concerns allometry. One prevalent hypothesis regarding allometry is that it mainly reflects functional equivalence across a size range (e.g., see Emerson and Bramble, 1993; Lockwood and Fleagle, 1999; see also Chapter 2). Therefore, allometric patterns may be the expression of underlying homologous processes (Lockwood and Fleagle, 1999). As such, allometry is often considered to be a source of homoplasy, and common allometric patterns are not considered useful for resolving phylogenetic relationships within a group of closely related species. Indeed, in many studies, attempts are made to mini-

mize or remove the effects of size on morphology when investigating the relationship between morphology and phylogeny (e.g., Gould, 1966; Lleonart et al., 2000; Marroig and Cheverud, 2004; Zelditch et al., 2004, 2004).

The hypothesis that allometric patterns reflect functional equivalence rather than adaptations to diet and activity patterns is well supported for cranium configuration in the whole primate order (see Chapter 2). However, this was not the case for mandible configuration. At a lower systematic level, it would be expected that allometric patterns convey an important adaptive signal. Therefore, the different strepsirrhine families exhibit specialization in diet, locomotion or activity patterns. For instance, most of the Lemuridae species are cathemeral, whereas all the other strepsirrhine families, with the exception of the Indridae, only comprise nocturnal species (e.g., see Curtis and Rasmussen, 2006; Curtis et al., 1999; Tattersall, 2006). Some families display unique specializations; for example, the lorisids are characterized by a form of slow locomotion that is unique among primates (e.g., see Osman Hill, 1953). These family-specific specializations may result in different allometric patterns. For instance, limb proportions in lemurids and indriids follow different allometric relationships (Jungers, 1979). Differences in allometric patterns of the limbs are linked by Jungers (1979) to the trend difference in locomotion between the Lemuridae (arboreal and terrestrial quadrupeds) and Indridae (vertical clingers and leapers). Hence, it may be asked whether family-specific allometric patterns also reflect differences in specialization for the cranium and the mandible in strepsirrhines.

We have addressed the following questions: does cranio-mandibular allometry differ among the strepsirrhine families? If so, can potential differences in allometry be related to differences in adaptation? Is allometry a source of homoplasy for the cranium and the mandible among strepsirrhines?

2. Materials and Methods

2.1 Sample composition

The sample consists of 112 skulls belonging to adult strepsirrhine specimens. 33 species are represented, of which 11 are Loriformes species and the remaining 22 are Malagasy lemurs. As the sample is composed of a greater number of Malagasy primate species, a greater number of specimens per species is included for the loriforms. As a whole, the extant sample consists of 48 loriform and 64 lemuriform skulls. The complete list of the specimens used in this chapter is presented in Appendix 1.

2.2 Methods

The landmark protocols used here are presented in Chapter 1, section 2.1. They correspond

to those used in Chapter 2.

2.2.1 PCA

The patterns of shape variability in the skull, cranium and mandible were assessed by performing a Principal Component Analyses (PCAs) on the shape data in linearized Procrustes space (see Chapter 1, sections 2.2 and 2.3).

2.2.2 Family-specific allometric patterns

For each pair of families, the significance of the angle of divergence between the family-specific allometric shape vectors (ASVs) was tested using resampling statistics (see Chapter 1, section 2.5). The direction of each family-specific ASV was visualized in a shape subspace formed by the first three axes of the PCA performed for the three configurations.

2.2.3 Is allometry a source of homoplasy?

In order to assess how size differs among the strepsirrhine families, one-way ANOVAs of size taking the factor "family" as the source of variation were computed for the three configurations. That way, the ANOVAs test whether inter-familial size variability is greater than intra-familial morphological variability. The extents to which the shapes of the skull, cranium, and mandible differ between the different strepsirrhine families were assessed in the following way: Canonical Variate Analyses (CVAs) were performed for the three configurations using family as the categorical variable, in order to assess whether inter-familial shape discrimination was better for data corrected for size than for raw shape data. *A posteriori* reallocation procedures were set up: each specimen was classified into the family to which it was most similar in shape. In order to assess whether inter-familial shape discrimination was better for data corrected for size than for raw shape data, CVA were performed on both raw data and data corrected for size. In a manner similar to that followed in Chapter 2, shape data corrected for size consisted of shape residuals resulting from the projection of the specimens on the common allometric shape vector (CASV). Here, the CASV was computed as the mean of the family-specific ASVs.

A higher percentage of correct *a posteriori* reallocation of shape data corrected for size would indicate that allometry is an important source of homoplasy.

2.2.4 Ancestral character estimation

Unambiguous fossil data are lacking for stem toothcombed strepsirrhines. However, we wanted to determine if it is possible to estimate the ancestral morphology of toothcombed strepsirrhines with confidence using the morphology of their extant representatives as the sole piece of information. On the basis of a hypothesis of phylogeny, the method of independent contrasts (Felsenstein, 1985) can be used to produce estimates of the phenotype at the nodes of a phylogenetic tree (see Garland et al., 1999, 1999). This method hypothesizes that continuous-valued

characters evolve through time following a specific model: the *Brownian motion* model of character evolution. This model of character change is acceptable under the neutral theory of phenotypic evolution (Felsenstein, 1985; Lynch, 1990). Such a model postulates that at some point on an evolutionary tree, the value of a character follows a Gaussian distribution. The variance of the character is proportional to the distance from the root node. Such a model certainly accounts well for evolutionary phenomena such as drift. However, evolutionary trends (Garland et al., 1999), selection or non-independence of characters due to phylogenetic constraints violate the hypothesis of *Brownian motion* evolution of characters. One must keep in mind that any violation of the *Brownian motion* model of character evolution will lead to biased estimations of the ancestral state of characters. However, independent contrasts may still provide a convenient null hypothesis to estimate the ancestral morphology of toothcombed strepsirrhines.

A subset of the phylogeny compiled by Spoor et al. (2007), in which only strepsirrhine species are kept, was used for the purpose of this analysis. The genera *Allocebus*, *Mirza*, and *Phaner* were integrated into this hypothesis of phylogeny following Roos et al. (2004). Species-specific mean shape configurations, consisting of Procrustes residuals, were used as the continuous input variables at each leaf of the phylogenetic tree. Procrustes distances were then computed between the estimated ancestral shape of toothcombed strepsirrhines and all the species at the leaves of the tree. It was then possible to estimate which families are more similar in shape to that of ancestral toothcombed strepsirrhines. Of course, the results of this analysis are valid only if the hypothesis of *Brownian motion* of evolution of characters is respected, and if the retained hypothesis of phylogeny is correct.

As noted by Garland et al. (1999), the ancestral estimation values computed by independent contrasts for all the nodes except the most basal node of the phylogeny (the root node) are not optimal by any criteria. Only the root node is a global parsimony reconstruction, which is the same as that computed by maximum likelihood (Schluter et al., 1997) and phylogenetic global least square (Martins and Hansen, 1997). However, when we re-root the phylogenetic tree at all the internal nodes, independent contrasts produce the same estimates as those computed by maximum likelihood and phylogenetic global least square (Garland et al., 1999). The package “APE” (Paradis et al., 2004) of “R” software 2.4 (Ihaka and Gentelman, 1996) was used to conduct the analysis of ancestral character estimation. “APE” provides methods to re-root phylogenetic trees, and to compute ancestral values of continuous characters using the method of independent contrasts.

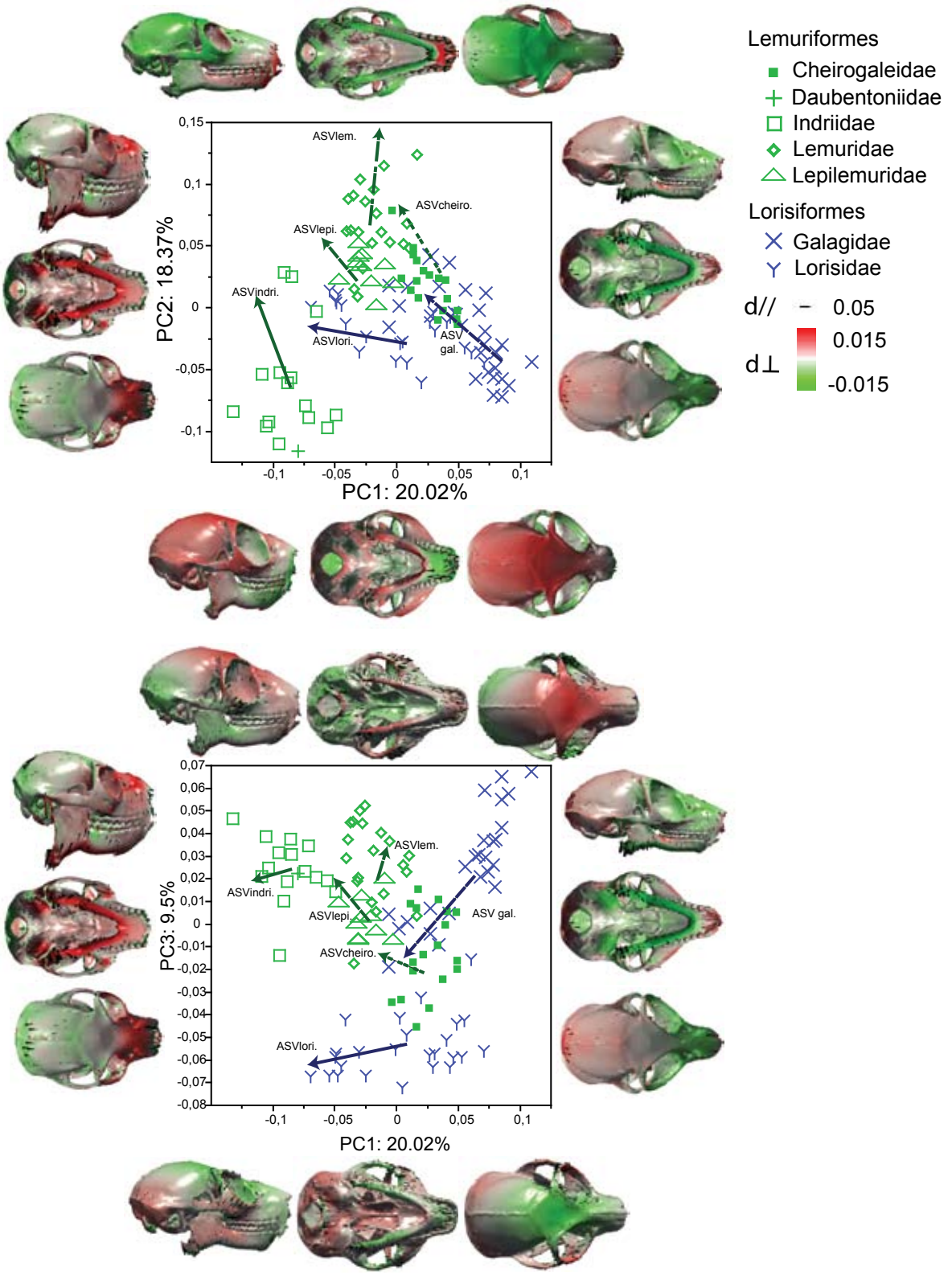

Figure 4.1: PCA of skull shape in extant strepsirrhines and associated patterns of shape variation. The skull of *Lepilemur ruficaudatus* is used to represent the deformations along the axes. The arrows represent the projections of the family-specific ASVs in PC1-PC2 and PC1-PC3 spaces. The lengths represent displacements of 0.1 in linearized Procrustes shape space along each vector. ASV cheiro, ASV gal, ASV indri, ASV lem, ASV lepi, ASV lori: ASVs computed respectively for the Cheirogaleidae, Galagidae, Indridae, Lemuridae, Lepilemuridae and Lorisidae. d//: displacement parallel to the surface. $d^{\perp}$: displacement perpendicular to the surface. Scales are in centroid size units.

3. Results

3.1 General patterns of shape variability

3.1.1 Whole skull (cranium + mandible):

The first principal component (PC1), which accounts for 20.02% of the total shape variance, summarizes the differences in skull shape between the indriids and the smallest galagid species. The other specimens project centrally on this axis. The shape differences corresponding to changes along PC1 are presented in Figure 4.1. Indriids display mandibles with high corpora, well-developed angular processes, and long and high mandibular symphyses. Such features correspond to the shape deformation associated with low values of projection on PC1 (see Figure 4.1). Indriids present crania with relatively more convergent and frontated orbits, and a shorter snout than the specimens belonging to other families. Skull shapes that project to high values on PC1 exhibit mandibles with gracile corpora, reduced gonial regions, and short and low symphyses. At the negative extreme of PC1, the crania display comparatively larger and less convergent orbits and a relatively larger braincase. Projection scores on PC1 are significantly correlated with the logarithm of centroid size (r^2=0.48; $p<0.001$). PC2 accounts for 18.37% of the total shape variance and separates the family Lemuridae from the other groups, especially the indriids, and the loriforms to a smaller extent. Lemurids, with the exception of the genus *Hapalemur*, display long snouts and long and low mandibles with a short mandibular symphysis. PC2 is also significantly correlated with the logarithm of centroid size (r^2=0.08; p=0.003). PC3 accounts for 9.5% of the total shape variance and separates the lorisids from other families. Lorisids display a high degree of orbital convergence and a low degree of frontation, and their orbits are orientated upwards. The galagids project the most in opposition to the lorisids on PC3. Galagids differ from the lorisids in their orbital region: they exhibit relatively less convergent orbits, which point in a more forward direction. The families Lepilemuridae, Cheirogaleidae and, to a lesser extent, Galagidae are not clearly discriminated on the first three PCs.

3.1.2 Cranium

PC1 accounts for 23.47 % of the total sample shape variance (Figure 4.2) and differentiates small species of galagids from the indriids and large lorisids. The crania of small galagids exhibit a relatively larger braincase, a relatively narrower snout, and large divergent orbits, whereas lorisids and indriids display comparatively smaller braincases, smaller and more convergent orbits, and a large snout. PC1 is significantly correlated with the logarithm of centroid size (r^2=0.44; $P<0.001$). PC2 accounts for 15.23 % of the total variance, and separates the lemurids from other taxa. PC2 describes shape variation related to the relative length of the snout and the configuration of the orbits. On the negative pole of PC2, crania exhibit a relatively

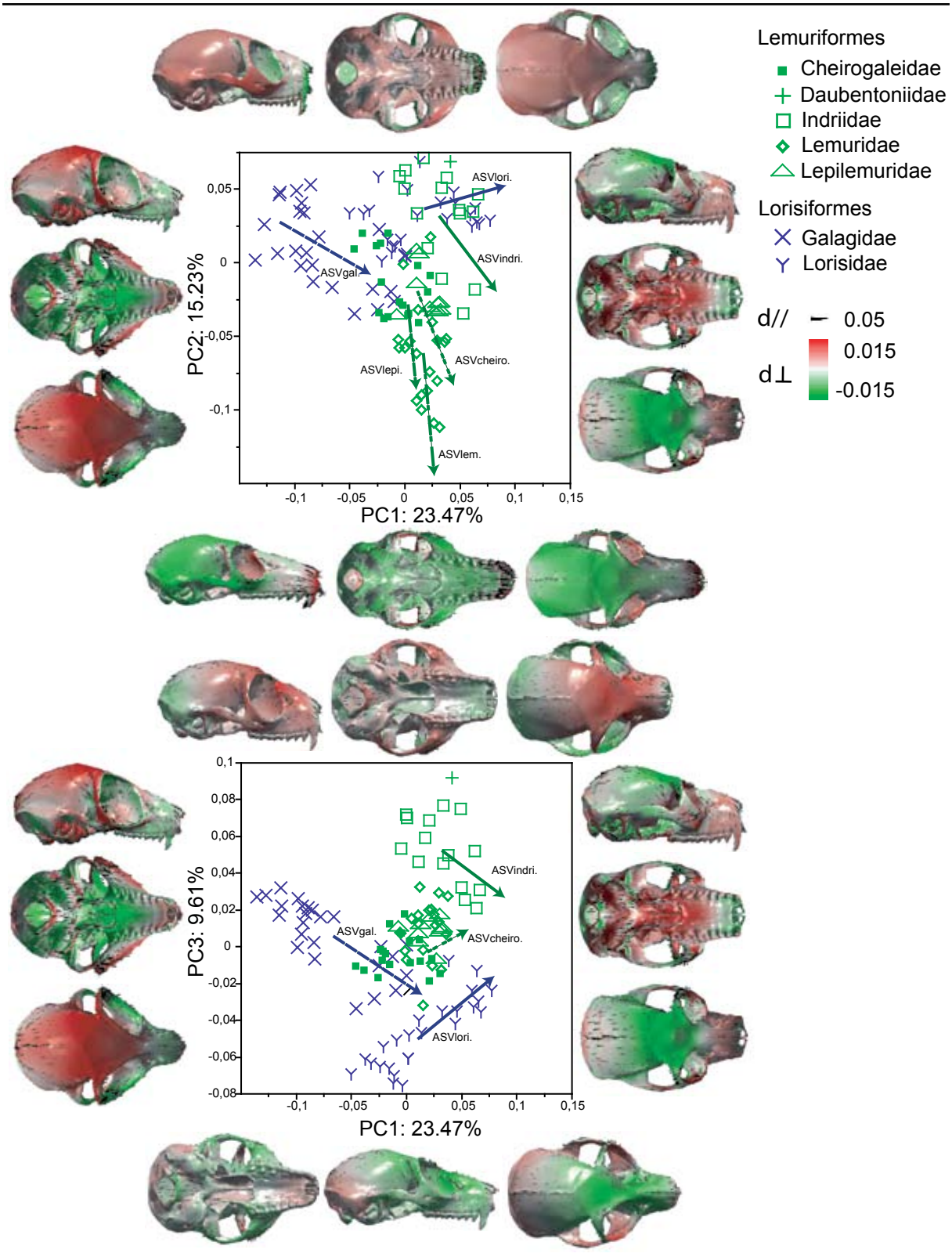

Figure 4.2: PCA of cranial shape in extant strepsirrhines and associated patterns of shape variation. The cranium of *Lepilemur ruficaudatus* is used to represent the deformations along the axes. The arrows represent the projections of the family-specific ASVs in PC1-PC2 and PC1-PC3 spaces. The lengths represent displacements of 0.1 in linearized Procrustes shape space along each vector. ASV cheiro, ASV gal, ASV indri, ASV lem, ASV lepi, ASV lori: ASVs computed respectively for the Cheirogaleidae, Galagidae, Indriidae, Lemuridae, Lepilemuridae and Lorisidae. d//: displacement parallel to the surface. d⊥: displacement perpendicular to the surface. Scales are in centroid size units.

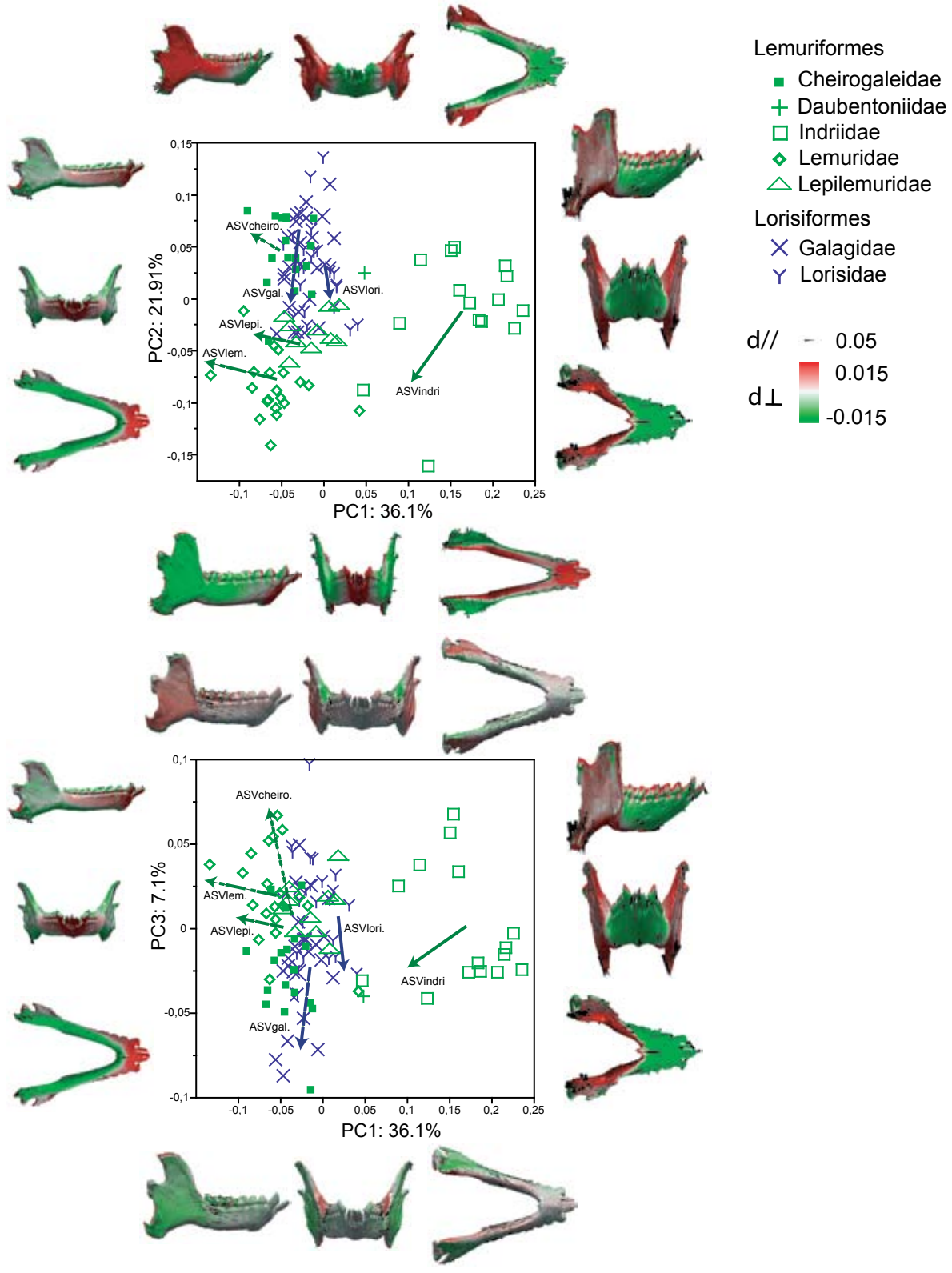

Figure 4.3: PCA of mandibular shape in extant strepsirrhines and associated patterns of shape variation. The cranium of *Lepilemur ruficaudatus* is used to represent the deformations along the axes. The arrows represent the projections of the family-specific ASVs in PC1-PC2 and PC1-PC3 spaces. The lengths represent displacements of 0.1 in linearized Procrustes shape space along each vector. ASV cheiro, ASV gal, ASV indri, ASV lem, ASV lepi, ASV lori: ASVs computed respectively for the Cheirogaleidae, Galagidae, Indriidae, Lemuridae, Lepilemuridae and Lorisidae. d//: displacement parallel to the surface. d⊥: displacement perpendicular to the surface. Scales are in centroid size units.

longer snout, a comparatively smaller neurocranium and divergent orbits. The specimens that project to high values on PC2 display crania with a shorter snout, more convergent orbits and a relatively more developed neurocranium. PC3 accounts for 9.5% of the variance in shape and separates extant indriids and *Daubentonia* from the lorisids. The crania of extant indriids have comparatively more frontated and less convergent orbits (features they share with *Daubentonia*) than the lorisids, which are characterized by crania harboring more convergent orbits orientated upwards. PC3 scores are significantly correlated with the logarithm of centroid size (r^2=0.1; p=0.004), probably because most indriids and *Daubentonia* are larger than the lorisids.

3.1.3 Mandible

PC1 accounts for 36.1 % of the total shape variance (Figure 4.3). PC1 describes patterns of variation in shape differentiating the mandibles of extant indriids and those belonging to other strepsirrhine species. PC2 accounts for 21.91% of the total shape variance, and is significantly correlated with the logarithm of centroid size (r^2=0.41; p<0.001). PC2 separates small mandibles exhibiting a wide angle between the two branches of the mandible from large and narrow

Tables 4.1-3: Pairwise comparisons of family-specific allometric shape vector (ASV) directions. Upper matrix: cosine of the angle of divergence computed for each pair. Negative values indicate an angle of divergence superior to 90°. Lower matrix: significance of this angle estimated by the resampling procedure. "*": p<0.05. "": p<0.005 "-": p>0.0.5. (see Chapter 1, section 2.5 for further details on the methodology).**

Table 4.1: skull configuration

	Galagidae	Lorisidae	Cheirogaleidae	Indridae	Lemuridae	Lepilemuridae
Galagidae	/	0.478	0.458	0.505	0.198	0.318
Lorisidae	**	/	0.2	0.185	0.028	0.261
Cheirogaleidae	**	**	/	0.371	0..356	0.274
Indridae	**	**	**	/	0.404	0.248
Lemuridae	**	**	**	**	/	0.35
Lepilemuridae	**	**	**	*	-	/

Table 4.2: cranium configuration

	Galagidae	Lorisidae	Cheirogaleidae	Indridae	Lemuridae	Lepilemuridae
Galagidae	/	0.402	0.524	0.507	0.310	0.303
Lorisidae	**	/	0.121	0.095	0.05	0.119
Cheirogaleidae	**	**	/	0.121	0.366	0.228
Indridae	**	**	**	/	0.371	0.271
Lemuridae	**	**	**	**	/	0.459
Lepilemuridae	**	**	*	**	-	/

Table 4.3: mandible configuration

	Galagidae	Lorisidae	Cheirogaleidae	Indridae	Lemuridae	Lepilemuridae
Galagidae	/	0.55	-0.219	-0.009	-0.215	-0.086
Lorisidae	*	/	-0.116	-0.026	-0.389	-0.09
Cheirogaleidae	**	**	/	-0.009	0.322	0.366
Indridae	*	*	*	/	0.459	0.129
Lemuridae	**	**	-	-	/	0.555
Lepilemuridae	**	**	-	-	-	/

mandibles. Small mandibles are relatively shorter and exhibit lower condyles and lower coronoid processes. Large mandibles are comparatively longer, display condyles at a higher position relatively to the alveolar plane and display comparatively vertically higher corpora.

3.2 Family-specific allometric patterns

There are marked differences in the direction of the family-specific ASVs (see Tables 4.1-3). With respect to the mandible configuration, in several pairs of families, the divergence in interspecific allometric direction is greater than 90° (see Table 4.3). In most pairs of families, and for the three configurations, the family-specific ASVs diverge significantly.

The directions of the family-specific ASVs in shape space are presented in Figure 4.1, Figure 4.2 and Figure 4.3

3.2.1 Skull and cranium configurations

All pairs of family-specific ASVs are found to diverge significantly, except the pair involving the Lemuridae and Lepilemuridae (see Table 4.1 and Table 4.2). However, all families still display ASVs that project in the same general direction in the space defined by the first three principal components (see Figure 4.1 and Figure 4.2). Only the lorisids differ markedly from other families in their interspecific cranial allometric patterns (see Figure 4.2). The largest lorisid species (belonging to the genera *Nycticebus* and *Perodicticus*) exhibit rather short snouts. In other families, the larger crania tend to exhibit relatively larger and longer snouts than the smaller ones (see Figure 4.2).

As a whole, the directions of the different ASVs correspond to the general allometric patterns of shape change already described in Chapter 2 for the whole primate order.

3.2.2 Mandible

The families Lemuridae, Lepilemuridae and Cheirogaleidae exhibit ASVs, the directions of which do not significantly diverge from one another (see Table 4.3). Conversely, the Lorisidae and Galagidae exhibit ASVs that diverge considerably from those of lemuriform families. Which morphological features account for the large difference between lemuriforms and loriforms in allometry? There is a difference in trend between the mandibles of 1) Galagidae and Lorisidae and 2) Cheirogaleidae, Lemuridae and Lepilemuridae (see Figure 4.4 and Figure 4.5). The largest galagids and lorisids exhibit robust, vertically high corpora as well as high condyles relatively to the alveolar plane and extended coronoid processes. The combination of these features gives the mandible a robust aspect (for example, *Perodicticus potto* and *Otolemur crassicaudatus* in Figure 4.4). In contrast, most of the largest cheirogaleids, lemurids and lepilemurids tend to exhibit relatively lower corpora and lower coronoid processes that point posteriorly, giving the mandible a gracile and elongated aspect (for example, *Cheirogaleus major*, *Varecia*

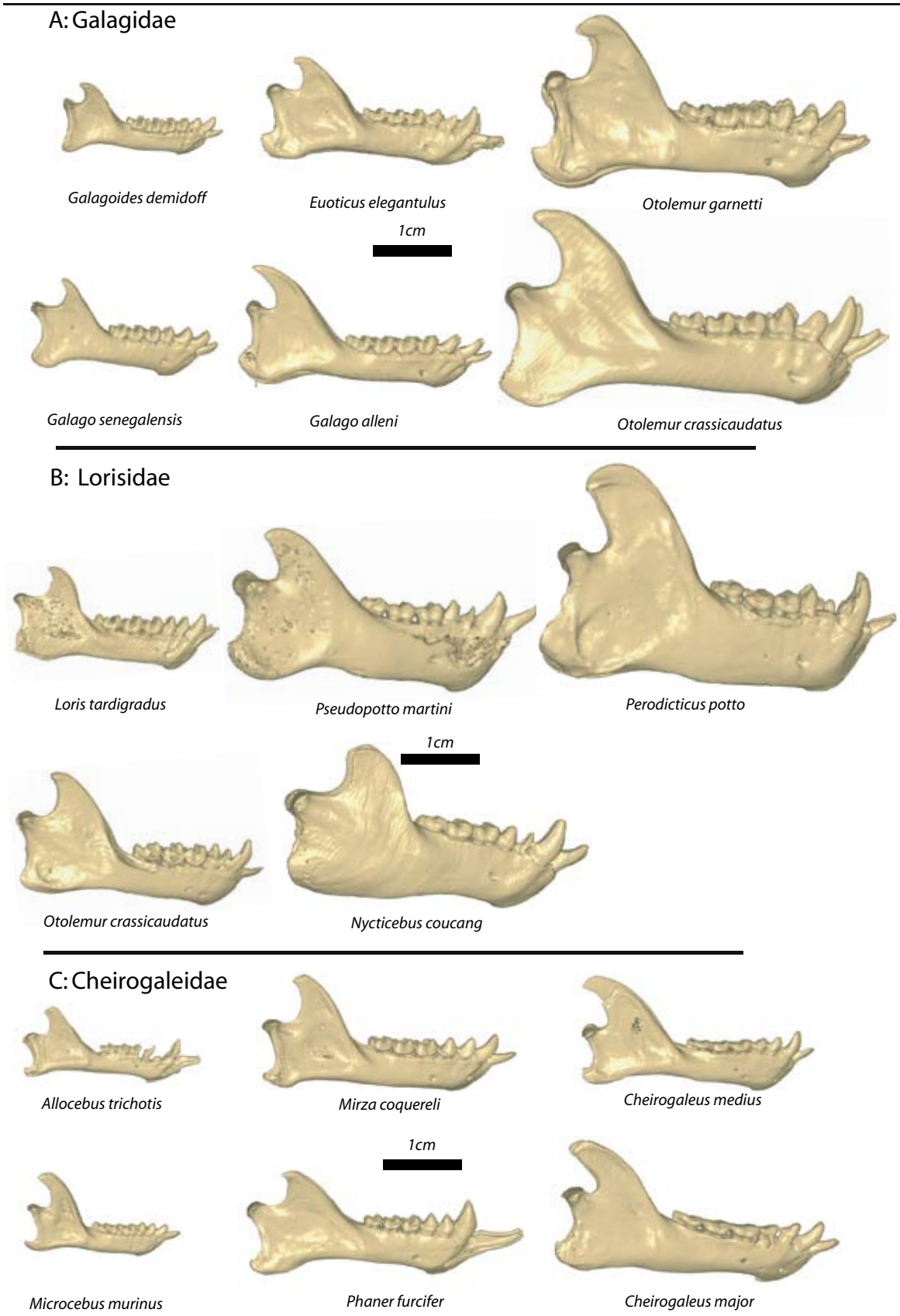

Figure 4.4: Mandibles belonging to different species of Galagidae, Lorisidae and Cheirogaleidae (virtual 3D surfaces derived from µCT image data).

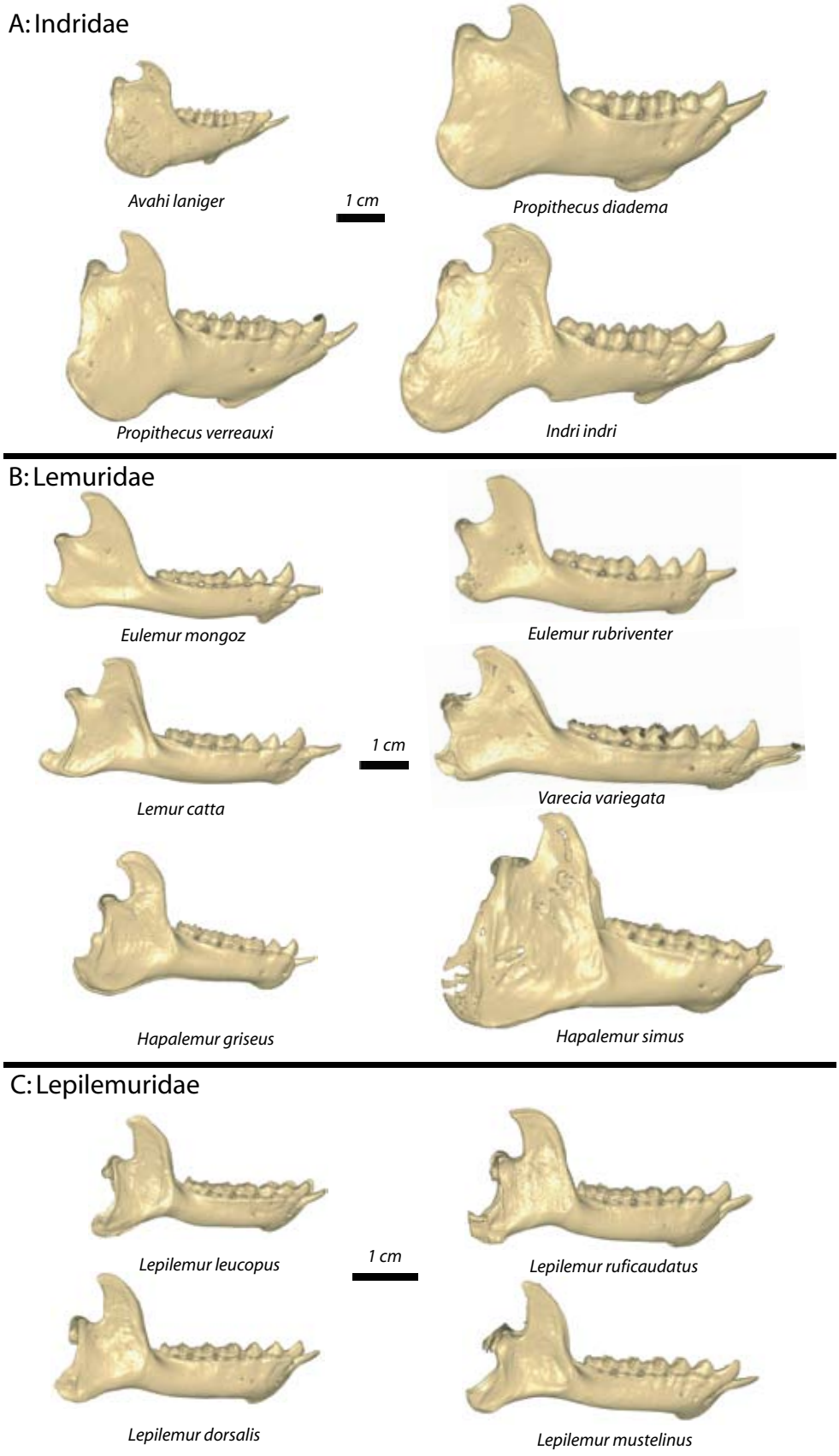

Figure 4.5: mandibles belonging to different species of Indridae, Lemuridae and Lepilemuridae (virtual 3D surfaces derived from µCT image data).

variegata and *Lepilemur mustelinus* in Figure 4.5). In lemurids, the genus *Hapalemur* constitutes an exception. The large *Hapalemur simus* exhibits a strongly developed angular region and a robust corpus, which reminds the typical indriid configuration (Figure 4.5). *Microcebus murinus* differs widely from all the other small species since it harbors highly developed coronoid processes that point upwards. In that respect, the mandibular shape of *Microcebus* shares morphological similarities with the mandible of the large *Otolemur garnetti* (Figure 4.4).

3.3 Morphology is distinctive at the family level

Table 4.4: Intra-familial and inter-familial variation in size. The intra-familial and inter-familial variations are compared using one-way analyses of variance of the centroid size, taking the factor "family" as the source of variation. *Daubentonia* is not included because only one specimen of this genus could be digitized. The genus *Archeolemur* is neither included.

	Effect	Df	Mean squares	F	P
Skull	Family	5	35129	38.8	$<10^{-15}$
	Residuals	107	905		
Cranium	Family	5	25402	38.4	$<10^{-15}$
	Residuals	107	661		
Mandible	Family	5	7186	34.7	$<10^{-15}$
	Residuals	107	207		

3.3.1 Size and shape differ across the families

For the three configurations, size and shape differ significantly across the strepsirrhine fami-

Table 4.5: Classification procedure derived from the CVA performed on the skull, taking "family" as the categorical variable. Top table: data not corrected for size. Bottom table: data corrected for size.

Shape data not corrected for size:

	Cheirogaleidae	Galagidae	Indridae	Lemuridae	Lepilemuridae	Lorisidae	%success
Cheirogaleidae (18)	18						100%
Galagidae (25)		23		1		1	92%
Indridae (15)			13	1	1		87%
Lemuridae(20)				19		1	95%
Lepilemuridae(10)					10		100%
Lorisidae(25)						25	100%
Total (113)							Total:96%

Shape data corrected for size:

	Cheirogaleidae	Galagidae	Indridae	Lemuridae	Lepilemuridae	Lorisidae	%success
Cheirogaleidae (18)	18						100%
Galagidae (25)		25					100%
Indridae (15)			15				100%
Lemuridae(20)				20			100%
Lepilemuridae(10)					10		100%
Lorisidae(25)						25	100%
Total (113)							Total:100%

Table 4.6: Classification procedure derived from the CVA performed on the cranium, taking "family" as the categorical variable. Top table: data not corrected for size. Bottom table: data corrected for size.

Shape data not corrected for size:

	Cheirogaleidae	Galagidae	Indridae	Lemuridae	Lepilemuridae	Lorisidae	%success
Cheirogaleidae (18)	18				1		100%
Galagidae (25)	1	22		1		1	88%
Indridae (15)			12	2	1		80%
Lemuridae(20)				18	1	1	90%
Lepilemuridae(10)					100		100%
Lorisidae(25)						25	100%
Total (113)							Total:93%

Shape data corrected for size:

	Cheirogaleidae	Galagidae	Indridae	Lemuridae	Lepilemuridae	Lorisidae	%success
Cheirogaleidae (18)	18						100%
Galagidae (25)		25					100%
Indridae (15)			15				100%
Lemuridae(20)				20			100%
Lepilemuridae(10)					10		100%
Lorisidae(25)						25	100%
Total (113)							Total:100%

Table 4.7: Classification procedure derived from the CVA performed on the mandible, taking "family" as the categorical variable. Top table: data not corrected for size. Bottom table: data corrected for size.

Shape data not corrected for size

	Cheiro.	Galagidae	Indridae	Lemuridae	Lepilemuridae	Lorisidae	%success
Cheirogaleidae (18)	13	5					72%
Galagidae (25)	4	18				3	72%
Indridae (15)			14		1		93%
Lemuridae(20)				20			100%
Lepilemuridae(10)					10		100%
Lorisidae(25)						25	100%
Total (113)							Total:89%

Shape data corrected for size

	Cheiro.	Galagidae	Indridae	Lemuridae	Lepilemuridae	Lorisidae	%success
Cheirogaleidae (18)	14	4					78%
Galagidae (25)	5	18				2	72%
Indridae (15)		1	13		1		87%
Lemuridae(20)				20			100%
Lepilemuridae(10)					10		100%
Lorisidae(25)	1	1		1		22	88%
Total (113)							Total:86%

lies (Table 4.4).

3.3.2 Canonical Variate Analyses:

Inter-familial shape discrimination is better when shape data corrected for size for the skull and the cranium configurations are used; when the effect of allometry is removed, the percentage of correct reallocation reaches 100% (see Tables 4.5, 4.6). For mandible configuration, discrimination is not better when using shape data corrected for size (see Table 4.7). All the misclassified mandibles of galagids are reallocated to the Cheirogaleidae family, and most of

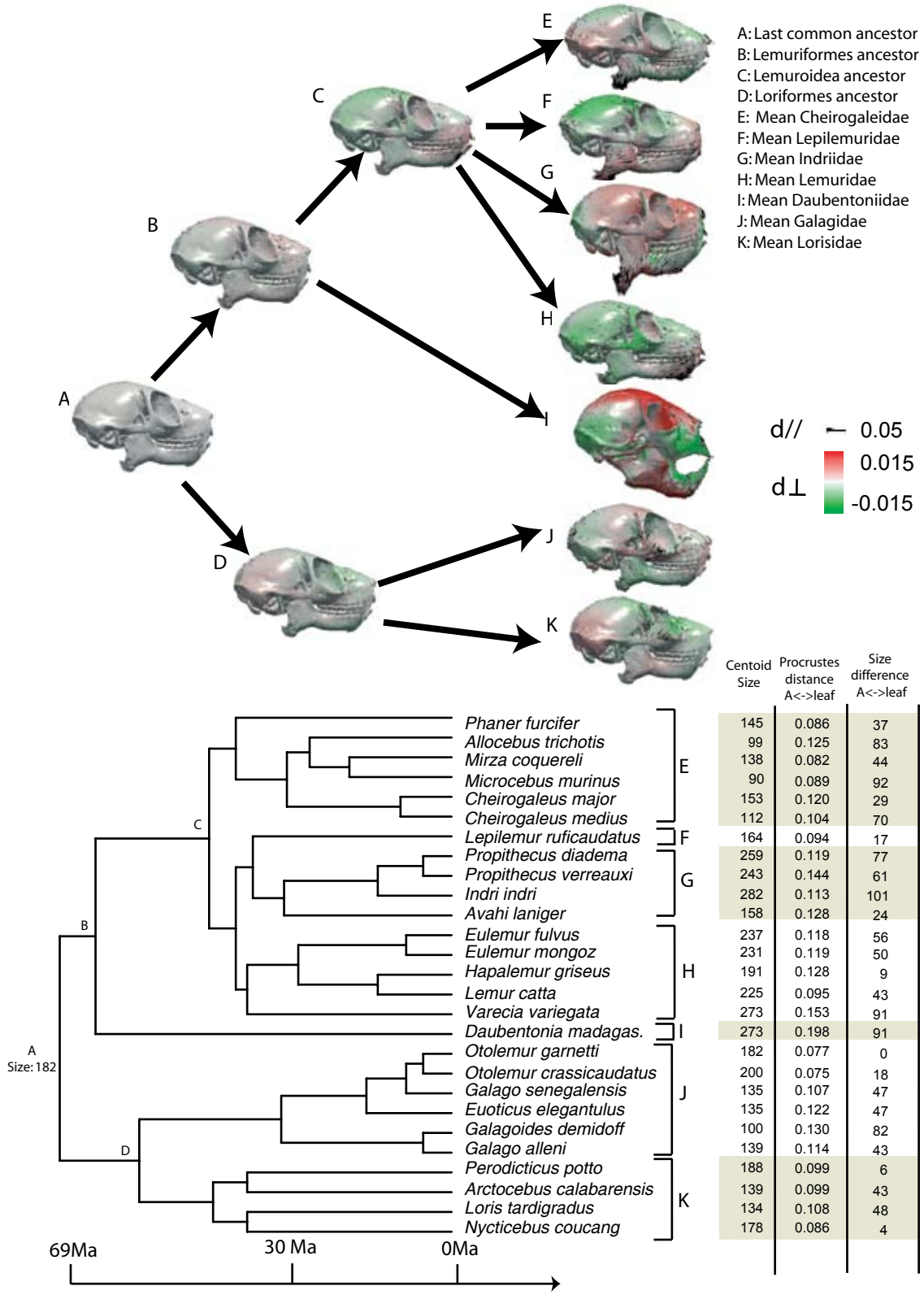

Figure 4.6: Estimation of the ancestral strepsirrhine skull morphology using the phylogenetic independent contrasts method. The associated phylogeny is a subset from the set compiled by Spoor et al. (2007). The associated molecular dating also came from Spoor (2007). This hypothesis of phylogeny is only slightly modified to incorporate the genera *Allocebus*, *Mirza*, and *Phaner*. The skulls of *Lepilemur ruficaudatus* (A,B,C,D,E,F,G,H,J,K) and of *Daubentonia madagascariensis* (I) are used as templates to represent the evolution of skull shape in toothcombed strepsirrhines. d//: displacement parallel to the surface. d⊥: displacement perpendicular to the surface. Scales in centroid size units.

the misclassified mandibles of cheirogaleids are reallocated to the Galagidae family.

3.4 Estimation of the ancestral morphology of toothcombed strepsirrhines.

The results of the comparative analysis using independent contrasts are presented in Figure 4.6. Under the Brownian motion model of character evolution, *Daubentonia* exhibits the highest Procrustes distance from the estimated ancestral strepsirrhine morphology. In contrast, the galagid *Otolemur crassicaudatus* and the cheirogaleid *Mirza coquereli* display the shortest Procrustes distance to the reconstructed ancestral shape. The smallest values of Procrustes distances between the computed ancestral morphology and each species are found in the Galagidae, Cheirogaleidae, Lepilemuridae and Lorisidae families. The shape computed at the basal root of the tree resembles that of Cheirogaleidae and Galagidae (Figure 4.6).

4. Discussion

4.1 Allometry

4.1.1 Cranium

In the current analysis, discrimination between the strepsirrhine families is improved using data corrected for size of the cranium and the skull configurations. Allometry differs across the families. However, the family-specific allometric patterns are still similar enough across the families to allow for the computation of a CASV that can be used to remove efficiently the effect of allometry from shape data. Therefore, for the cranium, the results support the hypothesis that allometry mainly reflects functional equivalence across a size range (e.g., see Lockwood and Fleagle, 1999 and Emerson and Bramble, 1993).

4.1.2 Mandibles: do differences in allometric patterns reflect differences in dietary specialization?

Conversely, it is not possible to improve the discrimination of mandibles belonging to the different strepsirrhine families using shape data corrected for size. As mentioned above, strepsirrhine families differ in their ecology. It may be expected that differences in adaptation would lead to difference in allometry. Could difference in diet across the strepsirrhine families be responsible for the high degree of variability in family-specific allometric patterns?

All Indridae and Lepilemuridae species are folivorous. In contrast, species belonging to the Cheirogaleidae, Galagidae, Lorisidae and Lemuridae families do not have homogeneous diets. In lemurids, for example, species belonging to the genus *Hapalemur* are bamboo feeding specialists (see for instance Grassi, 2006). The other Lemuridae genera are more generalist feeders, and are principally frugivorous (Mittermeier et al., 1994; Rowe, 1996; Vinyard and Hanna,

2005, and references therein). The Cheirogaleidae and Galagidae families comprise insectivore, frugivore and gummivore species. The Lorisids are principally insectivores and frugivores, and at least one species, *Nycticebus pygmaeus,* exhibits occasional gummivore behavior (Tan and Drake, 2001). If differences in diet across families influenced a lot allometry in the mandible, one would expect to find similarities in ASV direction in Lepilemuridae and Indridae because theses families comprise only folivore species. One would also expect that similar allometric patterns would be observed in the Galagidae and Cheirogaleidae families, which have mandibles that are morphologically close. However, the contrary appears to be the case, the analyses show that the allometric direction tends to be similar within the Lemuriformes and Loriformes, and widely differs between the two infraorders. Therefore, we find no strong support for the adaptive hypothesis to account for the differences in allometric patterns among the strepsirrhine families.

4.1.3 Allometry and the use of morphological information to infer phylogeny

The evidence presented here underlines the necessity to take the effect of allometry into account when attempting to extract phylogenetically relevant information from geometric morphometric data sets. This statement applies not only to geometric morphometric data but may

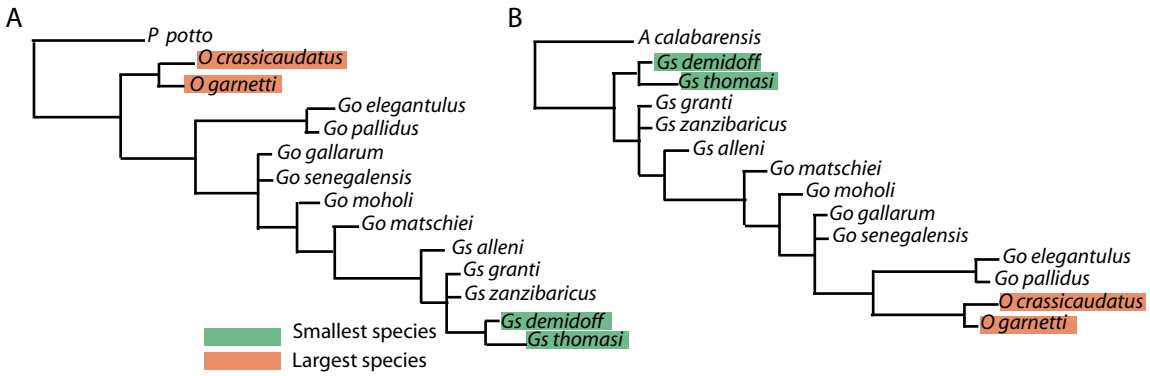

Figure 4.7: Cladistic reconstructions of the phylogeny of the Galagidae using morphological data, modified from Masters and Brothers (2002). A: Outgroup = *Perodicticus potto*. B: Outgroup = Arctocebus calabarensis. Taxonomy conserved from the original publication. Go: *Galago*. O: *Otolemur*. Gs: *Galagoides*. P: *Perodicticus*. A : *Arctocebus*.

be generalized to morphological information (Lockwood and Fleagle, 1999). Morphological cladistic reconstructions of phylogenetic relationships are based on the analysis of discrete morphological characters. Allometry is a source of homoplasy (Lockwood and Fleagle, 1999). Therefore, when attempting to infer phylogenetic relationships, one should exclude as many morphological characters influenced by size as possible. A very clear example of the influence of allometry in phylogenetic reconstructions is provided by the study of Masters and Brothers (2002). In an attempt to reconstruct the phylogeny of the Galagidae from a set of morphological data, Masters and Brothers (2002) found that the choice of the outgroup tends to signifi-

cantly influence the resulting tree. When the large-bodied lorisid *Perodicticus potto* was used as the outgroup (see Figure 4.7-A), the largest galagid species belonging to the genus *Otolemur* were placed in a basal position, whereas the small-bodied *Galagoides demidoff* was placed in a terminal position. Conversely, when the smaller *Arctocebus calabarensis* was used as the outgroup (see Figure 4.7-B), *Otolemur garnetti* and *Otolemur crassicaudatus* were placed in a much more terminal position on the resulting tree. In that case, the small *Galagoides demidoff* was placed in a basal position. Therefore, the phylogenetic trees presented in the study of Masters and Brothers (2002) are considerably polarized according to size. Several cranial characters from the study of Masters and Brothers (2002) may convey more allometric signals than phylogenetically relevant information. For instance, the 18th (lateral extension of orbits beyond zygomatic arch) and 20th characters (snout length relative to orbital width) are certainly strongly influenced by allometry. Furthermore, although they explicitly admitted that their 34th character (development of sagittal cresting) is largely a function of size, they have still included it in the analysis. The use of characters strongly influenced by allometry account certainly for the results of Masters and Brothers (2002).

4.2 The ancestral morphology of toothcombed strepsirrhines

The first striking feature of the ancestral morphological estimation using the phylogenetic independent contrast method is that this model fails to predict evolutionary trends. The morphology estimated at the basal node of strepsirrhines is extremely encephalized. The trend towards an increase in encephalization in strepsirrhine primates is well documented in the fossil record (Jerison, 1979). It is extremely unlikely that the common ancestor of modern toothcombed strepsirrhines possessed such a large braincase.

Considering this fact, we may approximate the selective pressure for an increase in encephalization as a constant through time during strepsirrhine evolution. Under this hypothesis, the morphological differences between the computed ancestral shape (see Figure 4.6-A) and the leaves of the tree (extant specimens) may still be meaningful. Under this hypothesis, could the *Brownian motion model* of evolution apply to the evolution of the strepsirrhine skull? This model postulates that the characters under study evolve randomly through time, and are therefore not determined by selection or specialization. Several taxa, among which *Daubentonia* is the most salient example, present extremely specialized morphologies. The existence of such a derived and specialized species provides evidence that the evolution of the strepsirrhine skull did not occur following a *Brownian motion model* of evolution. Therefore, the method of phylogenetic independent contrasts cannot give strong support to the hypothesis of Charles-Dominique and Martin (1970). Finally, we would like to stress on the fact that the *Brownian motion model* of evolution of characters represents a far too stringent hypothesis: this model proved to be of little help to depict the evolutionary morphology of toothcombed strepsirrhines. We want

to warn the reader regarding its use in such broad phylogenetic contexts.

The analyses of the skull, cranium, and mandible reveal that the Cheirogaleidae and Galagidae families share strong morphological similarities for these structures. For the three configurations, all of the families except the Cheirogaleidae and Galagidae are well separated in PC space. The results do not contradict the hypothesis of Charles-Dominique and Martin (1970), and the Cheirogaleidae and Galagidae may have retained a lot of the ancestral strepsirrhine condition. However, does this hold for most of the anatomical characters they share?

Among the different parts of the skull, the basicranium is thought to hold a lot of phylogenetic information (for a review, see MacPhee and Cartmill (1986). Molecular evidence supports the hypothesis that the Cheirogaleidae family is part of the Lemuriformes infraorder, and that *Daubentonia* is basal to all Malagasy primates (e.g., see Roos et al., 2004; Yoder et al., 1996). Therefore, among all the skull characters shared by Cheirogaleidae and Galagidae, it may be asked whether the basicranial characters they share consist of symplesiomorphies or result from parallelism. In particular, cheirogaleids and loriforms share similarities in their blood supply system for the brain, with both groups presenting an ascending pharyngeal artery. This feature has been considered by morphologists as a possible synapomorphy uniting the two families (Cartmill, 1975; Szalay and Katz, 1973). However, *Daubentonia,* which is basal to all Malagasy primates, does not present this character. No lemuriform family presents an ascending pharyngeal artery except the Cheirogaleidae. This character is not present in the Eocene adapiforms, considered as the sister group of the modern strepsirrhines (e.g., see Dagosto, 1994; Kay et al., 1997; Kay et al., 2004; Marivaux et al., 2001; Rosenberger, 1985), or as a group that may comprise the ancestors of toothcombed strepsirrhines (Beard et al., 1988; Beard and Godinot, 1988; Dagosto, 1988; Godinot, 1998, 2006). Therefore, the ascending pharyngeal artery is likely to be a derived feature that has emerged independently in Loriformes and one family of Lemuriformes, the Cheirogaleidae, and is not homologous for the two infraorders (but see Yoder, 1991). Therefore, at least some of the morphological similarities between the Cheirogaleidae and Galagidae families do not reflect the retention of ancestral features, but result from parallel evolution. New fossil evidence from stem toothcombed strepsirrhines is required in order to assess the importance of parallel evolution between the two families.

SUMMARY OF CHAPTER 4

Among the strepsirrhines, a popular hypothesis is to consider that the Cheirogaleidae and Galagidae have retained the most the ancestral strepsirrhine condition (Charles-Dominique and Martin, 1970). This hypothesis is examined for the skull using a geometric morphometric approach. The usefulness of phylogenetically-based comparative methods for estimating the morphology of the ancestors of modern strepsirrhines is investigated.

Allometric patterns are examined at the familial level. It is asked whether familial-specific allometry reflects adaptation or reflects functional maintenance across size range.

New arguments are provided to support the hypothesis that, among toothcombed strepsirrhines, cheirogaleids and galagids have retained the most the ancestral strepsirrhine skull morphology. This is especially true for the mandible, where close morphological affinities exist between the two families.

Evolutionary trends such as the increase of encephalization, which has occurred throughout the history of strepsirrhines, violate the *Brownian motion* model of character evolution upon which the phylogenetically-based comparative method relies. This method thus certainly fails to estimate the ancestral morphology of toothcombed strepsirrhines.

Allometric patterns differ relatively little across the strepsirrhine families for the cranium, favoring the hypothesis that allometry plays a major role in functional maintenance. For the mandible, there is a trend difference between the Lemuriformes and Loriformes infraorders in allometry that cannot be related to differences in dietary specialization across the families.

Chapter 5

The developmental origin of the diversity in the strepsirrhine skull.

Contents

1. Introduction

Modification of ontogeny has been recognized for a long time as an important source of morphological innovation. Since Haeckel (1866), the identification of general rules by which ontogeny (growth + development) and phylogeny are related has been an important issue in evolutionary biology. One powerful approach to studying the link between ontogeny and phylogeny centers on the notions of heterochrony and heterotopy: the temporal and spatial mechanisms of change in ontogeny. These concepts convey the idea that shifts in the timing and position of developmental events play a central role in the generation of new morphologies. Heterochrony is recognized when the timing of an event changes in relation to other events. Heterochronic and heterotopic processes that impinge on ontogenetic trajectories are the proximate causes of morphological novelty. The ultimate cause may be adaptation, and differences in the paces of cranial growth, development and teeth maturation in primates may be linked to life-history parameters and strategies (see for instance Godfrey et al., 2004; Godfrey et al., 2005). The terminology of heterochrony that prevails today has been proposed mainly by Gould (1977) and Alberch et al. (1979). It provides a useful framework for comparing ontogenetic sequences. Here, a clear distinction must be made between patterns and processes. Heterochrony was originally restricted to the description of developmental patterns (changes in shape). Now, the terminology has been extended to the analysis of growth (changes in size), and more recently to the analysis of the genetic processes responsible for observed differences in developmental patterns (e.g., see Ambros, 1997; Moss, 2007; Slack and Ruvkun, 1997). In this chapter, a top-down approach is followed: differences in morphological *patterns* are described within the framework of heterochrony. Only then can hypotheses concerning the evolution of the underlying morphogenetic *processes* be proposed.

Geometric morphometrics (GM) constitutes a powerful approach for quantifying phenotypic changes that occur during ontogeny: it allows growth and development to be analyzed separately. Furthermore, this approach permits to analyze complex patterns of shape variability in a visually comprehensive manner. Recent model considerations (Zollikofer and Ponce de León, 2004) suggest that similar ontogenetic processes may result in parallel ontogenetic trajectories in morphospacce, which can eventually be interpreted within the framework of heterochrony. Hence, homology in *patterns* may result from homologous underlying *processes.*

Studies exploring ontogenetic patterns among strepsirrhines rely on linear morphological measurements. The use of linear measurements has proven to be a powerful method in studies interpreting differences in patterns of morphological changes during ontogeny within the framework of several ecological hypotheses (see Godfrey et al., 2004; Godfrey et al., 2005; Smith, 2000). However, they convey little about the overall shape and size changes that occur in the mandible and the cranium during ontogeny, and how differences in ontogenetic trajectories influence morphological variability. Here, a GM approach is used to investigate the morpho-

logical diversity of strepsirrhines from the perspective of evolutionary developmental biology, i.e., in terms of differences in patterns of ontogeny.

In Chapter 2, the following hypothesis was proposed: the difference in the morphology of the skull between haplorrhines and strepsirrhines result from phylogenetic constraints. Here, this hypothesis is investigated from an evo-devo perspective: are there marked differences in the patterns of development and growth in haplorrhines and strepsirrhines? If strepsirrhine and haplorrhine ontogenetic trajectories differ markedly in direction, length, and position, it would support the hypothesis that differences in developmental constraints are responsible for the morphological differences between the two suborders.

In Chapter 4, greater morphological diversity was observed in lemuriforms than in the loriforms for the skull. This chapter attempts to explain the difference in morphological variability between the two strepsirrhine infraorders from an evo-devo perspective. The following issues are investigated: are there trend differences in ontogenetic trajectory length, direction, and position across strepsirrhine species? Do differences in postnatal ontogenetic trajectories in lemuriforms and loriforms explain the higher diversity in the morphology of the skull of Malagasy lemurs? What is the relative importance of prenatal and postnatal morphogenetic processes in the overall morphological variability?

Patterns of allometric grade in lemuriforms and loriforms are also investigated. Shifts in allometric grade (also referred to as allometric transposition by Meunier, 1959) relate to the uncoupling of size and shape across taxa. According to a hypothesis formulated by Gould (1971), patterns of allometric transposition are expected to occur in contexts of rapid diversification. Strepsirrhines provide an ideal test case to evaluate the hypothesis of Gould, since the different families specific to the Lemuriformes infraorder are thought to have differentiated rapidly in Madagascar (e.g., Martin, 1972; Yoder, 1997; Yoder and Yang, 2004). Thus, if the hypothesis of Gould is correct, one would expect to observe wide differences in allometric grade across Lemuriformes species. Conversely, one would expect to observe fewer differences in allometric grade among loriform species.

One last issue is investigated here. Yoder et al. (1996) suggested that the divergence between Lemuriformes and Loriformes took place 62 million years ago. The estimates of Bayesian and maximum likelihood models are always older than 63.3 million years for this node (Yang and Yoder, 2003). Furthermore, Yoder and Yang (2004), using multiple gene loci and several calibration points, proposed that the last common ancestor of lemuriforms lived between 62 and 65 million years. Such estimates imply that strepsirrhines differentiated during the earliest Paleocene or during the Cretaceous. Such estimates also imply that if the toothcomb is homologous in the Lemuriformes and Loriformes infraorders, it evolved during the Cretaceous or the early Paleocene, a view that is not supported by the present state of the fossil record. The Late Eocene remains of a stem galagid, *Wadilemur elegans* (Seiffert, 2005), provide the oldest evidence of a toothcomb in strepsirrhines. Thus the alternative hypothesis has to be considered: if those es-

timates are correct, it may indicate that the toothcomb is not homologous in the Lemuriformes and Loriformes infraorders. Under this scheme, *Daubentonia*, which is assumed to be basal for lemuriforms (Roos et al., 2004), may derive from a non-toothcombed ancestor. This chapter investigates the evidence for the hypothesis of non-homology of the toothcomb across the two strepsirrhine infraorders based on sequences of tooth eruption in lemuriform and loriform species.

2. Materials and methods

2.1 Sample composition

As mentioned in Chapter 1, postnatal ontogenetic series were collected for 10 strepsirrhine species, among which were five lemuriform species (*Lemur catta, Lepilemur ruficaudatus, Microcebus murinus, Propithecus diadema,* and *Propithecus verreauxi*) and five loriform species (*Arctocebus calabarensis, Nycticebus coucang, Perodicticus potto, Galago senegalensis, Otolemur garnetti*). In addition, ontogenetic series were acquired for two haplorrhine species (*Tarsius bancanus* and *Aotus trivirgatus*). The present sample comprises 83 skulls (crania + mandibles) and one isolated cranium belonging to a juvenile individual, and 52 skulls belonging to adults. Two mandibles belonging to individuals of the genus *Propithecus* were badly preserved, and could not be included for analysis. Altogether, the sample comprises 132 crania with associated mandibles, and three crania without mandibles or with badly preserved mandibles. A comprehensive list of the juvenile specimens is presented in Appendix 1. Additionally, information on the state of dental eruption for each specimen is provided in Appendices 3.1-12.

2.2 Landmark protocol

The landmark protocols used for the cranium and the mandibular configurations differ only slightly from those used in Chapters 2 and 4. Only landmarks corresponding to the permanent last molar were omitted (see Chapter 1, section 2.1).

2.3 Common time scales

Because the absolute age of most specimens in the sample was unknown, an appropriate time scale was needed to allow for interspecific comparisons. The use of absolute ages can be a good choice when the paces of development and growth are not extremely different between the species under investigation. In the present sample, however, species range from small *Microcebus murinus*, in which females give birth for the first time when they are about one year old (Rowe, 1996), to *Propithecus diadema,* in which females have their first offspring when they are

between three and five years old (Wright, 1995). Thus, in the present case, using dental eruption information to produce relative "time" scales is a better option. Therefore, we used a continuous dental variable (dental score) and an ordinal categorical dental variable (dental stage). Godfrey et al. (2004) proposed a continuous developmental scale, which they referred to as the "dental stage". This metric is useful for interspecific comparisons, especially when species differ in their dental formulae. In the present chapter, the "dental developmental stage" variable of Godfrey et al. (2005) is referred to by the term "dental score", whereas "dental stage" refers to the five following categories: neonate, infant (M1 has not yet erupted), juvenile (M1 has erupted and M2 has not yet erupted), sub-adult (M2 has erupted, but the individual is not a dental adult), and adult (complete dentition). The dental score is roughly equivalent to the proportion of teeth that have erupted, and varies between 0 and 1. A lot of the specimens consisted of dry skulls. Therefore, when assessing the state of eruption of a given tooth, it was not possible to determine whether it emerged through the gingiva. Rather, a tooth was labeled as "emerging" when the cusps were rising from the alveoli. So one should keep in mind that these data might not be directly comparable to data sets that use gingival emergence information, since alveolar emergence can long precede gingival emergence, at least for molariform teeth (Smith, 2000). For instance, in *Lemur catta*, Smith (2000) noted that M3 is the last tooth to erupt. However, the last molars emerge from the alveoli well before P2 and P3 (see Appendix 3.3).

2.4 The allometric component of ontogenetic shape change

Ontogenetic shape change along a linear taxon-specific trajectory can be quantified by the principal shape vector (PSV), which is the first axis of a PCA performed on the taxon-specific data scatter in shape space (e.g., see O'Higgins and Jones, 1998; Vioarsdóttir et al., 2002). In addition to calculating PSVs for each species, ontogenetic allometric shape vectors (ASVs) were computed. ASVs consist of the coefficients of a multivariate regression of shape coordinates against the logarithm of centroid size. For each species, the angle between its ASV and its PSV was computed in order to assess whether these vectors were collinear.

2.5 Patterns of shape change during ontogeny

As we expected that most of the ontogenetic shape change was allometric, a common allometric shape vector (CASV) was computed for the whole sample. This vector was used to identify common patterns of allometric shape changes that occurred during ontogeny. This vector was computed as the mean of the species-specific allometric shape vectors (ASVs). It must be kept in mind that the CASV is not necessarily biologically meaningful. Rather, it represents a useful reference axis in shape space, which comprises most ontogenetic allometric signals in the sample (see Chapter 1, section 2.5). In order to characterize patterns of shape changes that

were *not* related to ontogenetic shape change, the specimens were projected on the CASV, and a Principal Component Analysis (PCA) was performed on the resulting shape residuals. The projection of the specimens on the first principal component (PC1res), as well as the associated shape variations, were reported.

The directions in CASV-PC1res space of the two suborder-specific ASVs, which were computed as the means of the species-specific ASVs constitutive of each suborder, were reported together with the direction of several species-specific ASVs of interest (see Results).

2.6 Interspecific differences in ontogenetic trajectory direction, length and position

2.6.1 Ontogenetic trajectory direction

Early and late phases of cranial development are distinct and it can therefore be expected that ontogenetic trajectories depart from linearity through shape space (Ponce de León and Zollikofer, 2006). However, because departures from linearity were small in the present sample (see Results), postnatal ontogenetic trajectories were assumed to be linear in shape space.

To test for divergence between ontogenetic allometric vectors, two resampling protocols were designed. In the first protocol, the individuals were permuted randomly without attempting to represent each dental stage. However, since adults were over-represented in some species while younger ontogenetic stages were often under-represented or in a few cases simply missing, a second protocol was also employed. The design of this second protocol was inspired by the work and recommendations of McNulty et al. (2006). The five dental stages defined in the introduction (neonates, infants, juveniles, subadults, and adults) were used. Specimens were constrained to remain within their dental stages during the process of resampling. When a dental stage was not represented in one of the two ontogenetic series, the specimens belonging to that specific stage were not incorporated into the resampled groups. In both protocols, unequal sample sizes were allowed.

The angle of divergence between ontogenetic trajectories through shape space were computed for all possible pairs of species, and for each pair of species, the statistical significance of this angle was assessed by performing two resampling procedures. For a given pair of species, when one of the two tests was significant, divergence in ontogenetic trajectories was considered confirmed.

2.6.2 Ontogenetic trajectory length

Ontogenetic shape change was approximated by the displacement in shape space along a linear vector. Under this model, the amount of postnatal shape change in a given species could be estimated by the Procrustes distance between the end points of the trajectory: shape at birth and at adulthood. Thus, in this Chapter, species-specific postnatal ontogenetic trajectory lengths

Table 5.1: Gestation period, mean dental score at birth and weaning length for the species studied (data from Grzimek, 1989; Lindenfors, 2002; Rowe, 1996). The estimation of dental sore at birth of *Perodicticus potto* is done using a late term fetus (specimen n°9606). The logarithms of the centroid sizes of the skull (SK), cranium (CR) and mandible (MD) configurations at birth and adulthood are also given. * Data from *Lepilemur mustelinus*.

	Gestation (days)	Dental score at birth	Age at first birth (year)	Weaning (days after birth)	Log(centroid size) at birth			Log(centroid size) at adulthood		
					SK	CR	MD	SK	CR	MD
Haplorrhines										
Aotus trivirgatus	133	0	2.4	75	4.686	4.606	3.62	5.23	5.103	4.32
Tarsius bancanus	178	0.33	2.52	>42d	4.369	4.277	3.371	4.758	4.633	3.857
Lemuriformes										
Lemur catta	135	0	2.01	135	4.811	4.725	3.76	5.423	5.298	4.555
Lepilemur ruficaudatus	135*	<0.4	1. 88*	75*	<4.598	<4.486	<3.694	5.058	4.932	4.195
Microcebus murinus	62	0.275	1	40	3.894	3.801	2.897	4.483	4.375	3.565
Propithecus Diadema	162	0.3	4	180	<5.056	4.545	<4.06	5.574	5.433	4.706
Propithecus verreauxi	162	<0.4	3 .5	180	<5.183	<4.867	X	5.484	5.34	4.597
Loriformes										
Galago senegalensis	124.2	0.2666	2	101	4.235	4.155	3.178	4.863	4.758	3.909
Otolemur garnetti	131.6	0.31	1.25	140	4.611	4.524	3.567	5.196	5.082	4.284
Arctocebus calabarensis	134	<0.38	1.1	105	<4.508	<4.37	<3.397	4.956	4.854	4.005
Loris tardigradus	165	>0.233	1.5	169	X	X	X	X	X	X
Nycticebus coucang	192.2	0.4667	2.1	189	4.561	4.467	3.543	5.186	5.078	4.204
Perodicticus potto	170	>0.4	2.03	210	<4.803	<4.689	<3.853	5.226	5.09	4.384

were measured by the Procrustes distance between the mean neonatal shape and the mean shape at adulthood. This means that in each species, the length of postnatal ontogenetic trajectories was computed only when at least one neonate and one adult specimen were available. The unique neonate available for *Propithecus diadema* (MNHN 1962-2728) had a damaged mandible, such that only cranial ontogenetic trajectory length could be estimated only for this species. Because the number of neonatal and adult individuals per species was small, resampling statistics would be inadequate for comparing trajectory lengths between species. Therefore, one should note that not all interspecific differences in ontogenetic trajectory length may be significant. Furthermore, as stated above, it should be kept in mind that when two ontogenetic trajectories are not parallel, a difference in trajectory length cannot be interpreted in terms of heterochrony.

Finally, let us note that there may be an issue when trying to interpret the ontogenetic trajectory length: gestation length varies considerably among strepsirrhine species, even between species of similar body mass at adulthood (see Table 5.1). For instance, all lorisids except *Arctocebus calabarensis* have gestation periods longer than what is recorded in strepsirrhine species of similar body size. Hence, the question of whether postnatal trajectory length was inversely proportional to gestation length was investigated here. To do so, the correlation of

ontogenetic trajectory length with "gestation length" was assessed.

2.6.3 Ontogenetic trajectory position

There may be interspecific differences in ontogenetic trajectory position along the CASV. In a pair of species exhibiting similar ontogenetic trajectory length and direction, a difference in position along the CASV would indicate that one species is relatively paedomorphic, and that the other is relatively peramorphic. CASV scores were plotted against dental scores and dental stages (the common developmental time scales) to retrieve relatively paedomorphic and peramorphic species. In this analysis, mean species-specific specimens were computed for each dental stage (neonate, infant, juvenile, subadult, adult).

2.7 Differences between lemuriform and loriform species in ontogenetic trajectory divergence.

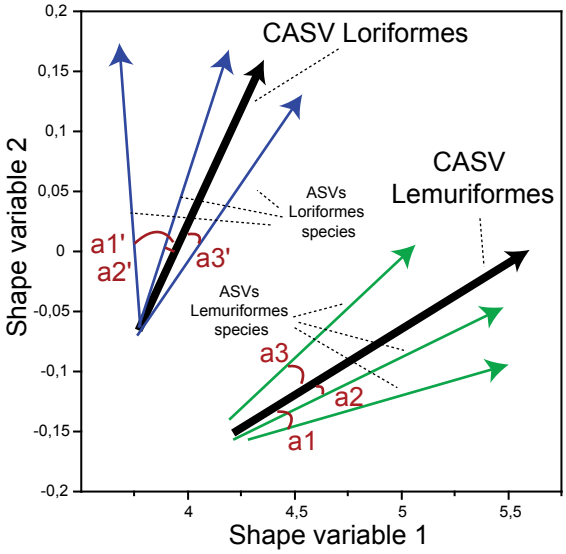

Figure 5.1: Scheme used to test for differences in the variability in direction of the ontogenetic allometric vector between Lemuriformes and Loriformes. For each species the angles of divergence between their ASV and their infraorder-specific CASV is computed (a1, a1', a2…).

Lemuriform species are more diverse in cranio-mandibular morphology than loriform species (see Chapter 4). If postnatal morphogenetic processes are responsible for this state of affairs, we may ask whether the amount of ontogenetic trajectory divergence is greater in lemuriform than in loriform species. To answer this question, each infraorder-specific CASV was computed as the mean of the ASVs computed for all the species specific to this infraorder (see Figure 5.1). Then, for each species, the angle of its species-specific ASV with its infraordinal-specific CASV was computed. This allows assessment of whether divergence in ontogenetic trajectories was more important within the lemuriform or loriform species of the present sample.

2.8 The prenatal and postnatal components of shape change

In all pairs of species for which neonate individuals could be measured, Procrustes distances were computed between the respective species-specific mean neonatal configurations.

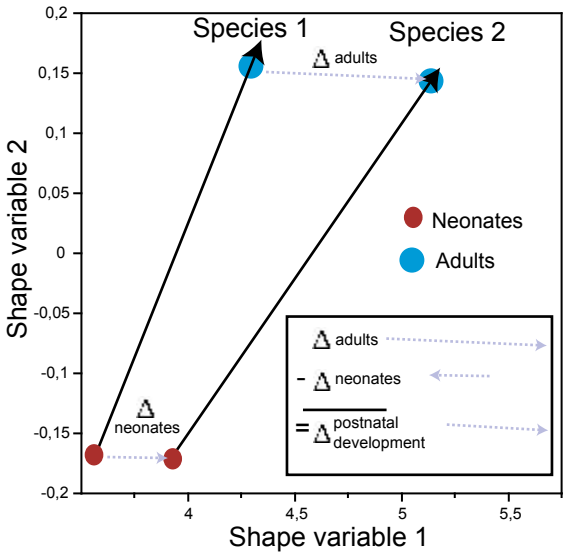

Figure 5.2: Computation of the vector of differential shape change during postnatal ontogeny of two species.

For a given pair of species, this distance represents the amount of difference in shape for which prenatal morphogenetic processes are responsible. In each pair of species, the interspecific Procrustes distance was computed between their respective mean adult configurations. Such a distance gives an estimate of the differences in shape that occur during the entire ontogeny (prenatal + postnatal) between the two species. Finally, a measurement of the differential shape changes that occur postnatally in pairs of species was established (see Figure 5.2): it was estimated as the length of the vector obtained by subtracting the vector of interspecific neonatal shape difference (vector "Δ neonates") from the vector of interspecific adult shape difference (vector "Δ adults").

3. Results

3.1 The allometric component of ontogenetic shape change

For each species, the PSV explains at least 40% of the overall species-specific shape variance (see Table 5.2). Furthermore, the principal shape and allometric shape vectors are always almost parallel: the cosine of their angles is always greater than 0.94, and is greater than 0.99 in the vast majority of cases. Therefore almost all of the changes in shape that occur during ontogeny for the mandible and cranium are allometric. In all subsequent analyses, ASVs are used to measure ontogenetic shape changes.

Table 5.2: Variance in shape explained by each species-specific principal shape vector (PSV), and divergence from the species-specific allometric shape vector (ASV). The PSV is the first principal component of a PCA performed on the corresponding species data. The angle between each species-specific ASV and PSV is given by their cosine.

Species	Skull		Cranium		Mandible	
Haplorrhines						
Aotus trivirgatus	60.60%	0.999	50.30%	0.996	73.50%	0.995
Tarsius bancanus	60.50%	0.998	55%	0.997	73.60%	0.993
Lemuriformes						
Lemur catta	61.40%	0.998	61.90%	0.998	68.40%	0.997
Lepilemur ruficaudatus	44.80%	0.999	41.90%	0.997	59%	0.997
Microcebus murinus	55%	0.998	55.80%	0.997	70.10%	0.993
Propithecus diadema	59.40%	0.996	48.50%	0.995	61.10%	0.978
Propithecus verreauxi	52.30%	0.997	55.90%	0.99	53.40%	0.94
Loriformes						
Galago senegalensis	58%	0.997	57.30%	0.997	71.30%	0.995
Otolemur crassicaudatus	73.40%	0.996	71.10%	0.993	85%	0.998
Arctocebus calabarensis	51.40%	0.997	52.30%	0.996	61.90%	0.987
Nycticebus coucang	62.20%	0.997	64%	0.998	60%	0.972
Perodicticus potto	41.80%	0.993	40.60%	0.987	41.70%	0.989

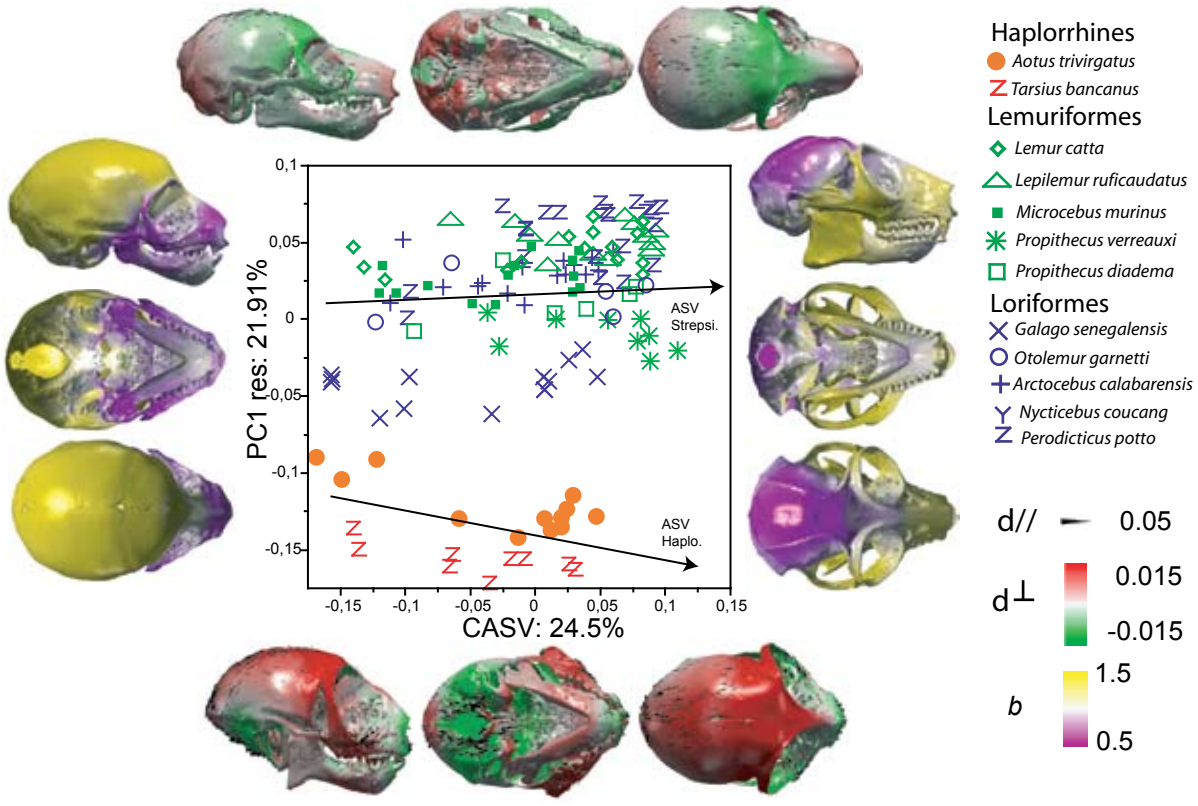

Figure 5.3: Patterns of shape variations for the skull in primates during ontogeny and interspecific differences. This figures presents the patterns of morphological change along the CASV, and along the first principal component of a PCA performed on shape residuals (PC1res) after projection of the specimens on the CASV. Figures around the central plot correspond to extreme shape variations. Templates: *Arctocebus calabarensis* 7704 (high values on CASV); *Arctocebus calabarensis* 7013 (all other cases). The arrows represent the projections of the suborder-specific ASVs on CASV-PC1res space. ASV Strepsi, ASV Haplo: ASVs computed respectively for the strepsirrhines and the haplorrhines. d//: displacement parallel to the surface. d⊥: displacement perpendicular to the surface. Scales are in centroid size units. The color scale (b) corresponds to the relative change in local area along the CASV.

3.2 Postnatal developmental patterns

3.2.1 Common developmental patterns

The CASVs computed for the skull, cranium and mandible configurations account respectively for 24.50%, 21.69% and 36.73% of the total sample shape variance (see Figures 5.3-5.5). CASV scores are significantly correlated with the logarithm of centroid size (r^2 = 0.546, $p<0.0001$ for the skull; r^2 = 0.36, $p<0.0001$ for the cranium; r^2 = 0.62, $p<0.0001$ for the mandible).

The CASVs illustrate the changes in shape that occur during ontogeny (see Figures 5.3-5.5). Young individuals exhibit skulls with relatively larger braincases and shorter snouts (Figures 5.3-5.4). Mandibles of young individuals are relatively shorter in the antero-posterior direction and exhibit rounded corpora, very small angular and coronoid processes, low condyles relatively to the occlusal plane and widely separated horizontal branches. The condyles and coronoid processes of those mandibles are oriented labially. These characters give an oblique aspect to the two branches of the mandible when viewed in frontal orientation (see Figure 5.5). During

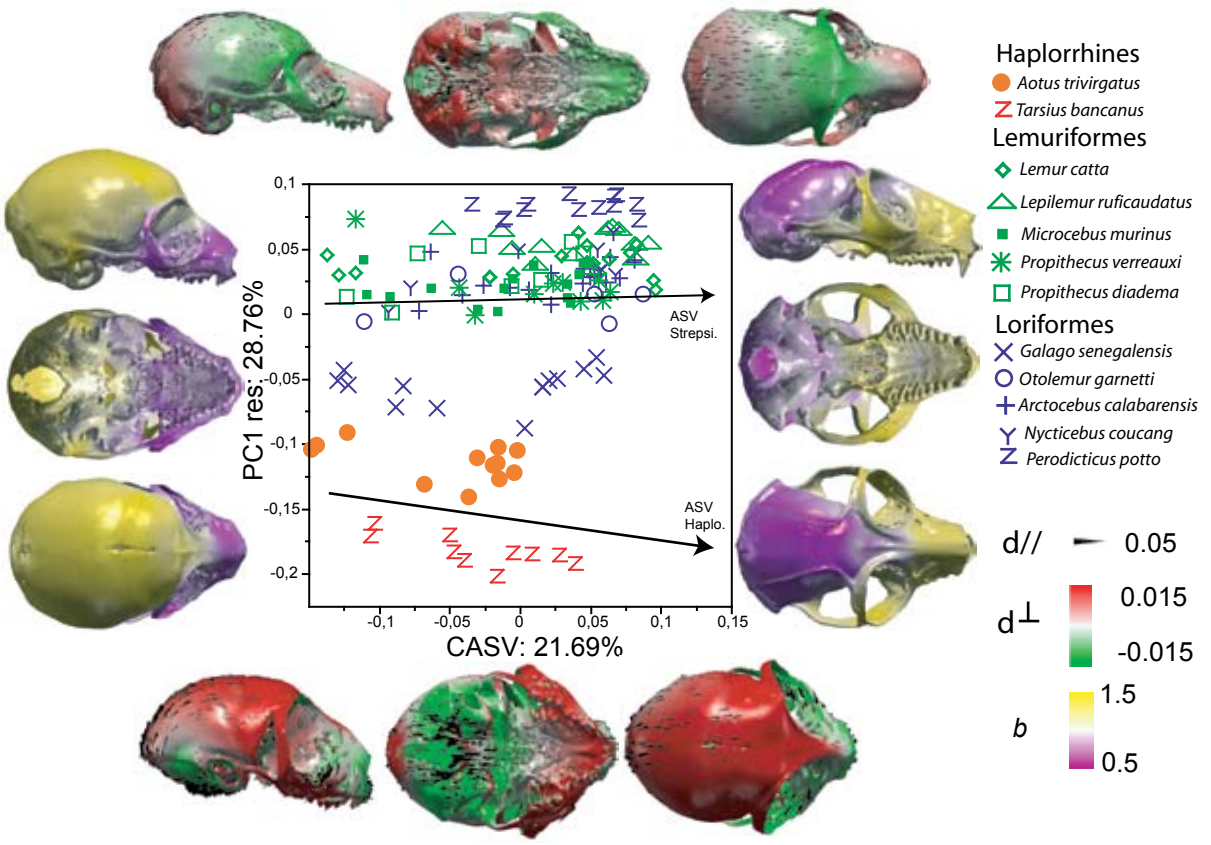

Figure 5.4: Patterns of shape variations for the cranium in primates during ontogeny and interspecific differences. Patterns of morphological change along the CASV, and along the first principal component of a PCA performed on shape residuals (PC1res) after projection of the specimens on the CASV. Figures around the central plot correspond to extreme shape variations. Templates: *Arctocebus calabarensis* 7704 (high values on CASV); *Arctocebus calabarensis* 7013 (all other cases). The arrows represent the projections of the suborder-specific ASVs on CASV-PC1res space. ASV Strepsi, ASV Haplo: ASVs computed respectively for the strepsirrhines and the haplorrhines. d//: displacement parallel to the surface. d⊥: displacement perpendicular to the surface. Scales are in centroid size units. The color scale (b) corresponds to the relative change in local area along the CASV.

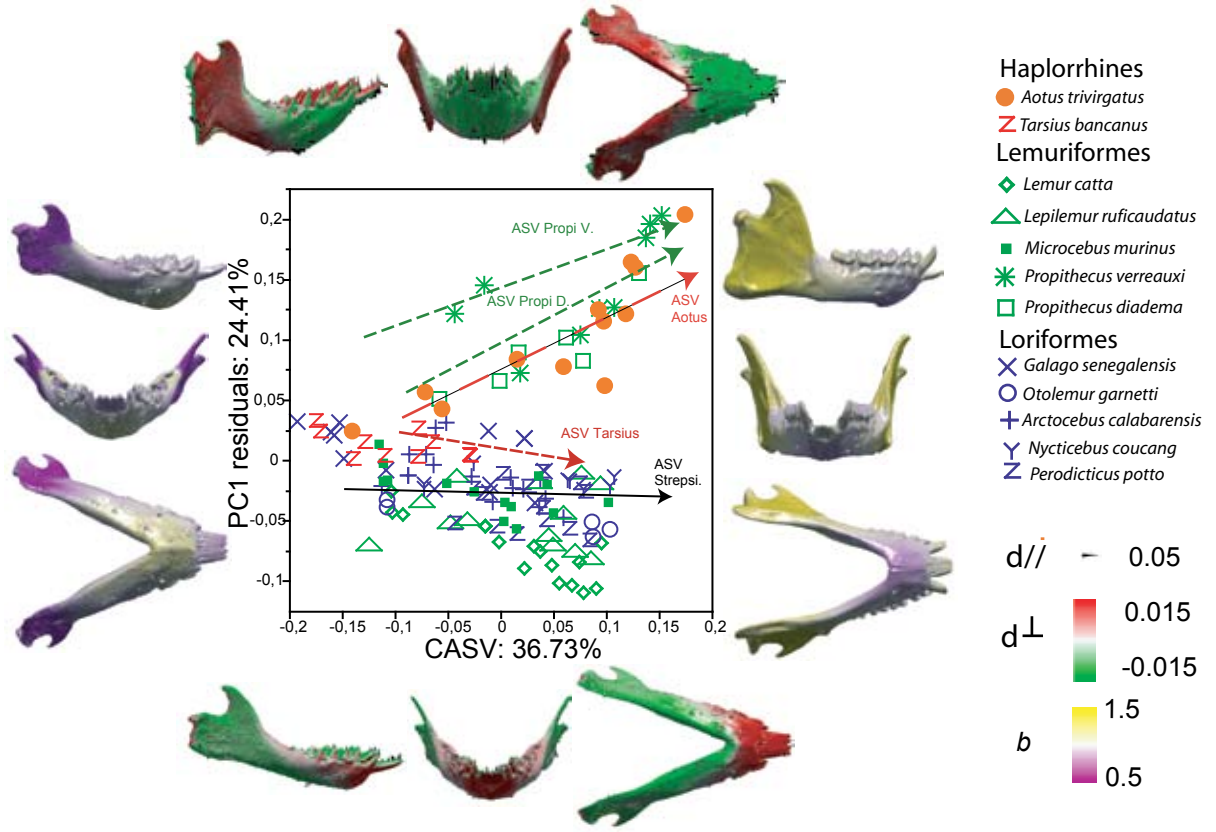

Figure 5.5: Patterns of shape variations for the mandible in primates during ontogeny and interspecific differences. The figures presents the patterns of morphological change along the CASV, and along the first principal component of a PCA performed on shape residuals (PC1res) after projection of the specimens on the CASV. Figures around the central plot correspond to extreme shape variations. Templates: *Arctocebus calabarensis* 7704 (high values on CASV); *Arctocebus calabarensis* 7013 (all other cases). The arrows represent the projections of the species-specific and strepsirrhine-specific ASVs on CASV-PC1res space. ASV Strepsi, ASV Aotus, ASV Prop D, ASP Prop V, ASV Tarsius: ASVs computed respectively for the strepsirrhines, *Aotus trivirgatus, Propithecus diadema* and *P. verreauxi* and *Tarsius bancanus.* d//: displacement parallel to the surface. d⊥: displacement perpendicular to the surface. Scales in centroid size units. The color scale (b) corresponds to the relative change in local area along the CASV. Note how *Propithecus diadema* and *Propithecus verreauxi* on the one hand, and *Aotus trivirgatus* on the other follow similar patterns of shape change during ontogeny.

development, the braincase undergoes relative reduction, whereas the mandible and maxilla regions expand widely. The orbits become positioned in a more convergent configuration and tend to point upwards. Older individuals exhibit mandibles with comparatively higher corpora, developed angular and coronoid processes, higher condyles, and a smaller angle between the two horizontal branches. The observation that the orbits move upward during development is probably partly due to the lorisids, which are unique in their orbital configuration (see Chapter 4). Orbits grow isometrically in the present sample.

3.2.2 Interspecific differences independent of postnatal development

For the skull and cranium configurations, PC1res accounts, respectively, for 21.19% and 28.76% of the total sample shape variance (see Figure 5.3 and Figure 5.4). The crania of strep-

sirrhine and haplorrhine species are well separated along PC1res, independently of the age of the individuals (Figure 5.4). Haplorrhines project to low values on this axis and exhibit relatively larger braincases, relatively flatter faces, a foramen magnum anteriorly placed, larger and more frontated orbits, and shorter mandibles. Strepsirrhine crania project to high values on PC1res and exhibit comparatively smaller braincases, well developed snouts, smaller and less frontated orbits, a foramen magnum placed posteriorly, and longer mandibles. The infraorder-specific ASVs diverge slightly in CASV-PC1res space.

For mandible configuration, PC1res accounts for 24.41% of the total sample shape variance (see Figure 5.5). *Aotus trivirgatus*, *Propithecus diadema,* and *Propithecus verreauxi* are well separated from other species on this axis. However, here, the projection scores of the individuals are age-dependent for *Aotus* and *Propithecus*: the older the specimens belonging to these genera, the higher they project on PC1res. Hence, PC1res reflects the variation in shape associated with developmental patterns specific to *Aotus* and *Propithecus* during postnatal ontogeny. The mandibles of *Aotus* and *Propithecus* develop longer and higher mandibular symphyses during ontogeny, vertically high corpora, expanded gonial regions, and condyles high above the alveolar plane. The mandible of *Tarsius* does not deviate markedly from the typical pattern of mandibular development of strepsirrhines.

3.3 Interspecific differences in allometric grade

3.3.1 Skull and cranium

There is large variability in the relationship between allometric score and centroid size across species (see Figure 5.6-A). For instance, for the same allometric score, lemurids, indriids, and *Aotus* are larger than *Microcebus murinus* specimens. For a given allometric score, all the loriforms, *Lepilemur ruficaudatus,* and *Tarsius* exhibit an intermediate size. Conversely, this means that for a given size, *Microcebus murinus* is more peramorphic than lemurids, indriids, and *Aotus*. Similar patterns of allometry can be observed on the cranium alone (see Figure 5.6-B). Here we advance the hypothesis that the allometric grades exhibited by *Microcebus murinus, Lemur catta*, *Propithecus diadema,* and *Propithecus verreauxi* do not reflect the ancestral condition for strepsirrhines, since they are extreme in comparison to other strepsirrhine species. On the contrary, because they are similar to one another, the allometric grades exhibited by loriform species and *Lepilemur* probably better reflect the ancestral condition of toothcombed strepsirrhines.

3.3.2 Mandible

Analogous observations can be made regarding mandible configuration (see Figure 5.6-C). However, there is one noticeable exception: at a given size, the mandible of *Aotus* displays higher allometric scores than those of *Lemur catta, Propithecus verreauxi,* and *Propithecus*

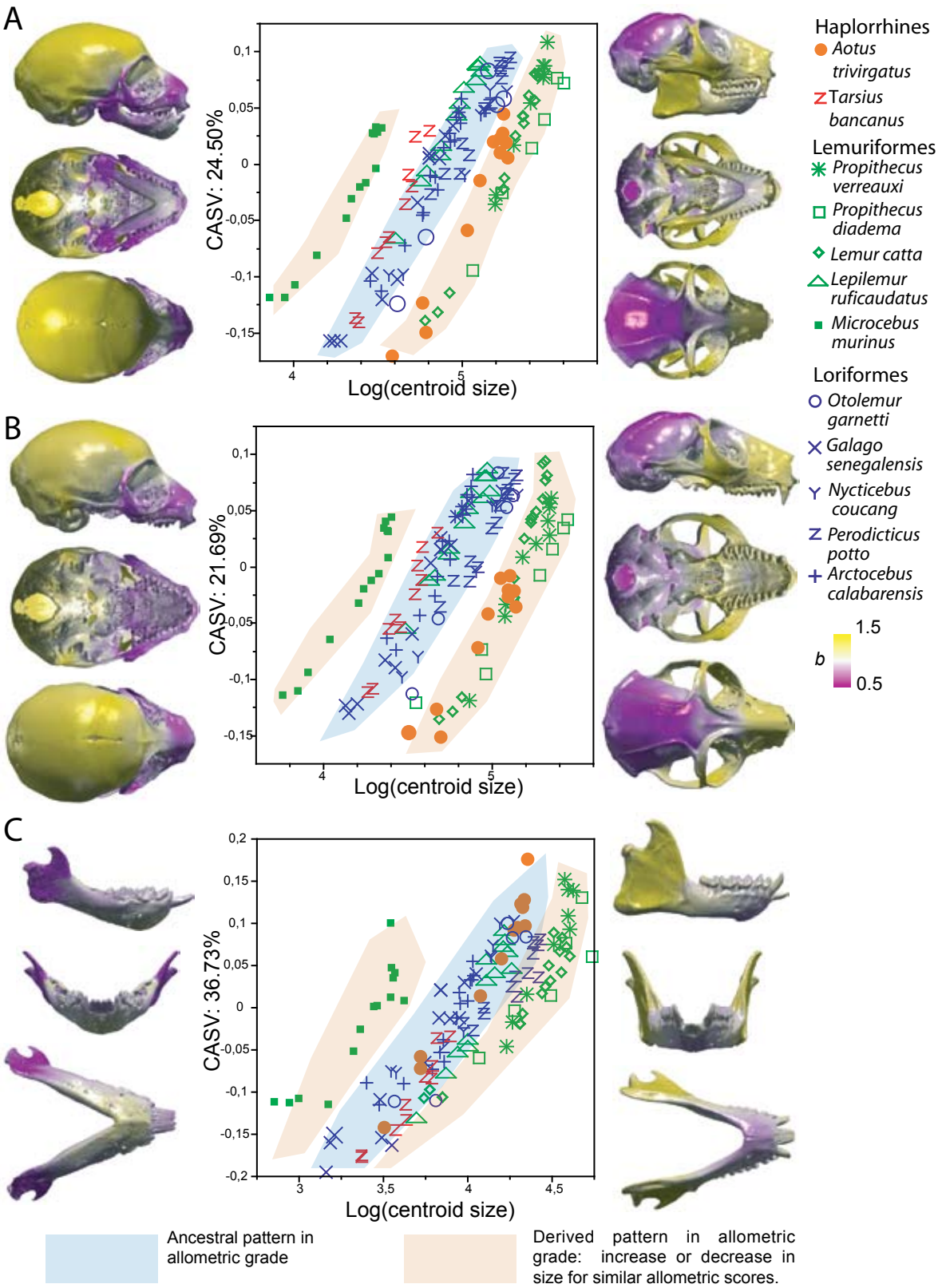

Figure 5.6: Variability in ontogenetic allometric grades. Common patterns of ontogenetic allometry and associated patterns of shape variations are also represented. Figures around the central plots correspond to extreme variations (templates: *Arctocebus calabarensis* 7013 for low values of projection on CASV and *Arctocebus calabarensis* 7704 for high values on CASV). The color scale (b) corresponds to the relative change in local area along the CASVs.

Tables 5.3-5: Species pairwise comparison of the trajectory direction, and species-specific ontogenetic trajectory lengths. Upper triangle: cosines of the angle of divergence computed for each pair of species. Lower triangle: significance of this angle estimated by resampling tests. First experiment: dental stage clustered test. Second experiment: normal test. "*": p<0.05. "-": p>0.0.5. See material and methods sections for details. Mean angle: mean angle of trajectory divergence between the given species and all the other species. Length: Procrustes distance between mean fetus and mean adult stage. When no foetus was available, the given value is the distance between the younger specimen and mean adult. Sign score (Significance score): sum of the tests involving the given species which proved statistically significant. A.t.: *Aotus trivirgatus*. A.c. *Arctocebus calabarensis*. G.s.: *Galago senegalensis*. L.c: *Lemur catta*. L.r. : *Lepilemur ruficaudatus* N.c.: *Nycticebus coucang*. P.p.: *Perodicticus potto*. P.d.: *Propithecus diadema*. P.v.: *Propithecus verreauxi*. T.b.: *Tarsius bancanus*. O.g.: *Otolemur garnetti*. The significance of the angle for *Otolemur garnetti* are not computed because its ontogenetic series is incomplete.

Table 5.3: skull configuration

	A.t.	T.b.	L.c.	L.r.	M.m	P.d.	P.v	G.s.	O.g.	A.c	N.c.	P.p.
A.t.	/	0.698	0.639	0.713	0.55	0.72	0.779	0.751	0.694	0.719	0.727	0.61
T.b.	*|-	/	0.681	0.675	0.588	0.649	0.616	0.807	0.721	0.758	0.676	0.689
L.c.	*|*	*|*	/	0.726	0.776	0.604	0.597	0.817	0.815	0.833	0.763	0.768
L.r	*|-	*|*	*|*	/	0.698	0.663	0.691	0.795	0.792	0.745	0.709	0.733
M.m.	*|*	*|*	*|*	*|*	/	0.602	0.462	0.775	0.742	0.715	0.748	0.688
P.d	-|-	-|-	*|-	*|-	-|-	/	0.608	0.672	0.619	0.669	0.71	0.631
P.v.	-|-	-|*	-|-	*|-	-|*	*|-	/	0.658	0.626	0.678	0.67	0.618
G.s.	*|*	*|-	*|*	-|*	*|*	-|-	*|-	/	0.864	0.872	0.825	0.786
O.g.	X	X	X	X	X	X	X	X	/	0.839	0.803	0.817
A.c.	*|*	-|-	-|-	*|*	*|*	*|-	*|-	-|-	X	/	0.838	0.802
N.c.	*|-	*|-	*|-	*|-	*|-	*|-	-|-	*|-	X	-|-	/	0.749
P.p.	*|*	-|*	*|*	*|*	*|*	*|-	-|*	*|-	X	*|-	-|-	/
Mean angle	0.691	0.687	0.729	0.722	0.668	0.65	0.637	0.784	0.757	0.77	0.747	0.717
Sign Score	13/20	11/20	14/20	15/20	17/20	06/20	07/20	10/20	/	09/20	07/20	13/20
Length	0.215	0.199	0.235	>0.18	0.185	>0.22	X	0.19	0.212	>0.18	0.19	>0.14

Table 5.4: cranium configuration

	A.t.	T.b.	L.c.	L.r.	M.m	P.d.	P.v	G.s.	O.g.	A.c	N.c.	P.p.
A.t.	/	0.604	0.631	0.703	0.538	0.628	0.682	0.712	0.67	0.638	0.694	0.627
T.b.	*|-	/	0.662	0.66	0.565	0.604	0.573	0.788	0.698	0.676	0.606	0.683
L.c.	*|*	*|*	/	0.808	0.78	0.789	0.74	0.83	0.802	0.84	0.76	0.777
L.r	-|-	*|*	-|-	/	0.648	0.668	0.759	0.79	0.789	0.778	0.682	0.791
M.m.	*|*	*|*	*|*	*|*	/	0.652	0.676	0.751	0.693	0.73	0.734	0.669
P.d	*|-	*|-	*|-	-|-	*|-	/	0.642	0.694	0.661	0.68	0.641	0.738
P.v.	-|-	-|*	*|-	-|-	*|*	*|-	/	0.736	0.729	0.713	0.656	0.744
G.s.	*|*	*|*	*|*	-|*	*|*	*|-	*|-	/	0.538	0.86	0.802	0.708
O.g.	X	X	X	X	X	X	X	X	/	0.841	0.789	0.828
A.c.	*|*	*|*	-|-	*|-	*|*	*|-	*|-	-|-	X	/	0.829	0.821
N.c.	*|-	*|*	*|-	*|-	*|-	*|-	*|-	*|-	X	-|-	/	0.778
P.p.	*|*	-|*	*|*	-|-	*|*	*|-	-|*	*|*	X	*|-	-|-	/
Mean angle	0.648	0.647	0.765	0.734	0.676	0.672	0.695	0.746	0.731	0.764	0.725	0.742
Sign Score	13/20	16/20	13/20	07/20	18/20	09/20	09/20	14/20	/	10/20	0/20	12/20
Length	0.165	0.176	0.23	>0.16	0.179	0.219	>0.2	0.172	0.199	>0.16	0.191	>0.12

Table 5.5: mandible configuration

	A.t.	T.b.	L.c.	L.r.	M.m	P.d.	P.v	G.s.	O.g.	A.c	N.c.	P.p.
A.t.	/	0.719	0.71	0.768	0.753	0.776	0.856	0.764	0.803	0.763	0.86	0.692
T.b.	*|*	/	0.806	0.797	0.762	0.691	0.68	0.779	0.828	0.848	0.811	0.757
L.c.	*|*	*|*	/	0.734	0.855	0.531	0.627	0.809	0.863	0.869	0.815	0.657
L.r	-|*	*|-	-|*	/	0.874	0.739	0.885	0.861	0.855	0.868	0.866	0.903
M.m.	*|*	*|*	*|*	-|-	/	0.571	0.746	0.946	0.93	0.908	0.894	0.843
P.d	-|-	-|-	*|*	*|-	*|-	/	0.841	0.569	0.569	0.605	0.746	0.603
P.v.	-|-	*|*	-|*	-|-	-|*	-|-	/	0.742	0.753	0.749	0.845	0.766
G.s.	*|*	*|*	*|*	-|*	-|-	*|*	-|*	/	0.954	0.877	0.902	0.781
O.g.	X	X	X	X	X	X	X	X	/	0.888	0.874	0.782
A.c.	*|*	"-|-	-|*	-|-	-|-	*|*	*|*	-|*	X	/	0.912	0.859
N.c.	*|-	*|-	*|-	-|-	*|-	*|-	-|-	*|-	X	-|-	/	0.82
P.p.	*|*	-|-	*|*	-|-	-|-	-|-	-|-	*|-	X	-|-	-|-	/
Mean angle	0.769	0.771	0.752	0.832	0.826	0.658	0.772	0.817	0.827	0.831	0.85	0.769
Sign Score	14/20	12/20	16/20	05/20	09/20	09/20	06/20	13/20	/	08/20	06/20	05/20
Length	0.258	0.166	0.196	>0.21	0.17	>0.21	X	0.195	0.23	>0.16	0.175	>0.13

diadema. Interspecific differences in allometric grade can thus be observed in the mandible, but they occur to a lesser degree. Again, we propose that the pattern exhibited by loriforms and *Lepilemur* is ancestral for strepsirrhines, whereas those displayed by *Microcebus, Lemur,* and *Propithecus* are derived.

3.4 Diversity in ontogenetic trajectories and morphological diversity

3.4.1 Divergence in direction

Altogether, 110 resampling tests were performed for each configuration (see Tables 5.3-5). For the skull and the cranium configurations, more than half of the resampling tests (skull, 61/110; cranium, 65/110; see Table 5.3 and Table 5.4) rejected the hypothesis of parallelism between trajectories. When one of the resampling tests is significant, divergence is considered confirmed (see Methods, section 2.6). Thus, a vast majority of species pairs exhibit divergent trajectories (skull, 43/55; cranium, 45/55). These findings are affected by the incompleteness of the data. In most species pairs for which the angle of divergence is not significant, at least one of the two species involved is represented by a small number of specimens, such as in the tests involving the genus *Propithecus*, or one of the dental stages is not represented in the sample, such as in the comparison between *Nycticebus coucang* and *Lepilemur ruficaudatus*. It therefore seems reasonable to postulate that if more complete ontogenetic series were available, most of these angles would become statistically significant. Hence, postnatal ontogenetic trajectories among the species included in the sample can be considered on the whole as divergent from one another.

For the mandible, less than half of the resampling tests (52/110) reject the hypothesis of parallelism between pairs of species (see Table 5.5). However, divergence in ontogenetic allometric vector direction is confirmed for the majority of the pairs of species (35/55).

To summarize, for cranium configuration, *Propithecus diadema* and *P. verreauxi, Aotus trivirgatus,* and *Microcebus murinus* exhibit the most divergent ontogenetic trajectories. For mandible configuration, the genera *Propithecus diadema, P. verreauxi*, *Aotus trivirgatus,* and *Lemur catta* exhibit a wide degree of divergence in the direction of the ontogenetic allometric vector.

The deviation of each species-specific ASV from its infraordinal-specific CASV is significantly greater in lemuriforms than in loriforms for skull and cranium configurations (see Table 5.6). For mandible configuration, the difference between lemuriforms and loriforms is not significant ($p=0.074$), although the mean angle found for lemuriforms is greater than that of loriforms. Nevertheless, the results strongly support the notion that the ontogenetic trajectories of lemuriform species diverge more significantly from each other than do the trajectories of loriforms.

Table 5.6: Deviation from each specific ASV from its infraorder-specific CASV. F-tests and t- tests are performed to test for significance of the difference in variance and mean for the angle of divergence in Lemuriformes and Loriformes.

Skull	**Lemuriformes**		**Angle : ASV/CASV(Lemuriformes)**
	Lemur catta		0.88
	Lepilemur ruficaudatus		0.89
	Microcebus murinus		0.84
	Propithecus diadema		0.82
	Propithecus verreauxi		0.79
	Loriformes		**Angle : ASV/CASV(Loriformes)**
	Arctocebus calabarensis		0.94
	Galago senegalensis		0.94
	Nycticebus coucang		0.91
	Perodicticus potto		0.9
	Otolemur garnetti		0.93
	F value : 4.43	p = 0.18	
	T value : 3.99	p= 0.004	
Cranium	**Lemuriformes**		**Angle : ASV/CASV(Lemuriformes)**
	Lemur catta		0.94
	Lepilemur ruficaudatus		0.88
	Microcebus murinus		0.85
	Propithecus diadema		0.85
	Propithecus verreauxi		0.87
	Loriformes		**Angle : ASV/CASV(Loriformes)**
	Arctocebus calabarensis		0.94
	Galago senegalensis		0.93
	Nycticebus coucang		0.91
	Perodicticus potto		0.92
	Otolemur garnetti		0.93
	F value : 6.7722	p = 0.091	
	T value : 2.7414	p = 0.025	
Mandible	**Lemuriformes**		**Angle : ASV/CASV(Lemuriformes)**
	Lemur catta		0.85
	Lepilemur ruficaudatus		0.95
	Microcebus murinus		0.91
	Propithecus diadema		0.82
	Propithecus verreauxi		0.92
	Loriformes		**Angle : ASV/CASV(Loriformes)**
	Arctocebus calabarensis		0.96
	Galago senegalensis		0.96
	Nycticebus coucang		0.95
	Perodicticus potto		0.89
	Otolemur garnetti		0.96
	F value : 3.524	p = 0.25	
	T value : 2.0502	p = 0.074	

3.4.2 Differences in trajectory length

Data on trajectory lengths are summarized in Tables 5.3-5. *Aotus* displays the shortest cranial trajectory, but the longest mandibular trajectory. *Tarsius bancanus* exhibits the shortest mandibular trajectory, and a short cranial trajectory. Within the strepsirrhines, cranial trajectories are longest in *Lemur catta* and *Propithecus diadema*, and shortest in *Galago senegalensis* and *Microcebus murinus.* Mandibular trajectories are longest in *Otolemur garnetti*, *Lepilemur ruficaudatus,* and *Propithecus diadema*, and shortest in *Microcebus murinus* and *Nycticebus coucang.* The only lorisid species for which neonates could be incorporated in the sample is *Nycticebus coucang*. In *Nycticebus coucang,* the ontogenetic trajectory is short for mandible configuration. However, *Nycticebus coucang* exhibits cranial and skull trajectory lengths that lie within the range of other observations.

A direct link between trajectory length and duration of gestation can not be established (skull, p= 0.82; cranium, p=0.66; mandible, p=0.83).

3.4.3 Relative position of ontogenetic trajectories.

For the cranium, the most paedomorphic species are *Aotus trivirgatus*, *Tarsius bancanus,* and *Galago senegalensis* (see Figure 5.7). The most peramorphic species are *Lemur catta* and *Perodicticus potto.* For the mandible, the most paedomorphic species are *Tarsius bancanus* and *Galago senegalensis*, whereas the most peramorphic species are *Aotus triviragatus, Perodicticus* potto, *Nycticebus coucang, Propithecus diadema,* and *P. verreauxi.*

Within the Galagidae, the smaller *Galago senegalensis* is more paedomorphic than the larger *Otolemur garnetti* (see Figure 5.7). Within the Lorisidae family, the smaller *Arctocebus calabarensis* is more paedomorphic than the larger *Nycticebus coucang* and *Perodicticus potto.* In Lemuriformes, however, the smallest species (*Microcebus murinus*) displays average scores along the CASV for all the dental stages.

3.4.4 Interspecific Procrustes distance at birth and at adulthood.

In strepsirrhines, the Procrustes distances between adults of any two species are usually of the same range as distances between neonates of the same two species (Table 5.7). One noticeable exception is the mandible of *Lemur catta*. Its interspecific Procrustes distance to any other species at adulthood is higher than the interspecific Procrustes distance at birth. This is exemplified by the fact that the postnatal ontogenetic trajectory of *Lemur catta* is one of the most divergent in the sample.

3.5 Patterns of eruption of the tooth-comb across strepsirrhines species.

The eruption of the toothcomb relative to molar eruption varies widely in strepsirrhines. In *Lepilemur ruficaudatus*, it erupts after the second permanent molar. In *Lemur catta* and *Mi-*

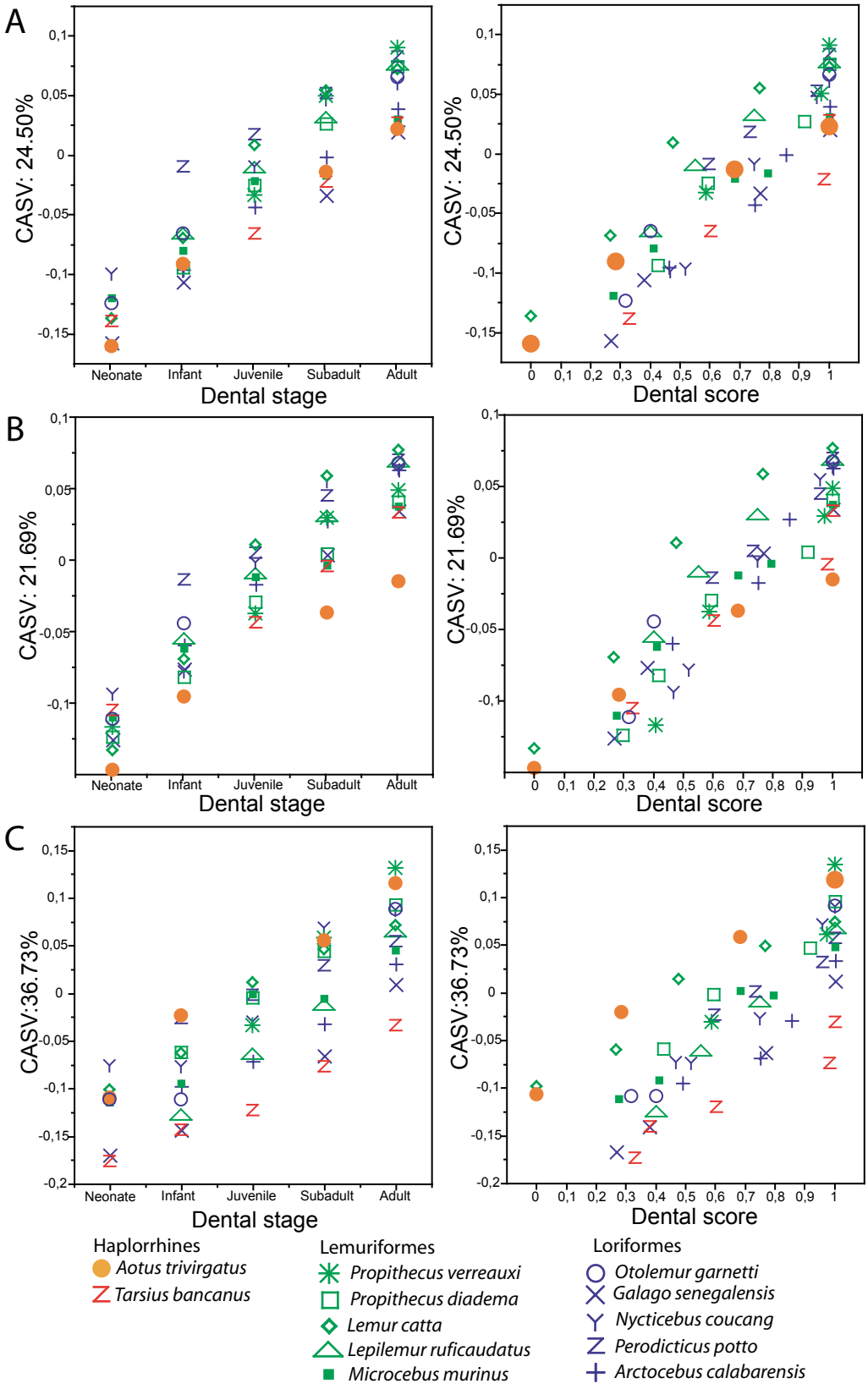

Figure 5.7: CASV scores, dental stages, and dental scores. A: skull. B: cranium. C: mandible. Left column: CASVscores-Dental stage plots. Note how these graphs separates peramorph from paedomorph species. Right column: CASV scores-Dental scores plots. CASV and dental scores consist of the species-specific mean values computed for each dental stage.

Table 5.7: Interspecific Procrustes distance at birth (left) and adulthood (middle), and length of differential postnatal developmental vector. A.t.: *Aotus trivirgatus*. A.c. *Arctocebus calabarensis*. G.s.: *Galago senegalensis*. L.c: *Lemur catta*. L.r. : *Lepilemur ruficaudatus* N.c.: *Nycticebus coucang*. P.p.: *Perodicticus potto*. P.d.: *Propithecus diadema*. T.b. : *Tarsius bancanus*. O.g.: *Otolemur garnetti*. No neonate belonging to the species *Propithecus diadema* presented a mandible in sufficiently good condition to be incorporated in the analysis.

Skull	At	T.b.	L.c.	M.m.	G. s.	O.g.
T.b.	0.186|0.224|0.16					
L.c.	0.198|0.241|0.180	0.231|0.244|0.172				
M.m.	0.213|0.221|0.189	0.210|0.240|0.174	0.131|0.131|0.153			
G. s.	0.154|0.201|0.143	0.151|0.193|0.123	0.149|0.160|0.134	0.141|0.110|0.130		
O.g.	0.184|0.232|0.154	0.166|0.211|0.168	0.119|0.110|0.138	0.130|0.107|0.154	0.107|0.109|0.104	
N. c.	0.172|0.207|0.168	0.206|0.263|0.174	0.130|0.150|0.164	0.127|0.126|0.141	0.151|0.147|0.121	0.125|0.119|0.146

Cranium	A.t.	T.b.	L.c.	M.m.	P.d.	G. s.	O.g.
T.b.	0.191|0.231|0.153						
L.c.	0.203|0.242|0.170	0.234|0.261|0.172					
M.m.	0.227|0.216|0.159	0.222|0.247|0.166	0.118|0.116|0.143				
P.d	0.210|0.216|0.176	0.237|0.272|0.174	0.136|0.125|0.163	0.166|0.129|0.189			
G. s.	0.163|0.196|0.129	0.156|0.198|0.117	0.139|0.146|0.130	0.141|0.111|0.122	0.156|0.173|0.170		
O.g.	0.172|0.209|0.149	0.192|0.242|0.146	0.113|0.097|0.138	0.134|0.105|0.155	0.150|0.127|0.188	0.102|0.105|0.101	
N. c.	0.177|0.213|0.153	0.209|0.280|0.176	0.130|0.144|0.162	0.127|0.114|0.139	0.158|0.125|0.197	0.142|0.150|0.118	0.123|0.114|0.140

Mandible	A.t.	T.b.	L.c.	M.m.	G. s.	O.g.
T.b.	0.146|0.230|0.188					
L.c.	0.120|0.247|0.173	0.136|0.173|0.107				
M.m.	0.100|0.206|0.171	0.147|0.265|0.170	0.101|0.162|0.113			
G. s.	0.096|0.200|0.164	0.107|0.161|0.136	0.130|0.174|0.127	0.099|0.076|0.073		
O.g.	0.115|0.212|0.162	0.120|0.198|0.137	0.085|0.111|0.119	0.092|0.102|0.114	0.104|0.127|0.086	
N. c.	0.114|0.185|0.153	0.175|0.203|0.118	0.083|0.139|0.113	0.114|0.131|0.082	0.154|0.125|0.095	0.122|0.109|0.136

crocebus murinus, it erupts well after M1 (see Appendices 3.1-12). In other lemur species for which sufficient data were available for study, the toothcomb erupts between the emergence of M1 and M2. In *Galago senegalensis*, the toothcomb erupts after M1, but no specimen in the sample allowed us to assess whether it erupts before or after M2. In the two galagid species incorporated in the sample (*Galago senegalensis,* and *Otolemur garnetti*), the permanent toothcomb had just started to mineralize in neonate specimens, which possibly indicates an earlier eruption compared to most lemuriform families. In lorisids (*Nycticebus coucang*, *Perodicticus potto*, and *Arctocebus calabarensis*), the deciduous toothcomb is replaced before the emergence of M1. This may also be the case in *Loris tardigradus* since a late-term fetus of this species exhibits an advanced degree of formation of the permanent toothcomb (Figure 5.8-B). Early mineralization of the definitive toothcomb is a pattern that is probably related to the early eruption of the definitive toothcomb. Therefore it seems reasonable to assume that the permanent toothcomb of *Loris tardigradus* also erupts before M1. Moreover, the crowns of P2 and M1 of these two fetus mandibles are already visible. Such early maturation of the permanent dentition is observed only in lorisids. Unsurprisingly, two lorisid species, *Nycticebus coucang* and *Perodictius potto,* exhibit the highest dental score at birth in the sample (see Table 5.1).

In contrast to the species considered so far, neonates of *Galago senegalensis* and *Lemur*

catta are dentally underdeveloped (see Figure 5.8 C,D; see also Figure 5.7). In *Galago senegalensis,* the crowns of the permanent toothcomb and P2 start to mineralize only at birth. In *Lemur catta*, permanent toothcomb and P2 crowns are not visible on CT images of neonates.

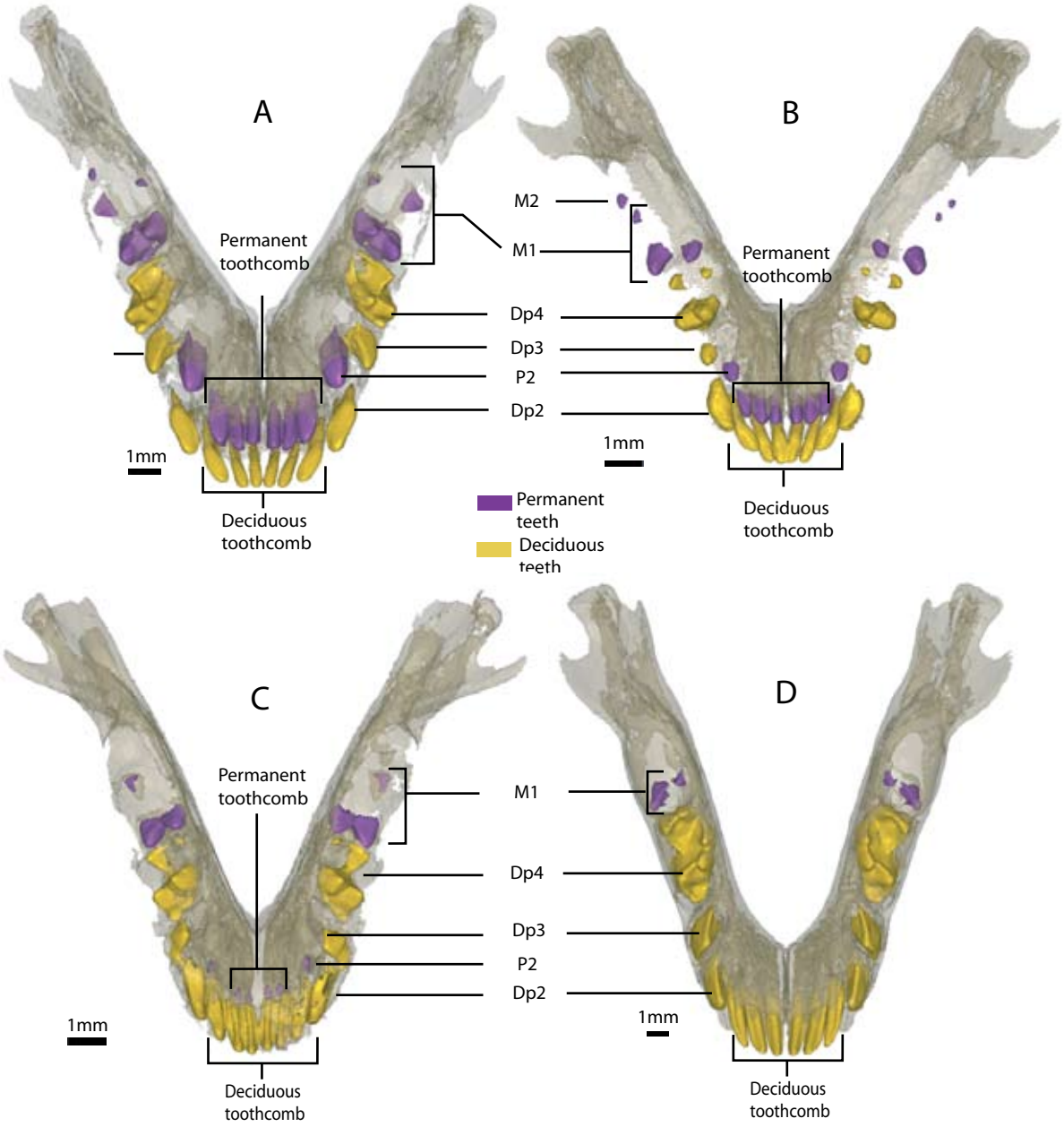

Figure 5.8: Variability of dental maturation in juvenile strepsirrhine mandibles. A: late-term fetus of *Nycticebus coucang* (PR-41, Hubrecht collections). B: late-term fetus of *Loris tardigradus* (PR-55, Hubrecht collections). C: neonate *Galago senegalensis* (8190, AIM-Zürich). D: neonate *Lemur catta* (15821, AIM-Zürich). The formation of a permanent toothcomb occurs earlier in Lorisidae species than in Galagidae and Lemuriformes species.

4. Discussion

4.1 Differences in developmental constraints between haplorrhines and strepsirrhines

Several arguments have been made to support the hypothesis that strepsirrhines and haplorrhines share different cranial developmental constraints. First of all, for cranium configuration, interspecific Procrustes distances at birth is greatest in pairs involving one haplorrhine species and one strepsirrhine species. This indicates that strepsirrhines and haplorrhines differ widely in their prenatal developmental processes. Furthermore, the Procrustes distance is always greater at adulthood than at birth, and postnatal ontogenetic trajectories diverge significantly in all pairs involving one strepsirrhine and one haplorrhine species. This indicates that the underlying postnatal morphogenetic processes also differ to a great extent between the two suborders. There are also trend differences in ontogenetic trajectory positions along the CASV between strepsirrhines and haplorrhines: at any dental stage, *Aotus* and *Tarsius* exhibit the most paedomorphic cranial shapes. Additionally, the cranium of *Aotus tirvirgatus* exhibits the shortest ontogenetic trajectory length of the entire sample. This leads to the proposal that the general trends towards paedomorphism in anthropoid primates (in comparison to strepsirrhine primates) is achieved both via the shortening of the ontogenetic trajectory and the displacement of the ontogenetic trajectory.

Concerning mandibular configuration, *Tarsius* and *Aotus* display differences in ontogenetic trajectory lengths, direction, and position along the CASV. The ontogenetic trajectory of the mandible of *Tarsius* does not deviate significantly from that of strepsirrhine species, with the exception of the genus *Propithecus*. The mandibles of *Aotus* and *Propithecus* show similarities in developmental patterns. As already stated in the preceding chapters, among strepsirrhines, the Indridae is the only strepsirrhine family that exhibits any morphological resemblance to anthropoids for the mandible. Thus, there is presently no evidence for differences in developmental constraints on the mandible between strepsirrhines and haplorrhines, when all strepsirrhines species are considered.

4.2 Trends in the evolution of morphology of the skull in strepsirrhines

Malagasy lemurs offer one of the best examples of adaptive radiation, and they occupy a wide range of ecological niches (Martin, 1972; Mittermeier et al., 1994). Loriforms are comparatively less diversified. Mittermeier et al. (1994) propose that competition with haplorrhines may have restricted their diversification.

Ontogenetic trajectory divergence occurs more frequently in lemuriform species than in loriform species. Coincidentally, lemuriforms also display wider diversity in their ontogenetic

allometric grades. For example, allometric transposition (Gould, 1971; Meunier, 1959), which allows for an uncoupling between size and shape, occurs in several taxa. The cheirogaleid *Microcebus murinus* is extremely small for the shape range it displays, whereas the lemurid *Lemur catta* and the indriids *Propithecus diadema* and *Propithecus verreauxi* are large for their shape. Conversely, loriforms are more restrained: the allometric scores of animals of the same size fall within a narrow range of values. Interestingly, the specimens belonging to the species *Lepilemur ruficaudatus* project similarly to loriforms in terms of allometric grade. The relationship between shape and size observed in *Lepilemur* and Loriformes is probably primitive for strepsirrhines. Conversely, the genera *Microcebus, Lemur,* and *Propithecus* are extremely derived in this respect.

The uncoupling between size and shape observed achieved via allometric transposition may seem maladaptive. Indeed, when shape does not change while size increases or decreases, there are important functional consequences. As stated by Gould (1971), maintaining geometric similarity in the face of changing size must be considered a problem and not an expectation. To account for the selective advantage of changing size while maintaining shape, Gould (1971) follows two lines of evidence. First, he argues that the genetic determinism of allometric transposition may be simple. A single mutation or a small number of mutations could account for modifications in size with only slight changes in shape. Such a mechanism would be favored in contexts of rapid diversification, or in contexts of strong selective pressure for a size change. The other, and in our view weaker, argument of Gould is that a change in allometric grade may represent a morphological innovation. Subsequent to a change in size, mechanical properties can be maintained only by changing shape. Thus an absence of shape change leads to changes - and potentially innovation - in the mechanical properties of the object.

In any case, the present evidence supports the hypothesis of Gould (1971) that large changes in size precede changes in shape in the adaptive radiation of different lemuriform families. Allometric grade shift is accompanied in lemuriforms with divergence in postnatal ontogenetic trajectory direction. However, it is not clear whether divergence in ontogenetic trajectory direction acts as an *a posteriori* compensatory mechanism for an initial change in allometric grade that was accompanied by a change in the mechanical properties of the skull, or whether this phenomenon forms part of the specialization specific to each taxon. Conversely, in the Loriformes infraorder, diversification may not have occurred as rapidly as in the case of the Lemuriformes infraorder. Ravosa (2007) proposes that the variation in morphology of the skull of the African lorises (*Arctocebus* and *Perodicticus*) results mainly from selection for differentiation in body-size. This proposal may be extended to all sister taxa in the Loriformes infraorder. In loriform species, a larger component of shape change is achieved via displacement of the ontogenetic trajectory position. All loriform species studied exhibit similar allometric grades, while differing in ontogenetic trajectory position. In loriforms, the largest species exhibit a trend toward peramorphism, whereas the small species tend to be paedomorphic. These trends toward

paedomorphism in smaller species and peramorphism in larger species do not seem to occur via changes in postnatal ontogenetic trajectory lengths. Indeed, at all dental stages and all dental scores, the smaller loriform species exhibit lower scores on CASV than larger species.

4.3 Is the toothcomb homologous in loriforms and lemuriforms?

The vast majority of extant strepsirrhines exhibit a distinctive morphology of the anterior mandibular teeth: they possess what is commonly referred to as a toothcomb, or a tooth scraper. The toothcomb is formed from the elongated, slender, and procumbent lower incisors and incisiform canines. The toothcomb forms a functional unit that is used during grooming (Buettner-Janusch and Andrew, 1962), and feeding (Martin, 1972).

4.3.1 Two hypotheses for the evolution of the toothcomb

Rosenberger and Strasser (1985) proposed that a functional link exists between the vomeronasal organ and the toothcomb. Under this interpretation, the toothcomb evolved as an extension of the vomeronasal organ. This organ is thought to be involved in the evolution of social behavior and grooming in strepsirrhines (for a review, see Asher, 1998). Asher (1998) gives morphological evidence that modern strepsirrhines (and not adapiforms) have an autapomorphic rostrum, and use their toothcomb as a means of collecting pheromones. There is a correlation between the width of the upper interincisal gap and social behavior in Strepsirrhines. However, species that spend a lot of active time with conspecifics (belonging to the genera *Eulemur, Hapalemur, Lemur, Avahi, Indri, and Phaner*) and that present a wide upper interincisal gap are well nested within Strepsirrhines (Asher, 1998). Therefore, Asher favors the diet-based hypotheses on the origin of the toothcomb, as formulated by Martin (1972) and Rose et al. (1981). According to these hypotheses, the toothcomb evolved primarily as a tool to collect plant exudates from damaged trunks. Under this scenario, the grooming function of the toothcomb would be a secondary adaptation.

The potential advantage of the early emergence of the toothcomb in lorisids may be linked to dietary habits. Among lorisids, there is evidence of gouging behavior in *Nycticebus pygmaeus* (Tan and Drake, 2001). Although there is no evidence of active gouging in other lorisid species, *Perodicticus* frequently consumes tree exudates (Charles-Dominique, 1977), and the mostly insectivore *Loris* occasionally feeds on gum (Nekaris and Rasmussen, 2003). This leads to the proposal that the relatively early emergence of the permanent; and more robust; toothcomb is part of the gummivory specialization observed in *Nycticebus pygmaeus*. This hypothesis would be consistent with early gouging behavior in young individuals. If this idea is true, then dietary specialization may have led to the evolution of the toothcomb in stem lorisids, whereas it was lost in *Arctocebus*, *Loris,* and *Perodicticus*.

4.3.2 Could the toothcomb have evolved twice during strepsirrhine phylogeny?

A few extant species depart from the typical toothcomb morphotype, including the indriids, which do not possess a lower canine, and *Daubentonia madagascariensis*, which possesses only a pair of very specialized hypsodont incisors. Several sub-fossil lemur species also deviate from the toothcomb morphology in their anterior lower teeth (Martin, 1972). Therefore, it is parsimonious to consider that the toothcomb emerged only once during the evolution of strepsirrhines (Martin, 1972; Rose et al., 1981; Szalay and Seligsohn, 1977). Seen in this way, the toothcomb may represent an apomorphy of Strepsirrhines. Martin (1972) detailed how non-toothcombed strepsirrhine species, and in particular *Daubentonia*, could have developed their dental morphology secondarily through the modification of a toothcomb.

In Lorisidae species, the permanent toothcomb erupts before the first molar. Lorisidae species also exhibit a very unusual configuration in the orbital region (see Chapter 2). Their orbits are convergent and oriented upward, which suggests a radical reorganization of the face. It is probable that the pattern of eruption of the toothcomb of the lorisids represents a supplementary apomorphy of this family, rather than evidence for non homology of the toothcomb between lemuriforms and loriforms.

SUMMARY OF CHAPTER 5

Modification of ontogeny has been recognized for a long time as an important source of morphological innovation (Haeckel, 1866). Here, we examined whether modifications of ontogenetic trajectories are responsible for a large part of the diversity of the skull in strepsirrhines and in primates in general. We investigated whether developmental constraints can be detected between haplorrhines and strepsirrhines. Ontogenetic patterns are compared between the two extant strepsirrhine infraorders, the Lemuriformes (Malagasy lemurs) and Loriformes (Galagidae and Lorisidae).

Strepsirrhine and haplorrhine species differ widely in cranial ontogenetic trajectory direction, position and length. These results support the hypothesis that different constraints act on cranial development and determine the morphological variability in both suborders. In contrast, no evidence of differences in developmental constraints on the mandible is found between haplorrhines and strepsirrhines.

Divergence in ontogenetic trajectory and allometric grade shifts occur more frequently and with a higher degree of intensity in the lemuriform than in loriform species. Ontogenetic trajectories are much less variable in the Loriformes infraorder. In small loriform species, there is a trend toward skull paedomorphism via a change in ontogenetic trajectory position.

Molecular dating suggests that the divergence between the Lemuriformes and the Loriformes infraorders occurred in the early Paleocene or during the Cretaceous. If this hypothesis were true, it would imply that the toothcomb of lemuriforms and loriforms is not necessarily homologous. A difference in trend exists in the relative timing of eruption of the permanent toothcomb in lorisids and lemuriforms. While it erupts before M1 emerges in lorisids, it always erupts afterwards in lemuriforms. However, the galagids display a pattern of eruption different from that observed in lorisids. Thus, the patterns observed in lorisids are interpreted as an apomorphy of this family. There is presently no developmental evidence for a non-homologous toothcomb in loriforms and lemuriforms.

Chapter 6

Adapiformes and the evolution of the strepsirrhine skull

Contents

1. Introduction

Unambiguous fossil data are lacking for the ancestors of modern strepsirrhines. The Adapiformes is a group of early strepsirrhine primates that performed a large radiation mostly during the Eocene (Godinot, 1998). The phylogenetic relationships between the adapiforms and extant strepsirrhines are still debated. The Adapiformes may be the sister group to modern strepsirrhines (Marivaux et al., 2001; Rosenberger et al., 1985) or may include the direct ancestors of modern strepsirrhines (Beard et al., 1988; Beard and Godinot, 1988; Dagosto, 1988; Godinot, 2006).

Recent studies have supported the hypothesis of an Afro-Arabian origin of the toothcombed strepsirrhines. Two stem loriform taxa, *Karanisia* and *Saharagalago*, were found in middle-Eocene deposits of Egypt (Seiffert et al., 2003,). Recent fossil evidence also supports the hypothesis that the Fayum late Eocene *Wadilemur,* which was formerly interpreted as an anchomomyin adapiform (Simons, 1997), is a stem galagid (Seiffert, 2005). Moreover, other taxa such as *Anchomomys milleri*, *Djebelemur martinezi,* and *Plesiopithecus teras* are potentially more related to extant strepsirrhines than any adapiform primate and may form part of an African radiation independent of that of adapiforms (Godinot, 2006; Seiffert, 2005,).

These fossils are known mostly through dental material only. A cranium of *Plesiopithecus teras* was described by Simons and Rasmussen (1994), but it is incomplete, crushed, and slightly distorted. The cranium of *Plesiopithecus* shows specialization in various respects. It possesses anterior tusk-like teeth, and its snout is unusually short (Rasmussen and Nekaris, 1998). Therefore, the skull morphology of the ancestors of the modern strepsirrhines remains unknown.

Nevertheless, several Eocene adapiform taxa, such as the notharctines *Smilodectes* and *Notharctus*, the adapines *Adapis*, *Leptadapis*, and *Palaeolemur*, are represented by fairly complete skulls. The adapine adapiforms form part of an important immigration wave, which brought in the European archipelago (see Figure 6.1) mammals in the middle Eocene, among which were perissodactyles, artiodactyles, rodents, and chiroptera (e.g., Franzen, 2003; Franzen and Haubold, 1986; Hartenberger, 1990; Sigé, 1977; Sudre, 1980). The European primates are probably of Asiatic origin (see Beard et al., 1994) and invaded the central Europe island during the late Lutetian (e.g., see Franzen, 2003; Godinot, 1998). The adapine evolved and diversified in Europe until the end of the Eocene (Godinot, 1998). The end of the Eocene is marked by a climatic deterioration (e.g., see Legendre and Hartenberger, 1992; Prothero, 1989), which caused a major faunal turnover around the Eocene-Oligocene transition (also referred to as the "Grande Coupure" of Stehlin, 1909). The adapine material that is included in this study comes from the "Phosphorites du Quercy" from the southwest of France. The adapine cranial material of the old Quercy collection has been subject to much debate and was reviewed by Lanèque (1990) in a comprehensive thesis. One major outcome of her analyses is that the morphological

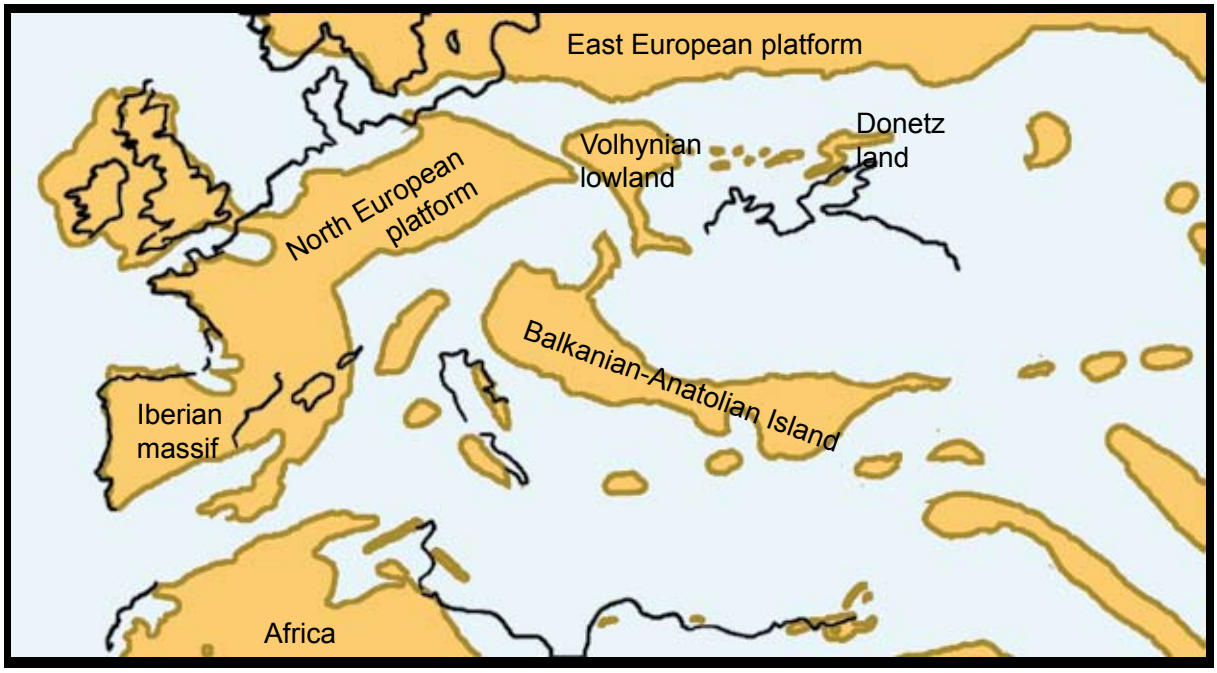

Figure 6.1: Paleogeography of Europe during the late Lutetian (44–41 million years). Modified after Meulenkamp et al. (2000).

variability within the *Adapis* and *Leptadapis* genera cannot be explained by the hypothesis of sexual dimorphism (e.g., see Gingerich, 1981a). Rather, the morphological variability reflects a phyletic diversity. For instance, Lanèque (1993) described patterns of orbital variability in the cranium of adapines. She observed that the degree in orbital frontation is variable within the genera *Leptadapis* and *Adapis*. However, it remains to be seen whether this degree of variability is an overestimate. Indeed, at least some of the specimens analyzed by Lanèque are incomplete or present severe distortion in the orbital region. Here, we reassess the morphological variability in the skull of adapine adapiforms using a GM approach. Virtual reconstructions of adapine crania belonging to the genera *Adapis*, *Palaeolemur*, and *Leptadapis* are proposed. Here, the orbits of incomplete or damaged specimens were restored when it was necessary (e.g., see Appendices 8, 9, 10 and 11).

Several adapiform primates for which the skull morphology is well known share characteristics that are usually found only among anthropoids. For example, *Leptadapis*, *Adapis,* and *Notharctus* have relatively vertical incisors and a fused mandibular symphysis. Hence, adapiform primates have been considered potential ancestors of anthropoids (e.g., Gingerich, 1973, 1984; Rasmussen, 1990; Simons and Rasmussen, 1989). This hypothesis has since been abandoned, and the characteristics shared by adapiforms and anthropoids are now considered homoplastic. Adapine and notharctine adapiforms are probably specialized in several respects, and the morphological features involved in these specializations may not be representative of the condition of stem strepsirrhines. Thus, we investigate whether both notharctine and adapine adapiforms present peculiarities in the 3D geometry of their skull that support the hypothesis that they are highly derived strepsirrhines: is the shape of their skull convergent in any respect

with that of anthropoid primates? What are the most important differences in the shape of the skull between adapiforms and extant strepsirrhines? What can be inferred about the evolution of cranio-mandibular developmental processes in strepsirrhine primates? Finally, do patterns of ontogeny of the strepsirrhine skull reflect known evolutionary trends, such as the general increase in the degree of encephalization?

2. Materials and methods

2.1 Sample composition

The fossil sample consists of 13 crania belonging to the Adapiformes infraorder. The subfamily Adapinae is represented by *Adapis sp*. (*N*=3), *Leptadapis* (*N*=6), the type specimen of *Palaeolemur betillei*, one cranium of *Notharctus tenebrosus* from the subfamily Notharctinae, and one cranium of *Smilodectes gracilis*.

Three different comparative samples were used. The first sample consisted of extant haplorrhines and strepsirrhines. This sample is used to assess the morphological affinities of the adapiforms with extant strepsirrhines and haplorrhines (see below). This first comparative sample is similar to that used in Chapter 2, with the exception of the genera *Alouatta, Archaeolemur*, and *Daubentonia*, which are not included. The second comparative sample consists of extant strepsirrhine individuals. This sample is used in the comparative analysis of extant and extinct strepsirrhine morphologies and is similar to that used in Chapter 4, but the genus *Daubentonia* was omitted. The third comparative sample consists of ontogenetic series. This sample is similar to that used in Chapter 5 and is used in an evolutionary analysis of the developmental patterns in strepsirrhines. The complete list of the specimens examined in this chapter is presented in Appendix 1.

2.2 Methods of analysis

The landmark protocols used in this chapter take into account the fact that several fossils are incomplete, especially in the nasal region (see Chapter 1, section 2.1).

2.2.1 Morphological variability of the adapine adapiforms

Shape and size variability were assessed for each extant strepsirrhine family and the Adapinae subfamily. A Principal Component Analysis (PCA) of data in linearized Procrustes shape space was conducted in order to permit an assessment of the patterns of shape variation within adapine adapiforms (see Chapter 1, sections 2.2 and 2.3) for cranium configuration.

2.2.2 Are there morphological similarities between the skull of adapine and notharctine adapiforms and those of haplorrhines?

To assess whether adapiforms are more similar morphologically to extant haplorrhines or strepsirrhines, Canonical Variate Analyses (CVA) were performed for the three landmark configurations. The suborder to which each extant specimen belongs (Haplorrhini or Strepsirrhini) was taken as the categorical variable. Reallocation procedures were subsequently performed in order to classify *a posteriori* all the specimens into the categories "haplorrhines" and "strepsirrhines". One result presented in Chapter 4 is that discrimination between monophyletic groups is more reliable using data corrected for cranium size and skull configuration. Accordingly, the same methodology was followed here for skull and cranium configurations: extant specimens were first projected on the common allometric shape vector (CASV) and computed as the mean of the allometric vectors obtained separately for each suborder. After projecting the extant specimens on the CASV, shape residuals were used as the input of the CVA. For mandible configuration, raw Procrustes residuals were used as the input into the CVA. All extant specimens were then classified *a posteriori*. It must be noted that the adapiforms were not used for computing the canonical axes. Rather, they were projected *a posteriori* on these axes, and their projection scores were used to classify them into the suborder to which they are closest in terms of shape without making any *a priori* assumptions that may influence the computation of the axes (see Chapter 1, sections 2.4 and 2.5). In this analysis, the first comparative sample was used (see above for a detailed description).

2.2.3 What are the main differences in cranio-mandibular morphology between the adapiforms and toothcombed strepsirrhines?

In order to assess the morphological features by which the adapiforms differ from extant strepsirrhines, CVAs were performed for the three landmark configurations Two classes were used: "extant strepsirrhine" and "adapiform". The morphological variation along the resulting canonical axis were represented for the skull, cranium, and mandible. This analysis involves the second comparative sample (see above).

2.2.4 An evo-devo perspective on adapiform skull morphology

Here we tackled the question of the evolution of ontogeny in both extant and extinct strepsirrhines by performing an analysis combining fossils and ontogenetic series of extent specimens. The third comparative sample was used for this purpose (see above for details). CASVs were computed for the skull, cranium, and mandible configurations as the mean values of species-specific ontogenetic allometric shape vectors (ASVs). As only adult adapiforms were available, it was not possible to compute fossil species-specific ontogenetic ASVs. Therefore, the fossils were simply projected on the CASV computed for the ontogenetic series data using extant specimens.

The first goal of this analysis was to evaluate whether allometric transposition occurred in adapine adapiforms, similarly to what was observed within extant lemuriforms in Chapter 5.

Allometric transposition was detected on plots of the logarithm of centroid size against CASV scores. As emphasized in Chapter 5, allometric grade shifts may indicate episodes of rapid diversification. The adapines invaded the central European island in the late Lutetian and radiated mostly during the late Eocene (Godinot, 1998). Within the framework of this radiation, *Adapis* species are interpreted by Gingerich (1981a) as dwarfed descendants of a *Leptadapis*-like ancestor, a view which is not shared by Godinot (1998). Similar to what was observed for the lemuriform species in Chapter 5, differences in allometric grade may exist between *Leptadapis* and *Adapis/Palaoelemur*. In such a case, new arguments could be made regarding the assessment of the polarity of the shift in size that occurred in the Adapinae subfamily.

The second goal of this analysis was to assess whether variability in the patterns of ontogenetic trajectories in extant and extinct species could be linked to the general trend toward increasing encephalization in primates since at least the Eocene (Jerison, 1979). Indeed, the most striking features in which adapiforms differ from extant primates are found in the basicranium and neurocranium: adapiforms display a low degree of basicranial flexion and a relatively smaller braincase. A metric that is widely used to compare the relative degree of encephalization in primates is the "Encephalization Quotient" (*EQ*), which was proposed by Jerison (1970). It measures the deviation of an animal's brain mass from the standard relationship between brain mass and body mass in living mammals. Jerison found that in a large sample composed of living mammals, brain mass E^m can be approximated by the equation:

$$E^m = 0.12\ P^{2/3},$$

where P is body mass. Accordingly, EQ is defined as

$$EQ = \mathrm{E}/(0.12\ P^{2/3})$$

where E is brain mass.

An *EQ* larger than 1 means that the degree of encephalization is larger than than of an average extant mammal. Similarly, an *EQ* smaller than 1 indicates that the degree of encephalization is lower than that of an average extant mammal.

We estimated the *EQ* for each species for which ontogenetic series were acquired plus the genera *Adapis*, *Palaeolemur,* and *Smilodectes* as follows: first, the CT images were used to segment manually the endocranial cavity. Endocranial volumes were derived from these virtual reconstructions. Three estimates of body mass were used to compute three corresponding estimations of *EQ*: the lower and upper range of body mass given by Rowe (1996) and Nowak (1999) and body mass estimated from cranial length, according to Jerison's equation (1979) for strepsirrhines. For *Adapis* and *Smilodectes, EQ* and body mass estimates provided by Jerison (1979) were used. The endocranial volume of *Palaeolemur* was measured using a scan of the type specimen, and its body mass was estimated using the equation that Jerison (1979) derived from cranial length for strepsirrhines.

For a given species, the CASV score at adulthood provides an indication of the total amount of shape change that occurs during ontogeny. Thus, it is a proxy for the total (prenatal + postnatal) ontogenetic trajectory length. The potential relationship between encephalization quotients and ontogenetic trajectory length was assessed by performing linear regression of *EQ* against CASV scores.

3. Results

3.1 Shape and size variance in the adapine cranium

Table 6.1: Shape and size variance of the cranium within each family.

	Group	Shape Variance	D.f.	Mean Size	Size Variance	D.f.
Cranium	Cheirogaleidae	5.39E-05	2227	92	356	17
	Indridae	6.12E-05	1834	171	1389	14
	Lemuridae	5.67E-05	2489	171	215	19
	Lepilemuridae	4.45E-05	1179	122	21	9
	Galagidae	7.68E-05	3144	117	487	24
	Lorisidae	6.88E-05	3144	123	354	24
	Adapinae	7.46E-05	1048	199	1393	8

Data on size variance and shape variance for the Adapinae subfamily are given in Table 6.1. Size variance is the same in the Adapinae subfamily and in the Indridae family ($p=0.48$), but it is significantly greater as compared to other families ($1e\text{-}7<p<0.03$). Moreover, in the Indridae family, there is a wide gap in size distribution between the genus *Avahi* and the largest species belonging to the *Indri* and *Propithecus* genera. Similarly, in the Adapinae subfamily, a wide gap in size range exists between the two genera *Adapis* and *Palaeolemur* on one side and *Leptadapis* on the other. Shape variance in Adapinae is equivalent to that of Lorisidae and Galagidae families ($0.05<p<0.3$), but it is significantly greater than in any Lemuriformes family ($1e\text{-}18<p<2e\text{-}4$). No sub-fossil Malagasy lemur is incorporated in the sample. Thus, it is likely that the shape variance computed for a Lemuriformes family such as the Indridae, which are represented by several recently extinct genera, would be larger than that computed for the Adapinae if representative specimens of all the indriid sub-fossil genera were included.

The patterns of cranial shape variation of adapine primates are presented in Figure 6.2. The first principal component (PC1) accounts for 27.75 % of the total sample shape variance. Shape variations at the negative pole of PC1 show crania with relatively larger, less frontated and less convergent orbits, vertically higher and broader snouts, and a relatively smaller braincase. Specimens that project to the positive pole of PC1 exhibit relatively larger braincases, smaller, more frontated and convergent orbits, and low and thin snouts. PC1 scores are significantly

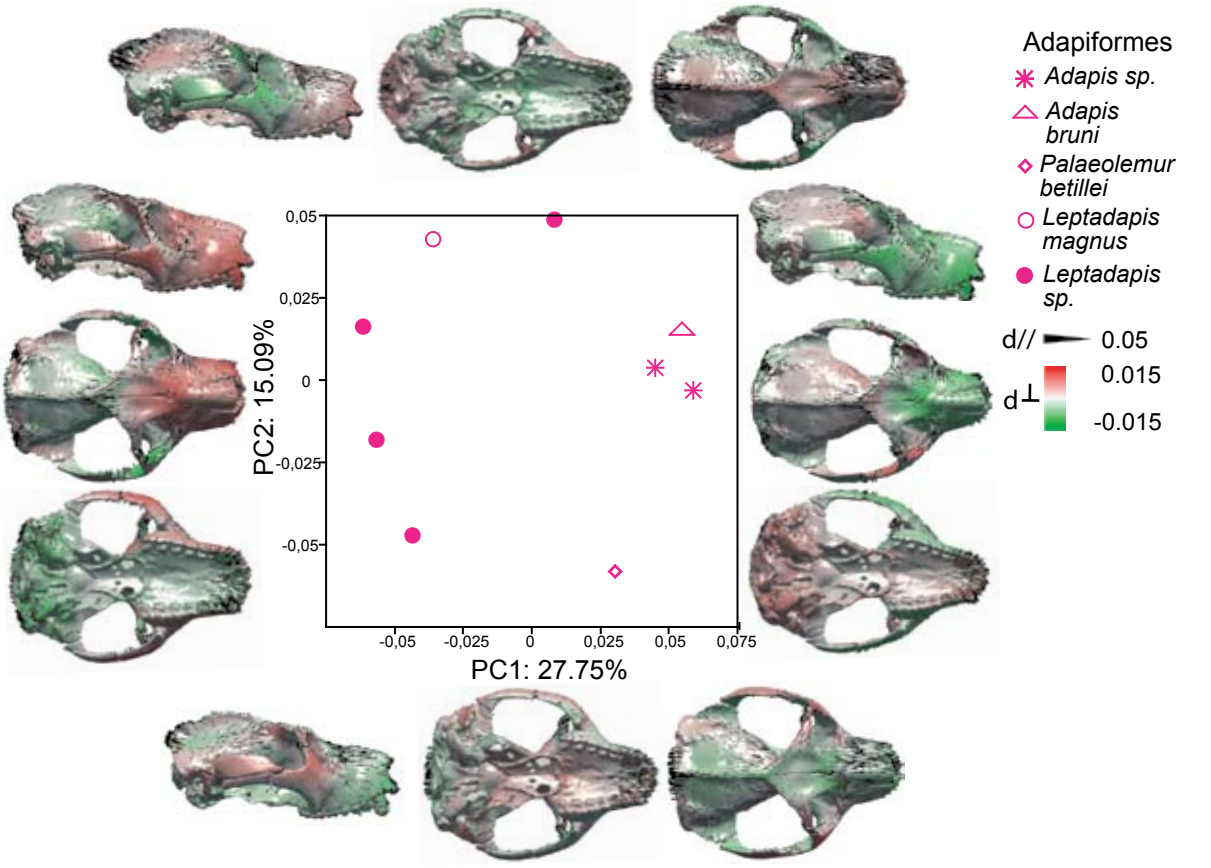

Figure 6.2: Major patterns of cranio-mandibular variation in shape within the adapine Adapiforms. A composite skull consisting of the back of the cranium of *Leptadapis* sp. ACQ 209 and of the snout of *Leptadapis sp.* MAPHQ 210 is used to represent the variations in shape. d//: displacement parallel to the surface. d⊥: displacement perpendicular to the surface. Scales in centroid size units.

correlated with size (p=0.003). The genera *Leptadapis* and *Adapis* and *Palaeolemur* are well separated on PC1. The second principal component (PC2) accounts for 15.09% of the total sample shape variance. PC2 quantifies shape change that describes primarily the breadth and length of the crania. PC2 separates short and broad crania with convergent and frontated orbits from narrow and long crania in the anteroposterior plane, which exhibit less frontated and divergent orbits. The largest crania of *Leptadapis* MAPHQ 210 and QU10870 and the small cranium *Palaeolemur betillei* are well separated from the other specimens on this axis.

3.2 Classification procedures

3.2.1 skull

Only two fossils in the sample are complete: *Notharctus tenebrosus* AMNH 127163 and *Leptadapis sp.* QU 10870. Therefore, only these two fossils were incorporated in the analysis of skull configuration. All extant strepsirrhines and haplorrhines are successfully reallocated *a posteriori* to their suborder. All the fossils are classified in the "strepsirrhine" suborder (Table 6.2).

Table 6.2: Classification procedure derived from the CVA of the skull shape taking "suborder" as the categorical variable. The analysis is performed on shape data corrected for size.

	Strepsirrhine	Haplorrhines	%success
Strepsirrhines (113)	113		100%
Haplorrhines (85)		85	100%
Total (198)			100%
Adapinae(1)	1		
Notharctinae(1)	1		

Table 6.3: Classification procedure derived from the CVA of the mandible shape taking "suborder" as the categorical variable. The analysis is performed on shape data corrected for size. All the misclassified mandibles belong to the family Indridae.

	Strepsirrhine	Haplorrhines	%success
Strepsirrhines (113)	101	12	89.4%
Haplorrhines (85)		85	100%
Total (198)			94%
Adapinae(1)	1		
Notharctinae(1)	1		

Table 6.4: Classification procedure derived from the CVA of the cranial shape taking "suborder" as the categorical variable. The analysis is performed on data corrected for size.

	Strepsirrhine	Haplorrhines	%success
Strepsirrhines (113)	113		100%
Haplorrhines (85)		85	100%
Total (185)			100%
Adapinae(9)	9		
Notharctinae(2)	2		

3.2.2 mandible

This classification procedure is not as powerful for discriminating strepsirrhines from the haplorrhines (Table 6.3). All misclassified mandibles belong to the Indridae family. The two fossil mandibles are classified as strepsirrhines.

3.2.3 cranium

All the extant specimens are successfully classified *a posteriori*. The eleven adapiform crania are allocated into the Strepsirrhini suborder (table 6.4).

3.3 Differences in morphology between adapiforms and toothcombed strepsirrhines

The canonical axes (CVs) are significantly correlated with centroid size (skull: $r^2= 0.57$, $p<0.001$; cranium: $r^2=0.35$, $P<0.001$; mandibles: $r^2=0.44$, $p<0.001$), which indicates that a large part of the shape differences between adapiforms and toothcombed strepsirrhines is of allometric origin (see Figure 6.3). However, for cranium configuration, even though *Adapis* and *Palaeolemur* are clearly not the largest specimens of the sample, they are also well discriminated on the canonical axis. This indicates that not only allometry explains the morphological differences between adapiforms and extant strepsirrhines. Toothcombed strepsirrhines differ

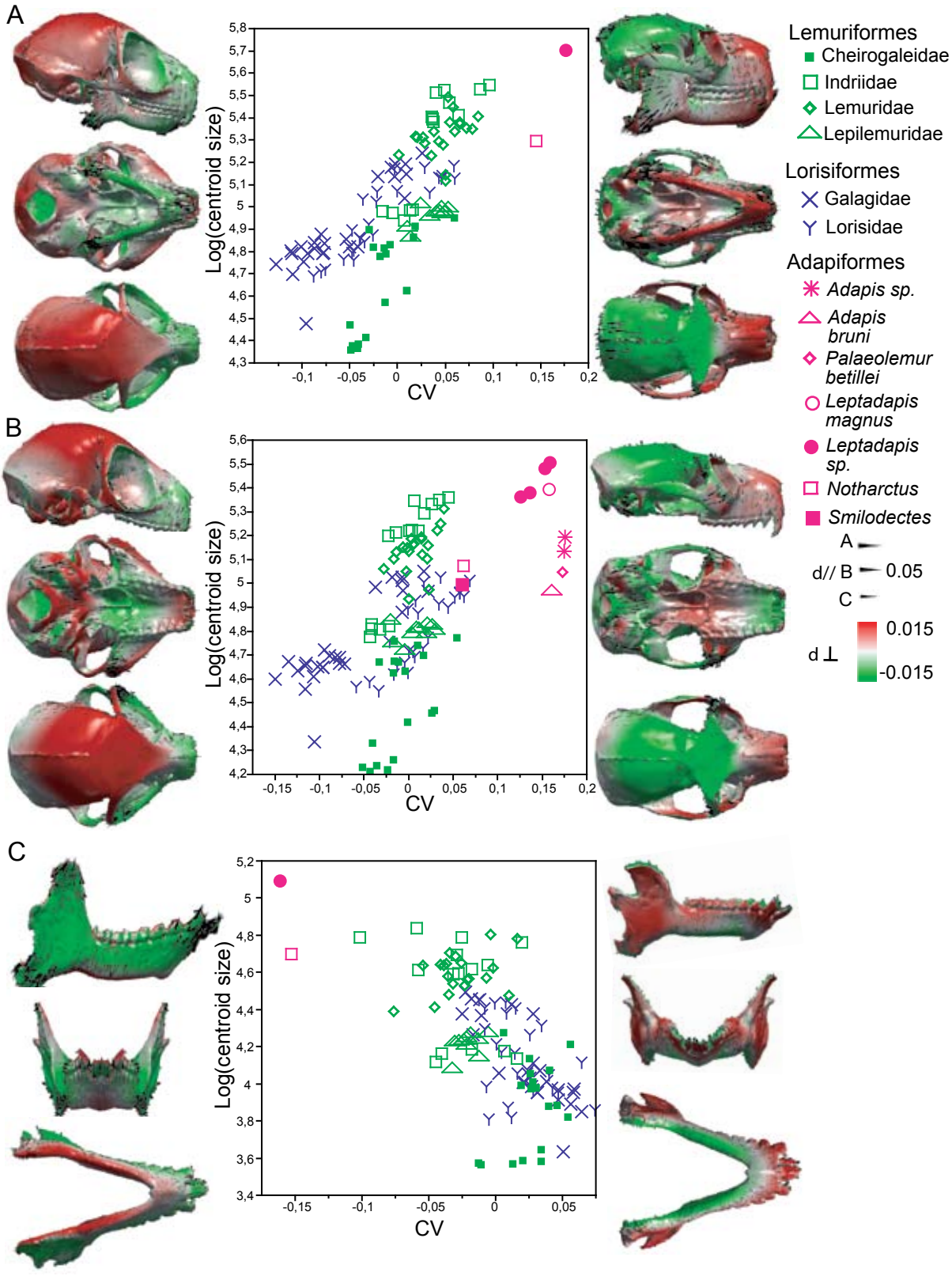

Figure 6.3: Major cranio-mandibular differences in shape between adapiforms and extant strepsirrhines. A: skull. B: cranium. C: mandible. CVAs were performed on the three configurations. Two classes were used: "adapiform" and "extant strepsirrhine". Note how the resulting canonical axes are significantly correlated with size for the 3 configurations ($p<0.001$), indicating that a large part of the differences in morphology between the adapiforms and extant strepsirrhines are of allometric origin. The skull of *Lepilemur ruficaudatus* is used to represent the shape deformations. d//: displacement parallel to the surface. d⊥: displacement perpendicular to the surface. Scales are in centroid size units.

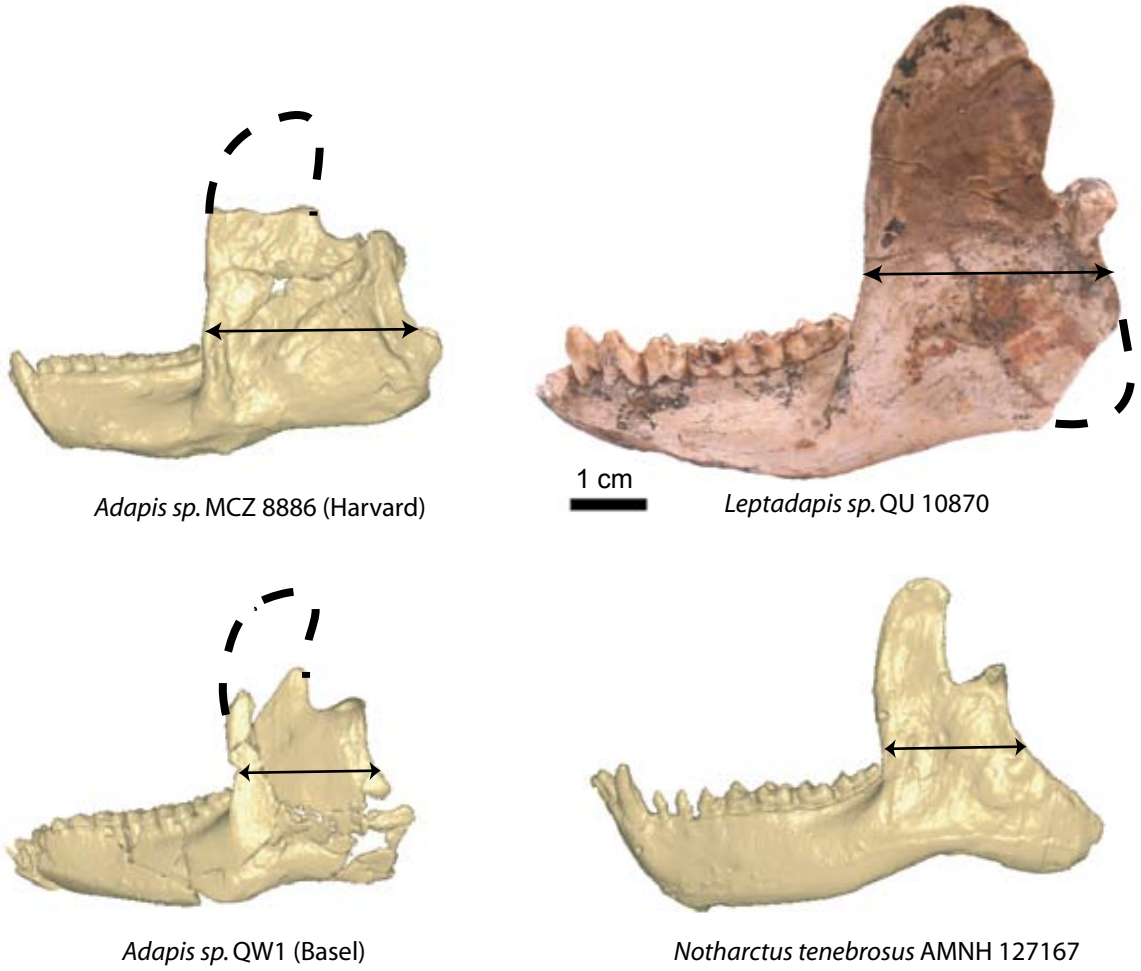

Figure 6.4: Comparison of the mandibles of four adapiform specimens. Dashed lines: estimation of the missing parts. Note the relative depth of the horizontal ramus (arrows), which is relatively longer in *Adapis* and *Leptadapis* than in *Notharctus*.

from adapiforms in the following features: they exhibit crania with relatively larger braincases, larger and more divergent orbits, a narrow and short snout, and a higher degree of basicranial flexion. Extant strepsirrhine skulls exhibit comparatively smaller and more gracile mandibles with lower condyles relatively to the occlusal plane and small angular processes. Conversely, the crania of adapiforms are characterized by a relatively smaller neurocranium, smaller and more convergent orbits, a comparatively longer and larger snout, and a posteriorly-placed foramen magnum. Concerning the cranium, among the adapiforms, *Notharctus* and *Smilodectes* are the least discriminated from extant strepsirrhines. Adapiforms also exhibit longer and more robust mandibles with high condyles, high mandibular corpora, vertically higher and longer mandibular symphyses in the anteroposterior plane, and extremely well developed coronoid processes. Adapiforms also exhibit a very narrow angle between the two horizontal branches of their mandibles. The mandibles of the adapines exhibit shorter corpora and tooth rows and a greater depth of the horizontal ramus than *Notharctus* (see Figure 6.4).

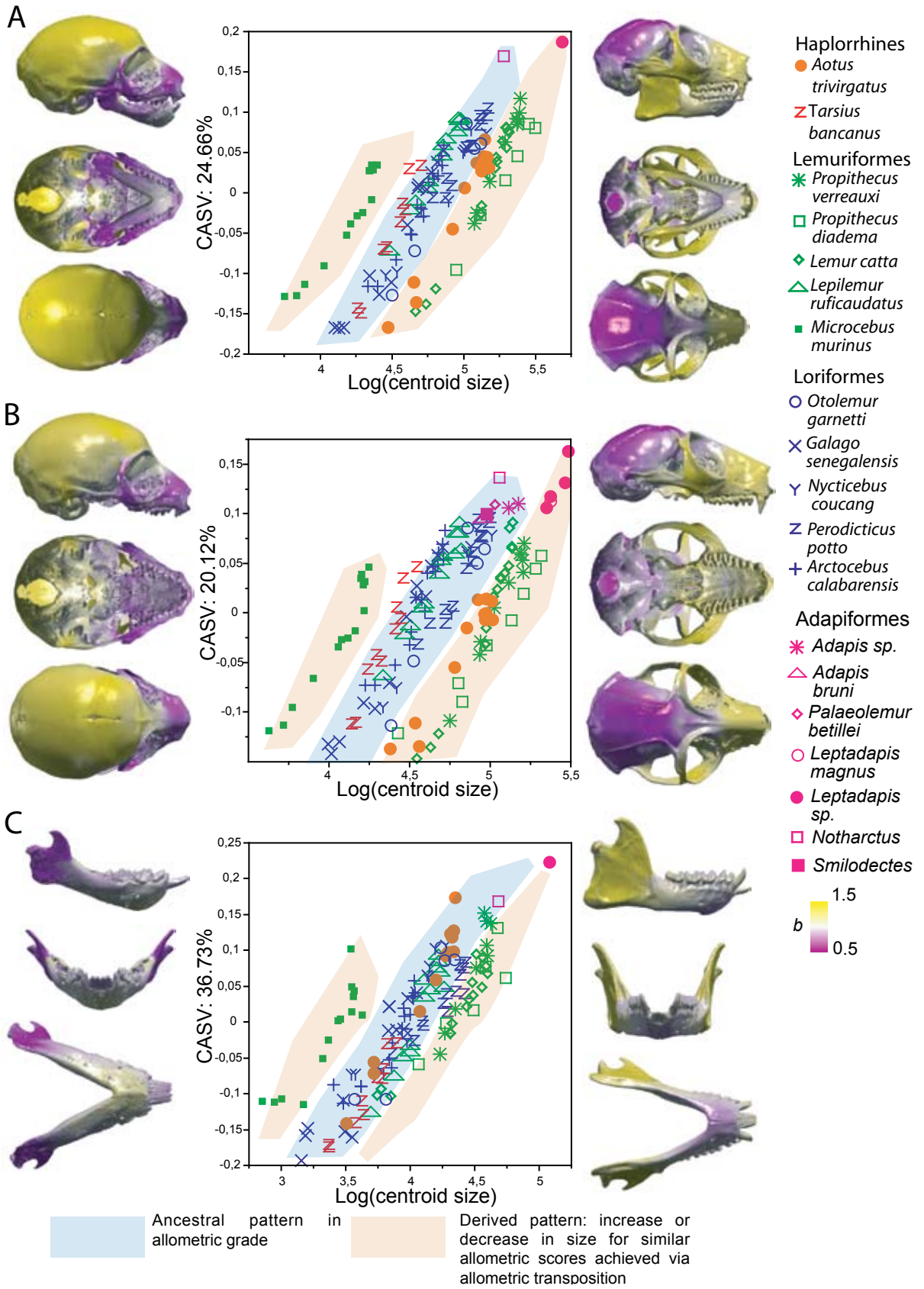

Figure 6.5: An evo-devo perspective on adapiform skull morphology. The CASV is computed as the mean of the different extant species-specific ASVs. The fossils are projected on the CASV a posteriori. Figures around the central plots correspond the extreme variations (templates: *Arctocebus calabarensis* 7013 for low values of projection on CASV and *Arctocebus calabarensis* 7704 for high values on CASV). The color scale (b) corresponds to the relative change in local area along the CASV.

3.4 Ontogenetic allometric patterns

The projection scores of the fossils on the CASVs are presented in Figure 6.5 for the three configurations. For skull configuration, *Notharctus* and *Leptadapis* project to values higher than any reached in the extant sample. As for cranium configuration, nearly all of the fossils exhibit high projection scores on the CASV. Among the fossils, *Smilodectes gracilis* projects to the lowest value, whereas *Notharctus* and the largest *Leptadapis* display the highest projection scores. Concerning the mandible configuration, *Leptadapis* displays the highest projection score of the samples, and *Notharctus* projects higher than any strepsirrhines.

Table 6.5: Endocranium volume, body mass, encephalization quotient (EQ) and projection scores on the CASV at adulthood. Only the species for which ontogenetic data could be collected are represented here, plus three fossil genera.

	Measured specimen	Endocranial volume (cm3)	Weight (litterature)*	EQ‘	EQ’’	Maximal cranial length (cm)	Weigth estimation from cranial length	EQ°	CASV Score at adulthood (cranium)
Haplorrhines									
Aotus trivirgatus	ZU-1775	15.73	920-950	1.36	1.39	5.65	539.14	1.98	0.003
Tarsius bancanus	ZU-1832	3.57	100-131	1.15	1.38	3.9	130.62	1.16	0.0409
Lemuriformes									
Lemur catta	ZU-9601	22.18	2678-2705	0.95	0.96	8.36	2444.27	1.02	0.0663
Lepilemur ruficaudatus	ZU-11054	6.89	600-915	0.61	0.81	5.731	552.60	0.85	0.0671
Microcebus murinus	ZU-10815	1.99	38-98	0.78	1.48	3.2	55.69	1.14	0.0358
Propithecus Diadema	ZU-7725	40.38	5633-7250	0.90	1.06	9.25	3640.54	1.42	0.0506
Propithecus verreauxi	ZU-AS131	26.99	3480-3637	0.95	0.98	8.221	2288.09	1.30	0.0563
Loriformes									
Galago senegalensis	ZU-6591	4.86	193-210	1.15	1.21	4.24	168.68	1.33	0.0345
Otolemur_garnetti	ZU-12251	11.85	721-822	1.13	1.23	6.49	901.82	1.06	0.0667
Arctocebus calabarensis	ZU-7059	6.28	266-465	0.87	1.27	5.5	469.95	0.87	0.0603
Nycticebus coucang	ZU-10573	9.91	230-1200	0.73	2.20	5.87	607.29	1.15	0.0765
Perodicticus potto	ZU-7425	12.63	850-1600	0.77	1.17	6.29	797.23	1.22	0.081
Adapiformes									
Palaeolemur betillei	BOR613	7.25	/			7	1214.78	0.53	0.1095**
Adapis sp.	/	9	1600	0.55					0.104**
Smilodectes gracilis	USNM 21812	9	1600	0.55					0.0983**

Encephalization quotients:
The formula used is: *EQ* = E/(0.12*P2/3) where E is the endocranium volume and P is body weight.
- *EQ*': computed using the upper range of body mass given in Rowe (1996) and Nowak (1999).
- *EQ*'': computed using the lower range of body mass given in Rowe (1996) and Nowak (1999).
- *EQ*°: *EQ* computed using body mass estimators determined from the equations of Jerison (1979):
  Aotus trivirgatus: the "ceboid" regression is used: logY = 3.566 logX + 0.0499
  Tarsius bancanus: the "ceboid + *tarsius*" regression is used: logY=3.6759 logX –0.0567
  Other specimens: the "strepsirrhine" regression is used: logY= 3.938 logX –0.2435
  Y stands for body mass (g), and X represents cranial length (cm).
- *Adapis* and *Smilodectes*: *EQ* from Jerison (1979).
*: weight ranges from Rowe (1996), with the following exceptions:
Adapis and *Smilodectes*: the estimates given by Jerison (1979) are employed.
Microcebus murinus: the value of 109 g (reported by Rowe,1996) seems overestimated, sothe range found in Nowak (1999) is followed instead.
**: CASV scores obtained by simple projection of the specimens on the CASV computed for cranium configuration (see Method paragraph for details concerning the computation of this vector). Concerning "*Adapis*", a mean individual is computed for all the specimens belonging to this genus and is projected on the CASV.

Table 6.6: Regressions of *EQ* against CASV scores at adulthood. The original data on which the regressions are performed is presented in Table 6. Regressions are conducted with and without the fossil genera *Adapis*, *Palaeolemur*, and *Smilodectes*.

EQ used in the regression	Coefficient of determination "r²"	p Value
EQ' with/without fossils	0.71/0.5	<0.0001/0.01
EQ" with/without fossils*	0.27/0.35	0.048/0.06
EQ° with/without fossils	0.76/0.54	<0.0001/0.007

- EQ': computed using the upper range of body mass given in Rowe (1996) and Nowak (1999).
- EQ": computed using the lower range of body mass given in Rowe (1996) and Nowak (1999).
- EQ°: EQ computed using body mass estimators determined from the equations of Jerison (1979).
*: *Nycticebus coucang* is removed. The specimen for which the endocranium volume is measured is large, and certainly weighs far more than the lower bound of body mass range given in Rowe (1996) for this species.

3.4.1 EQ and developmental patterns

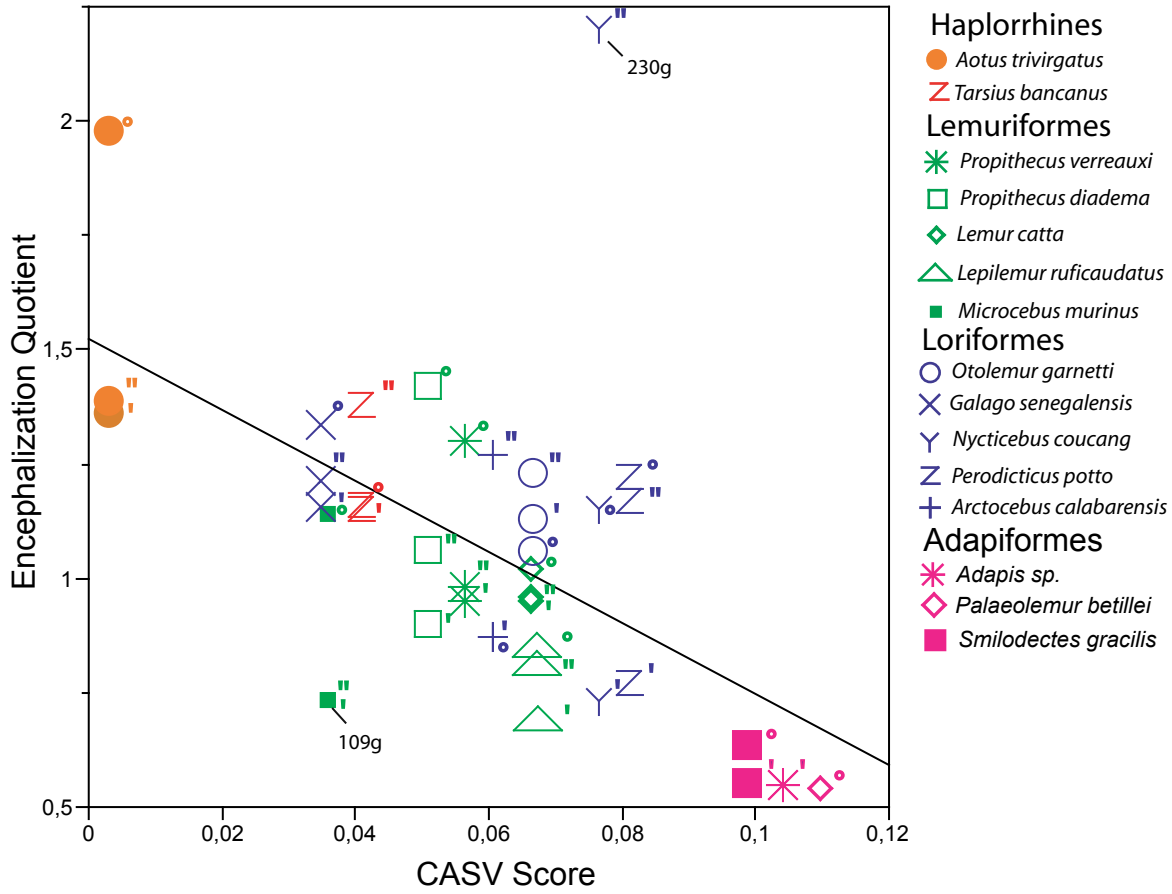

Figure 6.6: Relationship between the encephalization quotient (*EQ*) and CASV scores at adulthood (original data and explanations are exposed in Table 6.5).
***EQ* estimations : <<°>>: *EQ* computed following the equations given by Jerison (1979), using cranial length as a proxy for body mass; see Table 6.5 for details concerning these equations. <<">>: *EQ* computed using the lower bound of the body mass range given in Rowe (1996) and Nowak (1999). <<'>>: *EQ* is computed using the upper range of body mass given in in Rowe (1996) and Nowak (1999). *Adapis* and *Smilodectes*: *EQ* from Jerison (1979).**
***Nycticebus coucang*: the specimen for which the endocranium volume is measured is large, and certainly weighs more than the lower bound of body mass range given in Rowe (1996) for this species. The resulting *EQ*" is doubtless severely overestimated.**

Species-specific endocranial volumes, body mass estimates, *EQ* values, and CASV scores at adulthood are presented in Table 6.5. For the three *EQ* estimates, *EQ* is significantly and negatively correlated with CASV scores at adulthood, with one single exception (see Table 6.6): the regression using *EQ* estimates and the lower range of species-specific body mass are not significant (p=0.06) for a sample from which fossils are excluded. A plot of *EQ* against CASV scores at adulthood is presented in Figure 6.6. Taken as a whole, the length of the ontogenetic trajectory through shape space is inversely proportional to the degree of encephalization. The adapiforms present the smallest values of *EQ* and the highest scores on the CASV. This provides evidence that the trend toward the increase in encephalization in strepsirrhines was achieved via a reduction of cranial ontogenetic trajectory length.

4. Discussion

4.1 Adapiformes and the cranio-mandibular morphology of stem toothcombed strepsirrhines.

Among the adapiforms represented in this study, the adapines are more derived in shape than *Smilodectes* and *Notharctus.* Indeed, they are clearly more discriminated in the canonical analysis for cranium configuration than the notharctines. The adapines also display mandibles with the largest horizontal rami of the sample, and very well developed coronoid processes. These results support the hypothesis of Rosenberger et al. (1985): on the basis of the morphology of their anterior teeth, Rosenberger et al. (1985) proposed that the morphology of notharctine primates would be a better model for pre-toothcombed strepsirrhines than that of the adapines.

Smilodectes gracilis and *Notharctus tenebrosus* were animals that weighed probably around 1.5kg for *Smilodectes* and 7kg for *Notharctus* (Conroy, 1987; Fleagle, 1999; Gingerich et al., 1982; Jerison, 1979). A large number of studies support the hypothesis that the ancestors of modern strepsirrhines were small insectivore primates (e.g., see Charles-Dominique, 1977; Martin, 1972, 1979; Petter, 1962; Petter et al., 1977). Furthermore, most of the potential stem stepsirrhines are smaller than *Notharctus* and *Smilodectes*. For example, *Djebelemur* has an estimated body mass of 100g (Fleagle, 1999). *Anchomomys milleri* is slightly smaller than *Wadilemur elegans* (Simons, 1997), the latter estimated to be the size of *Microcebus rufus* (Seiffert, 2005). Hence, they must have differed widely from *Notharctus* and *Smilodectes.* It is therefore probable that the cranial morphology of *Notharctus* and *Smilodectes* reflects only partially the condition of stem tooth-combed strepsirrhines.

4.2 The morphology of the adapine skull

4.2.1 Systematic complexity and morphological variability

The results presented here suggest that cranial variability in the *Adapinae* subfamily is equivalent to that of families such as the Galagidae or the Lorisidae. Moreover, within the small adapine species, the genera *Adapis* and *Palaeolemur* are well distinct in shape space: the cranium of *Palaeolemur* is relatively shorter and displays more frontated and more convergent orbits than the crania of the genus *Adapis.* This supports the view shared by Godinot (1998) and Lanèque (1992a; 1992b) that *Palaeolemur* (Delfortrie, 1873) is a valid genus. Moreover, the present analysis shows complex patterns of shape variability in the orbit and snout regions. These results come in general agreement with those of Lanèque (1990; 1992a; 1992b; 1993): the variability in the morphology within the Adapiformes infraorder reflects a phyletic diversity.

4.2.2 Differences between Adapis/Palaeolemur and Leptadapis

Allometry is certainly responsible for several features differentiating the crania of *Lepdatapis* and *Adapis/Palaeolemur*: crania of *Leptadapis* present comparatively vertically higher, longer and larger muzzles than those of *Adapis* and *Palaeolemur.* Moreover, *Leptadapis* specimens present relatively smaller braincases. However, the variability in the dimensions of the sagittal and nuchal crests within *Adapis/Palaolemur* and *Lepdatapis* cannot be explained by differences in size between these genera. In both the *Adapis* and *Leptadapis genera*, several specimens possess almost no sagittal crest (e.g., *Leptadapis sp.* YPM 11481, not included in this study and *Adapis bruni* MAPHQ 221), whereas others exhibit strongly developed crests (e.g., see *Leptadapis sp.* MAPHQ 210 or *Adapis sp.* PQ 1700, not represented here). Also, one would expect that the small *Adapis* and *Palaeolemur* exhibit relatively larger orbits than the large *Leptadapis*. On the contrary, specimens belonging to the genus *Adapis* exhibit very small orbits. This has been interpreted by Gingerich and Martin (1981) and Kay and Kirk (2000) as proof of diurnal activity (but see Lanèque, 1993). Specimens belonging to the genus *Leptadapis*, on the contrary, display relatively normal orbits for their size. Still, Kay and Kirk (2000) favour the hypothesis that they were diurnal.

4.2.3 Specialization to folivory

Adapines were early on acknowledged to exhibit a high degree of variability in the morphology of their mandibles. Filhol (1883) defined six adapine categories based on the comparative morphology of the corpus of the mandible. Stehlin (1912) recognized the importance of the variation in the shape of the horizontal ramus and of the extension of the mandibular symphysis in this material. Large horizontal rami, fused mandibular symphyses, condyles placed high above the alveolar plane, and very developed coronoid processes are features associated with

the possession of well-developed masseter and temporal muscles. They are related to a high degree of specialization to a folivore regime (Gingerich and Martin, 1981; Szalay and Delson, 1979).

Even if there is variability in the configuration of their orbits, the adapines display orbits that are much more convergent than those of most toothcombed strepsirrhines and those of the notharctines. The orbital characteristics shared by the adapine fossils are reminiscent of the conditions observed in Lorisidae. Lanèque proposed that orbital convergence could be the result of the combination of different factors: it may be interpreted as additional evidence that adapines were not leapers, as the galagids, but rather were climbers, like the lorises. By analogy with the slow lorises, which exhibit the highest degree of orbital convergence among strepsirrhines, she also proposed that orbital convergence in *Adapis* may reflect adaptation to occasional predatorial behavior. However, another proposition may be advanced to account for the degree of orbital convergence in adapine. Well-developed nuchal and sagittal crests and large temporal fossae indicate the possession of large masseter and temporal muscles in adapines, features which reflects a high degree of specialization to a folivore regime (Gingerich and Martin, 1981; Szalay and Delson, 1979). Previous observations performed in the whole primate order show that the forms that display the larger temporal fossae also exhibit a higher degree of orbital convergence (Chapter 2, section 2.3). Besides, our results suggest that longer ontogenetic trajectories result in larger the temporal fossae and higher degree of orbital convergence. Here we propose that the high degree of orbital convergence observed in adapine primates has two main origins: it is the result of their specialization to folivory on the one hand, and the by-product of harbouring long cranial ontogenetic trajectories on the other.

4.3 Allometric grade shifts and phyletic gigantism in *Leptadapis*

4.3.1 Ancestral patterns in allometry.

Similarly to what was observed in Chapter 5, a clear ancestral pattern concerning the relationship between centroid size and shape can be observed: at a given size, loriform species and *Lepilemur* exhibit a narrow range of allometric scores. Alternatively, the genera *Lemur, Propithecus,* and *Microcebus* deviate from this pattern, which is likely to be derived. The fossils belonging to the genera *Notharctus, Smilodectes, Adapis,* and *Palaeolemur* clearly exhibit the ancestral pattern when one observes the skull and cranium configurations. Contrary to this, for a given allometric score, the crania, mandibles, and skulls belonging to *Leptadapis* tend to exhibit very large sizes, and they fit in the pattern exhibited by *Lemur* and *Propithecus.* It is less clear whether *Notharctus* exhibits the derived or ancestral pattern of mandible configuration. The mandible of *Leptadapis* is large relative to its allometric projection score.

4.3.2 Phyletic gigantism in the Leptadapis lineage

The evidence presented here favors the hypothesis that *Adapis* and *Palaeolemur* follow the ancestral allometric grade and that *Leptadapis* has increased in size from an *Adapis*-like ancestor. At a given allometric score, *Leptadapis* is larger than expected for the ancestral allometric pattern, but similar in allometric score to *Adapis* and *Palaeolemur. Leptadapis* is clearly more similar in its allometric grade to *Lemur catta* and *Propithecus verreauxi* or *Propithecus diadema.* This view is in agreement with the hypothesis of phylogeny of the Adapinae subfamily proposed by Godinot (1998). Nevertheless, at least one argument can be advanced against this hypothesis: the unusually small orbits of *Adapis* would be more easily explained in a context of isometric dwarfism from a larger ancestor. As shown by Gingerich (1981a) and reassessed in Chapter 2, larger crania tend to display smaller orbits.

4.4 Encephalization and the evolution of development in Strepsirrhines

One important result of this study lies in the finding that ontogenetic trajectories of the notharctine and adapine adapiforms were longer than those of any extant strepsirrhine species. For the three configurations, all fossils exhibit considerably higher CASV scores than the extant adult strepsirrhines.

Could specialization to folivory account for such long trajectories? Indeed, long ontogenetic trajectories imply larger temporal fossae, stronger zygomatic arches, smaller neurocrania, a more developed gonial region of the mandible, and larger mandibular corpora. Such features are indirect evidence for larger masticatory muscles and are often found in larger, folivore species (see above). However, as extant strepsirrhine folivore species exhibit relatively shorter trajectories, folivory alone cannot explain why adapiforms exhibit the largest ontogenetic trajectories of the sample

Another explanation is advanced here, that is related to the general trend toward an increase in encephalization exhibited by mammals (Jerison, 1970, 1973) and in particular by primates (Jerison, 1979) during the Cenozoic era. The predominent explanation for such a general trend in mammals lies in the predatory-prey “arms race” model proposed by Jerison (1973). Under this scheme, the co-evolution of encephalization in Carnivora and ungulates during the Cenozoic is well explained (Jerison, 1970). Adapiforms were less encephalized than their extant relatives (Jerison, 1979). The endocranium of *Leptadapis* is not known, but that of *Adapis* has been described: *Adapis* is known to have a low, elongated endocranium, with olfactory bulbs rostral to the frontal pole (Gingerich and Martin, 1981; Radinski, 1970). Its occipital and temporal lobes are broad, whereas the frontal lobes are less developed than what can be observed in extant strepsirrhines. Gingerich and Martin (1981) found an encephalization quotient (*EQ*) of 0.45 for *Adapis parisiensis.* Jerison (1979) gave a range in *EQ* of 0.47-0.61 for *Smilodectes*. These values fall well below the range found in extant strepsirrhines. Stephan et al. (1970) es-

tablished the range of 0.67-1.90 for modern strepsirrhines. Modern forms present more rounded endocrania with more developed frontal lobes, which cover the reduced olfactory bulbs.

It is interesting to note that high ontogenetic allometric scores at adulthood are significantly negatively correlated with encephalization quotients. This result also stands for samples composed uniquely of modern species. All modern forms look like "juvenilized" versions of their Eocene relatives. In modern strepsirrhines, differences in ontogenetic trajectories cannot be described using the vocabulary of heterochrony (see Chapter 5). "Pure" heterochronic mechanisms cannot account for differences in the developmental processes of the strepsirrhine skull. However, the results strongly support the hypothesis that the strepsirrhines experienced a general trend towards paedomorphism during their evolution. This trend primarily concerns the process of encephalization. A possible hypothesis is proposed to account for this result: selective pressures for an increase in brain size resulted in the emergence of "generally paedomorphic" crania, larger braincases, and shorter snouts. According to this hypothesis, we propose that the trend toward the shortening of cranial ontogenetic trajectories is the result of the expression of developmental constraints in a context of selection for high encephalization.

SUMMARY OF CHAPTER 6

The Adapiformes infraorder may include the ancestors of modern strepsirrhines. The skull is well known in two adapiform subfamilies, the Adapinae and the Notharctinae. The morphological affinities between adapines and notharctines with extant strepsirrhines is assessed.

The adapines are unique in their cranio-mandibular morphology, which may be linked with a highly specialised folivore regime.

Among the adapines, an increase in size through allometric transposition has probably occurred in the *Leptadapis* lineage. Gingerich (1981a), on the contrary, proposed that phyletic dwarfism has occurred in the *Adapis* genus.

Adapiforms exhibit longer ontogenetic trajectories than extent strepsirrhines. A trend to the shortening of ontogenetic trajectories occurred in the evolutionary history of strepsirrhines. We propose that the trend toward the shortening of cranial ontogenetic trajectories in strepsirrhines is the result of the expression of developmental constraints in a context of selection for high encephalization.

The understanding of the evolution and development of morphology is a challenge that requires arguments deriving from both bottom-up and top-down perspectives. In the field of human evolution and primatology, relatively few studies have adopted a bottom-up perspective, usually via computer simulation of ontogenetic trajectories (e.g., see Mitteroecker et al., 2004b; Zollikofer and Ponce de León, 2004). One compelling reason for the relative scarcity of studies following a bottom-up approach is that little is known about the genetic mechanisms involved in the developmental evolution of mammalian morphology in general, and primate morphology in particular. The complete genome of the rhesus monkey has been recently published (Gibbs et al., 2007), raising to three the number of complete primate genomes available after those of humans (Lander et al., 2001, 2004) and chimpanzees (Mikkelsen et al., 2005). Long lists of genes differs between humans, chimpanzees and rhesus monkeys (Gibbs et al., 2007; Mikkelsen et al., 2005), and several of these certainly imply important changes in development. However, relating genotype to phenotype is extremely difficult (e.g., see Carroll, 2003), and the genes that have played a major role in human evolution remain to be discovered. The understanding of the processes by which genotype generates phenotype in model organisms such as the mouse will be decisive for shedding light on human and primate developmental evolution from a bottom-up perspective (e.g., see Carroll, 2003; Lieberman, 2004;).

On the top-down front, the field of phenotypic analysis has recently seen both theoretical and technological progresses. The present work examining the evolution and development in the skull of strepsirrhines relies heavily on the latest advances in this field. Complex samples composed of extant adults, ontogenetic series, and fossils have been analyzed. The quantification of the morphology of specimens in various conditions of preservation, such as cadavers, dried skulls, or highly mineralized fossils, has been achieved using conventional X-ray microtomography and Synchrotron X-ray microtomography. For each specimen, a 3D model of the skull was computed using CT images, which served as a basis for analysis. The original morphologies of distorted and incomplete fossils were estimated following published reconstruction methods (Zollikofer and Ponce de León, 1995; Zollikofer and Ponce de León, 2005; Zollikofer et al., 1995) and with the help of dedicated software. Comparative geometric morphometric analysis was subsequently conducted using MorphoTools, an interactive and integrated application framework. Many of the functionalities of this software were implemented for the purposes of the present study. Now, let us review the major insights developed in this thesis concerning the evolution and development of strepsirrhine primates.

First of all, the developmental origin of the morphological differences between haplorrhines and strepsirrhines has been investigated. Haplorrhines and strepsirrhines differ widely in ontogenetic trajectory direction and length. Furthermore, the interspecific morphological distance at birth is greater between haplorrhines and strepsirrhines than within strepsirrhines. This supports the hypothesis that important differences in cranio-mandibular developmental constraints exist between the two primate suborders. Such constraints explain why similar dietary specialization

and activity patterns do not lead to similar morphologies in both groups for the skull, though common effects of adaptation on morphology could be quantified in both suborders. Haplorrhines and strepsirrhines differ not only in the anatomy of the skull, but also in the anatomy of their soft tissues: haplorrhines and strepsirrhines vary in their nasal regions (Hill, 1955; Pocock, 1918), in their placentation (Luckett, 1974), and in a series of traits in the orbital and auditory regions (Aiello, 1986; MacPhee and Cartmill, 1986). Three genera of basal haplorrhines belonging to the Omomyidae family (*Necrolemur*, *Microchoerus,* and *Rooneyia*) show more morphological resemblance in their craniofacial geometry to strepsirrhines than to haplorrhines, *Tarsius* included. This result strongly supports Beard's (1988) hypothesis that strepsirrhinism represents the ancestral condition in primates. Another outcome of this analysis is that it is probable that the shift towards a modern haplorrhine morphology of the skull occurred in one omomyid lineage, to the exclusion of the three genera mentioned above. The anatomy of soft tissues is not available in extinct lineages. However, the hypothesis formulated above may be extended to soft tissues: the anatomical features characteristic of haplorrhines (nasal region, placentation, orbital and auditory regions) may not have evolved in *Necrolemur, Microchoerus,* and *Rooneyia.* The omomyid skull is known in another genus, *Shoshonius*. The skull of *Shoshonius* resembles that of *Tarsius* (Beard and MacPhee, 1994). The analysis of *Shoshonius* may make it possible to assess whether omomyid members evolved "skeletal haplorrhinism", and thus potentially anatomical haplorrhinism.

The morphological variability in the craniofacial form of adult primates, and especially of strepsirrhines, can be understood in terms of diversity in postnatal ontogenetic trajectories. Among strepsirrhines, divergence between taxon-specific postnatal ontogenetic trajectories is more pronounced in Malagasy lemurs than in loriforms. Postnatal ontogenetic trajectory length, measured here by the Procrustes distance between neonates and adult, is variable across strepsirrhine species, although no evidence of trend differences between Loriformes and Lemuriformes infraorders was found. If differences in postnatal development partly explain the differences in morphological variability in lemuriforms and loriforms, prenatal morphogenetic processes may play an even more important role. In the present sample of primates, interspecific morphological distances at birth are of the same range as interspecific morphological distances among adults. Modifications of ontogeny in early stages of development certainly play a prominent role in the creation of new morphologies during evolution. These results are consistent with those of other studies showing that many differences in the primate skull morphology are set early in ontogeny (e.g., prenatally). These results also support the hypothesis that developmental modifications that occur early in ontogeny are a major source of morphological innovation (e.g., see Alberch et al., 1979; Gould, 1977). Conversely, postnatal ontogenetic trajectories are more often parallel or slightly divergent (Ackermann and Krovitz, 2002; O'Higgins et al., 2001; Ponce de León and Zollikofer, 2001; Ponce de León and Zollikofer, 2006; Vioarsdóttir et al., 2002). Postnatal morphogenetic processes may then be highly conserved processes during the

evolution of primates.

Another outcome of the analysis of ontogeny in strepsirrhines concerns the strong support it gives to the hypothesis of Gould that differences in allometric grades reflect contexts of rapid diversification. Lemuriforms have differentiated rapidly in Madagascar (e.g., Martin, 1972; Yoder, 1997; Yoder and Yang, 2004), and display marked differences allometric grades. On the contrary, loriform species exhibit very similar allometric grades to one another. The shared pattern in allometric grade exhibited by loriform species and that of *Lepilemur* are very likely to be ancestral for strepsirrhines, whereas those of species such as *Microcebus murinus, Propithecus diadema, P. verreauxi, and Lemur catta* are derived. If this hypothesis is true, the study of allometric grade provides a powerful tool for the analysis of fossil strepsirrhines: it makes it possible to assess the polarity of potential modification in allometric grade in extinct species. In fossil adapiforms, differences in allometric grades exist between *Adapis* and *Leptadapis*. The genus *Adapis* exhibits clearly the ancestral pattern of strepsirrhines, whereas at a given allometric score, *Leptadapis* is far larger than *Adapis*. These result strongly suggest that phyletic gigantism via allometric transposition occurred in the *Leptadapis* lineage.

The analysis of the morphology of fossils also sheds light on the trends in the evolution of development. In extinct species for which the juvenile morphology is often unknown, developmental information can be inferred from samples composed of adults only: as adult specimens provide an end point for ontogenetic trajectories, single adult fossils give information concerning the length of their ontogenetic trajectory (i.e. prenatal + postnatal amounts of morphological change). Here, we have demonstrated that adapiforms exhibited longer ontogenetic trajectories than their extant relatives. A general trend towards paedomorphism via neoteny or progenesis occurred in the strepsirrhine lineage. De Beer viewed paedomorphosis as an important mode of developmental evolution (e.g., see de Beer, 1962). De Beer offered several arguments for this point of view, the main one being that this mode of evolution allows for evolutionary plasticity (de Beer, 1958), since it leads to non over-specialized evolutionary lineages. Further differentiation would thus be possible in a flexible way (de Beer, 1930). A genetic explanation was advanced by de Beer (1958) to account for the importance of paedomorphosis in morphological evolvability. As in paeodomorph lineages, the genes responsible for the development of ancestral characters in adults are no longer employed, and they would remain available for the development of new variations and potentially new functions. However, the idea that evolvability is subject to natural selection seems to contradict the principle that event can not precede its own cause. Hence, would there be an immediate selective advantage to possessing paedomorphic skulls? In this thesis, such an explanation has been advanced to account for the trend toward paedomorphism in the skull of strepsirrhines. Paedomorphism can be related to a general increase in encephalization in this lineage. The neoteny hypothesis is often employed to account for the increase in encephalization observed in the hominid lineage (e.g., see Gould, 1977; Penin et al., 2002). As emphasized in this study, encephalization via paedomorphism is not ex-

clusive to the evolution of humans, but also applies to strepsirrhines and certainly to the whole primate order. Researchers are returning to the question of encephalization in primates, mostly because of the development of X-ray tomography. One major outcome from the development of this technique is that the inner structures of fossils, such as the endocranial cavity, are now available for study. The main difficulty in the analysis of endocasts is that there are only a few homologous locations between individuals and across species. However, recent developments in comparative analysis of endocasts (Specht et al., 2007) make possible the comprehensive analysis of large samples of endocranial cavities using a geometric morphometric approach. Since many strepsirrhine fossils crania are complete, combining X-ray microtomography and modern techniques of comparison offers new possibilities for shedding light on the encephalization of strepsirrhine primates.

Ackermann, R. R. and G. E. Krovitz (2002). Common Patterns of Facial Ontogeny in he Homonid Lineage. *The Anatomical Record (New Anat)* **267**: pp. 142-147.

Aiello, L. 1986. The relationships of the Tarsiiforms: a review of the case for the Haplorhini. In: B. Wood, L. Martin and P. Andrews, editors. *Major Topics in Primate and Human Evolution*. Cambridge: Cambridge University Press. pp. 47-65.

Alberch, P., S. J. Gould, G. F. Oster and D. B. Wake (1979). Size and shape in ontogeny and phylogeny. *Paleobiology* **5**: pp. 296–317.

Ambros, V. 1997. Heterochronic genes. In: D. L. Riddle, T. Blumenthal, N. J. Meyer and J. R. Priess, editors. *C. elegans II*. New York: Cold Spring Harbor Laboratory Press. pp. 501-518.

Anapol, F. and S. Lee (1994). Morphological adaptation to diet in platyrrhine primates. *American Journal of Physical Anthropology* **94**: pp. 239-261.

Andrews, P. 1988. A phylogenetic analysis of the primates. In: M. J. Benton, editor. *The Phylogeny and Classification of the Tetrapods*. Oxford: Clarendon press. pp. 143-175.

Asher, R. J. (1998). Morphological Diversity of Anatomical Strepsirrhinism and the Evolution of the Lemuriform Toothcomb. *American Journal of Physical Anthropology* **105**: pp. 355-367.

Baxter, B. and J. Sorenson (1981). Factors affecting the measurement of size and CT number in computed-tomography. *Investigative Radiology* **16**: pp. 337-341.

Beard, K. C. (1988). The phylogenetic significance of strepsirhinism in Paleogene primates. *International Journal of Primatology* **9**: pp. 83-96.

Beard, K. C. (1998). A new genus of Tarsiidae (Mammalia: Primates) from the middle Eocene of Shanxi Province, China, with notes on the historical biogeography of tarsiers. *Bulletin of the Carnegie Museum of Natural History* **34**: pp. 260-277.

Beard, K. C., M. Dagosto, D. L. Gebo and M. Godinot (1988). Interrelationships among primate higher taxa. *Nature* **331**: pp. 712-714.

Beard, K. C. and M. Godinot (1988). Carpal anatomy of Smilodectes-gracilis (Adapiformes, Notharctinae) and its significance for lemuriform phylogeny. *Journal of Human Evolution* **17**: pp. 71-92.

Beard, K. C., L. Krishtalka and R. K. Stucky (1991). First skulls of the Early Eocene primate *Shoshonius cooperi* and the anthropoid-tarsier dichotomy. *Nature* **349**: pp. 64-67.

Beard, K. C. and R. D. E. MacPhee. 1994. Cranial anatomy of Shoshonius and the antiquity of Anthropoidea. In: J. G. Fleagle and R. F. Kay, editors. *Anthropoid Origins*. New-York: Plenum Press.

Beard, K. C., T. Qi, M. R. Dawson, B. Wang and C. Li (1994). A diverse new primate fauna

from middle Eocene fissure-fillings in southeastern China. *Nature* **368**: pp. 604-609.

Bolk, L. (1926). On the problem of anthropogenesis. *Proc Sect Sci Kongr Akad Wetens (Amsterdam)* **29**: pp. 465–475.

Bookstein, F. L. (1991). *Morphometric tools for landmark data. Geometry and biology.* Cambridge, Cambridge University Press.

Bouvier, M. (1986a). A biomechanical analysis of mandibular scaling in Old World monkeys. *American Journal of Physical Anthropology* **69**: pp. 473-482.

Bouvier, M. (1986b). Biomechanical scaling of mandibular dimensions in New World monkeys. *International Journal of Primatology* **7**: pp. 551-567.

Buettner-Janusch, A. and R. M. Andrew (1962). Use of the incisors by primates in grooming. *American Journal of Physical Anthropology* **20**: pp. 127–129.

Burrows, A. M. and T. D. Smith (2005). Three-dimensional analysis of mandibular morphology in Otolemur. *American Journal of Physical Anthropology* **127**: pp. 219-230.

Carroll, S. B. (2003). Genetics and the making of Homo sapiens. *Nature* **422**: pp. 849–857.

Carroll, S. B. (2005). *Endless forms most beautiful. The new science of Evo Devo and the making of the animal kingdom.* New York, W. W. Norton & Company

Cartmill, M. 1972. Arboreal adaptations and the origins of the order Primates. In: R. Tuttle, editor. *The Functional and Evolutionary Biology of Primates.* Aldine, Chicago. pp. 97-122.

Cartmill, M. 1975. Strepsirhine basicranial structures and the affinities of the Cheirogaleidae. In: W. P. Luckett and F. S. Szalay, editors. *In Phylogeny of the Primates: A Multidisciplinary Approach*. New York: Plenum press. pp. 313-354.

Cartmill, M. 1977. Daubentonia, Dactylopsila, woodpeckers and klinorhynchy. In: R. D. Martin, G. A. Doyle and A. C. Walker, editors. *Prosimian Anatomy, Biochemistry, and Evolution*. London: Gerald Duckworth & Company. pp. 655–670.

Cartmill, M. 1994. Anatomy, antinomies, and the problem of anthropoid origins. In: J. Fleagle and R. F. Kay, editors. *Anthropoid Origins*. New York: Plenum. pp. 549-566.

Cartmill, M. and R. F. Kay. 1978. Cranio-dental morphology, tarsier affinities, and primate suborders. In: D. J. Chivers and K. A. Joysey, editors. *Recent Advances in Primatology*. London: Academic Press. pp. 205-214.

Cartmill, M., R. D. E. MacPhee and E. L. Simons (1981). Anatomy of the temporal bone in early anthropoids, with remarks on the problem of anthropoid origins. *American Journal of Physical Anthropology* **56**: pp. 3-21.

Cave, A. J. E. (1967). Observations on the platyrrhine nasal fossa. *American Journal of*

Physical Anthropology **26**: pp. 277-288.

Charles-Dominique, P. (1977). *Ecology and Behaviour of Nocturnal Primates. Prosimians of Equatorial West Africa.* New York, Columbia University Press.

Charles-Dominique, P. and R. D. Martin (1970). Evolution of Lorises and Lemurs. *Nature* **227**: pp. 257-260.

Cheverud, J. M. and M. M. Dow (1985). An autocorrelation analysis of genetic variation due to lineal fission in social groups of rhesus macaques. *American Journal of Physical Anthropology* **67**: pp. 113-121.

Cheverud, J. M., M. M. Dow and W. Leutenegger (1985). The quantitative assessment of phylogenetic constraints in comparative analyses: sexual dimorphism in body weight among primates. *Evolution* **39**: pp. 1335-1351.

Claude, J., E. Paradis, H. Tong and J. C. Auffray (2003). A geometric morphometric assessment of the effects of environment and cladogenesis on the evolution of the turtle shell. *Biological Journal of the Linnean Society* **79**: pp. 485-501.

Claude, J., P. Pritchard, H. Tong, E. Paradis and J. C. Auffray (2004). Ecological Correlates and Evolutionary Divergence in the Skull of Turtles: A Geometric Morphometric Assessment. *Systematic Biology* **53**: pp. 933-948.

Collard, M. and P. O. O'Higgins (2001). Ontogeny and homoplasy in the papionin monkey face. *Evolution & Development* **3**: pp. 322-331.

Conroy, G. C. (1987). Problems of body-weight estimation in fossil primates. *International Journal of Primatology* **8**: pp. 115-137.

Conroy, G. C. (2005). Ontogeny, auditory structures, and primate evolution. *American Journal of Physical Anthropology* **52**: pp. 443-451.

Coolidge, H. J. (1933). Pan paniscus: pygmy chimpanzee from south of the Congo river. *American Journal of Physical Anthropology* **18**: pp. 1–57.

Curtis, D. J. and M. A. Rasmussen (2006). The evolution of cathemerality in primates and other mammals: a comparative and chronoecological approach. *Folia Primatologica* **77**: pp. 178-193.

Curtis, D. J., A. Zaramody and R. D. Martin (1999). Cathemerality in the mongoose lemur, Eulemur mongoz. *American Journal of Primatology* **47**: pp. 279-298.

Dagosto, M. (1988). Implications of postcranial evidence for the origin of euprimates. *Journal of Human Evolution* **17**: pp. 35-56.

Dagosto, M. 1994. Postcranial anatomy and the origin of Anthropoidea. In: J. G. Fleagle and D. L. Gebo, editors. *Anthropoid origins*. New York: Plenum Press. pp. 567-593.

Dahl, J. F. and C. A. Hemingway (1988). An unusual activity pattern for the mantled howler monkey of Belize. *American Journal of Physical Anthropology* **75**: p 201.

Darwin, C. (1859). *On the origin of species by means of natural selection.* London, John Murray.

de Beer, G. R. (1930). *Embryology and evolution.* Oxford, Oxford University Press.

de Beer, G. R. (1958). *Embryos and ancestors, 3rd edition.* Oxford, Oxford University Press.

de Beer, G. R. 1962. Peter pan evolution. Broadcast by the BBC. *Reflections of a Darwinian: essays and addresses*. London: Thomas Nelson and Sons. pp. 58–66.

Delfortrie, E. (1873). Un singe de la famille des lémuriens dans les phosphates de chaux quaternaires du Département du Lot. *Actes de la Société Linnéenne de Bordeaux* **29**: pp. 87-95.

Dominy, N. J., P. W. Lucas, D. Osorio and N. Yamashita (2001). The sensory ecology of primate food perception. *Evolutionary Anthropology* **10**: pp. 171–186.

Dryden, I. L. and K. V. Mardia (1998). Statistical shape analysis. *Chichester : John Wiley & Sons*.

Dumont, E. R. (1997). Cranial shape in fruit, nectar, and exudate feeders: Implications for interpreting the fossil record. *American Journal of Physical Anthropology* **102**: pp. 187-202.

Emerson, S. B. and D. M. Bramble. 1993. Scaling and the evolution of skull design. In: J. Hanken and B. K. Hall, editors. *The Vertebrate Skull, volume III*. Chicago: University of Chicago Press. pp. 384-421.

Estes, R. (1972). The role of the vomeronasal organ in mammalian reproduction. *Mammalia* **36**: pp. 315–341.

Felsenstein, J. (1985). Phylogenies and the comparative method. *American Naturalist* **125**: pp. 1–15.

Felsenstein, J. (1989). PHYLIP - Phylogeny Inference Package (Version 3.2). *Cladistics* **5**: pp. 164-166.

Filhol, H. (1883). Observations relatives au mémoire de M. Cope intitulé “Relation des horizons renfermant des débris d’animaux vertébrés fossiles en Europe et en Amérique. *Annales des sciences geologiques, Paris* **14**: pp. 1-51.

Fleagle, J. (1999). *Primate adaptation and evolution, 2nd ed. San Diego: Academic Press.*

Fondon, J. W. and H. G. Garner (2004). Molecular origins of rapid and continuous morphological evolution. *Proceedings of the National Academy of Sciences of the United*

States of America **101**: pp. 18058–18063.

Franzen, J. L. (2003). Mammalian faunal turnover in the Eocene of central Europe. *Geological Society of America* **Special paper 369**: pp. 455-461.

Franzen, J. L. and H. Haubold (1986). The middle Eocene of European mammalian stratigraphy: Definition of the Geiseltalian. *Modern Geology* **10**: pp. 159–170.

Garland, T. J., P. E. Midford and A. R. Ives (1999). An Introduction to Phylogenetically Based Statistical Methods, with a New Method for Confidence Intervals on Ancestral Values. *American Zoologist* **39**: pp. 374-388.

Gibbs, R. A., J. Rogers, M. G. Katze, R. Bumgarner, et al. (2007). Rhesus Macaque Genome Sequencing and Analysis Consortium: Evolutionary and Biomedical Insights from the Rhesus Macaque Genome. *Science* **316**: pp. 222-234.

Gingerich, P. D. (1973). Anatomy of the temporal bone in the Oligocene anthropoid *Apidium* and the origin of Anthropoidea. *Folia Primatologica* **19**: pp. 329-337.

Gingerich, P. D. (1981a). Cranial morphology and adaptations in Eocene Adapidae. I. Sexual dimorphism in Adapis magnus and Adapis parisiensis. *American Journal of Physical Anthropology* **56**: pp. 217-234.

Gingerich, P. D. (1981b). Early Cenozoic Omomyidae and the evolutionary history of tarsiiform primates. *Journal of Human Evolution* **10**: pp. 345-374.

Gingerich, P. D. (1984). Primates evolution : evidence from the fosil record, comparative morphology, and molecular biology. *Yearbook of physical anthropology* **27**: pp. 57-72.

Gingerich, P. D. and R. D. Martin (1981). Cranial morphology and adaptations in Eocene *Adapidae.* II: The Cambridge skull of *Adapis parisiensis. American Journal of Physical Anthropology* **56**: pp. 235-257.

Gingerich, P. D., B. H. Smith and K. Rosenberg (1982). Allometric scaling in the dentition of primates and prediction of body-weight from tooth size in fossils. *American Journal of Physical Anthropology* **58**: pp. 81-100.

Godfrey, L. R., A. J. Petto and M. R. Sutherland. 2002. Dental ontogeny and life history strategies: The case of the giant extinct indroids of Madagascar. In: J. M. Plavcan, R. F. Kay, W. L. Jungers and C. P. van Schaik, editors. *Reconstructing Behavior in the Primate Fossil Record.* New York: Kluwer Academic/Plenum Publishers. pp. 113-157.

Godfrey, L. R., K. E. Samonds, W. L. Jungers, M. R. Sutherland and M. T. Irwin (2004). Ontogenetic Correlates of Diet in Malagasy Lemurs. *American Journal of Physical Anthropology* **123**: pp. 250-276.

Godfrey, L. R., K. E. Samonds, P. C. Wright and S. J. King (2005). Schultz's Unruly Rule: Dental Developmental Sequences and Schedules in Small-Bodied, Folivorous Lemurs. *Folia*

Primatologica **76**: pp. 77-99.

Godfrey, L. R. and M. R. Sutherland (1995). Flawed inference: why size-based tests of heterochronic processes do not work. *Journal of Theoretical Biology* **172**: pp. 43-61.

Godfrey, L. R. and M. R. Sutherland (1996). Paradox of peramorphic paedomorphosis: heterochrony and human evolution. *American Journal of Physical Anthropology* **99**: pp. 17–42.

Godinot, M. (1998). A Summary of Adapiform Systematics and Phylogeny. *Folia Primatologica* **69**: pp. 218-249.

Godinot, M. (2006). Lemuriform origins as viewed from the fossil record. *Folia Primatologica* **77**: pp. 446-464.

Gomez, A. M. (1992). Primitive and derived patterns of relative growth among species of lorisidae. *Journal of Human Evolution* **23**: pp. 219-233.

Gould, S. J. (1966). Allometry and size in ontogeny and phylogeny. *Biol. Rev. Cambridge. phil. soc.* **41**: pp. 587-640.

Gould, S. J. (1971). Geometric Similarity in Allometric Growth: A Contribution to the Problem of Scaling in the Evolution of Size. *American Naturalist* **105**: pp. 113-136.

Gould, S. J. (1975). Allometry in primates, with emphasis on scaling and the evolution of the brain. *Contributions to primatology* **5**: pp. 244-292.

Gould, S. J. (1977). *Ontogeny and Phylogeny.* C. Harvard University Press, editor.

Gould, S. J. (2000). Of coiled oysters and big brains: how to rescue the terminology of heterochrony, now gone astray. *Evolution and Development* **2**: pp. 241-248.

Gould, S. J. and R. C. Lewontin (1979). The Spandrels of San Marco and the Panglossian Paradigm: A Critique of the Adaptationist Programme. *Proceedings of the Royal Society of London. Series B. Biological Sciences* **205**: pp. 581-598.

Grandidier, G. (1905). *Recherches sur les lémuriens disparus et en particulier sur ceux qui vivaient à Madagascar.* Masson, editor Paris.

Grassi, C. (2006). Variability in habitat, diet, and social structure of Hapalemur griseus in Ranomafana National Park, Madagascar. *American Journal of Physical Anthropology* **131**: pp. 50-63.

Greaves, W. S. (1974). Functional implications of mammalian jaw joint position. *Forma Functio* **7**: pp. 363–376.

Groves, C. P. 1974. Taxonomy and phylogeny of the prosimians. In: R. D. Martin, G. A. Doyle and A. Walker, editors. *Prosimian Biology*. London: Duckworth. pp. 435-448.

Groves, C. P. (2001). *Primate taxonomy.* Washington, DC, Smithsonian Institute.

Grzimek, B. (1989). *Grzimek's Encyclopedia of Mammals (2nd edition).* McGraw-Hill Education.

Gunnell, G. F. and K. D. Rose. 2002. Tarsiiformes: Evolutionary History and adaptation. In: W. C. Hartwig, editor. *The primate fossil record*. Cambridge University Press.

Haeckel, E. (1866). *Generelle Morphologie der Organismen: Allgemeine Grundzüge der organischen Formen-Wissenschaft, mechanisch begründet durch die von Charles Darwin reformirte Descendenz-Theorie.* Berlin, Georg Reimer.

Hartenberger, J.-L. (1990). The origin of the Theridomyoidea (Mammalia, Rodentia) - New data and hypotheses. *Comptes rendus de l'Académie des Sciences de Paris, Série 2* **311**: pp. 1017-1023.

Heesy, C. P. and C. F. Ross (2001). Evolution of activity patterns and chromatic vision in primates: morphometrics, genetics and cladistics. *Journal of Human Evolution* **40**: pp. 111-149.

Hill, W. G. O. (1955). *Primates, Comparative Anatomy and Taxonomy. vol. II, Haplorrhini, Tarsioidea.* Edimburgh, Edimburgh Univertiy Press.

Hladik, C. M. 1979. Diet and ecology of prosimians. In: G. A. Doyle and R. D. Martin, editors. *The study of prosimian behavior*. New York: Academic Press. pp. 307–357.

Hylander, W. L. (1979). The functional significance of primate mandibular form. *Journal of Morphology* **160**: pp. 223-239.

Hylander, W. L. and K. R. Johnson (1994). Jaw muscle function and wishboning of the mandible during mastication in macaques and baboons. *American Journal of Physical Anthropology* **94**: pp. 523-547.

Ihaka, R. and R. Gentelman (1996). R: a language for data analysis and graphics. *Journal of Computational and Graphical Statistics* **5**: pp. 299-314.

Jerison, H. J. (1970). Brain evolution: new light on old principles. *Science* **170**: pp. 1224–1225.

Jerison, H. J. (1973). *Evolution of the Brain and Intelligence.* New York, Academic Press.

Jerison, H. J. (1979). Brain, Body and Encephalization in Early Primates. *Journal of Human Evolution* **8**: pp. 615-635.

Jolliffe, I. T. (1986). *Principal Component Analysis.* Berlin., Springer-Verlag.

Jungers, W. L. (1979). Locomotion, limb proportions and skeletal allometry in lemurs and

lorises. *Folia Primatologica* **52**: pp. 8-28.

Kay, R. F. 1984. On the use of anatomical features to infer foraging behavior in extinct primates. In: P. S. Rodman and J. G. Cant, editors. *Adaptations for Foraging in Nonhuman Primates*. New York: Columbia University Press.

Kay, R. F. and E. C. Kirk (2000). Osteological Evidence for the Evolution of Activity Pattern and Visual Acuity in Primates. *American Journal of Physical Anthropology* **113**: pp. 235-262.

Kay, R. F., C. Ross and B. A. Williams (1997). Anthropoid Origin. *Science* **275**: pp. 797-803.

Kay, R. F., B. A. Williams, C. F. Ross, M. Takai and N. Shigehara. 2004. Anthropoid origins: a phylogenetic analysis. In: C. F. Ross and R. F. Kay, editors. *Anthropoid origins: new visions*. New York: Plenum Press. pp. 91-135.

Kay, R. F. and B. A. Williams. 1994. Dental Evidence for Anthropoid Origins. In: J. G. Fleagle and R. F. Kay, editors. *Anthropoid Origins*. New-York: Plenum. pp. 361-446.

King, S. J., L. R. Godfrey and E. L. Simons (2001). Adaptive and phylogenetic significance of ontogenetic sequences in Archaeolemur, subfossil lemur from Madagascar. *Journal of Human Evolution* **41**: pp. 545-576.

Kirk, E. C. (2006). Effects of activity pattern on eye size and orbital aperture size in primates. *Journal of Human Evolution* **51**: pp. 159-170.

Klingenberg, C. P. 1996. Mutlivariate Allometry. In: L. F. Marcus, M. Corti, A. Loy, G. J. P. Naylor and D. E. Slice, editors. *Advances in Morphometrics*. New York: Plenum Press. pp. 29-43.

Klingenberg, C. P. (1998). Heterochrony and allometry: the analysis of evolutionary change in ontogeny. *Biological Reviews of the Cambridge Philosophical Society* **73**: pp. 79–123.

Lamberton, C. (1939). Contribution à la connaissance de la faune subfossile de Madagascar. Notes IV à VIII: lémuriens et cryptoproctes. *Mémoires de l'académie Malgache* **27**: pp. 1-203.

Lander, E. S., L. M. Linton, B. Birren, C. Nusbaum, et al. (2001). International Human Genome Sequencing Consortium: Initial sequencing and analysis of the human genome. *Nature* **409**: pp. 860–-920.

Lander, E. S., L. M. Linton, B. Birren, C. Nusbaum, et al. (2004). International Human Genome Sequencing Consortium: Finishing the euchromatic sequence of the human genome. *Nature* **431**: pp. 931-945.

Lanèque, L. 1990. *Diversité et variabilité des crânes chez les Adapinés (Primates, Eocène) des Phosphorites du Quercy. Comparaisons avec les primates actuels (Ph.D. Dissertation)*: Muséum National d'Histoire Naturelle, Institut de Paléontologie Humaine.

Lanèque, L. (1992a). Analyse de matrice de distance euclidienne de la région du museau chez *Adapis* (Adapiforme, Eocène). *Comptes rendus de l'Académie des Sciences de Paris* **314**: pp. 1387-1393.

Lanèque, L. (1992b). Variation in the shape of the palate in *Adapis* (Eocene, Adapiformes) compared with living primates. *Human Evolution* **7**: pp. 1-16.

Lanèque, L. (1993). Variation of orbital features in adapine skulls. *Journal of Human Evolution* **25**: pp. 287-317.

Le Gros Clark, W. F. (1959). *The Antecedents of Man.* Edinburgh, Edinburgh University Press. Reprinted in 1965 by Harper Torchbooks, New York.

Legendre, S. and J.-L. Hartenberger. 1992. Evolution of Mammalian Faunas in Europe during the Eocene and Oligocene. In: D. R. Prothero and W. A. Berggren, editors. *Eocene-Oligocene Climatic and Biotic Evolution*. Princeton: Princeton University Press.

Leigh, S. R. (2006). Cranial Ontogeny of Papio Baboons (Papio hamadryas). *American Journal of Physical Anthropology* **130**: pp. 71-84.

Leigh, S. R. (2007). Homoplasy and the evolution of ontogeny in papionin primates. *Journal of Human Evolution* **52**: pp. 536-558.

Lele, S. (1993). Euclidean Distance Matrix Analysis (Edma) - Estimation of Mean Form and Mean Form Difference. *Mathematical Geology* **25**: pp. 573-602.

Lele, S. and J. T. Richtsmeier (1991). Euclidean Distance Matrix Analysis - a Coordinate-Free Approach for Comparing Biological Shapes Using Landmark Data. *American Journal of Physical Anthropology* **86**: pp. 415-427.

Lieberman, D. (2004). Humans and primates: New model organisms for evolutionary developmental biology? *Journal of Experimental Zoology Part B-Molecular and Developmental Evolution* **302B**: pp. 195-195.

Lieberman, D. E., J. Carlo, M. S. Ponce de Leòn and C. P. E. Zollikofer (2007). A geometric morphometric analysis of heterochrony in the cranium of chimpanzees and bonobos. *Journal of Human Evolution* **52**: pp. 647-662.

Lindenfors, P. (2002). Sexually antagonistic selection on primate size. *Journal of Evolutionary Biology* **15**: pp. 595-607.

Lleonart, J., J. Salat and G. J. Torres (2000). Removing Allometric Effects of Body Size in Morphological Analysis. *Journal of Theoretical Biology* **205**: pp. 85-93.

Lockwood, C. A. and J. G. Fleagle (1999). The Recognition and Evaluation of Homoplasy in Primate and Human Evolution. *Yearbook of physical anthropology* **42**: pp. 189-232.

Lorenz von Liburnau, L. (1902). Über Hadropithecus Stenognathus Lz. Nebst Bemerkungen

zu einigen anderen ausgestorbenen Primaten von Madagaskar. *Denkschriften der Kaiserlichen Akademie der Wissenschaften in Wien* **72**: pp. 243- 254.

Luckett, W. P. (1974). Comparative development and evolution of the placenta in primates. *Contr. Primat.* **3**: pp. 142-234.

Lynch, M. (1990). The rate of morphological evolution in mammals from the standpoint of neutral expectation. *American Naturalist* **136**: pp. 727–741.

MacPhee, R. D. E. and M. Cartmill. 1986. Basicranial Structures and Primate Systematics. In: D. R. Swindler, editor. *Comparative Primate Biology. Vol. I. Systematics, Evolution, and Anatomy*. New York: Alan R. Liss. pp. 219-275.

Major, C. and I. Forsyth (1896). Preliminary notice on fossil monkeys from madagascar. *Geological Magazine* **3**: pp. 433-436.

Marcus, L. F., M. Corti, A. Loy, G. Naylor and D. E. Slice (1996). *Advances in Morphometrics.* L. F. Marcus, M. Corti, A. Loy, G. Naylor and D. E. Slice, editors New York, Plenum Press.

Marivaux, L., J.-L. Welcomme, P.-O. Antoine, G. Métais, I. M. Baloch, M. Benammi, Y. Chaimanee, S. Ducrocq and J.-J. Jaeger (2001). A Fossil Lemur from the Oligocene of Pakistan. *Science* **294**: pp. 587-591.

Marroig, G. and J. M. Cheverud (2004). Cranial Evolution in Sakis (Pithecia, Platyrrhini) I: Interspecific Differentiation and Allometric Patterns. *American Journal of Physical Anthropology* **125**: pp. 266-278.

Martin, R. D. (1972). Adaptative radiation and behavior of the malagasy lemurs. *Philosophical transactions of the Royal Society of London. Series B, Biological sciences* **264**: pp. 295-352.

Martin, R. D. 1979. Phylogenetic aspects of prosimian behavior. In: R. D. Martin and G. A. Doyle, editors. *The Study of Prosimian Behavior*. pp. 45-77.

Martin, R. D. (1990). *Primate Origins and Evolution: A Phylogenetic Reconstruction.* Princeton, Princeton University Press.

Martins, E. P. and T. F. Hansen (1997). Phylogenies and the comparative method: a general approach to incorporating phylogenetic information into the analysis of interspecific data. *American Naturalist* **149**: pp. 646–667.

Masters, J. C., N. M. Anthony, de Wit, M. J. and A. Mitchell (2005). Reconstructing the Evolutionary History of the Lorisidae Using Morphological, Molecular and Geological Data. *American Journal of Physical Anthropology* **127**: pp. 465-480.

Masters, J. C., M. Boniotto, S. Crovella, C. Roos, L. Pozzi and M. Delpero (2007). Phylogenetic relationships among the Lorisoidea as indicated by craniodental morphology

and mitochondrial sequence data. *American Journal of Primatology* **69**: pp. 6-15.

Masters, J. C. and D. J. Brothers (2002). Lack of Congruence Between Morphological and Molecular Data in Reconstructing the Phylogeny of the Galagonidae. *American Journal of Physical Anthropology* **117**: pp. 79-93.

Maynard Smith, J., R. Burian, S. Kauffman, P. Alberch, J. Campbell, B. Goodwin, R. Lande, D. Raup and L. Wolpert (1985). Developmental Constraints and Evolution: A Perspective from the Mountain Lake Conference on Development and Evolution *The Quarterly Review of Biology* **60**: pp. 265-287.

McNulty, K., S. R. Frost and D. S. Strait (2006). Examining affinities of the Taung child by developmental simulation. *Journal of Human Evolution* **51**: pp. 274-296.

Meulenkamp, J. E., W. Sissingh, J. P. Calvo, R. Daams, et al. 2000. Map 17: Early to Middle Ypresian (55–51 Ma), Map 18: Late Lutetian (44–41 Ma). In: J. Dercourt, et al., editor. *Atlas Peri-Tethys: Paleogeographical maps: Commission de la Carte Géologique du Monde, maps 17–18.* Paris.

Meunier, K. (1959). Die Allometrie des Vogelflügels. *Zeitschrift für wissenschaftliche Zoologie* **161**: pp. 444-482.

Mikkelsen, T. S., L. W. Hillier, E. E. Eichler, M. C. Zody, et al. (2005). The Chimpanzee Sequencing and Analysis Consortium: Initial sequence of the chimpanzee genome and comparison with the human genome. *Nature* **437**: pp. 69-87.

Mittermeier, R. A., I. Tattersall, W. R. Konstant, D. M. Meyers and R. B. Mast (1994). *The Lemurs of Madagascar.* Washington, D.C.: Conservation International

Mitteroecker, P., P. Gunz, M. Bernhard, K. Schaefer and F. L. Bookstein (2004a). Comparison of cranial ontogenetic trajectories among great apes and humans. *Journal of Human Evolution* **46**: pp. 679-698.

Mitteroecker, P., P. Gunz and F. L. Bookstein (2005). Heterochrony and geometric morphometrics: a comparison of cranial growth in Pan paniscus versus Pan troglodytes. *Evolution & Development* **7**: pp. 244-258.

Mitteroecker, P., P. Gunz, G. W. Weber and F. L. Bookstein (2004b). Regional dissociated heterochrony in multivariate analysis. *Annals of Anatomy* **186**: pp. 463-470.

Moss, E. G. (2007). Heterochronic genes and the nature of developmental time. *Current Biology* **17**: pp. 425-434.

Nekaris, K. A. and D. T. Rasmussen (2003). Diet and Feeding Behavior of Mysore Slender Lorises *International Journal of Primatology* **24**: pp. 33-46.

Nowak, R. M. (1999). *Walker's Primates of the World.* Baltimore and London, The Johns Hopkins University Press.

O'Higgins, P., P. Chadfield and N. Jones (2001). Facial growth and the ontogeny of morphological variation within and between the primates Cebus apella and Cercocebus torquatus. *Journal of Zoology* **254**: pp. 337-357.

O'Higgins, P. and N. Jones (1998). Facial growth in Cercocebus torquatus: an application of three-dimensional geometric morphometric techniques to the study of morphological variation. *Journal of Anatomy* **193**: pp. 251-272.

Osman Hill, W. C. (1953). *Primates: comparative anatomy and taxonomy, I, Strepsirhini.* Edinburgh:, Edinburgh University Press.

Paradis, E., J. Claude and K. Strimmer (2004). APE: analyses of phylogenetics and evolution in R language. *Bioinformatics* **20**: pp. 289–290.

Penin, X., C. Berge and M. Baylac (2002). Ontogenetic Study of the Skull in Modern Humans and the Common Chimpanzees: Neotenic Hypothesis Reconsidered With a Tridimensional Procrustes Analysis. *American Journal of Physical Anthropology* **118**: pp. 50-62.

Petter, J. J. (1962). Ecological and behavioral studies of madagascar lemurs in the field. *Annals of the New York Academy of Sciences* **102**: pp. 267-281.

Petter, J. J., R. Albignac and Y. Rumpler (1977). Mammifères lémuriens (Primates, Prosimii). *Faunes de Madagascar* **44**.

Pocock, R. I. (1918). On the external characters of the lemurs and of Tarsius. *Proceedings of the Zoological Society of London*: pp. 19–53.

Ponce de León, M. S. and C. P. E. Zollikofer (2001). Neanderthal cranial ontogeny and its implications for late hominid diversity. *Nature* **412**: pp. 534-538.

Ponce de León, M. S. and C. P. E. Zollikofer. 2006. Neanderthals and modern humans - chimps and bonobos: similarities and differences in development and evolution. In: K. Harvati and T. Harrison, editors. *Neanderthals Revisited: New Approaches and Perspectives*. Dordrecht, Netherlands: Springer.

Prothero, D. R. 1989. Stepwise extinctions and climatic decline during the later Eocene and Oligocene. In: S. K. Donovan, editor. *Mass Extinctions: Processes and Evidence*. New York: Columbia University Press. pp. 217-234.

Radinski, L. B. 1970. The fossil Evidence of Prosimian Brain Evolution. In: C. R. Noback and W. Montagna, editors. *The Primate Brain: Advances in primatology, Vol. 1*. New York: Appleton. pp. 209-224.

Raff, R. A. (1996). *The Shape of Life.* Chicago, University of Chicago Press.

Rasmussen, D. T. (1990). The phylogenetic position of *Mahgarita stevensi*: Protoanthropoid or lemuroid? *International Journal of Primatology* **11**: pp. 439-469.

Rasmussen, D. T. and K. A. Nekaris (1998). Evolutionary history of lorisiform primates. *Folia Primatologica* **69**: pp. 250-285.

Ravosa, M. J. (1991). Structural allometry of the prosimian mandibular corpus and symphysis. *Journal of Human Evolution* **20**: pp. 3-20.

Ravosa, M. J. (1992). Allometry and heterochrony in extant and extinct Malagasy primates. *Journal of Human Evolution* **23**: pp. 197-217.

Ravosa, M. J. (2007). Cranial ontogeny, diet, and ecogeographic variation in African lorises. *American Journal of Primatology* **69**: pp. 59-73.

Ravosa, M. J., V. E. Noble, W. L. Hylander, K. R. Johnson and E. M. Kowalski (2000). Masticatory stress, orbital orientation and the evolution of the primate postorbital bar. *Journal of Human Evolution* **38**: pp. 667-693.

Ravosa, M. J. and E. L. Simons (1994). Mandibular growth and function in Archaeolemur. *American Journal of Physical Anthropology* **95**: pp. 63-76.

Rice, S. H. (1997). The analysis of ontogenetic trajectories: When a change in size or shape is not heterochrony. *Proceedings of the National Academy of Sciences of the United States of America* **94**: pp. 907-912.

Richtsmeier, J. T. and S. Lele (1993). A Coordinate-Free Approach to the Analysis of Growth-Patterns - Models and Theoretical Considerations. *Biological Reviews of the Cambridge Philosophical Society* **68**: pp. 381-411.

Rohlf, F. J. and D. E. Slice (1990). Extensions of the Procrustes method for the optimal superimposition of landmarks. *Systematic Biology* **39**: pp. 40-59.

Roos, C., J. Schmitz and H. Zischler (2004). Primate jumping genes elucidate strepsirrhine phylogeny. *Proceedings of the National Academy of Sciences of the United States of America* **101**: pp. 10650-10654.

Rose, K. D., A. Walker and L. L. Jacobs (1981). Function of the mandibular tooth comb in living and extinct mammals. *Nature* **289**: pp. 583-585.

Rosenberger, A. L. (1985). In favor of the *Necrolemur*-tarsier hypothesis. *Folia Primatologica* **45**: pp. 179-194.

Rosenberger, A. L. (2006). Protoanthropoidea (Primates, Simiiformes): A New Primate Higher Taxon and a Solution to the Rooneyia Problem. *Journal of Mammal Evolution* **13**: pp. 139-146.

Rosenberger, A. L. and E. Strasser (1985). Toothcomb origins: Support for the grooming hypothesis. *Primates* **26**: pp. 73–84.

Rosenberger, A. L., E. Strasser and E. Delson (1985). Anterior Dentition of Notharctus and the Adapid-Anthropoid Hypothesis. *Folia Primatologica* **44**: pp. 15-39.

Rosenberger, A. L. and F. S. Szalay. 1980. On the Tarsiiform Origins of Anthropoidea. In: R. L. Ciochon and A. B. Chiarelli, editors. *Evolutionary Biology of the New World Monkeys and Continental Drift*. New York: Plenum Press. pp. 139-157.

Ross, C., B. Williams and R. F. Kay (1998). Phylogenetic analysis of anthropoid relationships. *Journal of Human Evolution* **35**: pp. 221-306.

Ross, C. F. 1994. The Craniofacial Evidence for Anthropoid and Tarsier Relationships. In: J. Fleagle and R. F. Kay, editors. *Anthropoid Origins*. New York: Plenum Press. pp. 469-547.

Ross, C. F. (1995). Allometric and functional influences on primate orbit orientation and the origins of the Anthropoidea. *Journal of Human Evolution* **29**: pp. 201-227.

Rossi, M., F. Casali, D. Romani, L. Bondioli, R. Macchiarelli and L. Rook (2003). MicroCT Scan in paleobiology: application to the study of dental tissues. *Nuclear Instruments and Methods in Physics Research Section B: Beam Interactions with Materials and Atoms* **213**: pp. 747-750.

Rossie, J. B., X. Ni and K. C. Beard (2006). Cranial remains of an Eocene tarsier. *Proceedings of the National Academy of Sciences of the United States of America* **103**: pp. 4381-4385.

Rowe, N. (1996). *The Pictorial Guide to the Living Primates.* East Hampton, New York, Pogonias Press.

Schluter, D., T. Price, A. O. Mooers and D. Ludwig (1997). Likelihood of ancestor states in adaptive radiation. *Evolution* **51**: pp. 1699-1711.

Schroeder, W., K. Martin and B. Lorensen (2006). *The Visualization Toolkit: An Object-Orientend Approach To 3D Graphics, 4th Edition.* Kitware, Inc. publishers.

Schultz, A. H. (1927). Studies of the growth of gorilla and other higher primates with special reference to a fetus of gorilla, preserved in the Carnegie Museum. *Memoirs of the Carnegie Museum* **11**: pp. 1–88.

Schwartz, G. T. and I. Tattersall (1974). Craniodental Morphology and the Systematics of the Malagasy Lemurs (Primates, Prosimii). *Anthropological Papers of the American Museum of Natural History* **52**: pp. 137-192.

Schwartz, J. H., I. Tattersall and N. Eldredge (1978). Phylogeny and classification of the primates revisited. *Yearbook of physical anthropology* **21**: pp. 95-133.

Schwarz, E. (1929). Das Vorkommen des Schimpansen auf den linken Kongo-Ufer. *Revue de zoologie et de botanique africaines* **16**: pp. 424-426.

Seiffert, E. R. (2005). Additional remains of Wadilemur elegans, a primitive stem galagid

from the late Eocene of Egypt. *Proceedings of the National Academy of Sciences of the United States of America* **102**: pp. 11396-11401.

Seiffert, E. R. (2007). Early Evolution and Biogeography of Lorisiform Strepsirrhines. *American Journal of Primatology* **69**: pp. 27–35.

Seiffert, E. R., E. L. Simons and Y. Attia (2003). Fossil evidence for an ancient divergence of lorises and galagos. *Nature* **422**: pp. 421-424.

Shea, B. T. (1983a). Allometry and heterochrony in the African apes. *American Journal of Physical Anthropology* **62**: pp. 275-289.

Shea, B. T. (1983b). Size and diet in the evolution of African ape craniodental form. *Folia Primatologica* **40**: pp. 32-68.

Shea, B. T. 1985. Ontogenetic allometry and scaling: A discussion based on the growth and form of the skull in African apes. In: W. L. Jungers, editor. *Size and Scaling in Primate Biology*. New York: Plenum Press. pp. 175-205.

Shea, B. T. (1989). Heterochrony in human evolution. The case of neoteny reconsidered. *Yearbook of physical anthropology* **32**: pp. 69–101.

Shoshani, J., C. P. Groves, E. L. Simons and G. F. Gunnell (1996). Primate Phylogeny: Morphological vs Molecular Results. *Molecular Phylogenetics and Evolution* **5**.

Sigé, B. (1977). Les insectivores et chiroptères du Paléogène moyen d'Europe dans l'histoire des faunes de mammifères sur ce continent. *Journal of the Palaeontological Society of India* **20**: pp. 178-190.

Silcox, M. T. (2003). New discoveries on the middle ear anatomy of Ignacius graybullianus (Paromomyidae, Primates) from ultra high resolution X-ray computed tomography. *Journal of Human Evolution* **44**: pp. 73-86.

Simons, E. L. (1997). Discovery of the smallest Fayum Egyptian primates (Anchomomyini, Adapidae). *Proceedings of the National Academy of Sciences of the United States of America* **94**: pp. 180-184.

Simons, E. L. and D. T. Rasmussen (1989). Cranial morphology of Aegyptopithecus and Tarsius and the question of the tarsier-Anthropoidean clade. *American Journal of Physical Anthropology* **79**: pp. 1-23.

Simons, E. L. and D. T. Rasmussen (1994). A remarkable cranium of Plesiopithecus teras (Primates, Prosimii) from the Eocene of Egypt. *Proceedings of the National Academy of Sciences of the United States of America* **91**.

Simpson, G. G. (1953). *The Major Features of Evolution.* New York, Columbia University Press.

Slack, F. and G. Ruvkun (1997). Temporal pattern formation by heterochronic genes. *Annual Review of Genetics* **31**: pp. 611-634.

Smith, B. H. 2000. 'Schultz's Rule' and the evolution of tooth emergence and replacement patterns in primates and ungulates. In: M. F. Teaford, M. M. Smith and M. W. J. Ferguson, editors. *Development, Function and Evolution of Teeth*. pp. 212-226.

Soligo, C. and R. D. Martin (2006). Adaptive origins of primates revisited. *Journal of Human Evolution* **50**: pp. 414-430.

Specht, M. 2007. *Spherical Surface Parameterization and its Application to Geometric Morphometric Analysis of the Braincase (Ph.D. Dissertation)*. Zürich: University of Zürich Irchel.

Specht, M., R. Lebrun and C. P. E. Zollikofer (2007). Visualizing Shape Transformation between Chimpanzee and Human Braincases. *The Visual Computer* **23**: pp. 743-751.

Spoor, C. (1998). Comparative review of the human bony labyrinth. *American Journal of Physical Anthropology* **Suppl 27**: pp. 211-251.

Spoor, C., F. Zonneveld and G. Macho (1993). Linear measurements of cortical bone and dental enamel by computed tomography: Applications and problems. *American Journal of Physical Anthropology* **91**: pp. 469-484.

Spoor, F., T. J. R. Garland, G. Krovitz, T. M. Ryan, M. T. Silcox and A. Walker (2007). The primate semicircular canal system and locomotion. *Proceedings of the National Academy of Sciences of the United States of America* **104**: pp. 10808-10812.

Stehlin, H. G. (1909). Remarques sur les faunules de mammifères des couches éocènes et oligocènes du Bassin de Paris. *Bulletin de la Société Géologique de France v.(4)* **9**: pp. 488-520.

Stehlin, H. G. (1912). Die Säugetiere des schweizerischen Eocaens. Siebenter Teil: Adapis. *Abh. schweiz. palaeont Gesch* **38**: pp. 1165-1298.

Stephan, H., R. Bauchot and O. J. Andy. 1970. Data on size of the brain and of various brain parts in insectivores and primates. In: C. R. Noback and W. Montagna, editors. *The Primate Brain*. New York: Appleton-Century-Crofts.

Sudre, J. (1980). Aumelasia gabineaudi n. g. n. sp. nouveau Dichobunidae (Artiodactyla, Mammalia) du gisement d'Aumelas (Hérault) d'âge lutétien terminal. *Paleovertebrata* **Mém. jubil. R. Lavocat**: pp. 197-211.

Sussman, R. W. (1991). Primate origins and the evolution of angiosperms. *American Journal of Primatology* **22**: pp. 209–223.

Szalay, F. S. (1976). Systematics of the Omomyidae (Tarsiiformes, Primates). Taxonomy, Phylogeny, and Adaptations. *Bull. Amer. Mus. Nat. Hist.* **156**: pp. 157-450.

Szalay, F. S. and E. Delson (1979). *Evolutionary History of the Primates.* New York, Academic Press.

Szalay, F. S. and C. C. Katz (1973). Phylogeny of lemurs, galagos and lorises. *Folia Primatologica* **19**: pp. 88-103.

Szalay, F. S., A. L. Rosenberger and M. Dagosto (1987). Diagnosis and Differentiation of the Order Primates. *Yearbook of physical anthropology* **30**: pp. 75-ą.

Szalay, F. S. and D. Seligsohn (1977). Why did the strepsirhine toothcomb evolve? *Folia Primatologica* **27**: pp. 75-82.

Tafforeau, P., R. Boistel, E. Boller, A. Bravin, et al. (2006). Applications of X-ray synchrotron microtomography for non-destructive 3D studies of paleontological specimens. *Applied Physics - Section A - Material Sciences and Processing* **83**: pp. 195-202.

Tan, C. L. and J. H. Drake (2001). Evidence of Tree Gouging and Exudate Eating in Pygmy Slow Lorises (Nycticebus pygmaeus). *Folia Primatologica* **72**: pp. 37-39.

Tan, Y., A. D. Yoder, N. Yamashita and W.-H. Li (2005). Evidence from opsin genes rejects nocturnality in ancestral primates. *Proceedings of the National Academy of Sciences of the United States of America*.

Tattersall, I. (1987). Cathemeral activity in primates: a definition. *Folia Primatologica* **49**: pp. 200-202.

Tattersall, I. (2006). The concept of cathemerality: History and definition. *Folia Primatologica* **77**: pp. 7-14.

Verberne, G. and J. de Boer (1976). Chemocommunication among domestic cats, mediated by the olfactory and vomeronasal senses. *Zeitschrift für Tierpsychologie* **42**: pp. 86-109.

Viguier, B. (2004). Functional adaptations in the craniofacial morphology of Malagasy primates: shape variations associated with gummivory in the family Cheirogaleidae. *Annals of Anatomy* **186**: pp. 495-501.

Viguier, B. and A. Tort (2000). Morphologie crânienne et mandibulaire des Indrinae. Apports des méthodes Procrustes et des analyses de Fourier. *Comptes rendus de l'Académie des Sciences de Paris* **323**: pp. 573-582.

Vinyard, C. J. and J. Hanna (2005). Molar scaling in strepsirrhine primates. *Journal of Human Evolution* **49**: pp. 241-269.

Vinyard, C. J., C. E. Wall, S. H. Williams and W. L. Hylander (2003). Comparative Functional Analysis of Skull Morphology of Tree-Gouging Primates. *American Journal of Physical Anthropology* **120**: pp. 153-170.

Vioarsdóttir, U. S., P. O'Higgins and C. Stringer (2002). A geometric morphometric study of regional differences in the ontogeny of the modern human facial skeleton. *Journal of Anatomy* **201**: pp. 211-229.

Williams, S. H., C. E. Wall, C. J. Vinyard and W. L. Hylander (2002). A Biomechanical Analysis of Skull Form in Gum-Harvesting Galagids. *Folia Primatologica* **73**: pp. 197-209.

Wright, P. C. (1989). The nocturnal primate niche in the New World. *Journal of Human Evolution* **18**: pp. 635–658.

Wright, P. C. (1995). Demography and life history of free-ranging Propithecus diadema edwardsi in Ranomafana National Park, Madagascar. *International Journal of Primatology* **16**: pp. 835–854.

Yang, Z. and A. D. Yoder (2003). Comparison of Likelihood and Bayesian Methods for Estimating Divergence Times Using Multiple Gene Loci and Calibration Points, with Application to a Radiation of Cute-Looking Mouse Lemur Species. *Systematic Biology* **52**: pp. 705-716.

Yoder, A. D. (1991). The applications and limitations of ontogenetic comparisons for phylogenetic reconstruction: the case of the strepsirhine internal carotid artery. *Journal of Human Evolution* **23**: pp. 183-195.

Yoder, A. D. (1997). Back to the future : a synthesis of Strepsirrhine systematics. *Evolutionnary Anthropology* **6**: pp. 11-22.

Yoder, A. D., M. Cartmill, M. Ruvolo, K. Smith and R. Vilgalys (1996). Ancient single origin for Malagasy primates. *Proceedings of the National Academy of Sciences of the United States of America* **93**: pp. 5122–5126.

Yoder, A. D. and Z. Yang (2004). Divergence dates for Malagasy lemurs estimated from multiple gene loci: geological and evolutionary context. *Molecular Ecology* **13**: pp. 757-773.

Zelditch, M., D. Swiderski, D. Sheets and W. Fink. 2004. Ordination methods. *Geometric Morphometrics For Biologists: A Primer*. New York and London: Elsevier Academic Press. pp. 178-179.

Zollikofer, C. P. E. and M. S. Ponce de León (1995). Tools for rapid prototyping in the Biosciences. *IEEE Transactions on Medical Imaging* **15**: pp. 48-55.

Zollikofer, C. P. E. and M. S. Ponce de León (2002). Visualizing patterns of craniofacial shape variation in Homo sapiens. *Proceedings of the Royal Society of London* **269**: pp. 801-807.

Zollikofer, C. P. E. and M. S. Ponce de León (2004). Kinematics of Cranial Ontogeny: Heterotopy, Heterochrony, and Geometric Morphometric Analysis of Growth Models. *Journal of Experimental Zoology (Mol Dev Evol)* **302B**: pp. 322-340.

Zollikofer, C. P. E. and M. S. Ponce de León (2005). *Virtual Reconstruction. A Primer in*

Computer-Assisted Paleontology and Biomedicine. John Wiley & Sons.

Zollikofer, C. P. E., M. S. Ponce de León, R. D. Martin and P. Stucki (1995). Neanderthal Computer Skulls. *Nature* **375**: pp. 283-285.

Introduction

Depuis Darwin (1859) et Haeckel (1866), il est reconnu que les processus évolutifs et développementaux influencent la morphologie des êtres vivants à différentes échelles temporelles. Sur le long terme, la morphologie reflète l'évolution par la sélection naturelle et l'adaptation à l'environnement. Sur le court terme, la morphologie est le résultat de l'ontogénèse, déterminée par des programmes génétiques et des contraintes de développement. L'idée maîtresse des études portant sur l'évolution du développement, ou « Evo-Devo », est que les changements dans l'ontogénèses sont une source majeure d'innovation au cours de l'évolution. Au sein d'un groupe, la diversité morphologique peut être décrite en termes de différences entre les modalités développementales propres à chaque espèce**.** Ces différences résultent de la modification de l'ontogénie au cours de la phylogénie. Aujourd'hui l'Evo-Devo est un domaine de recherche en expansion dont l'objectif est d'établir des liens entre le développement (l'ontogénie) et l'évolution (la phylogénie).

La théorie de la récapitulation d'Haeckel a marqué les travaux de recherche sur l'évolution du développement pendant près d'un siècle. Cette théorie prédit qu'au cours de l'ontogénèse, les espèces récapitulent les stades adultes de leurs ancêtres, et que l'innovation s'effectue principalement par addition terminale de caractères nouveaux. La proposition célèbre d'Haeckel « l'ontogénie récapitule la phylogénie » a inspiré une profusion de travaux de recherche sur les relations entre la phylogénie et l'ontogénie.

C'est Haeckel (1866) qui, afin de désigner les exceptions à la théorie de la récapitulation , a introduit la notion d'hétérochronie ; l'agent temporel du changement évolutif agissant au cours de l'ontogénie. De Beer (1930) a redéfini le concept d'hétérochronie comme le « décalage dans le temps de la formation d'un organe, relativement à celle du même organe chez son ancêtre ». Cette définition est toujours valable aujourd'hui, et la notion d'hétérochronie fait toujours partie aujourd'hui des concepts dominants en Evo-Devo.

Alors que la théorie de la récapitulation était progressivement réfutée au cours du XX^{ème} siècle et que la biologie évolutive se concentrait sur les changements adaptatifs via la sélection naturelle, l'ouvrage « Ontogénie et Phylogénie » de Gould (1977) suscita un regain d'intérêt considérable pour l'évolution du développement, et devait placer le cadre des hétérochronies à une place centrale de ce domaine de recherche. L'hétérochronie, selon Gould (1977, 2000), s'applique à l'analyse comparative de trajectoires forme-âge au cours de l'ontogénèse. Cette terminologie a été par la suite étendue à l'analyse comparative de trajectoires taille-âge (par exemple: Godfrey et Sutherland, 1995 ; Klingenberg, 1988 ; Rice, 1997). L'usage des hétérochronies devait initialement se restreindre à un rôle descriptif. Cependant, les avancée récentes en génétique du développement ont élargi l'emploi du vocabulaire lié aux hétérochronies aux processus génétiques responsables des différences observées dans les modalités de développement (e.g., Ambros, 1997 ; Moss, 2007 ; Slack et Ruvkun, 1997).

Parallèlement aux progrès en génétique du développement, l'introduction des méthodes de morphométrie géométrique a constitué une véritable révolution pour la biologie comparative (Bookstein, 1991 ; Dryden et Mardia, 1998 ; Marcus et al., 1996). Ces méthodes permettent de quantifier les changements phénotypiques au cours de l'ontogénie et de la phylogénie de manière globale, en préservant la géométrie de l'objet lors des analyses: ceci permet d'étudier des patrons de variabilité complexes à un niveau de détail qui n'avait pas été atteint jusqu'alors. Notamment, ces techniques ont relancé l'intérêt de la communauté scientifique pour la description et l'analyse des modalités de développement dans le domaine de l'anthropologie physique (par exemple: O'Higgins et al., 2001 ; O'Higgins et Jones, 1998 ; Ponce de Leòn et Zollikofer, 2001).

Un sujet central de l'Evo-Devo appliquée à l'anthropologie physique est l'hypothèse de néoténie du crâne humain, qui a été initialement proposée par Bolk (1926). Chez l'homme adulte, le crâne présente certaines caractéristiques correspondant à celles que l'on trouve chez les formes juvéniles de grands singes. Depuis son traitement par Gould (1977), cette hypothèse a fait l'objet d'une attention considérable, a engendré des débats houleux et ne fait toujours pas l'objet d'un consensus (par exemple : Godfrey et Sutherland, 1996 ; Penin et al., 2002 ; Raff, 1996 ; Rice, 1997 ; Shea, 1989). En primatologie, un autre sujet d'importance est le cas du bonobo, qui est considéré depuis sa découverte comme pédomorphe relativement à son espèce sœur, le chimpanzé (voir Coolidge, 1933 ; Schwarz, 1929).

Les études portant sur la diversité des primates anthropoïdes et particulièrement chez les hominoïdes ont une place importante car elles se rapportent à notre propre histoire évolutive. Il est néanmoins surprenant que la grande diversité chez les primates strepsirrhiniens ait jusqu'à présent été étudiée aussi peu au travers d'une approche Evo-Dévo. Ce travail s'inscrit dans cette perspective : cette thèse représente une tentative pour établir des liens entre les patrons de diversité morphologique au cours de l'ontogénie et de la phylogénie chez les primates strepsirrhiniens. Etant donné que la diversité concerne la majorité des aspects de la biologie des strepsirrhiniens, les perspectives d'une telle approche sont prometteuses. Les strepsirrhiniens actuels comprennent deux infraordres monophylétiques, les lémuriformes (les lémuriens malgaches) et les loriformes qui comprennent les galagos et les loris. Les lémuriens ont évolué en isolement sur Madagascar, et occupent un large éventail de niches écologiques (par exemple: Martin, 1972; Mittermeier et al., 1994). Les primates malgaches montrent une grande diversité dans leurs régimes alimentaires et leurs mode de vie. Ils sont également divers dans leurs modes de locomotion, et leur gamme de poids s'étale de 55g pour *Microcebus murinus* à plus de 200kg chez *Archaeoindri.* Ils offrent un des exemples les plus nets de radiation adaptative (Martin, 1972). Au contraire, les loriformes occupent des niches écologiques beaucoup plus restreintes, probablement en raison d'un phénomène de compétition avec les primates haplorrhiniens (Mittermeier et al., 1994).

Aussi, des questions se posent toujours quant à l'histoire évolutive des strepsirrhiniens. Il

n'existe aujourd'hui aucun reste fossile qui soit proche des ancêtres directs des strepsirrhiniens actuels. Bien que les adapiformes de l'Eocène n'aient pas développé au cours de leur évolution le peigne dentaire caractéristique des strepsirrhiniens actuels, l'hypothèse faisant actuellement l'objet du plus large consensus est celle que les strepsirrhiniens modernes descendent d'un ancêtre adapiforme, ou lié aux adapiformes (voir Beard et al., 1988 ; Beard et Godinot, 1988 ; Godinot, 1998, 2006). L'évolution des adapiformes est bien documentée dans les dépôts Eocènes d'Europe, d'Amérique du Nord et d'Asie (pour un récapitulatif, voir Godinot, 1998). Un des épisodes les mieux documentés de diversification au sein des adapiformes concerne la radiation de la sous famille des adapinés en Europe, qui s'étend de l'Eocène moyen à l'Eocène supérieur (Franzen, 2003 ; Godinot, 1998 ; Lanèque, 1992a, 1992b, 1993). Le registre fossile comporte un nombre important de crânes remarquablement bien préservés pour plusieurs genres d'adapiformes appartenant aux sous familles des adapinés et notharctinés, et il est donc possible de comparer leur morphologie avec celle des strepsirrhiniens actuels.

Les études qui ont porté jusqu'alors sur le développement crânien et mandibulaire chez les strepsirrhiniens ont été réalisées à l'aide de mesures linéaires (par exemple : Ravosa, 1992, 2007). Le principal objectif de ces études est d'établir des liens entre des modalités de changement morphologique au cours de l'ontogénie et des stratégie adaptatives (par exemple, voir Godfrey et al., 2004, 2005 ; Smith, 2000). Cependant, ces méthodologies ne permettent pas de séparer l'analyse de la morphologie en termes de croissance (changement de taille) et de développement (changement de forme) puisque les mesures linéaires *sont* des mesures de taille. Enfin, ces méthodologies ne permettent pas de visualiser les changements de forme au cours de l'ontogénie.

Ainsi, les liens entre les changements dans l'ontogénie du crâne et la diversification morphologique sont largement inconnus chez les primates strepsirrhiniens. Une raison importante peut être avancée pour expliquer cet état de fait : la plupart des collections de strepsirrhiniens actuels juvéniles comprennent des cadavres non préparés, ce qui rend difficile l'accès à la structure osseuse. Cependant, grâce aux développements de l'imagerie médicale et de la micro-tomographie tridimensionnelle (par exemple, Rossi et al., 2003 ; Silcox, 2003 ; Spoor, 1998 ; Tafforeau et al., 2006), il est aujourd'hui possible de scanner des spécimens tels que des microcèbes nouveaux nés avec une résolution spatiale suffisante pour accéder à la morphologie de leur crâne. De plus l'utilisation de techniques de reconstruction tridimensionnelle permet d'incorporer dans les analyses de géométrie morphométrique des fossiles incomplets et/ou déformés (Zollikofer et Ponce de Leòn, 1995, 2005 ; Zollikofer et al., 1995).

Le but de cette thèse est d'expliquer comment des modifications dans les modalités développementales ont contribué à la diversité observée chez les strepsirrhiniens fossiles et actuels. La morphologie du crâne est étudiée, car :

- le crâne comporte un signal phylogénétique fort, qui est utilisé dans les analyses de systématique et pour estimer les phylogénies (voir Cartmill, 1994 ; Fleagle,

1999 ; Kay et al., 1997 ; MacPhee et Cartmill, 1986 ; Shoshani et al., 1996).

- Le crâne comporte l'appareil masticateur, et il est le siège du cerveau et des principaux organes sensoriels. Sa morphologie reflète donc des adaptations fonctionnelles variées, qui sont d'un grand intérêt pour les études portant sur l'évolution d'un groupe.
- Le crâne est une structure tridimensionnelle présentant de nombreux caractères homologues quantifiables. Il est donc possible d'effectuer des analyses comparatives sur cette structure avec les outils de géométrie morphométrique.

Les questions suivantes sont abordées :

1) *Méthodes* : comment peut-on analyser de manière globale des patterns complexes de variation morphologique au cours de l'ontogénie et de la phylogénie au niveau du crâne et de la mandibule ?
2) *Adaptations et contraintes de développement* : quelles sont les contributions relatives des adaptations fonctionnelles et des contraintes liées au développement dans la morphologie du crâne ? Cette problématique rejoint le débat opposant les adaptationnistes aux structuralistes (Gould et Lewontin, 1971).
3) *Ontogénie et diversité phylétique* : quelles sont les relations entre la diversité en terme de croissance et de développement et la diversité morphologique ?
4) *Perspectives Evo-Dévo et taxons fossiles* : peut-on lier la tendance à l'augmentation du degré d'encéphalisation au cours de l'histoire évolutive des primates strepsirrhiniens à des changements particuliers dans les modalités de développement du crâne ?

Chapitre 1 : Matériel et méthodes

L'échantillon est composé de 311 individus. Au sein de cet échantillon, 205 spécimens ont été scannés par tomographie conventionnelle (N=8), microtomographie conventionnelle (N= 166) et microtomographie par rayonnement synchrotron (N=31). Des fossiles incomplets, déformés ou présentant des parties ayant été déplacées ont été reconstruits en suivant les recommandations de Zollikofer et Ponce de Leòn (2005).

Au sein de cet échantillon, les patrons de variabilité morphologique ont été analysés à l'aide de l'outil de géométrie morphométrique. 56 landmarks tridimensionnels ont été mesurés sur le crâne, et 18 sur la mandibule. En ce qui concerne les spécimens scannés, les landmarks ont été relevés directement sur des représentation surfaciques virtuelles obtenues à partir des scans. Pour le reste de l'échantillon, les landmarks ont été relevés à l'aide d'un Microscribe 3D.

Certaines méthodes d'analyse ont été employées plusieurs fois au cours des différents chapitres de la thèse. Dans ce chapitre, des détails sont donnés sur les sujets suivants :

- Alignement des spécimens grâce à la méthode de superposition Procrustes.

- Analyse en composantes principales.
- Analyse canonique.
- Traitement et quantification de l'allométrie.
- Visualisation des variations de forme.

Afin de permettre une analyse efficace de jeux de données morphométriques, un logiciel a été développé par Specht (2007) et Specht et al. (2007) : MorphoTools. Cette application intégrée permet d'effectuer des analyses interactives de jeux de données. Une présentation est donnée de l'architecture de cette application ainsi que des développements effectués sur ce projet au cours de cette thèse.

Chapitre 2. La variabilité morphologique du crâne chez les primates.

Le crâne présente une grande variabilité morphologique dans chacun des deux sous-ordres de primates, les haplorrhiniens et les strepsirrhiniens. De plus, les deux sous-ordres de primates diffèrent largement dans leur morphologie crânienne : l'origine de ces différences morphologiques se trouve-t-elle dans des contraintes phylogénétiques, ou dans des différences en terme d'adaptation ? L'allométrie, l'effet de la taille sur la forme, est également responsable d'une grande part de la variance morphologique. Les patrons d'allométrie reflètent-ils dans une certaine mesure l'adaptation à des régimes alimentaires donnés (frugivore, insectivore, folivore, gummivore) ou éventuellement le mode de vie (diurne, nocturne)? Ou bien l'allométrie agit-elle principalement comme un mécanisme de compensation qui influe sur la forme lorsqu'interviennent des changements de taille, comme le suggèrent par exemple Emerson et Bramble (1993) ? Les patrons d'allométrie diffèrent-ils entre les deux sous-ordres de primates ?

Afin de quantifier les contraintes phylogénétiques et les effets de l'adaptation sur la morphologie, l'approche proposée par Cheverud et al. (1985) a été utilisée. La variance morphologique est divisée en deux composantes. La première représente le fardeau phylogénétique. L'autre représente une évolution indépendante des contraintes phylogénétiques. C'est dans cette seconde fraction que des effets sur la morphologie crânienne communs aux deux sous-ordres, et liés à des adaptations à un régime alimentaire donné ou à un mode de vie, doivent être éventuellement observés.

L'adaptation à un régime alimentaire ou à un mode de vie donné se traduit par des effets similaires sur la taille (voir aussi Kay, 1984) et la forme du crâne dans chacun des deux sous-ordres. En ce qui concerne la forme, les espèces diurnes ont de plus petites orbites que les espèces nocturnes ; les espèces folivores ont des mandibules dont les branches horizontales sont plus hautes, des symphyses plus développées dans la direction antéropostérieure, et des condyles plus hauts relativement à la rangée dentaire. On retrouve dans les patrons d'allométrie de la mandibule des caractéristiques liées à l'adaptation aux régimes alimentaires. En ce qui

concerne le crâne, l'allométrie peut être résumée à un mécanisme permettant le maintien de la fonction pour un éventail de taille.

Néanmoins, les contraintes phylogénétiques expliquent une part importante de la variance de la forme du crâne et de la mandibule. Ces contraintes expliquent pourquoi il n'y a pas de chevauchement entre les haplorrhiniens et strepsirrhiniens actuels dans l'espace des formes pour le crâne, et relativement peu pour la mandibule. Les patrons d'allométrie diffèrent entre les haplorrhiniens et strepsirrhiniens, et il semble que ces contraintes phylogénétiques ont une origine développementale.

Chapitre 3. « Strepsirrhinisme »: est-ce une condition primitive ou dérivée chez les primates ?

La morphologie crânienne des omomyidés appartenant aux genres *Rooneyia, Necrolemur* et *Microchoerus* est beaucoup plus proche de celle des strepsirrhiniens actuels que de celle des haplorrhiniens actuels, *Tarsius* inclus. Ainsi, il est plus vraisemblable que la transition vers une morphologie caractéristique des haplorrhiniens modernes se soit déroulée au sein d'une lignée d'omomyidés, à l'exclusion des genres *Rooneyia, Necrolemur* et *Microchoerus*. Nos résultats contradisent l'hypothèse de Szalay et al (1987) : ces auteurs avaient proposé qu'une réorganisation de la face se soit effectuée chez les haplorrhiniens basaux (omomyidés inclus), et que cette réorganisation avait une origine développementale. Leur hypothèse impliquait que des différences dans les contraintes de développement du crâne sont à l'origine de différences profondes dans la morphologie crânienne entre haplorrhiniens et strepsirrhiniens, et que ces différences sont déjà présentes chez les omomyidés, ce qui est infirmé ici. De ce fait, de nouveaux arguments sont apportés pour soutenir l'hypothèse de Beard (1988). En effet, selon cet auteur, on ne peut pas écarter l'hypothèse que les omomyidés, considérés par la plupart des chercheurs comme des haplorrhiniens basaux, étaient peut-être plus proches dans leur anatomie des strepsirrhiniens que des haplorrhiniens actuels.,

Chapitre 4 : la variabilité morphologique crânio-mandibulaire au sein des strepsirrhiniens actuels.

Une hypothèse répandue est qu'au sein des strepsirrhiniens, ce sont les cheirogaleidés et des galagidés qui ont retenu le plus la condition ancestrale au niveau de l'écologie, du comportement et de l'anatomie. Cette hypothèse est testée à l'aide d'une approche de géométrie morphométrique, en ce qui concerne la morphologie crânio-mandibulaire.

Jungers (1979) a démontré que les patrons d'allométrie des membres étaient différents entre les différentes familles de lémuriens, et reflètent des différences interfamiliales en termes de mode de locomotion. De façon similaire, les patrons d'allométrie crâniens et mandibulaires

reflètent-ils les adaptations caractéristiques des différentes familles de strepsirrhiniens actuels ? L'allométrie est quantifiée pour chaque famille de strepsirrhiniens.

De nouveaux arguments sont apportés pour soutenir l'hypothèse que les cheirogaléidés et galagidés sont les moins dérivés des strepsirrhiniens par rapport à la condition ancestrale des strepsirrhiens modernes. C'est particulièrement vrai pour la mandibule : les mandibules des cheirogaleidés et des galagidés présentent des affinités morphologiques importantes.

Les patrons d'allométrie différent assez peu entre les familles de strepsirrhiniens pour le crâne, ce qui renforce l'hypothèse que l'allométrie joue un rôle majeur dans le maintien de la fonction lorsque la taille varie. En ce qui concerne la mandibule, il y a des différences importantes entre les lémuriformes et les loriformes dans l'allométrie, qui ne peuvent être mise en relation avec des différences de spécialisation entre les familles.

Chapitre 5 : l'origine développementale de la variabilité morphologique au sein des strepsirrhiniens.

Depuis Haeckel (1866), on sait que les changements dans l'ontogénèse sont une source majeure d'innovation morphologique. Dans le cas présent, est-ce que des modifications dans les trajectoires ontogénétiques sont à l'origine de la diversité morphologique au sein des primates en général, et parmi les strepsirrhiniens en particulier ? En premier lieu, des différences dans les contraintes de développement du crâne et de la mandibule peuvent-elles être détectées entre les haplorrhiniens et strepsirrhiniens ? Dans un deuxième temps, est-ce que la plus grande diversité morphologique observée au sein des lémuriformes par rapport aux loriformes est le reflet d'une plus grande diversité en termes de longueur, direction et position des trajectoires ontogénétiques ? Selon Gould et Lewontin (1971), des différences de grade allométrique reflètent des épisodes de diversification rapide. Si l'hypothèse de Gould et Lewontin (1971) est valide, on peut s'attendre à observer des différences de grade allométrique entre les espèces de lémuriens, et peu ou pas de différences de grade allométrique au sein des espèces de loriformes.

Une dernière question est abordée dans ce chapitre, et concerne l'évolution du peigne dentaire. Les études moléculaires situent la date de divergence entre les lémuriformes et loriformes au début du Paléocène ou même au cours du Crétacé (par exemple, voir Yoder, 1997 ; Yoder et al., 1996 ; Yoder et Yang, 2004). Si ces estimations sont valides, cela implique que le peigne dentaire caractéristique des primates malgaches et des loriformes pourrait ne pas être homologue dans les deux infraordres de strepsirrhiniens. Ce chapitre apporte des arguments tirés des données du développement dentaire en rapport avec l'homologie supposée du peigne dentaire.

Les espèces étudiées de strepsirrhiniens et d'haplorrhiniens diffèrent largement dans les directions, longueurs et positions de leurs trajectoires ontogénétiques, ce qui conforte l'hypothèse posée dans le second chapitre : des différences dans les contraintes de développement sont à

l'origine des différences de morphologie entre les haplorrhiniens et les strepsirrhiniens.

Chez les lémuriens malgaches, il y a une plus grande diversité en termes de direction, position et longueur de trajectoire ontogénétique que chez les loriformes. De plus, on observe des différences importantes de grade allométrique parmi les espèces de lémuriens, et une plus faible variabilité au sein des loriformes. Ces résultats renforcent l'hypothèse de Gould et Lewontin (1971). De plus, un pattern ancestral dans le grade allométrique se dégage nettement: le pattern ancestral correspond au grade allométrique de l'ensemble des Loriformes étudiés et du lémurien malgache *Lepilemur ruficaudatus*. On dispose donc d'un outil permettant d'inférer la polarité des changements de grade allométrique au sein des strepsirrhiens.

Concernant la question du peigne dentaire, on observe un pattern d'éruption original chez les lorisidés : au sein de cette famille, le peigne dentaire définitif émerge avant la première molaire. Chez les lémuriformes, il émerge toujours après la première molaire. Cependant, au sein des galagidés, le pattern d'éruption du peigne dentaire correspond à celui des lémuriformes. Le pattern observé chez les lorisidés correspond donc certainement à une apomorphie de ce groupe. Présentement, il n'y a donc pas d'argument développemental en faveur de l'hypothèse de non homologie du peigne dentaire entre les loriformes et les lémuriformes.

Chapitre 6 . Les adapiformes et l'évolution de la morphologie crânienne et mandibulaire chez les strepsirrhiniens.

Les strepsirrhiniens modernes descendent probablement d'un primate adapiforme ou apparenté aux adapiformes. Les affinités morphologiques entre les strepsirrhiniens actuels et un échantillon de crânes de primates adapiformes appartenant aux sous-familles des notharctinés et des adapinés sont examinées.

Les adapinés sont uniques dans la morphologie de leur orbite et de leur mandibule, ce qui reflète probablement une spécialisation marquée à un régime alimentaire de type folivore.

Au sein des adapinés, une augmentation de taille via une transposition allométrique caractérise la lignée des *Leptadapis*. Ceci contredit l'hypothèse de Gingerich (1981a), qui propose au contraire que le genre *Adapis* aurait évolué vers le nanisme depuis un ancêtre du genre *Leptadapis*.

Enfin, les adapiformes adapinés et notharctinés ont des trajectoires ontogénétiques plus longues en terme de quantité de changement de forme que les strepsirrhiniens actuels. Les strepsirrhiniens actuels ont des morphologies crâniennes et mandibulaires pédomorphes par rapport aux adapiformes étudiés. Une tendance vers le raccourcissement des trajectoires ontogénétiques caractérise donc l'évolution des strepsirrhiniens. Ceci est lié, au cours de leur histoire évolutive, à l'expression de contraintes de développement dans un contexte général de sélection en faveur de l'augmentation de leur degré d'encéphalisation.

Conclusion

La compréhension des relations entre la phylogénèse et l'ontogénèse est complexe, et nécessite des arguments provenant à la fois d'approches ascendantes (« bottom-up ») et descendantes (« top-down »). En primatologie et en anthropologie, relativement peu d'études ont adopté une approche montante (Mitteroecker et al., 2004b ; Zollikofer et Ponce de Leòn, 2004). Une raison majeure peut être avancée pour expliquer cet état de fait : jusqu'à présent, les mécanismes génétiques impliqués dans l'évolution du développement crânien chez les mammifères sont relativement peu connus. Le génome complet du macaque rhésus a été publié récemment (Gibbs et al., 2007), portant à trois le nombre de génomes séquencés chez les primates après ceux de l'homme (Lander et al., 2001, 2004) et du chimpanzé (Mikkelsen et al., 2005). De nombreux gènes diffèrent entre l'homme, le chimpanzé, et le macaque rhésus (Gibbs et al., 2007; Mikkelsen et al., 2005), certains étant probablement impliqués dans des différences notables en terme de développement. Cependant, relier le génotype au phénotype est extrêmement difficile (par exemple, voir Carroll, 2003), et les gènes qui ont joué un rôle majeur dans l'évolution de l'homme sont toujours inconnus. L'étude d'organismes modèles tels que la souris sera décisive pour améliorer la compréhension des processus génétiques qui gouvernent l'évolution phénotypique chez les primates et en particulier chez l'homme (Carroll, 2003; Lieberman, 2004).

Du côté de l'approche montante (depuis les patterns jusqu'au processus), les avancées récentes tant du point de vue théorique que du point de vue technique ont ouvert de nouvelles perspectives dans le domaine de l'analyse du phénotype. Au cours de cette thèse, nous avons profité pleinement de ces avancées : la morphologie osseuse a pu être quantifiée sur des spécimens de conditions aussi variées que des cadavres, des crânes préparés ou des fossiles très minéralisés. Des reconstructions de ces fossiles ont été élaborées en suivant les recommandations les plus récentes dans ce domaine (Zollikofer et Ponce de Leòn, 1995, 2005 ; Zollikofer et al., 1995). Des analyses comparatives ont été conduites en utilisant une application développée en grande partie pour les besoins de cette thèse, le MorphoTools.

Un résultat en particulier ouvre des perspectives nouvelles quant à l'analyse de fossiles. En effet, un des problèmes qui se posent pour les paléoanthropologues est que les séries ontogénétiques complètes sont rares chez les espèces éteintes de primates. En particulier, chez les adapinés, aucun crâne de spécimen juvénile assez complet n'a encore été décrit. Dans cette thèse, nous avons montré qu'il était possible d'effectuer des inférences quant à l'évolution du développement en utilisant un échantillon composé de séries ontogénétiques de primates actuels et de fossiles d'adultes : grâce à l'échantillon de fossiles il a été possible de démontrer que l'augmentation du degré d'encéphalisation se faisait via un raccourcissement des trajectoires ontogénétiques, ce qui aboutit à des formes actuelles relativement pédomorphes par rapport aux formes fossiles. De Beer (1962) considérait que les processus aboutissant à l'émergence

de formes pédomorphes (via la néoténie ou la progénèse) étaient importants d'un point de vue évolutif. En effet, de Beer (1930) propose que des formes pédomorphes présentent une plasticité évolutive accrue. De Beer (1958) a avancé une explication génétique en faveur de cette hypothèse: dans les lignées pédomorphes, les gènes responsables du développement des caractères adultes ancestraux ne sont plus employés. Ils seraient donc à nouveau disponibles pour développer de nouveaux caractères. Cependant, l'idée que l'évolvabilité puisse être l'objet de la sélection naturelle semble être contradictoire, dans le sens où un évènement ne peut précéder sa cause. Le fait de posséder un crâne pédomorphe pourrait-il présenter un avantage sélectif immédiat ? Ici, nos résultats suggèrent que dans un contexte de sélection pour une augmentation de l'encéphalisation, les contraintes de développements favorisent l'émergence de formes plus pédomorphes. La pédomorphie en tant que telle ne représenterait donc pas un avantage sélectif immédiat, mais serait un sous-produit de l'expression de contraintes de développement.

La compréhension de l'encéphalisation chez les primates actuels et fossiles est un domaine qui connaît actuellement un regain d'intérêt considérable, notamment grâce au déploiement des techniques de tomographie par rayons X : en effet, ces techniques permettent d'accéder de manière non destructive à des structures internes de fossiles telles que la cavité endocrânienne. Cependant, l'analyse comparative des endocrânes de fossiles et de primates actuels est un domaine qui reste aujourd'hui largement inexploré, la raison principale étant qu'il est difficile de localiser des points homologues sur cette structure. De récents développements en termes d'outils analytiques ouvrent de nouvelles possibilités pour l'analyse comparative des endocrânes (Specht et al., 2007). En effet, ces travaux proposent une manière d'appréhender la structure endocrânienne dans son ensemble et de comparer différents endocrânes tout en optimisant le critère d'homologie. De nombreux crânes de strepsirrhiniens fossiles possèdent une cavité endocrânienne bien préservée, et il est donc techniquement possible aujourd'hui d'entreprendre une analyse détaillée de l'encéphalisation chez les strepsirrhiniens.

Acknowledgements

This work would not have been possible without the support and motivation of many people. First of all, my great debt is to my parents for their constant support. I would like to thank Christoph Zollikofer, Marcia Ponce de León, and Jean-Jacques Jaeger for their longstanding support, advice, and trust. I would like especially to thank Matthias Specht for his help with programming issues and for welcoming me into the MorphoTools project. I would like to express my special gratitude to Paul Tafforeau for his constant enthusiasm, advice, his incredible energy, his friendship, for letting me access to the E.S.R.F, and for welcoming me in Grenoble. I warmly thank Franck Guy for his help, his detailed comments concerning early versions of this manuscript, and all his advice and enthusiasm.

I am also greatly indebted to the curators of the different Museums and researchers who let me access to the materials that were studied in this PhD. I want to thank Edmée Ladier from the Musée d'Histoire Naturelle de Montauban, Nathalie Mémoire from the Musée d'Histoire Naturelle de Bordeaux, Kurt Heissig from the Museum und Institut für Palaeontology of München, Burkart Engesser and Arne Ziems from the Naturhistorisches Museum Basel, Jacques Cuisin and Pascal Tassy from the Musée d'Histoire Naturelle de Paris, also Fabienne Aujard from the MNHN (Brunoy), Peter Giere and Robert Asher from the Museum für Naturkunde (Berlin), Suzane Jicquel, Bernard Marandat and Claude Requirand from the I.S.E.M. (Montpellier), Nadine Mestre-Francès from the Université Montpellier II, Christopher Beard from the Carnegie Museum of Natural History, and Charles Schaff from the Museum of Comparative Zoology (Harvard). I am also greatly indebted to Pr. Alfred Rosenberger from the Department of Anthropology and Archaeology, Brooklyn College, for kindly providing a copy of a scan of the cranium of *Rooneyia viejaensis*. This scan was performed with a laser scanner by Mr Sai Man Wong, the assistant of Pr. Alfred Rosenberger, .

I want to thank the staff of beamlines ID19 and ID17 from the E.S.R.F, and Peter Wyss from the E.M.P.A. for letting me access to their facilities.

I would also like to thank the personal of the different laboratories in which I was welcomed throughout these years. From Montpellier, I want to thank Monique Vianey-Liaud, Laurent Marivaux, Rodolphe Tabuce, Jean-Christophe Auffray, Henri Cappetta, Jacques Michaux, Anne-Marie Biglione, Sylvie Agret, Jean-Claude Plautin and Bernard Orth. I am greatly indebted to Julien Claude for his advice in statistics and pieces of code in "R". I want to thank Vincent Lazzari and Adelaïde Euriat for their friendship and for welcoming me in Montpellier several times. I thank also Julien Rossignol, Didine, Eudes Thouand, Céline Martin and Lionel Hautier for lots of good times spent there! Special thanks to Pierre-Henry Fabre for his suggestions regarding the use of DNA sequences. In Zürich, I warmly thank Claudia Zebib for her help. Thanks also to Gustl Anzenberger for resolving some difficult CITES issues. I express my gratitude to Tea Jashashvili for her support and generosity. I also thank Petter Holdener, Kris Carlson, and

Juan-Manuel Gimenez for welcoming me in Zürich. I thank Jody Weissman, Walther Fuchs, Fabian Hilti, Ann Margvelashvili and Naoki Morimoto for their friendship. In Poitiers, I want to thank Patrick Vignaud, Carine Noël, Ghislaine Florent and Anne Brunnelière for their support. Thanks to Michel Brunet for welcoming me in Poitiers. Thanks also to Olga Otero, Géraldine Garcia, Matthieu Schuster, Cécile Blondel, Xavier Valentin and Gildas Merceron. I especially want to express my gratitude to Aurélie Pinton and Soizic Le Fur for lots of hilarious moments in our shared office. And last but not least, I want to thank Olivier Chavasseau, Cyril Charles, Edouard-Georges Emonet, Thibault Bienvenue, and Pauline Coster for their company, support and friendship. Finally, I would like to thank Flora. Also thanks to those I may have forgotten!

1. Sample lists

Appendix 1: list of the extant specimens used in the study. S: Sex. M: male. F: female. N: unknown Prov: provenance of the specimens. AIM: Anthropologiches Institut und Museum. MNHN: Museum National d'Histoire Naturelle, laboratoire mammifères et oiseaux. BRUN: Museum National d'Histoire Naturelle, Brunoy. ISEM : Institut des Sciences de l'Evolution de Montpellier. MTP: Université Montpellier II. BERL: Museum für Naturkunde, Berlin MD: main diet. F: frugivore L: folivory I: insectivory. G: gummivory AP: activity patterns. N: nocturnal. D: diurnal. C: cathemeral. Age: category derived from the dental stage. Ad.: dental adults. Sub.: sub-adult, M2 is erupted. Juv: M1 is erupted, but M2 is not. Inf.: infant. M1 is not yet erupted. Neo: neonate. Protocol: protocol of data acquisation for the C.T. scans. Synchrotron data were acquired at the E.S.R.F., on beamlines ID17 and ID19.

N°	Genus	Species	Prov.	S	AP	MD	Cond	Protocol	Energy	Age	Used in Chapters:				
											2	3	4	5	6
2002-1	*Allocebus*	*trichotis*	MNHN	?	N	G	Cr+Md	µCT (voxel size: 36 µm)	70kv/110ma	Ad	X	X		X	X
10933	*Alouatta*	*belzebul*	AIM	f	D	L	Cr+Md	Microscribe		Ad	X				
10943	*Alouatta*	*belzebul*	AIM	f	D	L	Cr+Md	µCT (voxel size: 74 µm)	70kv/110ma	Ad	X				
10945	*Alouatta*	*belzebul*	AIM	?	D	L	Cr+Md	Microscribe		Ad	X				
10949	*Alouatta*	*belzebul*	AIM	f	D	L	Cr+Md	Microscribe		Ad	X				
10951	*Alouatta*	*belzebul*	AIM	f	D	L	Cr+Md	Microscribe		Ad	X				
8 279	*Aotus*	*trivirgatus*	AIM	?	N	F	Cr+Md	µCT Synchrotron light (voxel size: 30 µm) ID19	40kev	Ne				X	X
10630	*Aotus*	*trivirgatus*	AIM	m	N	F	Cr+Md	µCT (voxel size: 74 µm)	70kv/110ma	Ne				X	X
8446	*Aotus*	*trivirgatus*	AIM	m	N	F	Cr+Md	µCT Synchrotron light (voxel size: 60 µm) ID19	40kev	In				X	X
1781	*Aotus*	*trivirgatus*	AIM	m	N	F	Cr+Md	µCT Synchrotron light (voxel size: 45.71 µm) ID17	40kev	In				X	X
1175	*Aotus*	*trivirgatus*	AIM	f	N	F	Cr+Md	µCT Synchrotron light (voxel size: 45.71 µm)ID17	40kev	Sa				X	X
AS1775	*Aotus*	*trivirgatus*	AIM	m	N	F	Cr+Md	µCT (voxel size: 74 µm)	70kv/110ma	Ad	X	X		X	X
10750	*Aotus*	*trivirgatus*	AIM	?	N	F	Cr+Md	Microscribe		Ad	X	X		X	X
12250	*Aotus*	*trivirgatus*	AIM	f	N	F	Cr+Md	Microscribe		Ad	X	X		X	X
12261	*Aotus*	*trivirgatus*	AIM	?	N	F	Cr+Md	Microscribe		Ad	X	X		X	X
12320	*Aotus*	*trivirgatus*	AIM	m	N	F	Cr+Md	Microscribe		Ad	X	X		X	X
12322	*Aotus*	*trivirgatus*	AIM	?	N	F	Cr+Md	Microscribe		Ad	X	X		X	X
12323	*Aotus*	*trivirgatus*	AIM	m	N	F	Cr+Md	Microscribe		Ad	X	X	X	X	X
MAD8774	*Archaeolemur*	*sp*	MNHN	?	/	/	Cr	Mircoscribe		Ad	X				
MAD306	*Archaeolemur*	*sp*	MNHN	?	/	/	Cr	Microscribe		Ad	X				
MAD107	*Archaeolemur*	*edwarsii.*	MNHN	?	/	/	Cr	Microscribe		Ad	X				
MAD74	*Archaeolemur*	*sp.*	MNHN	?	/	/	Md	Microscribe		Ad	X				
MAD307	*Archaolemur*	*sp*	MNHN	?	/	/	Md	Microscribe		Ad	X				
MAD1931-6	*Archaeolemur*	*edwasii*	MNHN	?	/	/	Cr	Microscribe		Ad	X				
MAD63	*Archaeolemur*	*majori*	MNHN	?	/	/	Md	Microscribe		Ad	X				
7060	*Arctocebus*	*calabarensis*	AIM	m	N	I	Cr+Md	µCT (voxel size: 70 µm)	50kv/300ma	Inf				X	X
7 711	*Arctocebus*	*calabarensis*	AIM	f	N	I	Cr+Md	µCT (voxel size: 74 µm)	70kv/110ma	Inf				X	X
7013	*Arctocebus*	*calabarensis*	AIM	m	N	I	Cr+Md	µCT Synchrotron light (voxel size: 60 µm)ID19	40kev	Inf				X	X
7668	*Arctocebus*	*calabarensis*	AIM	m	N	I	Cr+Md	µCT (voxel size: 98 µm)	50kv/300ma	Juv				X	X
6985	*Arctocebus*	*calabarensis*	AIM	m	N	I	Cr+Md	µCT (voxel size: 98 µm)	50kv/300ma	Juv				X	X
7730	*Arctocebus*	*calabarensis*	AIM	m	N	I	Cr+Md	µCT (voxel size: 98 µm)	50kv/300ma	Sa				X	X

Appendix 1: list of the extant specimens used in the study (continued)

N°	Genus	Species	Prov.	S	AP	MD	Cond	Protocol	Energy	Age	Used in Chapters:				
											2	3	4	5	6
7800	*Arctocebus*	*calabarensis*	AIM	m	N	I	Cr+Md	µCT (voxel size: 103 µm)	50kv/300ma	Sa				X	X
6984	*Arctocebus*	*calabarensis*	AIM	f	N	I	Cr+Md	µCT (voxel size: 36 µm)	70kv/110ma	Sa				X	X
7024	*Arctocebus*	*calabarensis*	AIM	m	N	I	Cr+Md	µCT (voxel size: 50 µm)	70kv/110ma	Sa				X	X
7647	*Arctocebus*	*calabarensis*	AIM	?	N	I	Cr+Md	µCT (voxel size: 36 µm)	70kv/110ma	Sa				X	X
7103	*Arctocebus*	*calabarensis*	AIM	m	N	I	Cr+Md	µCT (voxel size: 113 µm)	50kv/300ma	Ad	X	X	X	X	X
7475	*Arctocebus*	*calabarensis*	AIM	?	N	I	Cr+Md	µCT (voxel size: 36 µm)	70kv/110ma	Ad	X	X	X	X	X
7059	*Arctocebus*	*calabarensis*	AIM	m	N	I	Cr+Md	µCT (voxel size: 103 µm)	50kv/300ma	Ad	X	X	X	X	X
7696	*Arctocebus*	*calabarensis*	AIM	?	N	I	Cr+Md	µCT (voxel size: 50 µm)	70kv/110ma	Ad	X	X	X	X	X
7704	*Arctocebus*	*calabarensis*	AIM	m	N	I	Cr+Md	µCT (voxel size: 50 µm)	70kv/110ma	Ad	X	X	X	X	X
7761	*Arctocebus*	*calabarensis*	AIM	f	N	I	Cr+Md	µCT (voxel size: 50 µm)	70kv/110ma	Ad	X	X	X	X	X
10754	*Ateles*	*paniscus*	AIM	m	D	F	Cr+Md	µCT (voxel size: 74 µm)	70kv/110ma	Ad	X	X			X
10674	*Ateles*	*paniscus*	AIM	m	D	F	Cr+Md	Microscribe		Sa	X	X			X
13884	*Avahi*	*occidentalis*	AIM	?	N	L	Cr+Md	µCT (voxel size: 74 µm)	70kv/110ma	Ad	X	X	X		X
AS-1827	*Avahi*	*laniger*	AIM	?	N	L	Cr+Md	µCT Synchrotron light (voxel size: 45.71 µm)ID17	40 kev	Ad	X	X	X		X
1932_3358	*Avahi*	*laniger*	MNHN	f	N	L	Cr+Md	Microscribe		Ad	X	X	X		X
2002_66	*Avahi*	*laniger*	MNHN	f	N	L	Cr+Md	Microscribe		Ad	X	X	X		X
2002_67	*Avahi*	*laniger*	MNHN	m	N	L	Cr+Md	Microscribe		Ad	X	X	X		X
10709	*Cacajao*	*calvus*	AIM	?	D	F	Cr+Md	µCT (voxel size: 74 µm)	70kv/110ma	Sa	X	X			X
10677	*Callicebus*	*personatus*	AIM	?	D	F	Cr+Md	µCT (voxel size: 74 µm)	70kv/110ma	Ad	X	X			X
12325	*Callicebus*	*sp*	AIM	m	D	F	Cr+Md	Microscribe		Ad	X	X			X
12326	*Callicebus*	*sp*	AIM	m	D	F	Cr+Md	Microscribe		Ad	X	X			X
12457	*Callicebus*	*sp*	AIM	m	D	F	Cr+Md	Microscribe		Ad	X	X			X
10150	*Callimico*	*goeldii*	AIM	m	D	I	Cr+Md	Microscribe		Ad	X	X			X
10317	*Callimico*	*goeldii*	AIM	f	D	I	Cr+Md	µCT (voxel size: 74 µm)	70kv/110ma	Sa	X	X			X
12362	*Callimico*	*goeldii*	AIM	?	D	I	Cr+Md	Microscribe		Ad	X	X			X
13349	*Callimico*	*goeldii*	AIM	?	D	I	Cr+Md	Microscribe		Ad	X	X			X
10692	*Callithrix*	*aurita*	AIM	f	D	I	Cr+Md	µCT (voxel size: 74 µm)	70kv/110ma	Sa	X	X			X
10157	*Callithrix*	*jacchus*	AIM	f	D	G	Cr+Md	Microscribe		Ad	X	X			X
10158	*Callithrix*	*jacchus*	AIM	m	D	G	Cr+Md	Microscribe		Ad	X	X			X
10159	*Callithrix*	*jacchus*	AIM	f	D	G	Cr+Md	Microscribe		Ad	X	X			X
10164	*Callithrix*	*jacchus*	AIM	m	D	G	Cr+Md	Microscribe		Ad	X	X			X
7152	*Cebuella*	*pygmaea*	AIM	f	D	G	Cr+Md	µCT (voxel size: 74 µm)	70kv/110ma	Ad	X	X			X
7107	*Cebus*	*apella*	AIM	f	D	F	Cr+Md	Microscribe		Ad	X	X			X
10802	*Cebus*	*apella*	AIM	m	D	F	Cr+Md	µCT (voxel size: 74 µm)	70kv/110ma	Sa	X	X			X
10981	*Cebus*	*apella*	AIM	f	D	F	Cr+Md	Microscribe		Ad	X	X			X
10983	*Cebus*	*apella*	AIM	f	D	F	Cr+Md	Microscribe		Ad	X	X			X
12112	*Cebus*	*apella*	AIM	m	D	F	Cr+Md	Microscribe		Ad	X	X			X
9887	*Cercocebus*	*torquatus*	AIM	f	D	F	Cr+Md	µCT (voxel size: 74 µm)	70kv/110ma	Sa	X	X			X
12755	*Cercopithecus*	*campbelli*	AIM	m	D	F	Cr+Md	Microscribe		Ad	X	X			X

Appendix 1: list of the extant specimens used in the study (continued)

N°	Genus	Species	Prov.	S	AP	MD	Cond	Protocol	Energy	Age	Used in Chapters:				
											2	3	4	5	6
12757	*Cercopithecus*	*campbelli*	AIM	m	D	F	Cr+Md	Microscribe		Ad	X	X			X
12763	*Cercopithecus*	*campbelli*	AIM	m	D	F	Cr+Md	Microscribe		Ad	X	X			X
12878	*Cercopithecus*	*campbelli*	AIM	f	D	F	Cr+Md	Microscribe		Ad	X	X			X
12882	*Cercopithecus*	*campbelli*	AIM	f	D	F	Cr+Md	Microscribe		Ad	X	X			X
10647	*Cercopithecus*	*mona*	AIM	f	D	F	Cr+Md	Microscribe		Ad	X	X			X
12213	*Cercopithecus*	*mona*	AIM	m	D	F	Cr+Md	µCT (voxel size: 74 µm)	70kv/110ma	Ad	X	X			X
2002_87	*Cheirogaleus*	*major*	MNHN	?	N	F	Cr+Md	µCT (voxel size: 36 µm)	70kv/110ma	Ad	X	X	X	X	X
1932_3362	*Cheirogaleus*	*major*	MNHN	m	N	F	Cr+Md	µCT (voxel size: 50 µm)	70kv/110ma	Ad	X	X	X	X	X
1940-1202	*Cheirogaleus*	*major*	MNHN	N	N	F	Cr+Md	µCT (voxel size: 36 µm)	70kv/110ma	Ad	X	X	X	X	X
8128	*Cheirogaleus*	*medius*	AIM	F	N	F	Cr+Md	µCT (voxel size: 74 µm)	50kv/110ma	Ad	X	X	X	X	X
1986-425	*Cheirogaleus*	*medius*	AIM	m	N	F	Cr+Md	µCT (voxel size: 36 µm)	70kv/110ma	Ad	X	X	X	X	X
1986-428	*Cheirogaleus*	*medius*	AIM	m	N	F	Cr+Md	µCT (voxel size: 36 µm)	70kv/110ma	Ad	X	X	X	X	X
10911	*Chiropotes*	*satanas*	AIM	f	D	F	Cr+Md	µCT (voxel size: 74 µm)	70kv/110ma	Ad	X	X	X	X	X
6812	*Chlorocebus*	*aethiops*	AIM	f	D	F	Cr+Md	µCT (voxel size: 74 µm)	70kv/110ma	Ad	X	X	X	X	X
/	*Daubentonia*	*madagascar-iensis*	ISEM	?	N	I	Cr+Md	µCT Synchrotron light (voxel size: 60 µm)ID19	40kev	Ad	X		X		
/	*Eulemur*	*fulvus*	ISEM	?	C	L	Cr+Md	µCT Synchrotron light (voxel size: 60 µm)ID19	40kev	Sa	X	X	X	X	X
1962_2776	*Eulemur*	*fulvus*	MNHN	m	C	L	Cr+Md	Microscribe		Ad	X	X	X	X	X
5053	*Eulemur*	*fulvus*	AIM	f	C	L	Cr+Md	Microscribe		Ad	X	X	X	X	X
5054	*Eulemur*	*fulvus*	AIM	m	C	L	Cr+Md	Microscribe		Ad	X	X	X	X	X
10598	*Eulemur*	*fulvus*	AIM	?	C	L	Cr+Md	Microscribe		Ad	X	X	X	X	X
10603	*Eulemur*	*fulvus*	AIM	?	C	L	Cr+Md	Microscribe		Ad	X	X	X	X	X
10608	*Eulemur*	*fulvus*	AIM	?	C	L	Cr+Md	Microscribe		Ad	X	X	X	X	X
1214	*Eulemur*	*mongoz*	MNHN	f	C	F	Cr+Md	µCT (voxel size: 74 µm)	70kv/110ma	Ad	X	X	X	X	X
1962-2757	*Eulemur*	*mongoz*	MNHN	?	C	F	Cr+Md	Microscribe		Ad	X	X	X	X	X
1932-3337	*Eulemur*	*rubriventer*	MNHN	f	C	F	Cr+Md	Microscribe		Ad	X	X	X	X	X
10599	*Eulemur*	*rubriventer*	AIM	?	C	F	Cr+Md	µCT (voxel size: 74 µm)	70kv/110ma	Ad	X	X	X	X	X
7712	*Euoticus*	*elegantulus*	AIM	?	N	G	Cr+Md	µCT Synchrotron light (voxel size: 45.71 µm)ID17	40 kev	Ad	X	X	X		X
7624	*Euoticus*	*elegantulus*	AIM	f	N	G	Cr+Md	Microscribe		Ad	X	X	X		X
7655	*Euoticus*	*elegantulus*	AIM	?	N	G	Cr+Md	Microscribe		Ad	X	X	X		X
7663	*Euoticus*	*elegantulus*	AIM	?	N	G	Cr+Md	Microscribe		Ad	X	X	X		X
7762	*Euoticus*	*elegantulus*	AIM	m	N	G	Cr+Md	Microscribe		Ad	X	X	X		X
12263	*Euoticus*	*elegantulus*	AIM	?	N	G	Cr+Md	µCT (voxel size: 74 µm)	70kv/110ma	Ad	X	X	X		X
7925	*Galago*	*alleni*	AIM	?	N	F	Cr+Md	µCT Synchrotron light (voxel size: 45.71 µm)ID17	40 kev	Ad	X	X	X		X
7634	*Galago*	*alleni*	AIM	?	N	F	Cr+Md	µCT (voxel size: 74 µm)	70kv/110ma	Ad	X	X	X		X
6619	*Galago*	*alleni*	AIM	?	N	F	Cr+Md	µCT (voxel size: 74 µm)	70kv/110ma	Ad	X	X	X		X
7930	*Galago*	*senegalensis*	AIM	?	N	I	Cr+Md	µCT Synchrotron lightID17 (voxel size: 45.71 µm)	40 kev	Ne				X	X
6 643	*Galago*	*senegalensis*	AIM	?	N	I	Cr+Md	µCT (voxel size: 50 µm)	50kv/110ma	Ne				X	X
8190	*Galago*	*senegalensis*	AIM	?	N	I	Cr+Md	µCT (voxel size: 50 µm)	50kv/110ma	Ne				X	X

Appendix 1: list of the extant specimens used in the study (continued)

N°	Genus	Species	Prov.	S	AP	MD	Cond	Protocol	Energy	Age	Used in Chapters:				
											2	3	4	5	6
7966	*Galago*	*senegalensis*	AIM	?	N	I	Cr+Md	µCT (voxel size: 60 µm)	50kv/110ma	In				X	X
1982-770	*Galago*	*senegalensis*	MNHN	?	N	I	Cr+Md	µCT (voxel size: 74 µm)	70kv/110ma	In				X	X
7983	*Galago*	*senegalensis*	AIM	?	N	I	Cr+Md	µCT (voxel size: 60 µm)	50kv/110ma	In				X	X
8025	*Galago*	*senegalensis*	AIM	?	N	I	Cr+Md	µCT (voxel size: 74 µm)	50kv/110ma	Sa				X	X
6591	*Galago*	*senegalensis*	AIM	m	N	I	Cr+Md	µCT Synchrotron light (voxel size: 45.71 µm)ID17	40 kev	Ad	X	X	X	X	X
8152	*Galago*	*senegalensis*	AIM	f	N	I	Cr+Md	Microscribe		Ad	X	X	X		
10610	*Galago*	*senegalensis*	AIM	m	N	I	Cr+Md	µCT (voxel size: 74 µm)	70kv/110ma	Ad	X	X	X	X	X
10611	*Galago*	*senegalensis*	AIM	m	N	I	Cr+Md	Microscribe		Ad	X	X	X		
10615	*Galago*	*senegalensis*	AIM	m	N	I	Cr+Md	µCT (voxel size: 74 µm)	70kv/110ma	Ad	X	X	X	X	X
9709	*Galago*	*senegalensis*	AIM	?	N	I	Cr+Md	µCT (voxel size: 74 µm)	70kv/110ma	Ad	X	X	X	X	X
6714	*Galago*	*senegalensis*	AIM	?	N	I	Cr+Md	µCT (voxel size: 74 µm)	70kv/110ma	Ad				X	
6768	*Galago*	*senegalensis*	AIM	?	N	I	Cr+Md	µCT (voxel size: 74 µm)	70kv/110ma	Ad				X	
6635	*Galago*	*senegalensis*	AIM	?	N	I	Cr+Md	µCT (voxel size: 74 µm)	70kv/110ma	Ad				X	
6535	*Galagoides*	*demidoff*	AIM	?	N	I	Cr+Md	µCT Synchrotron light (voxel size: 45.71 µm)ID17	40 kev	Ad	X	X	X		X
2002-83	*Hapalemur*	*griseus*	MNHN	?	D	L	Cr+Md	Microscribe		Ad	X	X	X	X	X
5055	*Hapalemur*	*griseus*	AIM	?	D	L	Cr+Md	µCT (voxel size: 74 µm)	70kv/110ma	Ad	X	X	X	X	X
AS1532	*Hylobates*	*lar*	AIM	m	D	F	Cr+Md	Microscribe		Ad	X	X			X
AS1538	*Hylobates*	*lar*	AIM	m	D	F	Cr+Md	Microscribe		Ad	X	X			X
AS1559	*Hylobates*	*lar*	AIM	f	D	F	Cr+Md	Microscribe		Ad	X	X			X
AS1574	*Hylobates*	*lar*	AIM	f	D	F	Cr+Md	Microscribe		Ad	X	X			X
AS919	*Indri*	*indri*	AIM	?	D	L	Cr+Md	µCT (voxel size: 74 µm)	70kv/110ma	Ad	X	X	X	X	X
10584	*Indri*	*indri*	AIM	?	D	L	Cr+Md	Microscribe		Ad	X	X	X	X	X
1962-2028	*Indri*	*indri*	MNHN	f	D	L	Cr+Md	Microscribe		Ad	X	X	X	X	X
10663	*Lagothrix*	*infumata*	AIM	f	D	F	Cr+Md	µCT (voxel size: 74 µm)	70kv/110ma	Ad	X	X			X
9791	*Lagothrix*	*lagothricha*	AIM	f	D	F	Cr+Md	Microscribe		Ad	X	X			X
9989	*Lagothrix*	*lagothricha*	AIM	m	D	F	Cr+Md	Microscribe		Ad	X	X			X
10359	*Lemur*	*catta*	AIM	?	D	F	Cr+Md	µCT (voxel size: 60 µm)	70kv/110ma	Ne				X	X
15821	*Lemur*	*catta*	BERL	m	D	F	Cr+Md	µCT (voxel size: 60 µm)	70kv/110ma	Ne				X	X
15869	*Lemur*	*catta*	BERL	m	D	F	Cr+Md	µCT (voxel size: 74 µm)	70kv/110ma	In				X	X
10522	*Lemur*	*catta*	AIM	?	D	F	Cr+Md	CT slice thickness: 0.5mm		In				X	X
8866	*Lemur*	*catta*	AIM	?	D	F	Cr+Md	CT slice thickness: 0.5mm		In				X	X
102840	*Lemur*	*catta*	AIM	?	D	F	Cr+Md	CT slice thickness: 0.5mm		Juv				X	X
9602	*Lemur*	*catta*	AIM	?	D	F	Cr+Md	CT slice thickness: 0.5mm		Juv				X	X
1871-254	*Lemur*	*catta*	AIM	?	D	F	Cr+Md	µCT (voxel size: 74 µm)	70kv/110ma	Juv				X	X
8368	*Lemur*	*catta*	AIM	?	D	F	Cr+Md	µCT (voxel size: 60 µm)	70kv/110ma	Sa				X	X
11051	*Lemur*	*catta*	AIM	?	D	F	Cr+Md	CT slice thickness: 0.5mm		Sa				X	X
10601	*Lemur*	*catta*	AIM	?	D	F	Cr+Md	CT slice thickness: 0.4mm		Sa				X	X
12365	*Lemur*	*catta*	AIM	?	D	F	Cr+Md	µCT (voxel size: 74 µm)	70kv/110ma	Ad	X	X	X	X	X

Appendix 1: list of the extant specimens used in the study (continued)

N°	Genus	Species	Prov.	S	AP	MD	Cond	Protocol	Energy	Age	Used in Chapters:				
											2	3	4	5	6
10600	*Lemur*	*catta*	AIM	m	D	F	Cr+Md	CT slice thickness: 0.4mm		Ad	X	X	X	X	X
8598	*Lemur*	*catta*	AIM	m	D	F	Cr+Md	µCT (voxel size: 60 µm)	70kv/110ma	Ad	X	X	X	X	X
9601	*Lemur*	*catta*	AIM	f	D	F	Cr+Md	µCT (voxel size: 74 µm)	70kv/110ma	Ad	X	X	X	X	X
1916-83	*Lemur*	*Catta*	MNHN	?	D	F	Cr+Md	Microscribe		Ad	X	X	X	X	X
11070	*Leontopithecus*	*rosalia*	AIM	?	D	F	Cr+Md	µCT (voxel size: 74 µm)	70kv/110ma	Ad	X	X	X	X	X
2002-6	*Lepilemur*	*dorsalis*	MNHN	f	N	L	Cr+Md	µCT (voxel size: 50 µm)	70kv/110ma	Ad	X	X	X	X	X
2002-7	*Lepilemur*	*dorsalis*	MNHN	M	N	L	Cr+Md	µCT (voxel size: 74 µm)	70kv/110ma	Ad	X	X	X	X	X
5058	*Lepilemur*	*leucopus*	AIM	f	N	L	Cr+Md	µCT Synchrotron light (voxel size: 45.71 µm)ID17	40 kev	Ad	X	X	X	X	X
5059	*Lepilemur*	*leucopus*	AIM	m	N	L	Cr+Md	µCT (voxel size: 74 µm)	70kv/110ma	Ad	X	X	X	X	X
2002-3	*Lepilemur*	*mustelinus*	MNHN	f	N	L	Cr+Md	µCT (voxel size: 74 µm)	70kv/110ma	Ad	X	X	X	X	X
1962_2721	*Lepilemur*	*ruficaudatus*	AIM	m	N	L	Cr+Md	µCT (voxel size: 74 µm)	70kv/110ma	Inf				X	X
1962_2716	*Lepilemur*	*ruficaudatus*	AIM	m	N	L	Cr+Md	µCT (voxel size: 74 µm)	70kv/110ma	Juv				X	X
1961_267f	*Lepilemur*	*ruficaudatus*	AIM	m	N	L	Cr+Md	µCT (voxel size: 74 µm)	70kv/110ma	Juv				X	X
1962_2717	*Lepilemur*	*ruficaudatus*	AIM	m	N	L	Cr+Md	µCT (voxel size: 74 µm)	70kv/110ma	Sa				X	X
1962_2718	*Lepilemur*	*ruficaudatus*	AIM	m	N	L	Cr+Md	µCT (voxel size: 74 µm)	70kv/110ma	Sa				X	X
1962_2733	*Lepilemur*	*ruficaudatus*	AIM	m	N	L	Cr+Md	µCT (voxel size: 74 µm)	70kv/110ma	Sa				X	X
1962-2728	*Lepilemur*	*ruficaudatus*	AIM	m	N	L	Cr+Md	µCT (voxel size: 74 µm)	70kv/110ma	Ad				X	X
1962-2719	*Lepilemur*	*ruficaudatus*	AIM	m	N	L	Cr+Md	µCT (voxel size: 74 µm)	70kv/110ma	Ad				X	X
1891-6	*Lepilemur*	*ruficaudatus*	AIM	?	N	L	Cr+Md	µCT (voxel size: 74 µm)	70kv/110ma	Ad	X	X	X	X	X
1891-696	*Lepilemur*	*ruficaudatus*	AIM	m	N	L	Cr+Md	µCT (voxel size: 74 µm)	70kv/110ma	Ad	X	X	X	X	X
10614	*Lepilemur*	*ruficaudatus*	AIM	m	N	L	Cr+Md	µCT (voxel size: 74 µm)	70kv/110ma	Ad	X	X	X	X	X
11054	*Lepilemur*	*ruficaudatus*	AIM	f	N	L	Cr+Md	µCT (voxel size: 50 µm)	70kv/110ma	Ad	X	X	X	X	X
2002_17	*Lepilemur*	*ruficaudatus*	MNHN	m	N	L	Cr+Md	Microscribe		Ad	X	X	X	X	X
10590	*Loris*	*tardigradus*	AIM	m	N	I	Cr+Md	Microscribe		Ad	X	X	X	X	X
11056	*Loris*	*tardigradus*	AIM	?	N	I	Cr+Md	µCT (voxel size: 74 µm)	70kv/110ma	Ad	X	X	X		X
11057	*Loris*	*tardigradus*	AIM	f	N	I	Cr+Md	Microscribe		Ad	X	X	X		X
9950	*Loris*	*tardigradus*	AIM	?	N	I	Cr+Md	µCT Synchrotron light (voxel size: 45.71 µm)ID17	40 kev	Ad	X	X	X		X
10628	*Macaca*	*arctoides*	AIM	f	D	F	Cr+Md	Microscribe		Ad	X	X			X
12465	*Macaca*	*fascicularis*	AIM	m	D	F	Cr+Md	Microscribe		Ad	X	X			X
12466	*Macaca*	*fascicularis*	AIM	f	D	F	Cr+Md	Microscribe		Ad	X	X			X
12469	*Macaca*	*fascicularis*	AIM	m	D	F	Cr+Md	Microscribe		Ad	X	X			X
12475	*Macaca*	*fascicularis*	AIM	m	D	F	Cr+Md	Microscribe		Ad	X	X			X
PAL34	*Macaca*	*fascicularis*	AIM	m	D	F	Cr+Md	Microscribe		Ad	X	X			X
AS2063	*Macaca*	*fuscata*	AIM	f	D	F	Cr+Md	Microscribe		Ad	X	X			X
AS2064	*Macaca*	*fuscata*	AIM	m	D	F	Cr+Md	Microscribe		Ad	X	X			X
AS8828	*Macaca*	*fuscata*	AIM	m	D	F	Cr+Md	Microscribe		Ad	X	X			X
AS1230	*Macaca*	*mulatta*	AIM	f	D	F	Cr+Md	Microscribe		Ad	X	X			X
AS1572	*Macaca*	*mulatta*	AIM	f	D	F	Cr+Md	Microscribe		Ad	X	X			X

Appendix 1: list of the extant specimens used in the study (continued)

N°	Genus	Species	Prov.	S	AP	MD	Cond	Protocol	Energy	Age	Used in Chapters:				
											2	3	4	5	6
AS1589	*Macaca*	*mulatta*	AIM	f	D	F	Cr+Md	Microscribe		Ad	X	X			X
AS2197	*Macaca*	*mulatta*	AIM	f	D	F	Cr+Md	Microscribe		Ad	X	X			X
6530	*Macaca*	*mulatta*	AIM	m	D	F	Cr+Md	Microscribe		Ad	X	X			X
7082	*Macaca*	*mulatta*	AIM	f	D	F	Cr+Md	Microscribe		Ad	X	X			X
8825	*Macaca*	*nemestrina*	AIM	m	D	F	Cr+Md	Microscribe		Ad	X	X			X
977b	*Microcebus*	*murinus*	MNHN	?	N	I	Cr+Md	µCT (voxel size: 36 µm)	50kv/110ma	Neo				X	X
Mtp1	*Microcebus*	*murinus*	MTP	m	N	I	Cr+Md	µCT Synchrotron light (voxel size: 30 µm)ID19	40 kev	Neo				X	X
153c	*Microcebus*	*murinus*	BRUN	?	N	I	Cr+Md	µCT (voxel size: 36 µm)	50kv/110ma	Inf				X	X
109	*Microcebus*	*murinus*	BRUN	?	N	I	Cr+Md	µCT (voxel size: 36 µm)	50kv/110ma	Inf				X	X
108	*Microcebus*	*murinus*	BRUN	?	N	I	Cr+Md	µCT (voxel size: 36 µm)	50kv/110ma	Inf				X	X
112	*Microcebus*	*murinus*	BRUN	?	N	I	Cr+Md	µCT (voxel size: 50 µm)	50kv/110ma	Juv				X	X
113	*Microcebus*	*murinus*	BRUN	?	N	I	Cr+Md	µCT (voxel size: 36 µm)	50kv/110ma	Sa				X	X
110	*Microcebus*	*murinus*	BRUN	?	N	I	Cr+Md	µCT (voxel size: 50 µm)	50kv/110ma	Sa				X	X
111	*Microcebus*	*murinus*	BRUN	?	N	I	Cr+Md	µCT (voxel size: 50 µm)	50kv/110ma	Sa				X	X
5065-10	*Microcebus*	*murinus*	AIM	f	N	I	Cr+Md	µCT (voxel size: 36 µm)	70kv/110ma	Ad	X	X	X	X	X
5065-12	*Microcebus*	*murinus*	AIM	f	N	I	Cr+Md	µCT (voxel size: 36 µm)	70kv/110ma	Ad	X	X	X	X	X
AS1815	*Microcebus*	*murinus*	AIM	f	N	I	Cr+Md	µCT (voxel size: 36 µm)	50kv/110ma	Ad	X	X	X	X	X
AS1816	*Microcebus*	*murinus*	AIM	f	N	I	Cr+Md	µCT (voxel size: 36 µm)	50kv/110ma	Ad	X	X	X	X	X
AS1818	*Microcebus*	*murinus*	AIM	f	N	I	Cr+Md	µCT (voxel size: 36 µm)	50kv/110ma	Ad	X	X	X	X	X
12542	*Mirza*	*coquereli*	AIM	f	N	F	Cr+Md	µCT (voxel size: 74 µm)	70kv/110ma	Ad	X	X	X	X	X
1869-198	*Mirza*	*coquereli*	MNHN	?	N	F	Cr+Md	µCT (voxel size: 36 µm)	70kv/110ma	Ad	X	X	X	X	X
1962-83	*Mirza*	*coquereli*	MNHN	?	N	F	Cr+Md	µCT (voxel size: 36 µm)	70kv/110ma	Ad	X	X	X	X	X
6833	*Miopithecus*	*talapoin*	AIM	f	D	F	Cr+Md	Microscribe		Ad	X	X			X
6834	*Miopithecus*	*talapoin*	AIM	f	D	F	Cr+Md	Microscribe		Ad	X	X			X
6990	*Miopithecus*	*talapoin*	AIM	m	D	F	Cr+Md	Microscribe		Ad	X	X			X
6991	*Miopithecus*	*talapoin*	AIM	f	D	F	Cr+Md	Microscribe		Ad	X	X			X
7602	*Miopithecus*	*talapoin*	AIM	m	D	F	Cr+Md	µCT (voxel size: 74 µm)	70kv/110ma	Ad	X	X			X
AS484	*Nasalis*	*larvatus*	AIM	f	D	L	Cr+Md	µCT (voxel size: 74 µm)	70kv/110ma	Ad	X	X			X
7726	*Nycticebus*	*coucang*	BERL	?	N	F	Cr+Md	µCT (voxel size: 74 µm)	70kv/110ma	Neo				X	X
326	*Nycticebus*	*coucang*	BERL	?	N	F	Cr+Md	µCT (voxel size: 74 µm)	70kv/110ma	Inf				X	X
10587	*Nycticebus*	*coucang*	AIM	?	N	F	Cr+Md	µCT (voxel size: 74 µm)	70kv/110ma	Juv				X	X
8596	*Nycticebus*	*coucang*	AIM	?	N	F	Cr+Md	µCT (voxel size: 74 µm)	70kv/110ma	Sa				X	X
8674	*Nycticebus*	*coucang*	AIM	?	N	F	Cr+Md	µCT (voxel size: 74 µm)	70kv/110ma	Sa				X	X
10586	*Nycticebus*	*coucang*	AIM	f	N	F	Cr+Md	µCT (voxel size: 74 µm)	70kv/110ma	Ad	X	X	X	X	X
AS10593	*Nycticebus*	*coucang*	AIM	f	N	F	Cr+Md	µCT (voxel size: 74 µm)	70kv/110ma	Ad	X	X	X	X	X
AS10594	*Nycticebus*	*coucang*	AIM	m	N	F	Cr+Md	µCT (voxel size: 74 µm)	70kv/110ma	Ad	X	X	X	X	X
1841	*Otolemur*	*crassicau-datus*	AIM	m	N	G	Cr+Md	µCT Synchrotron light (voxel size: 45.71 µm)ID17	40 kev	Ad	X	X	X		X
10588	*Otolemur*	*crassicau-datus*	AIM	?	N	G	Cr+Md	Microscribe		Ad	X	X	X		X
10612	*Otolemur*	*crassicau-datus*	AIM	f	N	G	Cr+Md	Microscribe		Ad	X	X	X		X

Appendix 1: list of the extant specimens used in the study (continued)

N°	Genus	Species	Prov.	S	AP	MD	Cond	Protocol	Energy	Age	Used in Chapters:				
											2	3	4	5	6
AS921	*Otolemur*	*crassicaudatus*	AIM	?	N	G	Cr+Md	µCT (voxel size: 74 µm)	70kv/110ma	Ad	X	X	X		X
AS1569	*Otolemur*	*crassicaudatus*	AIM	?	N	G	Cr+Md	µCT (voxel size: 74 µm)	70kv/110ma	Ad	X	X	X		X
9974	*Otolemur*	*garnetti*	AIM	?	N	F	Cr+Md	µCT (voxel size: 50 µm)	70kv/110ma	Neo				X	
AS-327	*Otolemur*	*garnetti*	AIM	?	N	F	Cr+Md	µCT (voxel size: 74 µm)	70kv/110ma	Inf				X	
9984	*Otolemur*	*garnetti*	AIM	?	N	F	Cr+Md	µCT (voxel size: 74 µm)	70kv/110ma	Ad				X	
12251	*Otolemur*	*garnetti*	AIM	?	N	F	Cr+Md	µCT (voxel size: 50 µm)	70kv/110ma	Ad				X	
AS926	*Otolemur*	*garnetti*	AIM	?	N	F	Cr+Md	µCT Synchrotron light (voxel size: 45.71 µm)ID17	40 kev	Ad	X	X	X	X	X
AS790	*Otolemur*	*sp.*	AIM	?	N	F	Cr+Md	µCT (voxel size: 74 µm)	70kv/110ma	Ad	X	X	X		X
7151	*Perodicticus*	*potto*	AIM	m	N	F	Cr+Md	µCT Synchrotron light (voxel size: 60 µm)ID19	40 kev	Inf				X	X
7031	*Perodicticus*	*potto*	AIM	m	N	F	Cr+Md	µCT Synchrotron light (voxel size: 45.71 µm)ID17	40 kev	Inf				X	X
7076	*Perodicticus*	*potto*	AIM	m	N	F	Cr+Md	µCT Synchrotron light (voxel size: 60 µm)ID19	40 kev	Inf				X	X
6976	*Perodicticus*	*potto*	AIM	m	N	F	Cr+Md	µCT Synchrotron light (voxel size: 60 µm)ID19	40 kev	Inf				X	X
7030	*Perodicticus*	*potto*	AIM	m	N	F	Cr+Md	µCT Synchrotron light (voxel size: 45.71 µm)ID17	40 kev	Juv				X	X
7046	*Perodicticus*	*potto*	AIM	m	N	F	Cr+Md	µCT Synchrotron light (voxel size: 45.71 µm)ID17	40 kev	Sa				X	X
7192	*Perodicticus*	*Potto*	AIM	m	N	F	Cr+Md	µCT Synchrotron light (voxel size: 45.71 µm)ID17	40 kev	Sa				X	X
AS1833	*Perodicticus*	*potto*	AIM	f	N	F	Cr+Md	µCT Synchrotron light (voxel size: 45.71 µm)ID17	40 kev	Ad	X	X	X	X	X
7425	*Perodicticus*	*potto*	AIM	?	N	F	Cr+Md	µCT Synchrotron light (voxel size: 60 µm)ID19	40 kev	Ad	X	X	X	X	X
6620	*Perodicticus*	*potto*	AIM	m	N	F	Cr+Md	µCT (voxel size: 74 µm)	70kv/110ma	Ad	X	X	X	X	X
7014	*Perodicticus*	*potto*	AIM	f	N	F	Cr+Md	µCT (voxel size: 74 µm)	70kv/110ma	Ad	X	X	X	X	X
7029	*Perodicticus*	*potto*	AIM	f	N	F	Cr+Md	µCT (voxel size: 74 µm)	70kv/110ma	Ad	X	X	X	X	X
7050	*Perodicticus*	*potto*	AIM	f	N	F	Cr+Md	µCT (voxel size: 74 µm)	70kv/110ma	Sa	X	X	X	X	X
7054	*Perodicticus*	*Potto*	AIM	m	N	F	Cr+Md	µCT (voxel size: 74 µm)	70kv/110ma	Sa	X	X	X	X	X
1962-2712	*Phaner*	*furcifer*	MNHN	?	N	G	Cr+Md	µCT (voxel size: 36 µm)	70kv/110ma	Ad	X	X	X	X	X
1912-8	*Phaner*	*furcifer*	MNHN	?	N	G	Cr+Md	µCT (voxel size: 36 µm)	70kv/110ma	Ad	X	X	X	X	X
2880-2535	*Phaner*	*furcifer*	MNHN	?	N	G	Cr+Md	µCT (voxel size: 50 µm)	70kv/110ma	Ad	X	X	X	X	X
8608	*Pithecia*	*pithecia*	AIM	f	D	F	Cr+Md	µCT (voxel size: 74 µm)	70kv/110ma	Ad	X	X			X
10804	*Pithecia*	*pithecia*	AIM	m	D	F	Cr+Md	Microscribe		Ad	X	X			X
8599	*Pithecia*	*pithecia*	AIM	?	D	F	Cr+Md	Microscribe		Ad	X	X			X
10751	*Presbytis*	*comata*	AIM	f	D	L	Cr+Md	µCT (voxel size: 74 µm)	70kv/110ma	Ad	X	X			X
2811	*Propithecus*	*diadema*	MNHN	?	D	L	Cr	µCT (voxel size: 74 µm)	70kv/110ma	Neo				X	X
1909_264	*Propithecus*	*diadema*	MNHN	?	D	L	Cr+Md	µCT (voxel size: 74 µm)	70kv/110ma	Inf				X	X
1909_265	*Propithecus*	*diadema*	MNHN	?	D	L	Cr+Md	µCT (voxel size: 74 µm)	70kv/110ma	Inf				X	X
1892_664	*Propithecus*	*diadema*	MNHN	?	D	L	Cr+Md	µCT (voxel size: 74 µm)	70kv/110ma	Juv				X	X
10597	*Propithecus*	*diadema*	MNHN	?	D	L	Cr+Md	µCT (voxel size: 74 µm)	70kv/110ma	Sub				X	X
1879_341	*Propithecus*	*diadema*	MNHN	?	D	L	Cr+Md	µCT (voxel size: 74 µm)	70kv/110ma	Sub				X	X
7255	*Propithecus*	*diadema*	AIM	?	D	L	Cr+Md	µCT (voxel size: 74 µm)	70kv/110ma	Ad	X	X	X	X	X
10597	*Propithecus*	*diadema*	AIM	?	D	L	Cr+Md	Microscribe		Ad	X	X	X	X	X

Appendix 1: list of the extant specimens used in the study (continued)

N°	Genus	Species	Prov.	S	AP	MD	Cond	Protocol	Energy	Age	Used in Chapters:				
											2	3	4	5	6
1962-2810	*Propithecus*	*diadema*	MNHN	m	D	L	Cr+Md	Microscribe		Ad	X	X	X	X	X
1912_28	*Propithecus*	*verreauxi*	AIM	?	D	L	Cr+Md	µCT (voxel size: 74 µm)	70kv/110ma	Inf				X	X
1854_1261	*Propithecus*	*verreauxi*	AIM	?	D	L	Cr+Md	µCT (voxel size: 74 µm)	70kv/110ma	Juv				X	X
1909_267	*Propithecus*	*verreauxi*	AIM	?	D	L	Cr+Md	µCT (voxel size: 74 µm)	70kv/110ma	Juv				X	X
2005_255	*Propithecus*	*verreauxi*	AIM	?	D	L	Cr+Md	µCT (voxel size: 74 µm)	70kv/110ma	Sa				X	X
1962_2833	*Propithecus*	*verreauxi*	AIM	?	D	L	Cr+Md	µCT (voxel size: 74 µm)	70kv/110ma	Sa				X	X
1909_268	*Propithecus*	*verreauxi*	AIM	?	D	L	Cr+Md	µCT (voxel size: 74 µm)	70kv/110ma	Sa				X	X
10606	*Propithecus*	*verreauxi*	AIM	?	D	L	Cr+Md	Microscribe		Ad	X	X	X	X	X
AS131	*Propithecus*	*verreauxi*	AIM	?	D	L	Cr+Md	µCT (voxel size: 74 µm)	70kv/110ma	Ad	X	X	X	X	X
10607	*Propithecus*	*verreauxi*	AIM	?	D	L	Cr+Md	Microscribe		Ad	X	X	X	X	X
5068	*Propithecus*	*verreauxi*	AIM	m	D	L	Cr+Md	Microscribe		Ad	X	X	X	X	X
1730	*Pseudopotto*	*martini*	AIM	m	?	?	Cr+Md	µCT (voxel size: 50 µm)	70kv/110ma	Ad	X	X	X		X
6698	*Pseudopotto*	*martini*	AIM	f	?	?	Cr+Md	µCT (voxel size: 50 µm)	70kv/110ma	Ad	X	X	X		X
AS1263	*Pygathrix*	*sp.*	AIM	m	D	L	Cr+Md	Microscribe		Ad	X	X			X
10772	*Pygathrix*	*Nemaeus*	AIM	f	D	L	Cr+Md	µCT (voxel size: 74 µm)	70kv/110ma	Ad	X	X			X
11043	*Saguinus*	*leucopus*	AIM	m	D	F	Cr+Md	µCT (voxel size: 74 µm)	70kv/110ma	Ad	X	X			X
9159	*Saimiri*	*sciureus*	AIM	f	D	I	Cr+Md	µCT (voxel size: 74 µm)	70kv/110ma	Ad	X	X			X
AS164	*Semnopithecus*	*entellus*	AIM	f	D	L	Cr+Md	Microscribe		Ad	X	X			X
AS1902	*Semnopithecus*	*entellus*	AIM	f	D	L	Cr+Md	Microscribe		Ad	X	X			X
17197	*Tarsius*	*bancanus*	BERL	?	N	I	Cr+Md	µCT (voxel size: 36 µm)	50kv/110ma	Neo				X	
482	*Tarsius*	*bancanus*	BERL	?	N	I	Cr+Md	µCT (voxel size: 50 µm)	50kv/110ma	Neo				X	
88793	*Tarsius*	*bancanus*	BERL	?	N	I	Cr+Md	µCT (voxel size: 50 µm)	50kv/110ma	Inf				X	
84055	*Tarsius*	*bancanus*	BERL	?	N	I	Cr+Md	µCT (voxel size: 50 µm)	50kv/110ma	Juv				X	
84052	*Tarsius*	*bancanus*	BERL	?	N	I	Cr+Md	µCT (voxel size: 50 µm)	50kv/110ma	Juv				X	
84054	*Tarsius*	*bancanus*	BERL	?	N	I	Cr+Md	µCT (voxel size: 50 µm)	50kv/110ma	Sa				X	
2892	*Tarsius*	*bancanus*	BERL	?	N	I	Cr+Md	µCT (voxel size: 50 µm)	50kv/110ma	Sa				X	
1035	*Tarsius*	*bancanus*	BERL	?	N	I	Cr+Md	µCT (voxel size: 50 µm)	50kv/110ma	Sa				X	
PAL44	*Tarsius*	*bancanus*	AIM	f	N	I	Cr+Md	µCT (voxel size: 36 µm)	70kv/110ma	Ad	X	X		X	
1838	*Tarsius*	*bancanus*	AIM				Cr	µCT (voxel size: 74 µm)	70kv/110ma	Ad	X	X			
AS1732	*Tarsius*	*syrichta*	AIM	f	N	I	Cr+Md	µCT (voxel size: 78 µm)	50kv/300ma	Ad	X	X			
AS1821	*Tarsius*	*spectrum*	AIM	f	N	I	Cr+Md	µCT (voxel size: 36 µm)	70kv/110ma	Ad	X	X			
AS1202	*Tarsius*	*sp*	AIM	?	N	I	Cr+Md	µCT (voxel size: 36 µm)	70kv/110ma	Ad	X	X			
AS1558	*Trachypithecus*	*cristatus*	AIM	m	D	L	Cr+Md	Microscribe		Ad	X	X			
10736	*Trachypithecus*	*vetulus*	AIM	f	D	L	Cr+Md	µCT (voxel size: 74 µm)	70kv/110ma	Ad	X	X			
AS805	*Varecia*	*variegata*	AIM	m	D	F	Cr+Md	µCT (voxel size: 74 µm)	70kv/110ma	Ad	X	X	X	X	X
10604	*Varecia*	*variegata*	AIM	?	D	F	Cr+Md	µCT (voxel size: 74 µm)	70kv/110ma	Ad	X	X	X	X	X

Appendix 2: List of the fossils included in the analyses, and the corresponding data acquisition protocol. *: following Lanèque (1992 a, b). **: Data courtesy: Pof. A. Rosenberger. Bordeaux: Musée d'Histoire Naturelle de Bordeaux. MNHN: Museum National d'Histoire Naturelle. ISEM : Institut des Sciences de l'Evolution de Montpellier. AIM: Anthropologisches Institut und Museum. TMM: Texas Memorial Museum. Montauban: Musée d'Histoire Naturelle de Montauban. SI: Smithsonian Institution. AMNH: American Museum of Natural History. Marseille: Faculté des Sciences de Marseille.

N°	Genus	Species	Prov.	Cond	Protocol	Energy	Used in chapter				
							2	3	4	5	6
BOR 613	*Paleolemur*	*betillei*	Bordeaux	Cr	µCT Synchrotron light (voxel size: 60 µm) ID19	60 kev					X
MAPHQ 221	*Adapis*	*bruni**	Montauban	Cr	µCT Synchrotron light (voxel size: 60 µm)ID19	60 kev					X
PQ1700	*Adapis*	*sp.*	Marseille	Cr	Microscribe 3D on a cast						X
Cambridge	*Adapis*	*sp.*	AIM	Cr	µCT of a cast, 74 µm						X
QU 11002	*Leptadapis*	*magnus*	MNHN	Cr	µCT of a cast, 74µm						X
MAPHQ 210	*Leptadapis*	*sp.*	Montauban	Cr	µCT (voxel size: 74 µm)	70 kv/110ma					X
QU 10870	*Lepdadapis*	*sp.*	MNHN	Cr	Microscribe 3D on the original fossil						X
QU 10875	*Leptadapis*	*sp.*	MNHN	Cr+Md	Microscribe 3D on the original fossil						X
ACQ 209	*Leptadapis*	*sp.*	ISEM	Cr	µCT Synchrotron light (voxel size: 45.71 µm) ID17	70 kev					X
AMNH 127167	*Notharctus*	*tenebrosus*	AMNH	Cr+Md	µCT of a cast, 74 µm						X
USNM21815	*Smilodectes*	*gracilis*	SI	Cr	CT of a cast, slice thickness: 0.5 mm						X
MAPHQ289	*Necrolemur*	*antiquus*	MNHN	Cr	µCT Synchrotron light (voxel size: 30 µm)ID19	60 kev		X			
QQ11060	*Necrolemur*	*antiquus*	MNHN	Cr	Mircoscribe 3D on the original fossil			X			
PR1771	*Microchoerus*	*erinaceus*	ISEM	Cr	µCT (voxel size: 50 µm)	70 kv/110ma		X			
TMM40688-7**	*Rooneyia*	*viejaensis*	TMM	Cr	Laser scan of a cast **			X			

Appendices 3.1-12 : List of the sample used in the ontogenetic series analyses. First sequence: upper teeth. Second sequence: lower teeth. Normal number: deciduous teeth. Roman characters: permanent and replacement teeth. For each specimen, each tooth was examined in order to establish its maturation status. (1/I = crown mineralizing, 2/II crown formed, 3/III tooth erupting, 4/IVtooth fully erupted). Explanations for the dental score index are given in Chapter 5.

Appendix 3.1: *Aotus trivirgatus.*

		Cranium									Mandible									
Specimen	Stage	I1	I2	C	P2	P3	P4	M1	M2	M3	I1	I2	C	P2	P3	P4	M1	M2	M3	Dental score
8 279	Neonate	1	1	1	1	1	1	X	X	X	1	1	1	1	1	X	X	X	X	0
10630	Neonate	2	2	1	1	1	1	X	X	X	2	2	1	1	1	1	X	X	X	0
8446	Infant	4	3	2	3	2	2	I	X	X	4	3	2	3	2	2	X	X	X	0.13
1781	Infant	4	4	4	4	4	4	III	I	X	4	4	4	4	4	4	III	I	X	0.43
1175	Subadult	III	III	4	4	4	4	IV	IV	III	IV	IV	4	4	4	4	IV	IV	IV	0.68
1775	Adult	IV	IV	IV	IV	IV	IV	IV	IV	IV	IV	IV	IV	IV	IV	IV	IV	IV	IV	1
12261	Adult	IV	IV	IV	IV	IV	IV	IV	IV	IV	IV	IV	IV	IV	IV	IV	IV	IV	IV	1
10750	Adult	IV	IV	IV	IV	IV	IV	IV	IV	IV	IV	IV	IV	IV	IV	IV	IV	IV	IV	1
12250	Adult	IV	IV	IV	IV	IV	IV	IV	IV	IV	IV	IV	IV	IV	IV	IV	IV	IV	IV	1
12320	Adult	IV	IV	IV	IV	IV	IV	IV	IV	IV	IV	IV	IV	IV	IV	IV	IV	IV	IV	1
12322	Adult	IV	IV	IV	IV	IV	IV	IV	IV	IV	IV	IV	IV	IV	IV	IV	IV	IV	IV	1
12323	Adult	IV	IV	IV	IV	IV	IV	IV	IV	IV	IV	IV	IV	IV	IV	IV	IV	IV	IV	1

Appendix 3.2: *Tarsius bancanus* (*though dentally adults, the development of the skull is obviously not finished)

		Cranium									Mandible									
Specimen	Stage	I1	I2	C	P2	P3	P4	M1	M2	M3	I1	I2	C	P2	P3	P4	M1	M2	M3	Dental score
17197	Neonate	4/I	4	4	3	4	4	I	I	X	4/II		4/I	3	4	4/I	I	I	X	0.328
482	Neonate	4/I	?	4	3	4	4	I	I	X	4/I		4/I	3	4	4/I	I	I	X	0.328
88793	Infant	4/II	III	4	3	4	4	III	II	X	III		4	3	4	4	II	I	I	0.379
84055	Juvenile	III	III	4	III	4	4	IV	III	I	IV		4	4	4	4	III	X	I	0.534
84052	Juvenile	IV	IV	II	III	4/III	4/III	IV	III	II	IV		III	4	4	4	IV	III	II	0.672
84054	Subadult	IV	IV	IV	IV	III	IV	IV	IV	IV	IV		IV	IV	III	IV	IV	IV	III	0.948
2892	Subadult*	IV	IV	IV	IV	IV	IV	IV	IV	IV	IV		IV	IV	IV	IV	IV	IV	IV	1
1035	Subadult*	IV	IV	IV	IV	IV	IV	IV	IV	IV	IV		IV	IV	IV	IV	IV	IV	IV	1
Pal44	Adult	IV	IV	IV	IV	IV	IV	IV	IV	IV	IV		IV	IV	IV	IV	IV	IV	IV	1
1838	Adult	IV	IV	IV	IV	IV	IV	IV	IV	IV	IV		IV	IV	IV	IV	IV	IV	IV	1

Appendices 3.1-12 : List of the sample used in the ontogenetic series analyses (continued).

Appendix 3.3: *Lemur catta*

		Cranium									Mandible									
Specimen	Stage	I1	I2	C	P2	P3	P4	M1	M2	M3	I1	I2	C	P2	P3	P4	M1	M2	M3	Dental score
10359	Neonate	2	2	2	2	2	1	X	X	X	2	2	2	2	2	2	1	X	X	0
15821	Neonate	2	2	2	2	2	1	X	X	X	2	2	2	2	2	2	1	X	X	0
15869	Infant	3	3	3	2	2	2	1	X	X	3	3	3	2	2	2	2	X	X	0.1
10522	Infant	4?	4?	4	4	4	4	III	X	X	4	4	4	4	4	4	III	X	X	0.433
8866	Infant	4?	4?	4	4	4	4	III	X	X	4	4	4	4	4	4	III	I	X	0.433
102840	Juvenile	4?	4?	4	4	4	4	IV	I	X	4	4	4	4	4	4	IV	II	X	0.467
9602	Juvenile	4?	4?	4	4	4	4	IV	I	X	4	4	4	4	4	4	IV	II	X	0.467
1871-254	Juvenile	4?	4?	4	4	4	4	IV	III	II	III	III	III	4/I	4/I	4	IV	II	II	0.533
8368	Subadult	IV	IV	4	4	4	4	IV	IV	II	IV	IV	IV	4	4	4	IV	IV	II	0.7
11051	Subadult	IV	IV	4	4	4	III	IV	IV	III	IV	IV	IV	4	4	III	IV	IV	III	0.767
10601	Subadult	IV	IV	4	4	4	IV	IV	IV	IV	IV	IV	IV	4	4	IV	IV	IV	IV	0.833
9601	Adult	IV	IV	IV	IV	IV	IV	IV	IV	IV	IV	IV	IV	IV	IV	IV	IV	IV	IV	1
10600	Adult	IV	IV	IV	IV	IV	IV	IV	IV	IV	IV	IV	IV	IV	IV	IV	IV	IV	IV	1
8598	Adult	IV	IV	IV	IV	IV	IV	IV	IV	IV	IV	IV	IV	IV	IV	IV	IV	IV	IV	1
12365	Adult	IV	IV	IV	IV	IV	IV	IV	IV	IV	IV	IV	IV	IV	IV	IV	IV	IV	IV	1
1916-83	Adult	IV	IV	IV	IV	IV	IV	IV	IV	IV	IV	IV	IV	IV	IV	IV	IV	IV	IV	1

Appendix 3.4: *Lepilemur ruficaudatus*

		Cranium									Mandible									
Specimen	Stage	I1	I2	C	P2	P3	P4	M1	M2	M3	I1	I2	C	P2	P3	P4	M1	M2	M3	Dental score
1962_2721	Infant	4	4	4	4	4	4/I	II	II	X	4/I	4/I	4/I	4	4	4/I	II	I	X	0.4
1962_2716	Juvenile	4	4	4/I	4/I	4/I	4/I	IV	III	II	4/II	4/II	4/II	4/I	4	4/I	IV	III	I	0.5
1961_267f	Juvenile	IV	IV	4/I	4/I	4/I	4/I	IV	III	II	III	III	III	4/II	4	4/II	IV	II	I	0.6
1962_2717	Subadult	IV	IV	4/I	4/I	4/I	4/I	IV	IV	II	4/II	4/II	4/II	4/I	4	4/II	IV	IV	II	0.6
1962_2718	Subadult	IV	IV	4/II	4/II	4/II	4/III	IV	IV	III	IV	IV	IV	4/II	4/I	III	IV	IV	III	0.767
1962_2733	Subadult	IV	IV	III	III	III	IV	IV	IV	IV	IV	IV	IV	II	III	IV	IV	IV	IV	0.883
1962_2728	Adult	IV	IV	IV	IV	IV	IV	IV	IV	IV	IV	IV	IV	IV	IV	IV	IV	IV	IV	1
1962_2719	Adult	IV	IV	IV	IV	IV	IV	IV	IV	IV	IV	IV	IV	IV	IV	IV	IV	IV	IV	1
10614	Adult	IV	IV	IV	IV	IV	IV	IV	IV	IV	IV	IV	IV	IV	IV	IV	IV	IV	IV	1
11054	Adult	IV	IV	IV	IV	IV	IV	IV	IV	IV	IV	IV	IV	IV	IV	IV	IV	IV	IV	1
2002_17	Adult	IV	IV	IV	IV	IV	IV	IV	IV	IV	IV	IV	IV	IV	IV	IV	IV	IV	IV	1
1891-6	Adult	IV	IV	IV	IV	IV	IV	IV	IV	IV	IV	IV	IV	IV	IV	IV	IV	IV	IV	1
1891-696	Adult	IV	IV	IV	IV	IV	IV	IV	IV	IV	IV	IV	IV	IV	IV	IV	IV	IV	IV	1

Appendices 3.1-12 : List of the sample used in the ontogenetic series analyses (continued).

Appendix 3.5: *Microcebus murinus*

		Cranium									Mandible									
Specimen	Stage	I1	I2	C	P2	P3	P4	M1	M2	M3	I1	I2	C	P2	P3	P4	M1	M2	M3	Dental score
977b	Neonate	4	4	4	2	1	1	I	X	X	4	4	4	4	3	3	I	X	X	0.267
Mtp1	Neonate	4	4	4	3	1	1	I	X	X	4	4	4	4	3	3	I	I	X	0.283
153c	Infant	4	4	4	4	4	4	I	I	X	4	4	4	4	4	4	I	X	X	0.4
109	Infant	4/I?	4	4	4	4	4	I	I	X	4	4	4	4	4	4	I	I	X	0.4
108	Infant	4/II	4/II	4/I	4/I	4	4	III	I	X	4/I	4/I	4/I	4/I	4	4	III	I	X	0.433
112	Juvenile	IV	IV	4/I	4/I	4/I	4/I	IV	III	I	IV	IV	IV	4/I	4/I	4/I	IV	IV	I	0.683
113	Subadult	IV	IV	4/I	4/I	4/I	4/I	IV	IV	I	IV	IV	IV	4/I	4/I	4/I	IV	IV	I	0.7
110	Subadult	IV	IV	4/III	III	4/I	4/I	IV	IV	II	IV	IV	IV	IV	4/I	4/I	IV	IV	II	0.767
111	Subadult	IV	IV	IV	IV	4/III	4/III	IV	IV	III	IV	IV	IV	IV	IV	4/III	IV	IV	III	0.917
5065-10	Adult	IV	IV	IV	IV	IV	IV	IV	IV	IV	IV	IV	IV	IV	IV	IV	IV	IV	IV	1
5065-12	Adult	IV	IV	IV	IV	IV	IV	IV	IV	IV	IV	IV	IV	IV	IV	IV	IV	IV	IV	1
Mtp2	Adult	IV	IV	IV	IV	IV	IV	IV	IV	IV	IV	IV	IV	IV	IV	IV	IV	IV	IV	1
1818	Adult	IV	IV	IV	IV	IV	IV	IV	IV	IV	IV	IV	IV	IV	IV	IV	IV	IV	IV	1
1815	Adult	IV	IV	IV	IV	IV	IV	IV	IV	IV	IV	IV	IV	IV	IV	IV	IV	IV	IV	1
1816	Adult	IV	IV	IV	IV	IV	IV	IV	IV	IV	IV	IV	IV	IV	IV	IV	IV	IV	IV	1

Appendix 3.6: *Propithecus diadema*

		Cranium									Mandible									
Specimen	Stage	I1	I2	C	P2	P3	P4	M1	M2	M3	I1	I2	C	P2	P3	P4	M1	M2	M3	Dental score
2811	Neonate	4	4	4	4?	1	1	I	X	X	4/I?	4/I?	4?	4?	1	2	I	X	X	0.296
1909_264	Infant	4/I	4	4/I	4?	4	4/I	II	I	X	4/II	4/II	4	4	4	4	II	I	X	0.407
1909_265	Infant	4/II	4	4/I	4?	4	4/I	III	I	X	4/II	4/II	4	4	4	4	II	I	X	0.426
1892_664	Juvenile	IV	4/II	4/I	4?	4/I	4/I	IV	II	I	IV	IV	X	4	4	4	IV	II	I	0.593
10597	Subadult	IV	IV	III	X	IV	IV	IV	IV	III	IV	IV	X	X	IV	IV	IV	IV	IV	0.963
1879_341	Subadult	IV	IV	I	X	III	IV	IV	IV	III	IV	IV	X	X	IV	IV?	IV	IV	III	0.870
7255	Adult	IV	IV	IV	X	IV	IV	IV	IV	IV	IV	IV	X	X	IV	IV	IV	IV	IV	1
1962_2810	Adult	IV	IV	IV	X	IV	IV	IV	IV	IV	IV	IV	X	X	IV	IV	IV	IV	IV	1

Appendix 3.7: *Propithecus verreauxi*

		Cranium									Mandible									
Specimen	Stage	I1	I2	C	P2	P3	P4	M1	M2	M3	I1	I2	C	P2	P3	P4	M1	M2	M3	Dental score
1912_28	Infant	4	4/I	4	4?	4	4/I	III	II		/	/	/	/	/	/	/	/	/	0.407
1854_1261	Juvenile	4/III	4/II	4/I	4?	4/I	4/I	IV	II	I	4/II	4/II	4	4	4/I	4/I	III	I		0.574
1909_267	Juvenile	III	4/III	4/I	4?	4/I	4/I	IV	III	II	IV	IV	X	4	4/I	4/II	IV	III	II	0.6
2005_255	Subadult	IV	IV	III	X	IV	IV	IV	IV	IV	IV	IV	X	X	IV	IV	IV	IV	IV	0.981
1962_2833	Subadult	IV	IV	III	X	IV	IV	IV	IV	IV	/	/	X	X	/	/	IV	IV	IV	0.981
1909_268	Subadult	?	IV	III	X	?	IV	IV	IV	II	IV	IV	X	X	III	?	IV	IV	II	0.963
AS131	Adult	IV	IV	IV	X	IV	IV	IV	IV	IV	IV	IV	X	X	IV	IV	IV	IV	IV	1
10607	Adult	IV	IV	IV	X	IV	IV	IV	IV	IV	IV	IV	X	X	IV	IV	IV	IV	IV	1
10606	Adult	IV	IV	IV	X	IV	IV	IV	IV	IV	IV	IV	X	X	IV	IV	IV	IV	IV	1
5068	Adult	IV	IV	IV	X	IV	IV	IV	IV	IV	IV	IV	X	X	IV	IV	IV	IV	IV	1

Appendices 3.1-12 : List of the sample used in the ontogenetic series analyses (continued).

Appendix 3.8: *Galago senegalensis*

		Cranium									Mandible									
Specimen	Stage	I1	I2	C	P2	P3	P4	M1	M2	M3	I1	I2	C	P2	P3	P4	M1	M2	M3	Dental score
7930	Neonate	4	4	4	4	1	1	I	X	X	4/I	4/I	4/I	4	4	3	I	X	X	0.317
6 643	Neonate	4	4	4	2	2	1	I	X	X	4	4	4	3	1	1	I	X	X	0.217
8190	Neonate	?	4	4	4	1	1	I	X	X	4/I	4/I	4	4/I	1	1	I	X	X	0.267
7966	Infant	4?	4	4	4	3	4	II	I	X	4/I	4/I	4/I	4/I	3	4	II	I	X	0.35
1982-770	Infant	X	4	4	4	4	4	II	I?	X	4/I	4/I	4/I	4/I	4	3	II	II	X	0.383
7983	Infant	4	4	4	4	4	4	II	I	X	4/I	4/I	4/I	4/I	4	3	III	I	X	0.4
8025	Subadult	IV	IV	III	III	III	4	IV	IV	III	IV	IV	IV	4	4	4	IV	III	III	0.767
6714	Adult	IV	IV	IV	IV	IV	IV	IV	IV	IV	IV	IV	IV	IV	IV	IV	IV	IV	IV	1
6768	Adult	IV	IV	IV	IV	IV	IV	IV	IV	IV	IV	IV	IV	IV	IV	IV	IV	IV	IV	1
6591	Adult	IV	IV	IV	IV	IV	IV	IV	IV	IV	IV	IV	IV	IV	IV	IV	IV	IV	IV	1
6635	Adult	IV	IV	IV	IV	IV	IV	IV	IV	IV	IV	IV	IV	IV	IV	IV	IV	IV	IV	1
10615	Adult	IV	IV	IV	IV	IV	IV	IV	IV	IV	IV	IV	IV	IV	IV	IV	IV	IV	IV	1
10610	Adult	IV	IV	IV	IV	IV	IV	IV	IV	IV	IV	IV	IV	IV	IV	IV	IV	IV	IV	1
9709	Adult	IV	IV	IV	IV	IV	IV	IV	IV	IV	IV	IV	IV	IV	IV	IV	IV	IV	IV	1

Appendix 3.9: *Otolemur garnetti*

		Cranium									Mandible									
Specimen	Stage	I1	I2	C	P2	P3	P4	M1	M2	M3	I1	I2	C	P2	P3	P4	M1	M2	M3	Dental score
9974	Neonate	4	4	4	4	1	1	I	X	X	4/I	4/I	4/I	4	4	3	I	X	X	0.317
326	Infant	4/I	4/I	4/I	4/I	4	4	I	I	X	4/I	4/I	4/I	4/I	4	4	I	I	X	0.4
12251	Adult	IV	IV	IV	IV	IV	IV	IV	IV	IV	IV	IV	IV	IV	IV	IV	IV	IV	IV	1
9884	Adult	IV	IV	IV	IV	IV	IV	IV	IV	IV	IV	IV	IV	IV	IV	IV	IV	IV	IV	1
AS-926	Adult	IV	IV	IV	IV	IV	IV	IV	IV	IV	IV	IV	IV	IV	IV	IV	IV	IV	IV	1

Appendix 3.10: *Arctocebus calabarensis*

		Cranium									Mandible									
Specimen	Stage	I1	I2	C	P2	P3	P4	M1	M2	M3	I1	I2	C	P2	P3	P4	M1	M2	M3	Dental score
7060	Infant	4	4	4/I	4	4	3	X	X	X	4/III	4/III	4/III	4/II	4	4	I	X	X	0.38
7 711	Infant	4	4	4	4	3	4	I	X	X	III	III	III	4/I	4	4	I	I	X	0.43
7013	Infant	4	4	4/III	III	4	4	I	I	X	IV	IV	IV	III	4	4	III	I	X	0.567
7668	Juvenile	IV	IV	IV	III	4	4	IV	III	X	IV	IV	IV	IV	4	4	IV	III	I	0.75
6985	Juvenile	IV	IV	IV	III	4	4	IV	III	X	IV	IV	IV	IV	4	4	IV	III	I	0.75
7647	Subadult	IV	IV	IV	IV	4	4	IV	IV	X	IV	IV	IV	IV	4	4	IV	IV	II	0.8
7730	Subadult	IV	IV	IV	IV	4	4	IV	IV	X	IV	IV	IV	IV	4	4	IV	IV	II	0.8
7800	Subadult	IV	IV	IV	IV	4	4	IV	IV	X	IV	IV	IV	IV	4	4	IV	IV	II	0.8
6984	Subadult	IV	IV	IV	IV	4/III	4/III	IV	IV	IV	IV	IV	IV	IV	4/III	4/III	IV	IV	IV	0.93
7024	Subadult	IV	IV	IV	IV	III	III	IV	IV	IV	IV	IV	IV	IV	III	III	IV	IV	IV	0.93
7059	Adult	IV	IV	IV	IV	IV	IV	IV	IV	IV	IV	IV	IV	IV	IV	IV	IV	IV	IV	1
7103	Adult	IV	IV	IV	IV	IV	IV	IV	IV	IV	IV	IV	IV	IV	IV	IV	IV	IV	IV	1
7475	Adult	IV	IV	IV	IV	IV	IV	IV	IV	IV	IV	IV	IV	IV	IV	IV	IV	IV	IV	1
7696	Adult	IV	IV	IV	IV	IV	IV	IV	IV	IV	IV	IV	IV	IV	IV	IV	IV	IV	IV	1
7704	Adult	IV	IV	IV	IV	IV	IV	IV	IV	IV	IV	IV	IV	IV	IV	IV	IV	IV	IV	1
7761	Adult	IV	IV	IV	IV	IV	IV	IV	IV	IV	IV	IV	IV	IV	IV	IV	IV	IV	IV	1

Appendices 3.1-12 : List of the sample used in the ontogenetic series analyses (continued).

Appendix 3.11: *Nycticebus coucang*

		Cranium									Mandible									
Specimen	Stage	I1	I2	C	P2	P3	P4	M1	M2	M3	I1	I2	C	P2	P3	P4	M1	M2	M3	Dental score
7726	Neonate	4/II	4/?	4/II	4/I	4	4	I	X	X	4/III	4/III	4/III	4/II	4	4	I	I	X	0.467
326	Infant	4/III	4/III	4/III	4/I	4	4	I	I	X	III	III	4/III	4/III	4	4	I	I	X	0.517
10587	Juvenile	IV	IV	IV	IV	4/II	4/II	IV	II	X	IV	IV	IV	IV	4/II	4/II	IV	III	I	0.75
8596	Subadult	IV	IV	IV	IV	III	IV	IV	IV	IV	IV	IV	IV	IV	4/III	IV	IV	IV	IV	0.967
8674	Subadult	IV	IV	IV	IV	III	IV	IV	IV	IV	IV	IV	IV	IV	III	III	IV	IV	IV	0.95
10 594	Adult	IV	IV	IV	IV	IV	IV	IV	IV	IV	IV	IV	IV	IV	IV	IV	IV	IV	IV	1
10593	Adult	IV	IV	IV	IV	IV	IV	IV	IV	IV	IV	IV	IV	IV	IV	IV	IV	IV	IV	1
10586	Adult	IV	IV	IV	IV	IV	IV	IV	IV	IV	IV	IV	IV	IV	IV	IV	IV	IV	IV	1

Appendix 3.12: *Perodicticus potto*

		Cranium									Mandible									
Specimen	Stage	I1	I2	C	P2	P3	P4	M1	M2	M3	I1	I2	C	P2	P3	P4	M1	M2	M3	Dental score
7151	Infant	III	III	4/III	4/II	4	4	X	X	X	III	III	4/III	II	4	4	I	X	X	0.5
7031	Infant	IV	IV	III	4/III	4	4	III	X	X	IV	IV	IV	III	4	4/I	II	X	X	0.633
7076	Infant	IV	IV	III	4	4	4	II	X	X	IV	IV	IV	III	4	4	II	I	X	0.6
6976	Infant	IV	IV	III	III	4/I	4/I	III	X	X	IV	IV	IV	III	4/I	4	III	I	X	0.65
7030	Juvenile	IV	IV	IV	IV	4/II	4/II	IV	I	X	IV	IV	IV	IV	4/I	4/I	IV	II	X	0.733
7046	Subadult	IV	IV	IV	IV	IV	IV	IV	IV	II	IV	IV	IV	IV	IV	IV	IV	IV	III	0.95
7192	Subadult	IV	IV	IV	IV	IV	IV	IV	IV	III	IV	IV	IV	IV	IV	IV	IV	IV	III	0.967
7024	Adult	IV	IV	IV	IV	IV	IV	IV	IV	IV	IV	IV	IV	IV	IV	IV	IV	IV	IV	1
1833	Adult	IV	IV	IV	IV	IV	IV	IV	IV	IV	IV	IV	IV	IV	IV	IV	IV	IV	IV	1
6620	Adult	IV	IV	IV	IV	IV	IV	IV	IV	IV	IV	IV	IV	IV	IV	IV	IV	IV	IV	1
7014	Adult	IV	IV	IV	IV	IV	IV	IV	IV	IV	IV	IV	IV	IV	IV	IV	IV	IV	IV	1
7029	Adult	IV	IV	IV	IV	IV	IV	IV	IV	IV	IV	IV	IV	IV	IV	IV	IV	IV	IV	1
7050	Adult	IV	IV	IV	IV	IV	IV	IV	IV	IV	IV	IV	IV	IV	IV	IV	IV	IV	IV	1
7054	Adult	IV	IV	IV	IV	IV	IV	IV	IV	IV	IV	IV	IV	IV	IV	IV	IV	IV	IV	1

2. Reconstructions

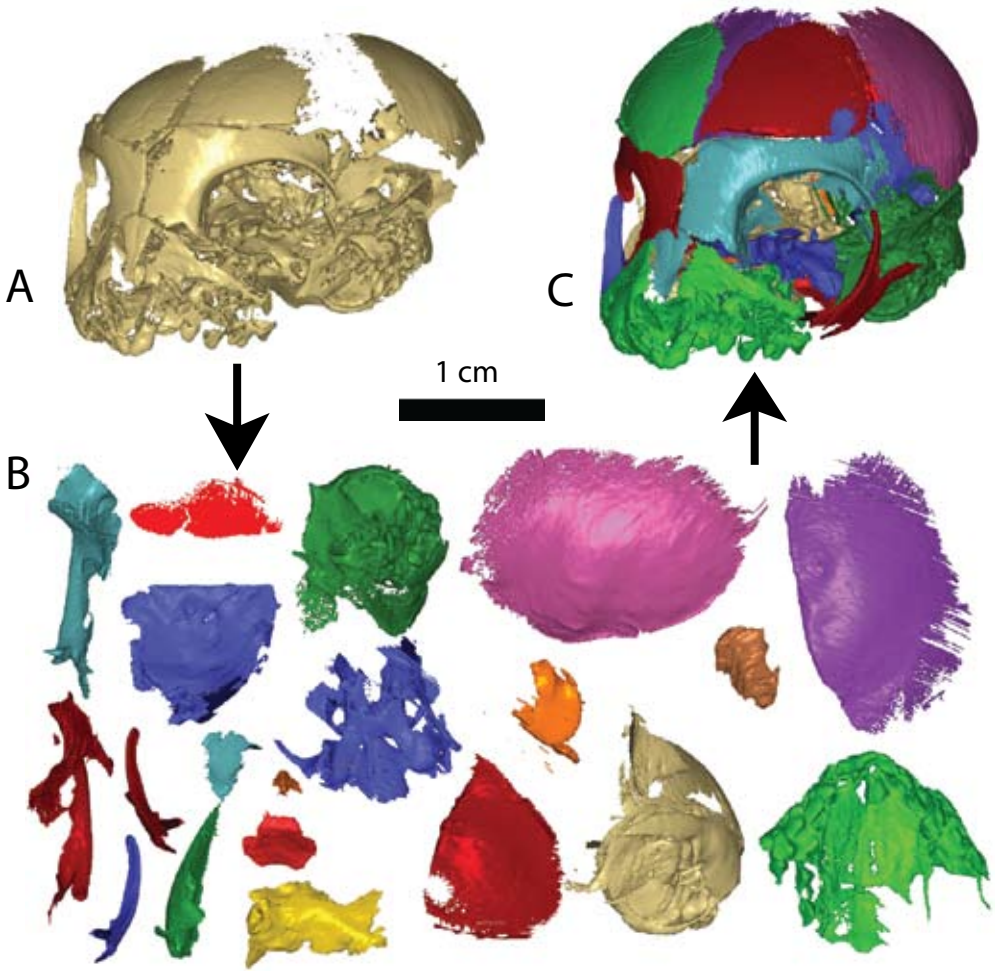

Appendix 4: µCT-based virtual reconstruction of specimen *Propithecus diadema* 1962-2811. A: original specimen. B: decomposition into distinct bones or groups of bones. C: reconstruction

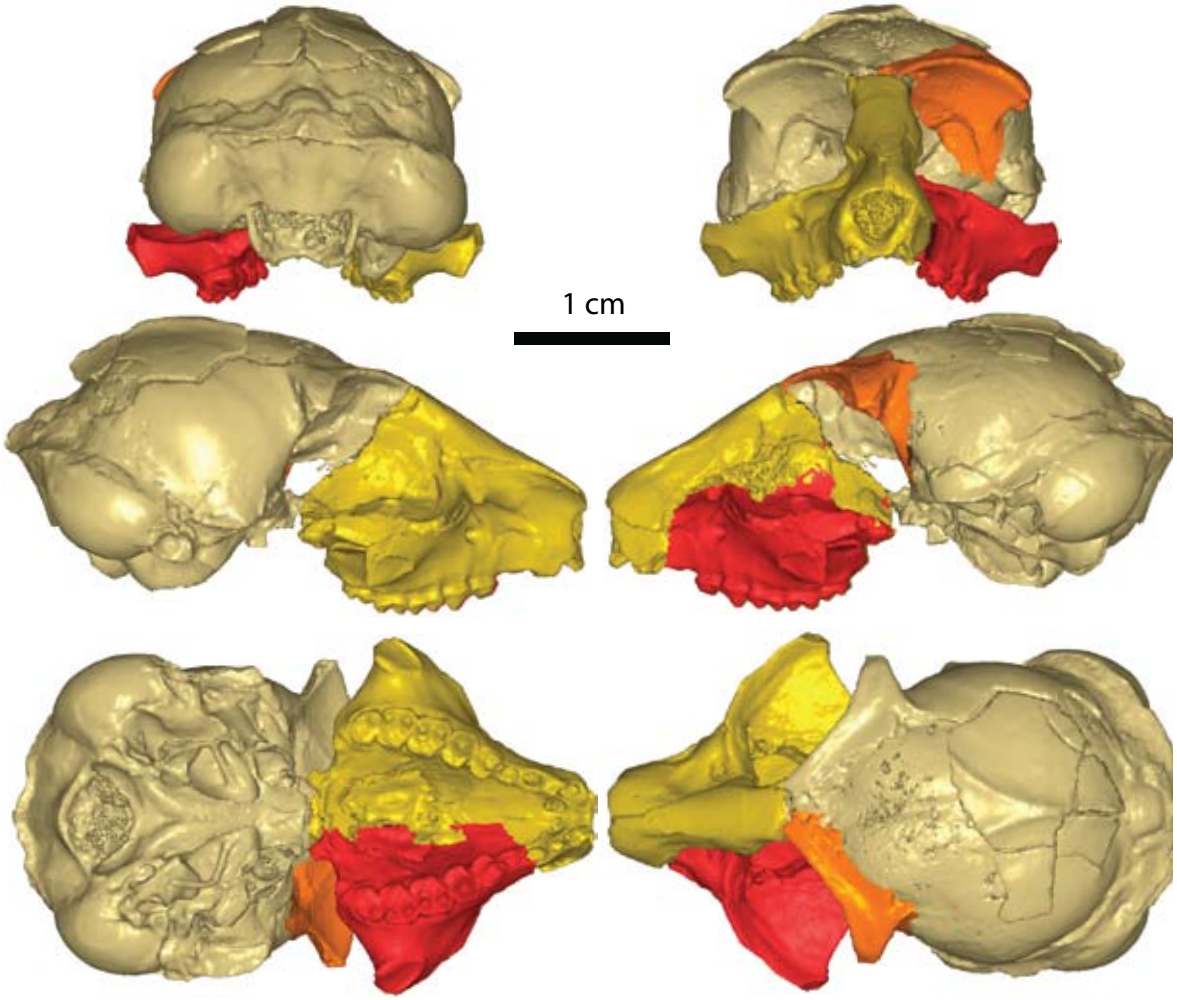

Appendix 5: µCT-based virtual reconstruction of MAHQ 289 (*Necrolemur antiquus*). Colored regions indicate parts that have been given a new position and/or mirror images.

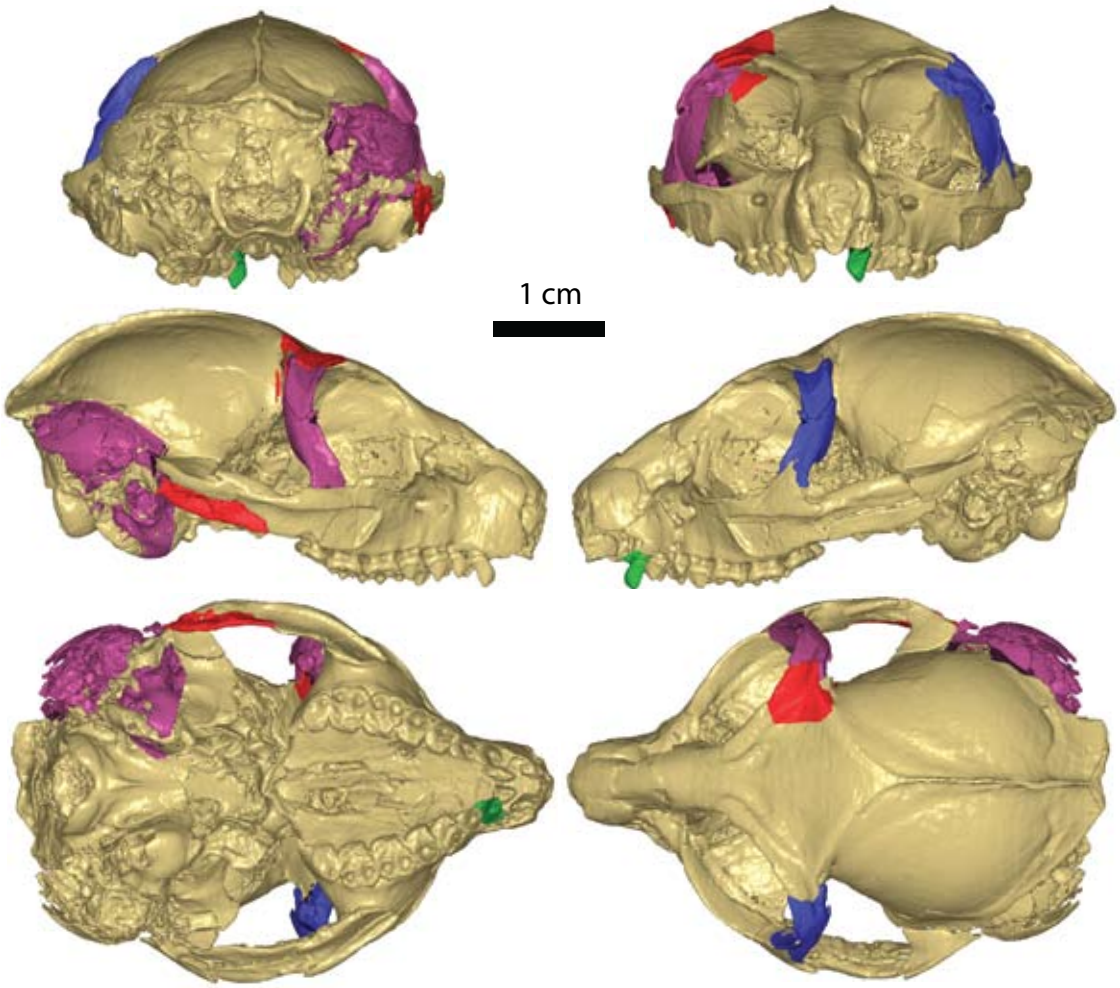

Appendix 6: µCT-based virtual reconstruction of the cranium of *Microchoerus sp.* (Montpellier PR1771). Colored regions indicate parts that have been given a new position and/or mirror images.

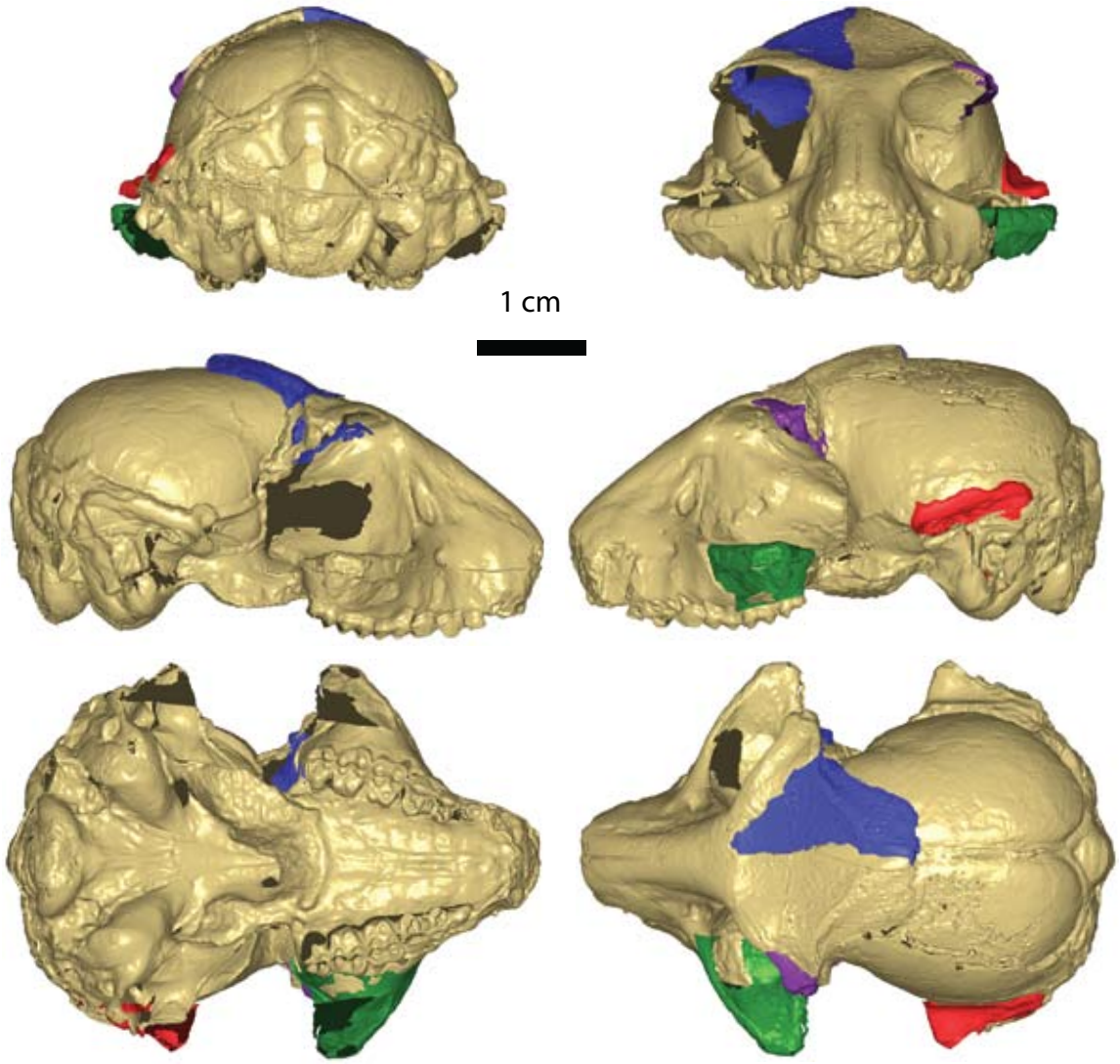

Appendix 7: µCT-based virtual reconstruction of the cranium of *Rooneyia viejaensis* (TMM 40688-7); cast provided by Prof. A. Rosenberger). Colored regions indicate parts that have been given a new position and/ or mirror images.

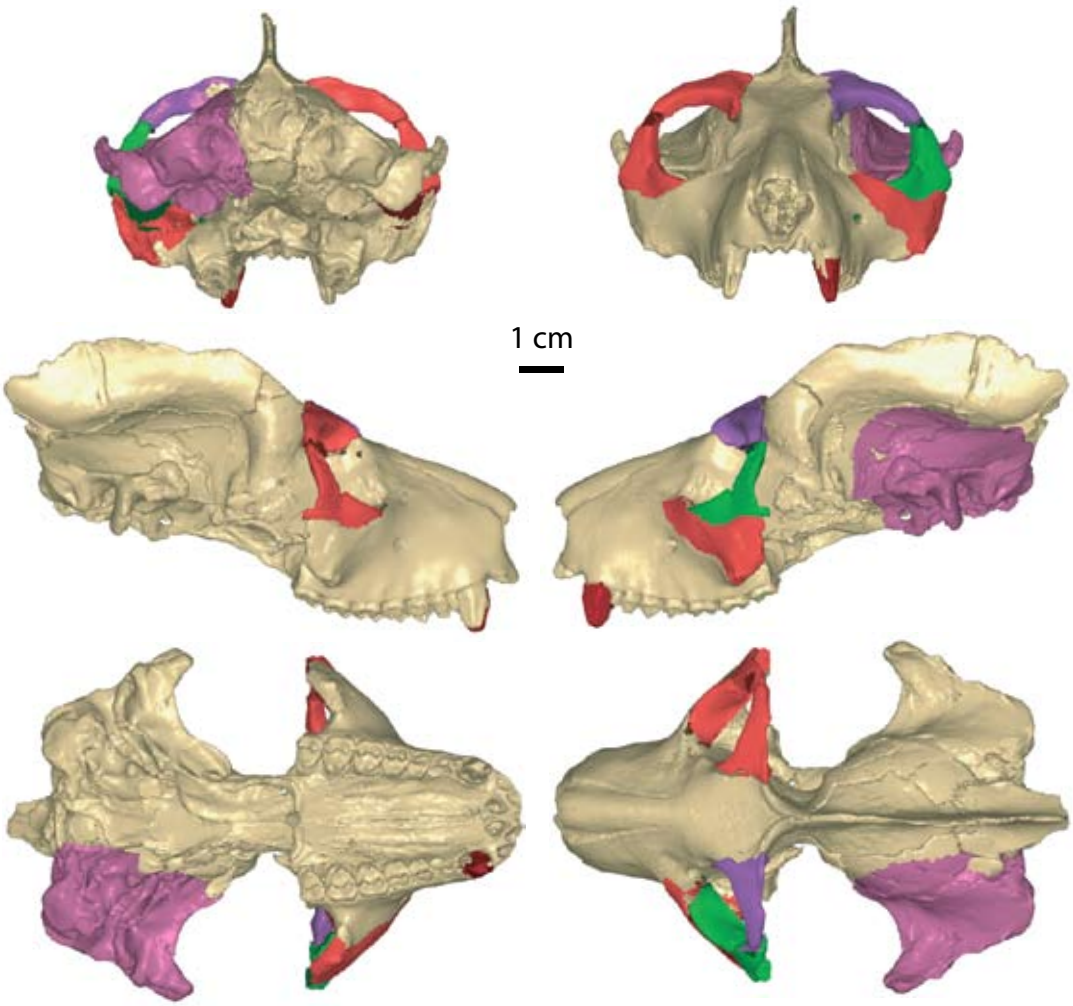

Appendix 8: µCT-based virtual reconstruction of the specimen MAPHQ 210 (*Leptadapis sp.*). The original specimen was scanned. Colored regions indicate parts that have been given a new position and/or mirror images.

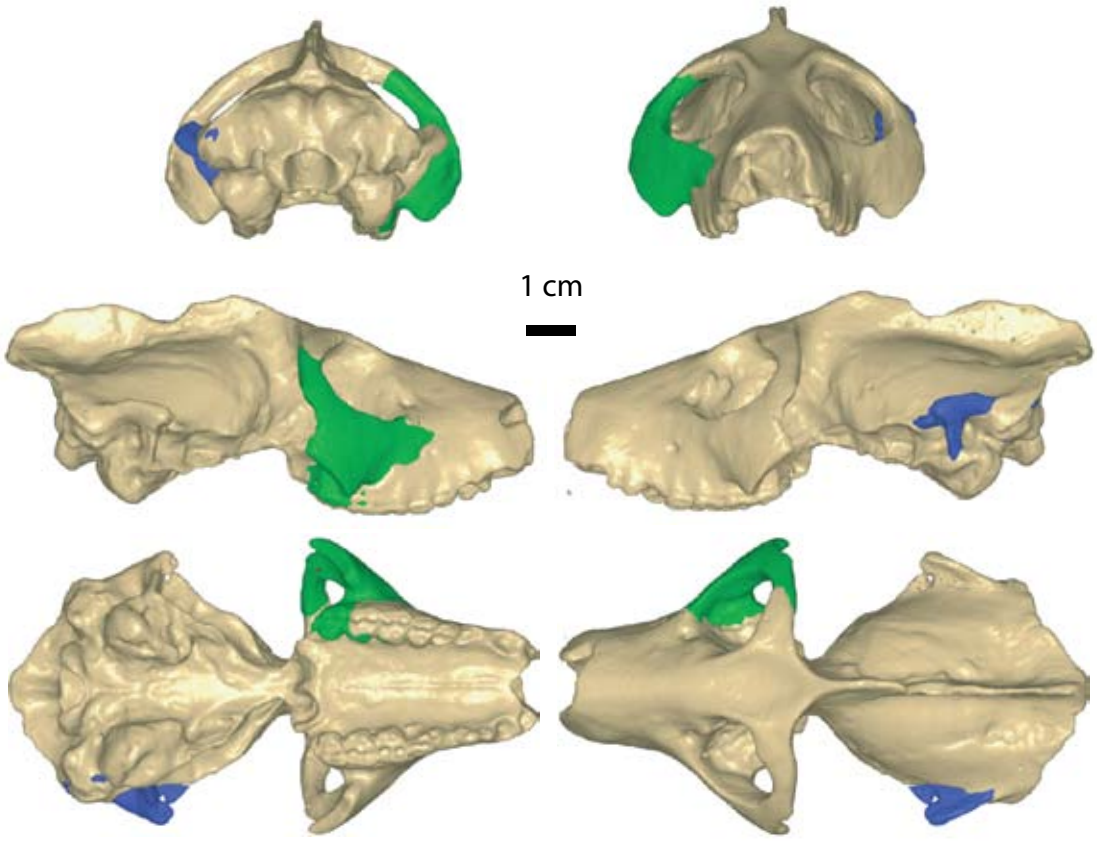

Appendix 9: µCT-based virtual reconstruction of the type specimen of *Leptadapis magnus* (QU 11002) A cast was used. Colored regions indicate parts that have been given a new position and/or mirror images.

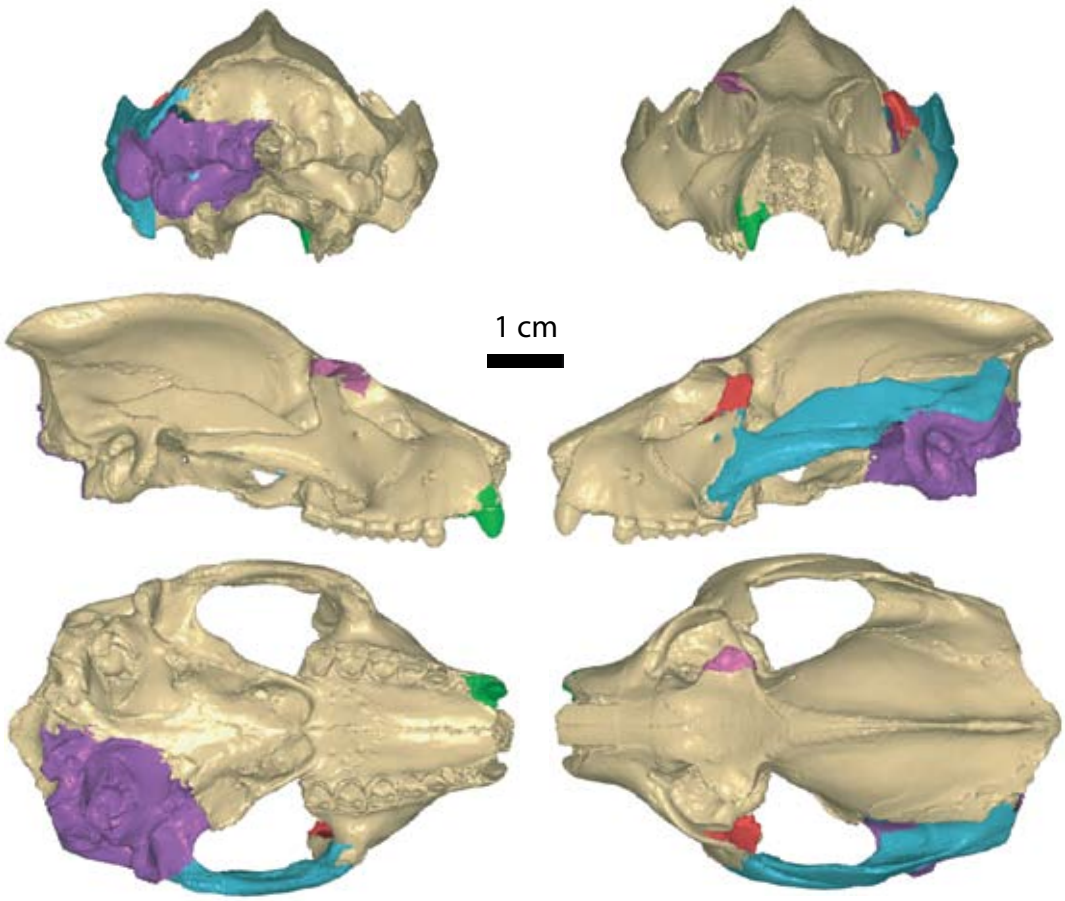

Appendix 10: µCT-based virtual reconstruction of MAHQ 221 (*Adapis bruni*). The original fossil was scanned. Colored regions indicate parts that have been given a new position and/or mirror images.

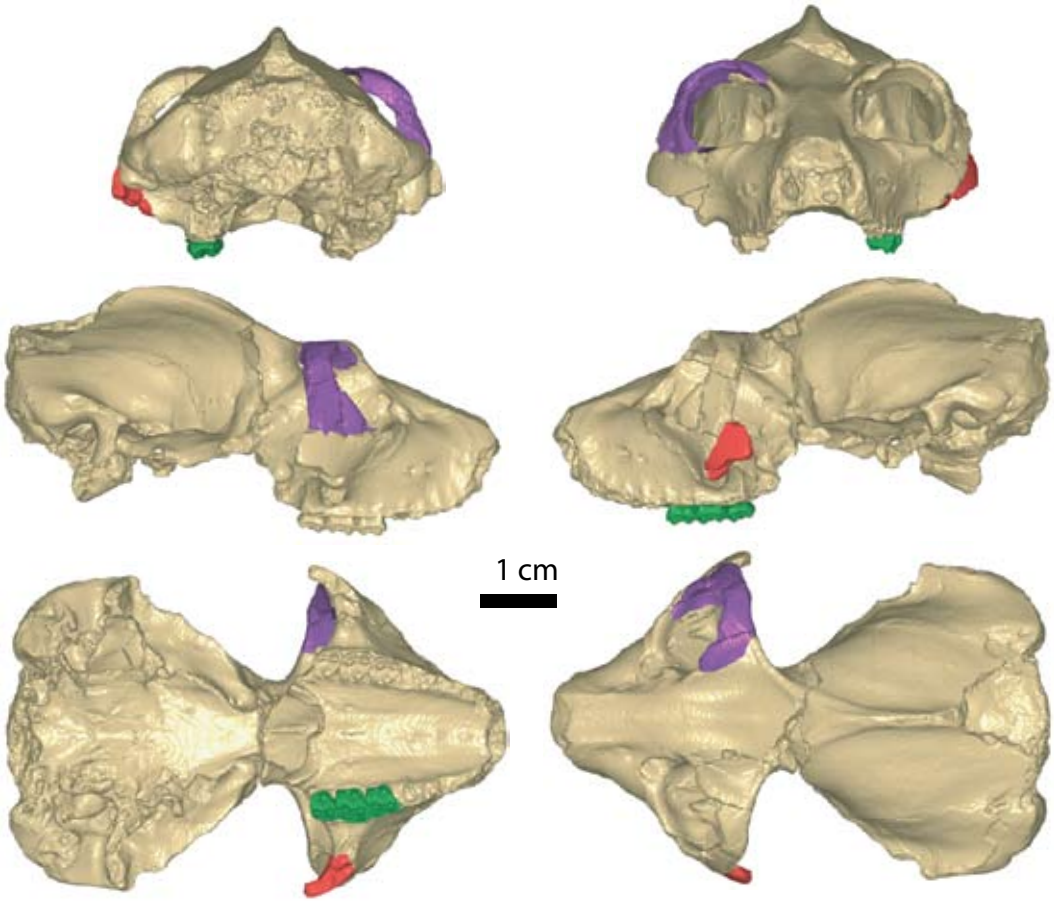

Appendix 11: µCT-based virtual reconstruction of the type specimen of *Paleolemur betillei* (Bor 613). The original fossil was scanned. Colored regions indicate parts that have been given a new position and/or mirror images.

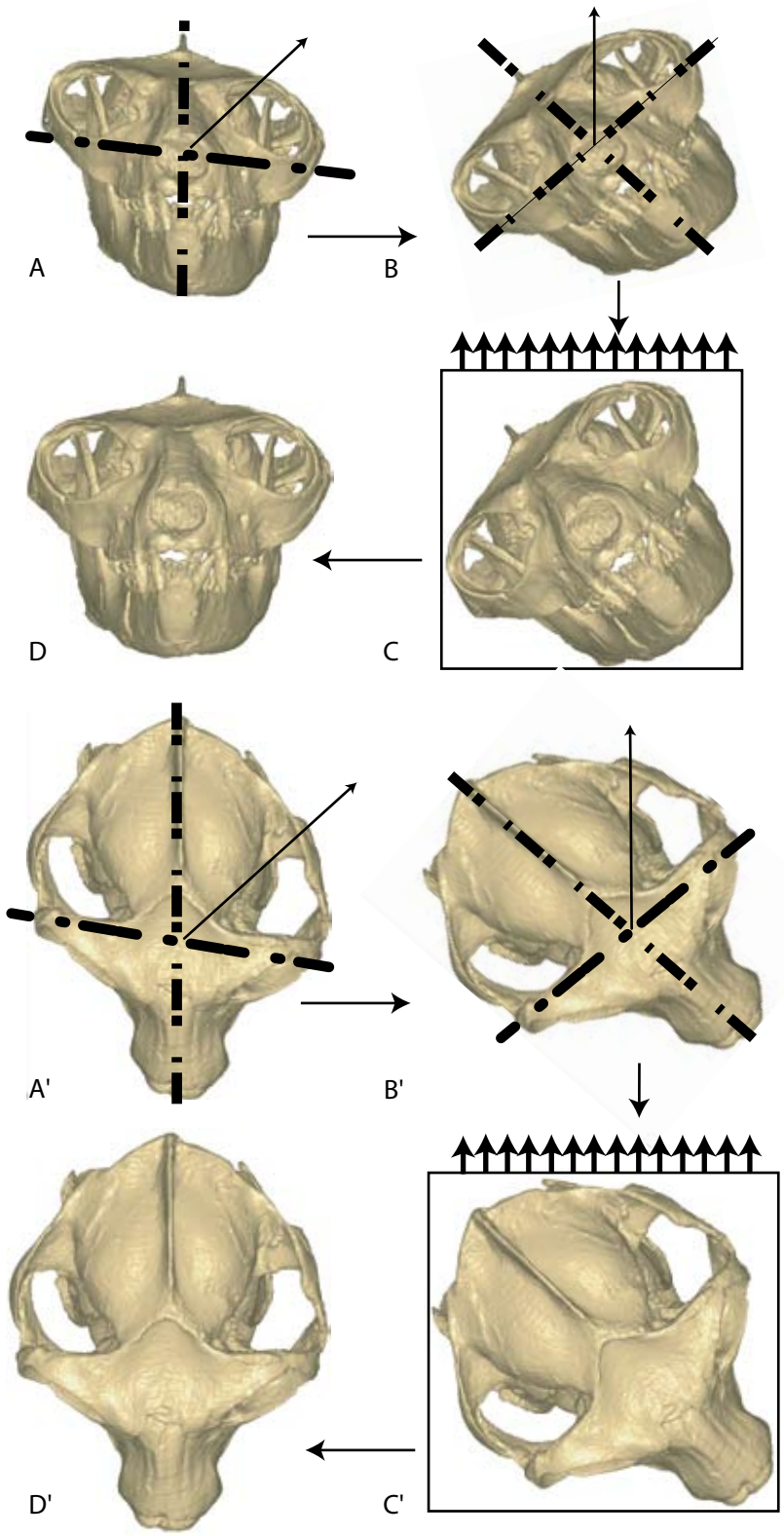

Appendix 12: µCT-based virtual reconstruction of the cranium of *Notharctus tenebrosus* (AMNH 163167). A, A': original state of the fossil in frontal and dorsal views. B, B': estimation of the orientation of maximal compression. C, C': estimation of the amplitude of relaxation necessary to give back the original shape. D, D': reconstructed fossil.

Evolution and Development of the Strepsirrhine Primate Skull.

Summary:

Due to recent advances in developmental genetics and phenotypic analysis, evolutionary developmental (evo-devo) studies regained considerable interest, and led to fundamental changes in our understanding of how ontogeny and phylogeny are related. This thesis investigates the relationship between ontogeny and phylogeny in strepsirrhine primates. Here, the focus is on cranial diversity, which is analyzed from a developmental perspective, and with a new set of geometric morphometric tools. A comparative geometric morphometric analysis of cranio-mandibular development is conducted in ten strepsirrhine and two haplorrhine species. Haplorrhines and strepsirrhines differ widely in ontogenetic trajectory direction, length and position. Within the strepsirrhines, divergence between taxon-specific ontogenetic trajectories and allometric grade shifts are more pronounced in lemurs than in lorises. The insights obtained from the evolutionary developmental analysis of extant taxa are used for a comparative analysis of Eocene fossil strepsirrhine taxa belonging to the infraorder Adapiformes. Among the adapine adapiforms, an increase in size via allometric grade shift has occurred in the *Leptadapis* lineage, which suggests phyletic gigantism in this genus. Adapiforms exhibit longer ontogenetic trajectories than extant strepsirrhines. A trend toward a shortening of ontogenetic trajectories has occurred in the evolutionary history of strepsirrhines. This trend can be related to the expression of developmental constraints in a context of selection for increase in encephalization.

Résumé:

Les récents progrès de la génétique du développement et de l'analyse du phénotype ont engendré un regain d'intérêt considérable pour l'étude de l'évolution du développement (evo-devo). Cette thèse présente une étude des relations entre ontogénie et phylogénie dans le sous-ordre des primates strepsirrhiniens. Ici, on s'intéresse au complexe crânio-mandibulaire, dont la croissance et le développement sont analysés à l'aide d'un ensemble d'outils dédiés de géométrie morphométrique. Une analyse comparative de l'ontogénie du crâne et de la mandibule est conduite sur un ensemble de dix espèces de strepsirrhiniens et de deux espèces d'haplorrhiniens. Les haplorrhiniens et les strepsirrhiniens diffèrent largement dans la direction, la position, et la longueur de leurs trajectoires ontogénétiques. Chez les lémuriens malgaches, il y a une plus grande diversité de direction, de position et de longueur des trajectoires ontogénétiques que chez les loriformes. De plus, on observe des différences importantes de grade allométrique parmi les espèces de lémuriens, et une plus faible variabilité au sein des loriformes. Une analyse comparative est conduite sur un échantillon de primates Eocènes adapiformes et de strepsirrhiniens actuels. Au sein des adapinés, une augmentation de taille via transposition allométrique caractérise la lignée des *Leptadapis*. Enfin, les adapiformes adapinés et notharctidés ont des trajectoires ontogénétiques plus longues en terme de quantité de changement de forme que les espèces de strepsirrhiniens actuels. Une tendance au raccourcicement des trajectoires ontogénétiques caractérise l'évolution des strepsirrhiniens. Ceci est lié, au cours de leur histoire évolutive, à l'expression de contraintes de développement dans un contexte général de sélection en faveur de l'augmentation de leur degré d'encéphalisation.

Keywords	Strepsirrhines, Primates, Adapiformes, Ontogeny, Phylogeny, Development, Evolution, Geometric Mophometric, 3D Reconstruction, Computed Tomography.

Laboratoires d'accueil:
- Institut des Sciences de l'Evolution, UMR 5554 -Montpellier II
- Anthropologisches Institut und Museum, Universität Irchel - Zürich
- Institut International de Paléoprimatologie, Paléontologie Humaine : Evolution et Paléoenvironnements, UMR 6046 - Poitiers